

N72-20340

ADVANCED STUDY OF GLOBAL OCEANOGRAPHIC REQUIREMENTS FOR EOS A/B

FINAL REPORT SUMMARY VOLUME

CASE FILE COPY

Prepared for

THE NATIONAL AERONAUTICS AND SPACE ADMINISTRATION
HEADQUARTERS
WASHINGTON, D.C.



Prepared by

TRW SYSTEMS GROUP/EARTHSAT

JANUARY 1972

TRW
SYSTEMS GROUP

REPRO VELLUM

***ADVANCED STUDY OF GLOBAL OCEANOGRAPHIC
REQUIREMENTS FOR EOS A/B***

***FINAL REPORT
SUMMARY VOLUME***

Prepared for

THE NATIONAL AERONAUTICS AND SPACE ADMINISTRATION
HEADQUARTERS
WASHINGTON, D.C.

Prepared by

TRW SYSTEMS GROUP/EARTHSAT

JANUARY 1972

TRW
SYSTEMS GROUP

INTRODUCTION

This volume summarizes the objectives, approach and conclusions reached in the "Advanced Study of Global Oceanographic Requirements for EOS A/B," NASw-2163; NASA Headquarters; January 1972.

OBJECTIVES

The global ocean, for the purposes of this study, is defined as the ocean domain of phenomena requiring a spatial resolution of at least several kilometers. The coastal zone, on the other hand, required a resolution on the order of meters.

In addressing the open ocean province, the specific study objectives were as follows:

- Define the global ocean information needs and evaluate their relative importance
- Establish the synoptic measurements required to provide useful data on these information needs
- Determine the sensor and orbital requirements needed to obtain the desired measurements
- Analyze the complex problems associated with data management
- Evaluate the possible synergistic aspects of the EOS oceanographic with existing and planned in situ measurement programs and other remote measuring platforms

The overall purpose of the study was to determine what, if any, relevant problem-oriented information can be best provided by a spacecraft dedicated to global oceanography in the 1976 time period. Therefore, the study was directed at problems confronting the open ocean rather than defining the classical oceanographic data obtainable from remote platforms.

APPROACH

Under the auspices of marine resource management and ecological exploitation, the study commenced by identifying specific priorities and their associated information needs. The specific priorities chosen were as follows:

- Monitoring and Prediction of Physical Phenomena - Understanding and predicting those phenomena which determine the physical environment of the global ocean ecosystem.
- Management of Living Marine Resources - Optimum exploitation and conservation of the living components of the global ocean ecosystem based on the understanding and prediction of the phenomena associated with these components.
- Detection, Monitoring and Control of Global Ocean Pollution - Monitoring and controlling those man-made phenomena which significantly perturb the natural system.

Once these information needs were identified, the study was performed in the following manner (See Figure 1).

1. The general all-inclusive national needs were broken down into more specific implied information needs and their associated space observables, features, processes, or phenomena
2. The synoptic measurements that provide information on these features, processes, and phenomena were then identified. Measurement requirements most likely accommodated by other space programs of expected operational status during the EOS A/B time frame were eliminated.
3. Requirements for these synoptic measurements, in terms of electromagnetic spectral region, spatial resolution, sensitivity, field of view and temporal characteristics were considered in order to arrive at sensor concepts. Tables 1, 2, and 3 give examples of the measurement requirements.
4. The widest range of sensor concepts was evaluated for its ability to meet the minimum and maximum performance goals. Table 4 is given as an example of this selection process and Table 5 shows the ultimate sensor design goals for all three information needs.
5. Under the requirements of the work statement a minimum sensor payload grouping for each priority that maximized effectiveness in achieving global problem solutions were synthesized. The minimum group established the most limited mission worth implementing. A description of each instrument in terms of size, weight, power, and performance was provided.
6. Beginning with the phenomenology requirements associated with the information categories and the sensor requirements, parametric orbital analyses were performed. Consideration was given to such factors as global areas to be covered, frequency of coverage, ground station visibility times, sun-angle variations, sensor field of view constraints, and atmospheric drag.

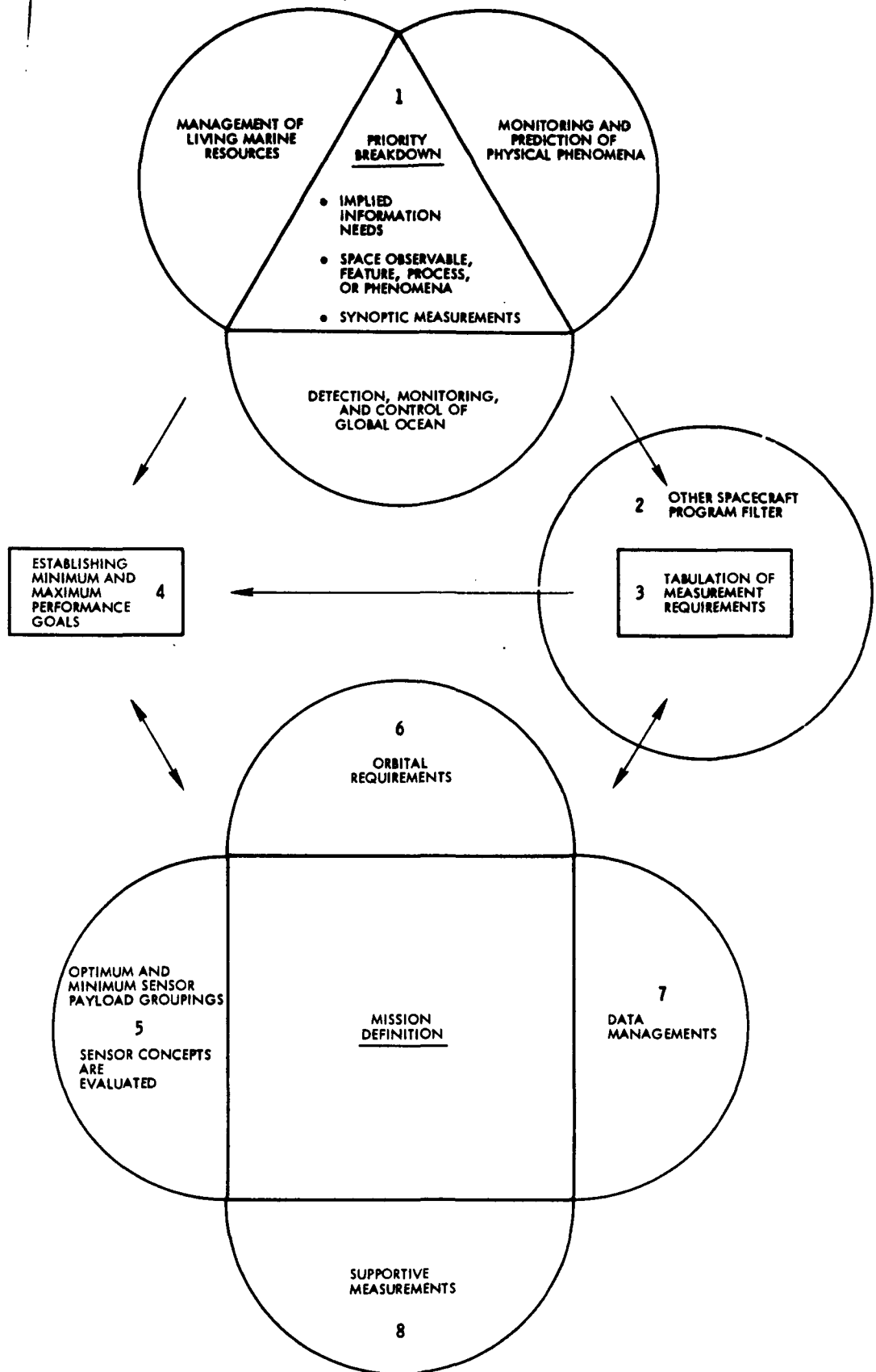


Figure 1. Study Approach Schematic

Table 1. Measurement Requirements - Monitoring and Prediction of Physical Phenomena

Space Observable	Frequency of Observation (Days)	Resolution or Grid Spacing (Km)	Accuracy/Sensitivity	Possible Measurement Technique
Atmospheric Measurements:				
Transparency	1	3-5 Res	1%	Visible Radiometry
Temperature profile	1	50 GS	1° C Abs	IR or Microwave sounding
Humidity profile	1	50 GS	±5% RH	IR sounding
Heat Flux	1-3	150 GS	± 10%	IR Radiometry
Cloud patterns	1-3	3-5 Res	NEΔρ=0.01	Visible imaging IR imaging
Sea State and Surface Winds:				
Wind vector, fetch and duration	1	3-5 Res	± 10%	Visible imaging (cloud patterns)
Directional wave spectrum	1	0.015-0.03 Res	± 10%	Visible imaging
Sea state	1	50 GS	Nearest Beaufort No.	Glitter pattern sensing Passive microwave radiometry
Sea Surface: Temperature	1-3	5-10 Res	0.2-0.5° C Abs	IR Radiometry Passive microwave radiometry
Salinity	1-3	5-10 Res	0.5 PPT	Passive microwave radiometry
Slopes	1	5 GS	10 ⁻⁴ to 10 ⁻⁷	Radar or laser altimetry
Sea ice: Boundaries	1-3	0.5-1 Res	1 Km	Visible imaging Synthetic aperture radar imaging IR imaging
Thickness	2-14	1 Res	NEΔρ = 0.01	Multispectral visible imaging
Turbidity (color)	3-5	5-10 Res	NEΔρ = 0.01	Multispectral visible imaging
Bottom topography	60-365	0.5 Res	NEΔρ = 0.01	Multispectral visible imaging
Configuration changes	190-365	0.5 Res	ΔS = 0.5 Km	Visible imaging
Magnetic anomalies	365	1 Res	1-2 Gamma	Magnetic flux measurement

Table 2. Measurement Requirements - Management of Living Marine Resources

Space Observable	Frequency of Observation (Days)	Resolution or Grid Spacing (Km)	Accuracy/Sensitivity	Possible Measurement Technique
Ocean Color (phytoplankton pigment)	3-5	1-2 Res estuaries and currents 5-10 other	NE $\Delta\rho$ = 0.001	Multispectral visible imaging
Ocean color (turbidity, anomalous water chemistry)	1/2-7	0.5-1 Res estuaries and coasts 5-10 other	NE $\Delta\rho$ = 0.01	Multispectral visible imaging
Cloud patterns	1/2-2 (storms, etc.) 7-14 (other)	1-2 Res	NE $\Delta\rho$ = 0.01 NE ΔT = 0.5 $^{\circ}$ C	Visible imaging IR imaging
Sea Surface:				
Temperature	1/2-2	0.5-1 Res estuaries 5-10 other	0.2-0.5 $^{\circ}$ Abs	IR radiometry
Salinity	3-7	0.5-1 Res	0.5 PPT	Passive microwave radiometry
Slopes	3-7	10-20 GS	10 $^{-5}$ to 10 $^{-8}$	Passive microwave radiometry Radar or laser altimetry
Sea state and surface winds:				
Sea state	1/2-1	10-100 Res	NBN	Glitter Pattern sensing Passive microwave radiometry
Directional wave spectrum	2-8		$\pm 10\%$	Visible imaging
Swell wavelength/direction	2-8	100 GS	$\pm 10\%$	Passive microwave radiometry
Slicks	1/2-2	0.5-1 Res	NBN	Glitter pattern sensing Passive microwave radiometry
Atmospheric temperature profile	1.2-1	100 GS	1 $^{\circ}$ C Abs	IR sounding Microwave sounding
Shallow water:				
Bottom topography	180-365	0.05-1 Res	NE $\Delta\rho$ = 0.01	Visible imaging
Swell wavelength foreshortening	180-365	0.05 Res	$\pm 10\%$	Visible imaging

Table 3. Measurement Requirements - Detection, Monitoring and Control of Global Ocean Pollution

Space Observable	Frequency of Observation (Days)	Resolution or Grid Spacing (Km)	Accuracy / Sensitivity	Possible Measurement Technique
Ocean Color (phytoplankton)	7	1-2 to 10 Res	$NE\Delta\rho = 0.001$	Multispectral visible imaging
Ocean Color (current boundaries, convergences, etc.)	3-14	1-2 to 10 Res	$NE\Delta\rho = 0.01$	Multispectral visible imaging
Sea Surface:				
Temperature	3-7	1-2 to 10 Res 150 GS	0.2 - 0.5°C	Infrared Radiometry
Salinity	3-7	1-2 to 10 Res	0.5 PPT	Passive microwave radiometry
Slopes	14	10-20 GS	10^{-5} to 10^{-8}	Radar or laser altimetry
Ice Cap Size	30	5-10 Res	Bdries to 5 km	Visible imaging Synthetic aperture radar imaging
Reduced sea state (oil films)	7	2 Res	NBN with boundaries to 2 km	Visible imaging Glitter pattern sensing Passive microwave radiometry

Table 4. Sensor Requirement Summary

Detection, Monitoring and Control of Global Ocean Pollution

Information Needs	ΔS IFOV (km)	S Swath Width (km)	λ_1 λ_2 Spectral Range (μ)	Δ Spectral Bandwidth (μ)	NE $\Delta\rho$ Sensitivity
I. Marine Ecosystem Modifications					
A. Power Plant Effects					
1) Current location boundaries					
a) Water color contrast	1-2	200	0.4-0.7	0.05	0.01
4) Phytoplankton dynamics	1-2	200	0.4-0.7	0.01	0.001
II. Global Temperature Alteration					
A. Albedo Modification due to haze					
1) Ice caps	5-10	--	0.4-0.7	Broad	0.01
III. Heavy Metals					
A. Phytoplankton standing stock					
	10	200	0.4-0.7	0.01	0.001
B. Global Monitoring System					
1) General surface circulation					
a) Water color contrast	10	200	0.4-0.7	0.05	0.01
2) Convergences					
a) Water color contrast	20	500	0.4-0.7	0.05	0.01
3) River Plumes					
a) Water color contrast	1-2	200	0.4-0.7	0.05	0.01
Maximum	1-2	500	0.4-0.7	0.01	0.001
Minimum	10	200	0.4-0.7	0.05	0.01

Table 5. Sensor Design Goals (Visible and Near IR Spectrometry/Imaging)

OBJECTIVE	SPECTRAL RANGE	SPECTRAL BANDWIDTH (μ)	RESOLUTION (KM)	SWATH WIDTH (FOV) (KM)	SENSITIVITY NEAP
DETECTION, MONITOR, AND CONTROL GLOBAL OCEAN POLLUTION					
OCEAN COLOR					
MAXIMUM PERFORMANCE GOALS	1-2	500	0.4 - 0.7	0.01	0.00
MINIMUM PERFORMANCE GOALS	10	200	0.4 - 0.7	0.05	0.01
GLITTER					
MAXIMUM PERFORMANCE GOALS	0.4 - 0.7		10	100	
MINIMUM PERFORMANCE GOALS	0.4 - 0.7		10	100	
MONITOR AND PREDICT PHYSICAL PHENOMENA					
OCEAN COLOR					
MAXIMUM PERFORMANCE GOALS	0.4 - 0.7	0.01	0.1 - 0.5	100	NEAP = 0.01
MINIMUM PERFORMANCE GOALS	0.4 - 0.7	0.1	3 - 5	100	NEAP = 0.01
GLITTER					
MAXIMUM PERFORMANCE GOALS			5 - 10	1000	NBN 10%
MINIMUM PERFORMANCE GOALS			5 - 10	1000	NBN 10%
MANAGEMENT OF LIVING MARINE RESOURCES					
OCEAN COLOR					
MAXIMUM PERFORMANCE GOALS	0.4 - 1.0	0.01	0.5 - 1	1000	0.001
MINIMUM PERFORMANCE GOALS	0.4 - 1.0	0.05	5 - 10	100	0.01
GLITTER					
MAXIMUM PERFORMANCE GOALS					
MINIMUM PERFORMANCE GOALS					

7. A review of planned or existing terrestrial programs that may be relevant to the EOS mission was conducted as well as the supporting terrestrial measurements that would be needed to maximize the effectiveness of the EOS mission.
8. The complex problem of data management and some representative solutions are discussed. Data rates and total daily data load were calculated on the basis of mission characteristics (e. g. , sensor data outputs, coverage requirements, etc.) Data-link bandwidths and data storage requirements were determined on the basis of a review of state-of-the-art data handling technology, including projected capabilities for data compression and storage. Three representative ground data station locations (Goddard Space Flight Center; Fairbanks, Alaska; and Goldstone, California) were considered in conjunction with onboard data storage and orbital parameters which would indicate maximum data handling capability.

RESULTS

The final product of the study of global oceanographic requirements for EOS A/B is the recommendation of optimum and minimum sensor groupings and their associated orbital requirements for each of the national priorities. The optimum and minimum sensors and their characteristics are displayed in Figures 2, 3, and 4 as well as their relevance to particular mission categories. In each list, the sensors are shown in their order of importance. The degree of satisfaction within each priority is expressed below:

Monitoring and Predicting Physical Phenomena

- The optimum payload satisfies all information needs except for two categories under geophysical research: geodesy and dynamic topography, and geomagnetism.
- The minimum payload emphasizes environmental monitoring and prediction for transportation and hazards.

Management of Living Marine Resources

- Both the optimum and minimum payloads are capable of completely satisfying all the information needs, except for weather effects on fishing operations.

Detection, Monitoring, and Control of Global Ocean Pollution

- The optimum payload possesses a positive capability for all the information needs.

INFORMATION NEEDS TO BE SATISFIED	CONTRIBUTION BY OPTIMUM PAYLOAD	CONTRIBUTION BY MINIMUM PAYLOAD
I. ENVIRONMENTAL MONITORING AND PREDICTION FOR TRANSPORTATION AND HAZARDS		
A. SHORT-TERM FORCING FUNCTIONS - INSOLATION	X	X
B. SHORT-TERM COUPLING MECHANISMS	X	X
1) WIND STRESS ON SURFACE WATER	X	X
2) HEAT EXCHANGE, EVAPORATION/PRECIPITATION AND FREEZING/MELTING	X	X
C. SHORT-TERM RESPONSE PATTERNS		
1) SEA ICE: PACK AND SHELF ICE FORMATION AND BREAKUP	X	X
2) REGIONAL WEATHER CONDITIONS (FOG, SEA STATE, WIND, ETC.)	X	X
3) CURRENTS (RESPONSE OF SURFACE WATERS TO WIND AND CORIOLIS FORCES) - CURRENT BOUNDARIES (FRONTS, DIVERGENCES, CONVERGENCES, UPWELLING AREAS)	X	X
D. SHOAL WATER AREAS (REEFS BANKS, ETC.)	X	X
II. BASIC GEOPHYSICAL RESEARCH		
A. GEODESY AND DYNAMIC TOPOGRAPHY	M	-
B. GEOMORPHOLOGY		
1) SHALLOW WATER BOTTOM TOPOGRAPHY	X	X
2) VOLCANIC ISLANDS, CORAL REEFS, CONTINENTAL AND INSULAR COASTLINES	X	X
C. CONDITIONS AND PROCESSES IN POLAR REGIONS	X	X

X = POSITIVE CAPABILITY
M = MARGINAL CAPABILITY
- = NO CAPABILITY

PAYLOAD GROUPING

SENSOR DEFINITION	MEASUREMENTS PERFORMED			
<u>OPTIMUM GROUP</u>				
I. VISIBLE IMAGER	OCEAN COLOR			
II. IR-MULTISPECTRAL SCANNER	SEA SURFACE TEMPERATURE			
III. SYNTHETIC APERTURE RADAR	SURFACE ROUGHNESS AND SEA ICE			
IV. MICROWAVE RADIOMETER	SEA STATE			
V. GLITTER FRAMING CAMERA	GLITTER PATTERN			
VI. RADAR ALTIMETER	SEA SLOPE			
PAYLOAD CHARACTERISTICS				
<u>SENSORS</u>	<u>SIZE (M²)</u>	<u>WEIGHT (KG)</u>	<u>POWER (WATTS)</u>	<u>DATA RATE (MB/S)</u>
I.	0.15	18	18	0.3
II.	1.2	43	45	1.5
III.	0.3	73	140	8.0
IV.	0.4	91	175	NILL
V.	0.1	18	45	0.2
VI.	0.05	23	30	NILL
TOTAL	2.2	266	450	10.0
<u>MINIMUM GROUP</u>				
I. VISIBLE IMAGER	OCEAN COLOR			
II. IR-MULTISPECTRAL SCANNER	SEA SURFACE TEMP.			
III. SYNTHETIC APERTURE RADAR	SURFACE ROUGHNESS AND SEA ICE			
PAYLOAD CHARACTERISTICS				
<u>SENSOR</u>	<u>SIZE (M²)</u>	<u>WEIGHT (KG)</u>	<u>POWER(WATTS)</u>	<u>DATA RATE (MB/S)</u>
I.	0.15	18	18	0.3
II.	1.2	43	45	1.5
III.	0.3	73	140	8.0
TOTAL	1.65	134	200	9.8

Figure 2. Mission Relevancy Summary - Physical Processes Priority

INFORMATION NEEDS TO BE SATISFIED	CONTRIBUTION BY OPTIMUM PAYLOAD	CONTRIBUTION BY MINIMUM PAYLOAD	PAYLOAD GROUPING	
			SENSOR DEFINITION	MEASUREMENT PERFORMED
I. RESOURCE ABUNDANCE/DYNAMICS				
A. TOTAL GLOBAL RESOURCE ABUNDANCE/YIELD POTENTIAL	X		OPTIMUM GROUP	
B. YIELD POTENTIAL OF SPECIFIC OCEAN SECTORS, YEAR-TO-YEAR STOCK SIZE VARIATIONS, MAXIMUM SUSTAINABLE STOCK YIELDS.		X	I. VISIBLE IMAGER	OCEAN COLOR
1) REGIONAL PRIMARY PRODUCTIVITY (STANDING CROP DYNAMICS)		X	II. IR MULTISPECTRAL SCANNER	SEA SURFACE TEMPERATURE
2) ENVIRONMENTAL LETHAL OR SUB-LETHAL FACTORS	X	X	III. MICROWAVE RADIOMETER	SEA STATE
II. RESOURCE DISTRIBUTION			IV. GLITTER FRAMING CAMERA	GLITTER PATTERN
A. BROAD BIOGEOGRAPHY OF RESOURCES	X		V. SYNTHETIC APERTURE RADAR	SURFACE ROUGHNESS AND SEA ICE
B. ADULT STOCK MIGRATION ROUTES, LOCATION OF SPAWNING GROUNDS/NURSERY AREAS.		X	VI. RADAR ALTIMETER	SEA SLOPE
1) REGIONAL PRIMARY PRODUCTIVITY (STANDING CROP DYNAMICS)	X			
2) MAJOR CURRENT/WATER MASS DISPLACEMENTS	X	X		
3) CURRENT MEANBERS	X	X		
4) RIVER PLUMES, ETC.	X	X		
5) SEASONAL MIGRATIONS OF ISOTHERMS	X	X		
C. CONCENTRATION OF FISH NEAR DISCONTINUITIES		X		
1) OCEANIC FRONTS	X			
2) CURRENT EDDIES	X			
III. STOCK AVAILABILITY/ACCESSIBILITY				
A. WEATHER EFFECTS ON FISHING OPERATIONS			MINIMUM GROUP	
1) STORMS	X		I. VISIBLE IMAGER	OCEAN COLOR
2) ENVIRONMENTAL CONDITIONS	X	X	II. IR-MULTISPECTRAL SCANNER	SEA SURFACE TEMPERATURE
3) ICING CONDITIONS	M	M	III. MICROWAVE RADIOMETER	SEA STATE
4) LOCATION OF SHOALS	X	X		
B. VULNERABILITY OF FISH				
1) THERMOCLINE TOPOGRAPHY	X	X		
2) WATER CLARITY	X	X		

PAYLOAD CHARACTERISTICS	
SENSOR	DATA RATE (MBS)
I.	0.15
II.	1.2
III.	0.4
IV.	0.1
V.	0.3
VI.	0.05
TOTAL	2.2

PAYLOAD CHARACTERISTICS	
WEIGHT (KG)	POWER (WATTS)
18	18
43	45
91	175
18	45
73	140
23	30
266	450

PAYLOAD CHARACTERISTICS	
SIZE (M ³)	DATA RATE (MBS)
0.15	0.3
1.2	1.5
0.4	NILL
0.1	0.2
0.3	8.0
0.05	NILL
2.2	10.0

PAYLOAD CHARACTERISTICS	
WEIGHT (KG)	POWER (WATTS)
18	18
43	45
91	175
152	240

PAYLOAD CHARACTERISTICS	
SIZE (M ³)	DATA RATE (MBS)
0.15	0.3
1.2	1.5
0.4	NILL
1.75	1.8

X = POSITIVE CAPABILITY
M = MARGINAL CAPABILITY
- = NO CAPABILITY

Figure 3. Mission Relevancy Summary - Living Marine Resources Priority

INFORMATION NEEDS TO BE SATISFIED	CONTRIBUTION BY OPTIMUM PAYLOAD	CONTRIBUTION BY MINIMUM PAYLOAD
I. THERMAL POLLUTION		
A. POWER PLANT LOCATION AND POWER PLANT EFFECTS		
1) CURRENT LOCATION AND BOUNDARIES	X	X
2) UPWELLINGS	X	X
3) RIVER PLUMES	X	X
4) PHYTOPLANKTON STANDING CROP DYNAMICS	X	X
B. GLOBAL MEAN TEMPERATURE ALTERATION	X	X
II. HEAVY METALS AND RADIONUCLIDES		
A. PHYTOPLANKTON STANDING CROP DYNAMICS - SPECTRAL SIGNATURES	X	X
B. GENERAL SURFACE CONDITIONS		
1) GENERAL OCEAN SURFACE CIRCULATION	X	X
2) CONVERGENCES	X	X
3) RIVER PLUMES	X	X
III. CHLORINATED HYDROCARBONS		
A. PHYTOPLANKTON STANDING CROP DYNAMICS - SPECTRAL SIGNATURES	X	X
B. GENERAL SURFACE CONDITIONS		
1) GENERAL OCEAN SURFACE CIRCULATION	X	X
2) CONVERGENCES	X	X
3) RIVER PLUMES	X	X
4) OIL FILMS	X	M

X = POSITIVE CAPABILITY
M = MARGINAL CAPABILITY
- = NO CAPABILITY

PAYLOAD GROUPING

SENSOR DEFINITION		MEASUREMENTS PERFORMED	
OPTIMUM GROUP			
I.	VISIBLE IMAGER		OCEAN COLOR
II.	R-MULTISPECTRAL SCANNER		SEA SURFACE TEMPERATURE
III.	GLITTER PLANNING CAMERA		GLITTER PATTERN
IV.	MICROWAVE RADIOMETER		SEA STATE
V.	SYNTHETIC APERTURE RADAR		SURFACE ROUGHNESS
VI.	SARAR ALTIMETER		SEA SLOPE
PAYLOAD CHARACTERISTICS			
SENSOR	SIZE (M ²)	WEIGHT (KG)	POWER (WATTS)
I.	0.15	18	18
II.	1.2	43	45
III.	0.1	18	45
IV.	6.4	91	175
V.	0.3	73	148
VI.	0.85	22	39
TOTAL	3.2	266	488
PAYLOAD CHARACTERISTICS			
SENSOR	SIZE (M ²)	WEIGHT (KG)	POWER (WATTS)
I.	0.15	18	18
II.	1.2	43	45
III.	0.1	18	45
IV.	6.4	91	175
V.	0.3	73	148
VI.	0.85	22	39
TOTAL	3.2	266	488

Figure 4. Mission Relevancy Summary - Pollution Priority

- The minimum payload completely satisfies all the information needs except the detection and monitoring of oil films which is marginally accommodated.

The multiple priority payload grouping, in order of importance, is contained in Figure 5. The minimum sensor grouping nearly fulfills the measurements requirements as shown in Figures 2, 3 and 4. It should be noted that the sensors in the multi-priority grouping, except MOCS, are design concepts and require development. This could be accomplished before the EOS-A launch if appropriate action were taken to establish the parametric design specifications, including aircraft flights.

<u>SENSORS</u>		<u>MEASUREMENTS</u>		
I.	VISIBLE IMAGER	OCEAN COLOR		
II.	IR-MULTISPECTRAL SCANNER	SEA SURFACE TEMPERATURE		
III.	MICROWAVE RADIOMETER	SEA STATE		
IV.	SYNTHETIC APERTURE RADAR	SURFACE ROUGHNESS		

PAYLOAD CHARACTERISTICS				
<u>SENSOR</u>	<u>SIZE (M³)</u>	<u>WEIGHT (KG)</u>	<u>POWER (WATTS)</u>	<u>DATA RATE (MBS)</u>
I.	0.15	18	18	0.3
II.	1.2	43	45	1.5
III.	0.4	91	175	NILL
IV.	0.3	73	140	8.0
TOTAL	2.0	225	380	9.8

Figure 5. Payload Grouping - All Priorities

The recommended orbit for all priorities was a near-polar, sun-synchronous orbit with a high cyclic frequency to meet the distributive and dynamic nature of the phenomena. Depending upon the sensor field of view, the size of and the latitude of the geographical regions of interest, coverage can be acquired at intervals of from one to four days. A parametric summary of the global oceanographic orbit is shown in Table 6.

To satisfy the scene contrast and instrument sensitivity requirements associated with visible spectroscopy and obtain favorable coverage in the Northern Hemisphere, particularly the Continental United States, a 2:00 P. M. ascending orbit was selected.

Table 6. Selected Orbits

	Q (ORBITS/DAY)	S (NMI)	P (MINUTES)	H (NMI)	I (DEGREES)	Ω (DEGREES)	LOCAL TIME *
ALL PRIORITIES	13 3/4	1571	104.73	531	99.37	30	2 PM

*ASCENDING EQUATORIAL CROSSING

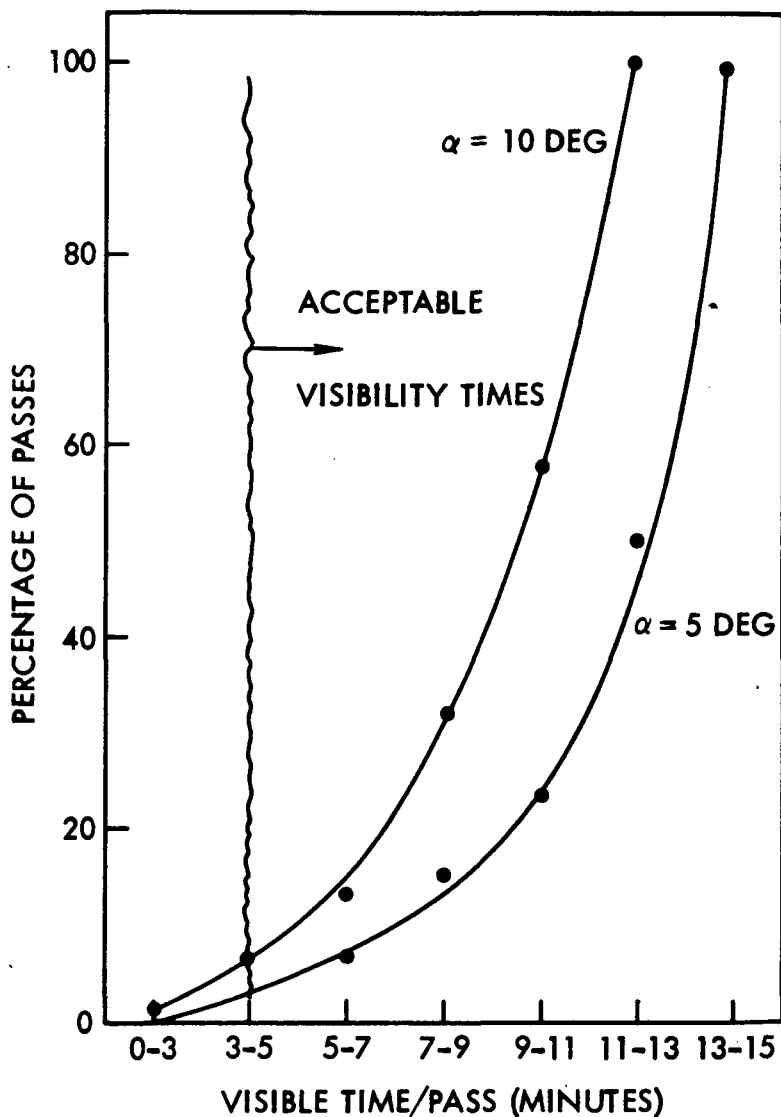
The ground data handling problem for the chosen orbit was evaluated by considering the three representative ground data stations previously mentioned. Rise and set times were then calculated for visibility circles with 5 and 10 degree elevation angles over one complete orbital coverage cycle of 4 days. As shown in Figure 6 for an elevation angle of 10 degrees less than 7 percent of the passes have unacceptable visibility times and 68 percent have visibility times greater than 7 minutes. Lowering the elevation angle to 5 degrees brings the number of unacceptable passes below 4 percent and over 85 percent of the passes have visibility times greater than 7 minutes.

To estimate the amount of data that will be acquired, the total payload was taken to consist of six separate sensor assemblies. Each assembly was analyzed in terms of the operating data rate, the average coverage factor and the average total data per orbit. The results are summarized in Table 7.

Table 7. Data Acquisition

Sensor	Operating Data Rate (MB/S)		Average Coverage Factor		Average Total Data Per Orbit (MB)
	Instantaneous	Average	Fraction of orbit	Operating time/orbit(sec)	
SLR	8 MB/S	8 MB/S	0.25	1550	1.24×10^4 MB
Multispectral Scanner	1.5	1.0	0.3	1850	} 2.8×10^3
	0.75	0.5	0.3	1850	
Visible Spectrometer	0.3	0.2	0.2	1240	3.7×10^2
Glitter Sensor	0.2	0.04	0.2	1240	50
Microwave Radiometer	0.0002	0.0002	0.6	3700	0.74
Radar Altimeter	0.0001	0.0001	0.6	3700	0.37
Total					1.56×10^4 MB

One final note should be added to place spacecraft oceanography in its proper perspective. While remote sensing of the ocean's surface shows great potential in meeting the needs of the oceanographic community, it is still in the research and development phase and there is a lack of sensor hardware experience and software utility.



α = ELEVATION ANGLE

Figure 6. Number of Passes with Available Visibility Times

N72-20340

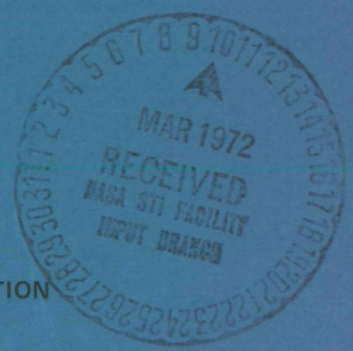
Contract No. NASW-2163

No. 17683-6001-R0-00

**CASE FILE
COPY**

***ADVANCED STUDY OF GLOBAL OCEANOGRAPHIC
REQUIREMENTS FOR EOS A/B***

***FINAL REPORT
TECHNICAL VOLUME***



Prepared for

THE NATIONAL AERONAUTICS AND SPACE ADMINISTRATION
HEADQUARTERS
WASHINGTON, D.C.

Prepared by

TRW SYSTEMS GROUP/EARTHSAT

JANUARY 1972

REPRO VELLUM

TRW
SYSTEMS GROUP

***ADVANCED STUDY OF GLOBAL OCEANOGRAPHIC
REQUIREMENTS FOR EOS A/B***

***FINAL REPORT
TECHNICAL VOLUME***

Prepared for

THE NATIONAL AERONAUTICS AND SPACE ADMINISTRATION
HEADQUARTERS
WASHINGTON, D.C.

Prepared by

TRW SYSTEMS GROUP/EARTHSAT

JANUARY 1972

TRW
SYSTEMS GROUP

ABSTRACT

This report considers the characteristics of the global ocean in terms of the nation's social, scientific and economic priorities and in terms of the measurements that can best be made from a spacecraft. It discusses the kinds of information that are needed to advance the basic ocean sciences as well as to improve marine transportation and fisheries operations and provide information for pollution control. It relates these information needs to logically feasible sensor concepts and presents an optimum sensor complement together with the related orbital considerations.

The report then relates the data-gathering capabilities of an oceanographic spacecraft to those of terrestrial oceanographic programs, using airborne, surface, and submarine platforms. Finally, it examines the data management problem and concludes that it is solvable with current technology.

CONTENTS

	<u>Page</u>
1. INTRODUCTION	1-1
2. PRIORITY ANALYSIS	2-1
3. MISSION DEFINITION	3-1
3.1 Measurement Requirements	3-1
3.1.1 Monitoring and Prediction of Physical Phenomena	3-1
3.1.2 Management of Living Marine Resources	3-4
3.1.3 Detection, Monitoring, and Control of Global Ocean Pollution	3-6
3.2 Sensors	3-8
3.2.1 Visible Imaging Spectrometer	3-8
3.2.2 Infrared Multispectral Scanner	3-10
3.2.3 Microwave Radiometer	3-11
3.2.4 Synthetic Aperture Radar	3-12
3.2.5 Glitter Pattern Sensor	3-13
3.2.6 Altimeter	3-15
3.3 Spacecraft Requirements	3-17
3.3.1 EOS Payload Limitations	3-17
3.3.2 Orbital Selection	3-18
3.3.3 Attitude Control	3-19
3.4 Data Requirements	3-19
3.5 Payload Groupings	3-20
3.6 Conclusions and Recommendations	3-21
4. MONITORING AND PREDICTION OF PHYSICAL PHENOMENA	4-1
4.1 Solar-Polar Interactions	4-3
4.1.1 Insolation	4-3
4.1.2 Polar Ice Caps	4-5
4.2 The Response Patterns	4-6

CONTENTS

(Continued)

	<u>Page</u>
5. MANAGEMENT OF LIVING MARINE RESOURCES	5-1
5.1 Dynamics of Resource Abundance	5-3
5.1.1 Global Primary Productivity	5-4
5.1.2 Variation in Abundance of Specific Stocks	5-5
5.2 Distribution of Living Marine Resources	5-9
5.3 Accessibility of Fishing Grounds and Stock Catchability	5-15
6. MONITORING OCEAN POLLUTION	6-1
6.1 "Hard" Chemicals	6-2
6.2 Thermal Effects	6-7
7. SENSORS	7-1
7.1 Visible Imaging Spectrometry	7-2
7.1.1 Sensor Description	7-2
7.1.2 Visible Imaging Spectrometry - Rationale for Design Parameters	7-8
7.2 Glitter Pattern Sensor	7-23
7.2.1 Objective	7-23
7.2.2 Theory	7-23
7.2.3 Glitter Sensor Description	7-25
7.2.4 Mode of Operation	7-26
7.2.5 Coverage	7-31
7.2.6 Expected Results	7-38
7.2.7 Data Rates	7-41
7.3 Infrared Imaging/Radiometer	7-42
7.4 Laser and Radar Instrumentation for Precision Ocean Altimeter	7-50
7.4.1 Instrumentation Characteristics for Altimetry	7-51
7.4.2 Geoid Effects in Altimetry	7-55
7.4.3 Perturbations of the Satellite	7-60
7.4.4 Interaction of Oceanographic and Geopotential Effects in Altimetry	7-63

CONTENTS

(Continued)

	<u>Page</u>
7.5 Microwave Radiometry, Imaging	7-66
7.5.1 Microwave Radiometer	7-67
7.6 Synthetic Aperture Radar	7-73
7.6.1 General Considerations	7-73
7.6.2 Transmitter Average Power	7-74
7.6.3 Parameter Values	7-75
7.7 Instrument Specification Sheets	7-76
8. ORBITAL ANALYSIS	8-1
8.1 Statement of the Problem and Summary of the Requirements	8-1
8.2 Theory	8-6
8.2.1 Parametric Development	8-6
8.2.2 Trace Pattern	8-9
8.3 Orbit Selection Criterion	8-13
8.3.1 Orbital Considerations	8-13
8.3.2 Coverage Schemes	8-36
8.4 Range of Acceptable Orbits	8-48
9. SUPPORTING MEASUREMENTS AND EXISTING DATA PROGRAMS	9-1
9.1 Background	9-1
9.2 Relevant Data Programs	9-7
9.2.1 Routine Data Programs	9-7
9.2.2 Special Operational Data Programs	9-27
9.2.3 Special Experimental Data Programs	9-38
9.2.4 Aircraft Programs	9-44
9.3 Dedicated Ground Truth Program for the EOS A/B Mission	9-50
9.3.1 Gulf of Mexico Sensor Evaluation Area	9-50
9.3.2 Baja California Sensor Evaluation Area	9-51
9.4 Summary	9-54

CONTENTS

(Continued)

	<u>Page</u>
10. DATA MANAGEMENT	10-1
10.1 Data Acquisition	10-2
10.1.1 Synthetic Aperture Radar	10-2
10.1.2 Multispectral Mechanical Scanner	10-4
10.1.3 Visible Imaging Spectrometer	10-4
10.1.4 Glitter Pattern Sensor	10-5
10.1.5 Microwave Radiometer	10-5
10.1.6 Radar Altimeter	10-5
10.1.7 Summary	10-5
10.2 Data Storage and Transmission	10-6
10.2.1 Space-to-Ground Considerations	10-6
10.2.2 Ground Data Links	10-8
10.3 Data Handling at NDPF	10-9
10.3.1 Processing	10-9
10.3.2 Data Storage	10-14
10.3.3 Distribution from NDPF	10-16

1. INTRODUCTION

For the purposes of this study, the global ocean can be defined as the ocean domain of mesoscale* or larger phenomena. It includes all coastal zones as well as the high seas and extends around the world in an irregular but unbroken envelope. It is the primary factor in maintaining a climate that is hospitable to life as we know it. It is the ultimate sink for most terrestrially derived substances, both natural and man-made. It provides a habitat for plants and animals far greater in area and volume than the life zone of the land, so that marine organisms can be thought of as the more representative life forms of the earth. Moreover, billions of years in the past, the global ocean is believed to have been the birthplace of life.

Yet we are only beginning to understand the oceans in definitive terms. Such detailed knowledge as we have is limited to a few small areas and has relatively little historical depth.

Over the past decade, however, the United States has shown an increasing interest in oceanography, as evidenced by major national and international activities. These efforts have, without exception, recognized the need to increase our understanding of the actions and interactions of the global ocean as a component of the biosphere.

With improved understanding, a start can be made toward controlling pollution, improving our management of marine food resources, and increasing the effectiveness with which marine hazards can be located, monitored, and countered. Without a vast increase in detailed factual knowledge of ocean dynamics, mankind has no basis for the national and decisive action that is necessary for the solution of these problems.

Given, therefore, that much basic information is lacking and urgently needed, what are the specific information needs and in what order of priority should they be treated? This was the first question to which the study team addressed itself and our conclusions are summarized in Section 2 of this report.

*Phenomena requiring spatial resolution on the order of kilometers rather than, as was the case for the coastal zone studies previously sponsored by NASA, on the order of meters.

Section 3 discusses the main categories of needed information in terms of the synoptic measurements that can, and indeed must, be made in order to provide the information and summarizes the instrumentation capabilities available for making these measurements.

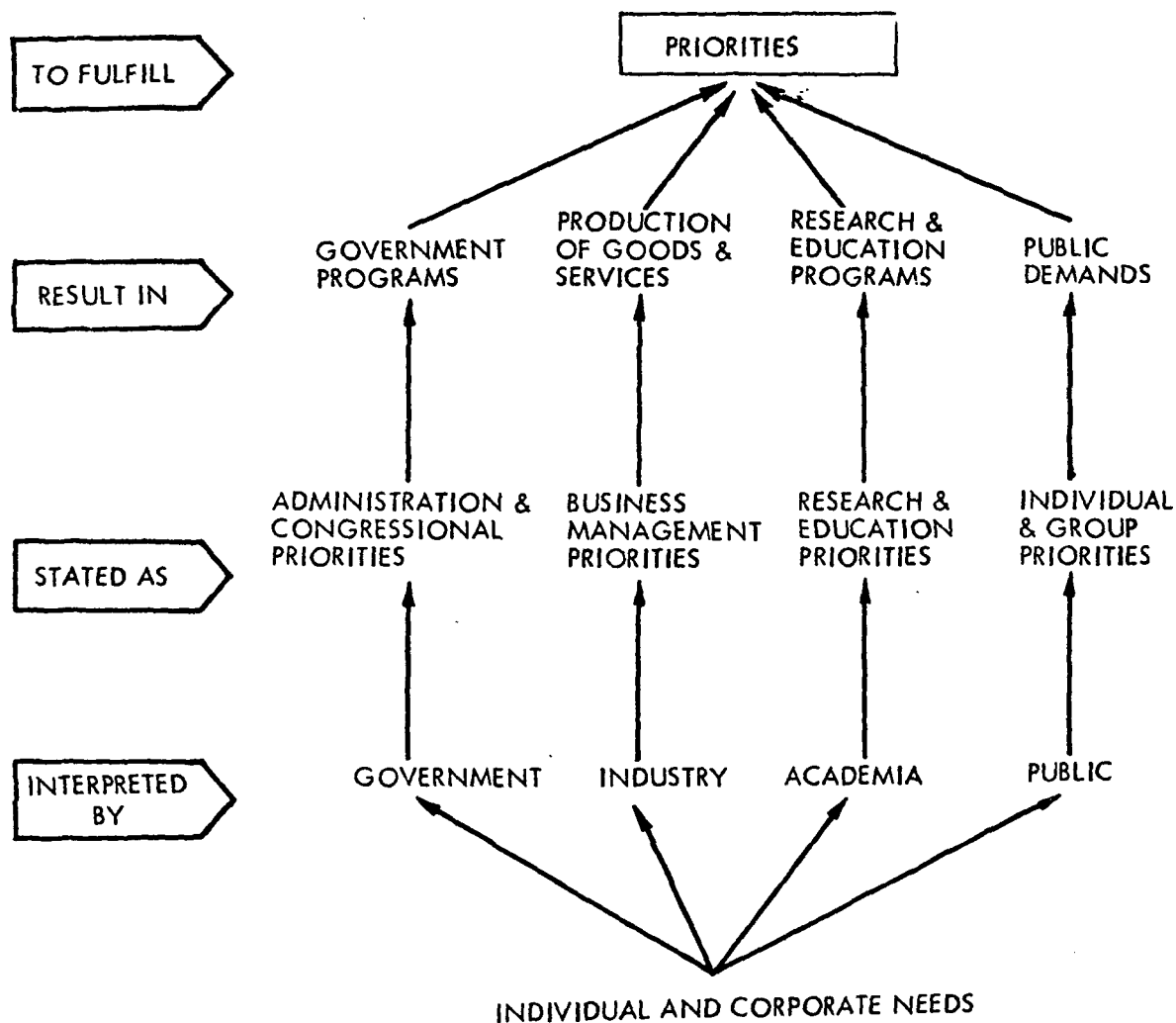
Sections 4, 5 and 6 present more detailed discussions of the three main categories of information needed to meet the priorities discussed in Section 2.

Section 7 analyzes a selection of spacecraft sensors in detail while Section 8 considers an optimum orbit for the preferred sensors and the information needs they are expected to satisfy.

Section 9 reviews existing programs that may be relevant to the EOS mission and the supporting terrestrial measurements that would be needed to make the EOS mission as effective as possible. Section 10 discusses the complex problems of data management and presents some solutions.

2. PRIORITY ANALYSIS

Government, industry, academia, and the public all participate in determining priorities (see Figure 2-1) but the information on which they can base decisions relevant to the global ocean is limited. Consequently, there are deep and widespread disagreements on the subject of what needs to be done first.



To government economists, for example and other officials who are responsible for trying to keep unemployment down and international trade in balance, the highest priorities for a global oceanographic satellite might be improvement of weather forecasting and charting services for the benefit of transportation and fisheries. This is because, as shown in Table 2-1, high seas transportation (including naval shipping) and fishing

Table 2-1. Principal Global Ocean Industrial Users
(date of information given in brackets)

Industry	Income (million dollars)		Number Persons Employed	Comments
Transportation	4,000	(1969)	87,000 (1967)	High seas transportation only
Offshore Petroleum	2,350	(1968)	30,000 (1967)	Persons employed computed from dollar/person ratio for entire industry
Fishing	602	(1970)	128,000 (1965)	Persons employed do not include 87,000 shore workers

employ a great many people and produce a large amount of income. Both the people who work in these industries and those who derive less direct economic benefits from them would presumably also support this priority.

To fisheries people and the general public, data that could provide a basis for effective control of industrial pollution would probably also rank high on the list of priorities.

To the oil, chemical, and agricultural industries, however, (though they may be willing to support pollution control measures in the long run), there is a near-term threat in such measures. Their highest priority problem tends to be information in support of the contention that pollution is not as imminent a danger as environmentalists claim it to be.

To the scientists, who are scattered throughout government, industry and academia, the paramount priority is for basic and objective information that would permit logical planning to meet all the other priorities.

The need to improve charting services, for example, is obvious (if not particularly urgent) because presently available charts are not only admittedly inaccurate and incomplete for vast areas of the globe, they are often also (except in areas of the heaviest traffic) embarrassingly out of date.

The need to improve weather forecasting, particularly the longer-term (5-14 day) forecasts, is equally obvious since ships still founder in storms and large efforts have to be expended in rescue operations.

The danger of seafood pollution by "hard" industrial chemicals has already been proven by the condemnation of fish catches contaminated with mercury.

There is widespread awareness of the potential danger of pollution by waste heat, industrial and agricultural smokes, and CO₂ and a very sharp awareness of the dangers of oil pollution. But not enough information is available to determine with any certainty whether or when these dangers will become so acute that decisive action must be taken to actually curtail industrial growth. There is only enough information to encourage loud arguments between environmentalists and the oil industry or environmentalists and the Atomic Energy Commission. There is not enough information to settle any of the arguments to anybody's satisfaction.

The need for background information appears, therefore, to be the most urgent need of all. And, since highly trained specialists are required to process and interpret such background information, the "community" with the most urgent need for data from a global oceanographic satellite would appear to be the technical people who are scattered throughout academia, industry, and the governments of the world.

The specific kinds of global oceanographic information that are needed by this community and that can be directly or indirectly provided by a satellite system may be categorized as follows:

- Monitoring and Prediction of Physical Phenomena. Understanding and predicting those phenomena which determine the physical environment of the global ocean ecosystem.
- Management of Living Marine Resources. Optimum exploitation and conservation of the living components of the global ocean ecosystem based on the understanding and prediction of the phenomena associated with these components.
- Detection, Monitoring, and Control of Global Ocean Pollution. Monitoring and controlling those man-made phenomena which significantly perturb the natural system.

These categories are closely interrelated. The first represents the ultimate goal of much of the directed research of marine scientists. It will contribute basic information needed for the management of the marine ecosystem required by the other two priorities, and for the improvement of weather forecasting. More directly it will provide the data base for optimum ship scheduling, including departures from scheduled routing and emergency planning. It also will include information applicable to off-shore mapping and utilization of drilling platforms.

The second priority is primarily associated with the assessment, harvesting, and management of commercial fisheries, but since every component of life in the ocean affects the status of every other, it must be concerned with the entire system, including the effects of physical phenomena and of pollution trends.

The addition of pollutants to the marine environment poses a serious threat to the biological resources of the ocean. The monitoring and control of global ocean pollution depend strongly for their effectiveness on an understanding of the physical environment. A satisfactory solution to this priority is vital to the preservation of the marine ecosystem.

The detailed analysis leading to establishment of the global ocean priorities is presented in Appendix I.

3. MISSION DEFINITION

On the basis of the priorities and information needs outlined in Section 2 and Sections 4, 5, and 6, the study team has defined in general terms the measurement requirements for the EOS mission and the sensor capabilities that would be needed to fill those requirements. This section also summarizes spacecraft and data requirements and presents summary conclusions and recommendations.

3.1 MEASUREMENT REQUIREMENTS

Measurements made from satellites represent the only feasible way to satisfy many of the information needs of the global ocean priorities. However, it is evident that they will not provide all the required information. Thus the role of a global ocean monitoring spacecraft system is that of a component of a total system designed to provide the information necessary for the implementation of the management and control aspects of the national priorities. This system should include aircraft and surface platforms as well as the spacecraft and, moreover, should draw upon data from other spacecraft, particularly those concerned with making meteorological measurements. The measurement requirements are discussed in terms of missions directed toward each of the priorities but, because of the interrelationships among these priorities and the frequent commonality of the accessible space observables, many of the requirements are similar for more than one priority.

3.1.1 Monitoring and Prediction of Physical Phenomena

The information needs for the monitoring and prediction of broad-scale ocean physical phenomena which must be met by a comprehensive program are discussed in detail in Section 4.1. They comprise three groups. The first of these is associated with environmental monitoring and prediction for transportation and hazards, with prediction periods of about two to five days. This group involves primarily measurements pertinent to short-term forcing functions, coupling mechanisms, and response patterns, but it also includes concern with shoal water areas which need to be monitored only once or twice a year.

Long-term meteorological prediction needs for periods of five days to two weeks entail a second group of measurement requirements. These

prediction periods are desirable for adequate transportation planning and hazard warning times, since the average open ocean transit time for ships is greater than the two to five day short-term period. The measurement requirements are primarily meteorological, and are most effectively met by satellites devoted to meteorological missions. A separate study concerned with this subject, Requirements for Earth Observations Satellite - Meteorology, is now in process. Since the oceans and the atmosphere cannot be separated when considering the dynamic interaction processes which affect them both, oceanographic measurements are necessary for long-term as well as short-term weather forecasting. It should be noted that meteorological mission planning recognizes the importance of such measurements as sea surface temperature, sea state, and sea ice conditions.

The third group of measurement requirements which are best addressed by a separate satellite such as GEOS, is concerned with basic geophysical research. It includes the areas of geodesy and dynamic topography, geomorphology, conditions and processes in polar regions, and geomagnetism.

The foregoing information needs lead to the measurement requirements on space observables listed in Table 3-1. A mission payload sensor group can be identified to fill most of these requirements. However, the temperature and humidity profile measurements will be obtained by meteorological satellites and need not be included. Magnetic anomaly measurements are incompatible with the other measurements because of their need for a clean magnetic environment; moreover, since they are required only once a year, they are inappropriate for a payload that is primarily concerned with frequently repetitive coverage. Therefore, these measurements should be made from another satellite. Bottom topography and configuration change measurements are similarly infrequently required, but they can be obtained, with somewhat less than the optimum resolution, by a sensor needed for other purposes. Directional wave spectrum measurements require a resolution level far in excess of that consistent with a global mission payload. Finally, the salinity measurements are beyond the foreseeable state of the art within the weight, size, and power constraints of the EOS spacecraft. The mission payload appropriate for the rest of the measurement requirements is discussed in the remainder of this section.

Table 3-1. Measurement Requirements - Monitoring and Prediction of Physical Phenomena

Space Observable	Frequency of Observation (Days)	Resolution or Grid Spacing (Km)	Accuracy / Sensitivity	Possible Measurement Technique
Atmospheric Measurements:				
Transparency	1	3-5 Res	1%	Visible Radiometry
Temperature profile	1	50 GS	1° C Abs	IR or Microwave sounding
Humidity profile	1	50 GS	±5% RH	IR sounding
Heat Flux	1-3	150 GS	± 10%	IR Radiometry
Cloud patterns	1-3	3-5 Res	NEΔρ=0.01	Visible imaging IR imaging
Sea State and Surface Winds:				
Wind vector, fetch and duration	1	3-5 Res	± 10%	Visible imaging (cloud patterns)
Directional wave spectrum	1	0.015-0.03 Res	± 10%	Visible imaging
Sea state	1	50 GS	Nearest Beaufort No.	Glitter pattern sensing Passive microwave radiometry
Sea Surface: Temperature	1-3	5-10 Res	0.2-0.5° C Abs	IR Radiometry Passive microwave radiometry
Salinity	1-3	5-10 Res	0.5 PPT	Passive microwave radiometry
Slopes	1	5 GS	10 ⁻⁴ to 10 ⁻⁷	Radar or laser altimetry
Sea ice: Boundaries	1-3	0.5-1 Res	1 Km	Visible imaging Synthetic aperture radar imaging IR imaging
Thickness	2-14	1 Res	NEΔρ = 0.01	Multispectral visible imaging
Turbidity (color)	3-5	5-10 Res	NEΔρ = 0.01	Multispectral visible imaging
Bottom topography	60-365	0.5 Res	NEΔρ = 0.01	Multispectral visible imaging
Configuration changes	190-365	0.5 Res	ΔS = 0.5 Km	Visible imaging
Magnetic anomalies	365	1 Res	1-2 Gamma	Magnetic flux measurement

3.1.2 Management of Living Marine Resources

The information needs and measurement requirements for the living marine resources priority are discussed in detail in Section 4.2. The first category of information needs is concerned with resource abundance and dynamics. Estimates of the magnitude of the ocean's food potential vary widely; an urgent need exists for accurate data on population sizes both for species of established importance, and for those currently unexploited and subject to limited exploitation. The most important need is information on population dynamics -- the response to environmental perturbations, including the effects of natural predators and of fishing operations -- to permit accurate estimation of sustainable yields. The abundance data, however, are essential to provide a baseline against which population change data can be compared. Moreover, because of the interdependency of all forms of marine life, including those not directly useful to man, the measurement requirements are very broad-based.

The distributions of living marine resources, and the variations in these distributions, are required for the practical exploitation of these resources. This information is needed to determine the extent to which apparent fluctuations in population densities are real or are the results of changes in distribution of otherwise stable populations. In addition, the information is needed directly to facilitate the planning of effective harvesting operations.

Data on the accessibility of fishing grounds and the catchability of the stock complete the information needs for the living marine resources priority. These include data on existing and forecast weather conditions and other environmental factors (such as sea state and currents) which affect the ability of fishermen to get to the fishing grounds and to carry out their harvesting operations. A number of environmental factors also influence the vulnerability of fish to the strategies and gear employed. For example, a shallow thermocline increases the efficiency of purse seines for catching tuna, and water turbidity is important in gillnet fisheries, since the ability of the fish to see the net enhances their chance for escape.

The measurement requirements implied by the information needs just summarized are listed in Table 3-2. These requirements cover

Table 3-2. Measurement Requirements - Management of Living Marine Resources

Space Observable	Frequency of Observation (Days)	Resolution or Grid Spacing (Km)	Accuracy/Sensitivity	Possible Measurement Technique
Ocean Color (phytoplankton pigment)	3-5	1-2 Res estuaries and currents 5-10 other	NEΔρ = 0.001	Multispectral visible imaging
Ocean color (turbidity, anomalous water chemistry)	1/2-7	0.5-1 Res estuaries and coasts 5-10 other	NEΔρ = 0.01	Multispectral visible imaging
Cloud patterns	1/2-2 (storms, etc.) 7-14 (other)	1-2 Res	NEΔρ = 0.01 NEΔT = 0.5°C	Visible imaging IR imaging
Sea Surface:				
Temperature	1/2-2	0.5-1 Res estuaries 5-10 other	0.2-0.5° Abs	IR radiometry
Salinity	3-7	0.5-1 Res	0.5 PPT	Passive microwave radiometry
Slopes	3-7	10-20 GS	10 ⁻⁵ to 10 ⁻⁸	Passive microwave radiometry Radar or laser altimetry
Sea state and surface winds:				
Sea state	1/2-1	10-100 Res	NBN	Glitter Pattern sensing Passive microwave radiometry
Directional wave spectrum	2-8		± 10%	Visible imaging
Swell wavelength/direction	2-8	100 GS	± 10%	Passive microwave radiometry
Slicks	1/2-2	0.5-1 Res	NBN	Glitter pattern sensing Passive microwave radiometry
Atmospheric temperature profile	1.2-1	100 GS	1°C Abs	IR sounding Microwave sounding.
Shallow water:				
Bottom topography	180-365	0.05-1 Res	NEΔρ = 0.01	Visible imaging
Swell wavelength foreshortening	180-365	0.05 Res	±10%	Visible imaging

measurements possible by observations from space; the information needed to accomplish the marine resources priority must be inferred from surface and aircraft observations as well as those from a spacecraft. A set of sensors capable of substantial satisfaction of these requirements can be configured within the constraints of the EOS Spacecraft, with exceptions similar to those for the physical phenomena priority. The atmospheric temperature profiles should be obtained from meteorological satellites which will also contribute supplementary data on other meteorological parameters and probably sea state and surface temperatures as well. Sea surface salinity, directional wave spectra, and swell wavelength forecasting measurements are not feasible for the reasons given in Section 7.

3.1.3 Detection, Monitoring and Control of Global Ocean Pollution

The most significant global ocean pollution problems are concerned with thermal pollution and modifications to radiative balance, chlorinated hydrocarbons, and heavy metals and radionuclides. These problems are considered in Section 6. Global ocean pollution can disturb the natural order of the marine ecosystem in a number of ways. Toxic materials can kill marine organisms directly or produce unacceptable levels of contamination in marine products desired for human consumption. These and other pollutants can also act more subtly by reducing the suitability of the environment, or by affecting biological processes such as reproduction or photosynthesis.

The need for knowledge of pollution effects and distribution mechanisms is urgent. Most direct measurements of actual pollution concentrations must be made from aircraft, surface or subsurface observations. However, satellite monitoring can contribute measurements of great value for the understanding of distribution patterns and for the indication of significant areas for detailed surface observations. In particular, ocean color measurements from a satellite promise a unique contribution to monitoring of phytoplankton distributions and vigor, and to the location of current boundaries, convergences and upwelling areas. Thus the measurement requirements, listed in Table 3-3, stress ocean color measurements as well as measurements of other surface parameters from which possible pollution effects can be inferred or located. All the requirements

Table 3-3. Measurement Requirements - Detection, Monitoring and Control of Global Ocean Pollution

Space Observable	Frequency of Observation (Days)	Resolution or Grid Spacing (Km)	Accuracy / Sensitivity	Possible Measurement Technique
Ocean Color (phytoplankton)	7	1-2 to 10 Res	$NE\Delta\rho = 0.001$	Multispectral visible imaging
Ocean Color (current boundaries, convergences, etc.)	3-14	1-2 to 10 Res	$NE\Delta\rho = 0.01$	Multispectral visible imaging
Sea Surface:				
Temperature	3-7	1-2 to 10 Res 150 GS	$0.2 - 0.5^{\circ}C$	Infrared Radiometry
Salinity	3-7	1-2 to 10 Res	0.5 PPT	Passive microwave radiometry
Slopes	14	10-20 GS	10^{-5} to 10^{-8}	Radar or laser altimetry
Ice Cap Size	30	5-10 Res	Bdrries to 5 km	Visible imaging Synthetic aperture radar imaging
Reduced sea state (oil films)	7	2 Res	NBN with boundaries to 2 km	Visible imaging Glitter pattern sensing Passive microwave radiometry

can be met quite well except, as with the other priorities, the sea surface salinity measurements.

3.2 SENSORS

In Section 7 the measurement requirements are considered in terms of electromagnetic spectral regions, spatial and spectral resolutions, sensitivities, and observation frequencies in order to arrive at sensor concepts. Along with spacecraft constraints, orbital parameters, and present or predictable state-of-the-art capabilities, these concepts have been used to define particular sensor configurations and specifications. Six sensors have been identified in this way to meet the feasible measurement requirements given in Section 3.1. Descriptions of these sensors are given in the following subsections.

3.2.1 Visible Imaging Spectrometer

The sensor selected for making ocean color measurements is an electronically scanned imaging spectrophotometer. A slit in the image plane of an objective lens defines the instantaneous sensor field of view. A collimating lens directs light passing through the slit to a transmission diffraction grating where it is dispersed into a spectrum. A re-imaging lens focuses the light onto the face of an image dissector tube. The resulting two-dimensional image gives the spectral signature, in one direction, of each pixel in a cross-track strip, positioned along the other direction. Scanning in a conventional raster thus produces spectral data for the light from each pixel along a cross-track line, and successive raster scans provide spectral data for a complete strip map. The instrument has no moving parts. It is capable of high spectral resolution and sensitivity and excellent radiometric accuracy.

A model of this device, the Multichannel Ocean Color Sensor (MOCS) is currently under development in the NASA Langley Advanced Applications Flight Experiments (AAFE) program which very closely satisfies the EOS global ocean requirements. Its performance characteristics are given in Table 3-4. In order to achieve the coverage necessary for global mapping applications, three MOCS sensors can be used with adjacent fields of view, providing a swath width of 925 km from a 925 km altitude. The use of three discrete instruments reduces development requirements,

Table 3-4. Visible Imaging Spectrometer Specification

<u>General Description</u>	
Function	To measure the spectra of reflected sunlight in an imaging mode
Configuration, Major Elements	Imaging spectrometer: objective lens, collimating lens, diffraction grating, re-imaging lens, image dissector
Developmental Status	Presently under development by TRW Systems for AAFE: MOCS (Multichannel Ocean Color Sensor)
<u>Performance Characteristics</u>	
Wavelength Range	.4-.7 μ
Spectral Resolution	.015 μ
Field of View	51 $^{\circ}$ (3 MOCS sensors, 17.1 $^{\circ}$ each) (925 km swath @ 925 km alt.)
Spatial Resolution	1.8 km
Sensitivity	NE $\Delta\rho$ = .001 or better
Absolute Accuracy	\pm .003
<u>Physical Characteristics</u>	
Size	.035 cubic meters (total of 3)
Weight	18 kg (6 kg, each of 3 sensors)
Power	18 watts total
<u>Platform/Data Considerations</u>	
Pointing Accuracy	.07 $^{\circ}$ (1 pixel)
Line of Sight Rate	.05 $^{\circ}$ /sec
Data Output	0.3 MBS (all 3 sensors)
<u>Comments</u>	No moving parts 3 MOCS sensors sweep adjacent swaths providing 925 km swath (3 day coverage)

provides for substantial coverage in the event of failure of one instrument, and isolates possible saturation or flare effects from sun glitter to no more than one third of the total field of view.

The choice of 20 spectral channels, as indicated in Table 3-4, is somewhat arbitrary. Design analyses show that an adequate S/N can be achieved with this spectral resolution, so that reduction of the number of channels is not necessary to achieve the desired performance. The currently available evidence is not conclusive with respect to the spectral resolution required, but it does seem to indicate the desirability of 20 to 30 channels in the visible range, particularly if the information so obtained can be fully exploited. In this respect, recent studies by P. G. White, Manager of the MOCS AAFE Project, indicated that a novel technique making use of the second differentials of the reflection curves facilitates the interpretation of ocean color data while making full use of high spectral resolution.¹ This technique, since it makes use of the relationships among reflectances in wavelengths very close to one another, should also greatly reduce the requirements for calibration of the atmosphere.

3.2.2 Infrared Multispectral Scanner

A single channel (8-13 μ band) and a multichannel infrared spectrometer are discussed in Section 7. Both employ a mechanical conical scan technique. This type of scan produces a (nearly) circular motion of the instantaneous field of view and is produced by the rotation of a mirror at a suitable angle to the axis of rotation. This scan technique has several distinct advantages over the conventional linear scan:

- Resolution element size and velocity on the ground are nearly constant.
- The obliquity angle and atmospheric path length are constant throughout the scan.
- Scan efficiency is higher than with a rotating mirror producing a linear trace, while mechanical complexity and power requirements are reduced from those for an oscillating mirror.

The single channel radiometer is obviously much simpler than the multichannel device, but the greater capability and flexibility of the multichannel instrument make it the recommended approach. Anding, Kauth, and Turner² have recently described a technique for removing atmospheric

effects from infrared surface temperature measurements which is implemented in this device. Simultaneous radiometric measurements are made in three narrow spectral intervals centered at 4.9, 9.1 and 11.0 μ . With the data from these three intervals, the effects of a non-cloudy atmosphere on the observed radiance can be nearly completely compensated for and estimated of sea temperature to an accuracy of 0.15 $^{\circ}$ K can be obtained. The three channels also provide some information on cloud cover when some clouds are within the field of view. It is, however, recommended that a broad-band visible channel be included to aid in cloud cover determination and to provide panchromatic imagery precisely registered with the infrared data. In addition a near infrared and/or an ultraviolet band can aid in recognizing oil slicks and other special targets. Performance characteristics of the Multispectral Infrared Mechanical Scanner are given in Table 3-5. The Multichannel Infrared Radiometer not only given more accurate data, it also eliminates the need for obtaining auxilliary atmospheric measurements and introducing them into the data processing procedures.

Table 3-5. Performance Characteristics of Multispectral Infrared Mechanical Scanner

Channels:	4.75 to 5.15 μ , 8.85 to 9.35 μ , 10.5 to 11.5 μ , 0.4 to 0.7 μ , 0.3 to 0.4 μ and 0.7 to 1.0 μ
Spatial Resolution	1 km
Swath Width:	Adjustable, 100 km to horizon-to-horizon (sensitivity given for 360 km swath)
Sensitivity:	NE Δ T = 0.16, 0.07 and 0.05 $^{\circ}$ K respectively for thermal IR channels NE Δ ρ = 0.01 for the other channels
Absolute Accuracy:	0.2 $^{\circ}$ C

3.2.3 Microwave Radiometer

The radiance observed with a single passive microwave radiometer measurement depends on water temperature, surface roughness, atmospheric conditions, and, to a slight extent, water salinity. The conditions of observation which affect the dependence are frequency, polarization, and the angle between the surface and the line of sight. Measurement

conditions can be chosen to maximize the sensitivity to any particular parameter while having low sensitivities to the others, but no one measurement can be made to be completely independent of all parameters but one. Thus a combination of carefully selected measurements is required, even if only one environmental quantity, e. g., sea surface temperature, is desired.

No one combination of microwave radiometer design and mode of operation is superior in all respects to any other. The recommendation of a two frequency, dual polarization, multiple angle radiometer is based on a primary interest in sea surface temperature and roughness. Size and weight are reduced over a radiometer sensitive to more frequencies; less information is obtained on cloud and rain droplet sizes, but this information is not as important for global ocean applications. The radiometer uses frequencies near 9 and 19 GHz, and angles of about 40° to 60° with the surface. Fixed planar array antennas are electrically scanned to provide conical scanning of the surface. For the smallest angle with the local vertical used, 40° , a swath width of up to about 1250 km can be obtained. A spatial resolution of 50 km and a temperature sensitivity of 0.5°K can be achieved with a radiometer weighing about 90 kg and using about 175 watts of power.

3.2.4 Synthetic Aperture Radar (SAR)

At frequencies below about 10 GHz there is very little attenuation by the atmosphere, even with heavy clouds in the path. Consequently imaging radar operating below 10 GHz can provide all-weather imagery of the surface. The synthetic aperture technique can be used to achieve high resolution with a feasible antenna size. The required radiation pattern is a fan beam tilted to one side of the orbit plane, so the antenna is very long in the along-track direction compared to its height in the cross-track direction. Scanning is provided in the cross-track direction by the time delay of the signal reflected from the surface at points successively farther from the nadir, while in the along-track direction the scanning comes from the spacecraft motion, (see Table 3-6).

Table 3-6. SAR Performance Characteristics

Wavelength:	10 cm (3 GHz)
Bandwidth:	0.5 MHz
Resolution:	1 km (both directions)
Sensitivity:	Good image above σ_0 of -20 db
Antenna Size:	6 m by 0.3 m by 8 cm
Weight:	73 kg
Power:	140 watts

3.2.5 Glitter Pattern Sensor

A sun glitter pattern sensor can provide the speed and direction of the near surface wind averaged over a substantial fraction of the glitter pattern, and make possible the detection and delineation of areas of reduced sea state arising from regions of upwelling or from natural or man-made slicks. The proposed sensor is essentially a medium resolution TV camera with a field of view which can be centered on the glitter pattern and cover a substantial fraction of its area. The wind data are deduced from relative measurements of constant brightness contours in the pattern, i. e., the "size" and "shape" of the pattern, along with the use of the relationships between the frequency of occurrence of local surface slopes and near-surface winds developed by Cox and Munk.³

Performance characteristics of the proposed sensor are summarized in Table 3-7. The glitter pattern sensor is in a sense in competition with the passive multichannel microwave radiometer, which also gives a measure of near-surface winds. It suffers in comparison with microwave techniques both in that its applicability is limited to the sun glitter region in the absence of excessive interference from cloud cover, and that the area over which the wind measurement is averaged is larger than a typical microwave footprint. The latter point may, however, not be a disadvantage for applications such as Numerical Weather Prediction, in which averages over fairly large areas are desired. On the other hand, the glitter pattern sensor provides information on the wind direction, while microwave measurements do not. In addition, the fairly high resolution of the

Table 3-7. Glitter Framing Camera

<u>General Description</u>	<p>Primary: To obtain images of glitter pattern from which to deduce average sea state and detect and locate areas of reduced sea state.</p>
Function	<p>Secondary: To obtain moderate resolution images of areas outside glitter pattern</p>
Configuration, Major Elements	<p>1000 TV line camera (RBV or Sec Vidicon); f/4 optics with adjustable iris diaphragm f/4 to f/16; two axis gimbaling or 2 axis pointing mirror</p>
Developmental Status	<p>State-of-the-art</p>
<u>Performance Characteristics</u>	
Wavelength Range	<p>0.58-0.7μ - not critical but should be at red end of visible spectrum</p>
Spectral Resolution	<p>Broadband - one band only</p>
Field of View	<p>40$^{\circ}$ x 40$^{\circ}$; 777 km across at 30$^{\circ}$ from nadir</p>
Spatial Resolution	<p>2500 feet; 0.78 km (per TV line) (925 km altitude)</p>
Sensitivity	<p>64:1 dynamic range at any given exposure, additional 16:1 by varying exposure</p>
Absolute Accuracy	<p>20 percent photometric</p>
<u>Physical Characteristics</u>	
Size	<p>.03 cu. meters</p>
Weight	<p>18 kg</p>
Power	<p>45 watts average, 52 watts peak</p>
<u>Platform/Data Considerations</u>	
Pointing Accuracy	<p>0.5$^{\circ}$ (+ 5 nmi)</p>
Line of Sight Rate	<p>0.35$^{\circ}$/sec</p>
Data Output	<p>100 KHz video, 10 sec/frame, 1 frame/30 sec</p>
<u>Comments</u>	<p>Brightness at center of glitter pattern varies from about 200Lum/ft²/ster to 2500 Lum/ft²/ster. 2 frames/min give about 4 images of any point on surface. Pointing required 0 to 40$^{\circ}$ from nadir, 360$^{\circ}$ in azimuth</p>

glitter pattern sensor imagery permits the detection and delineation of slicks which microwave radiometry could miss entirely. On a relatively short term basis, it should also be observed that the Cox and Munk statistics require some, as yet not firmly determined, modifications for application to microwave measurements. Thus, sun glitter measurements could serve as a form of "ground truth" for use in validating microwave data reduction procedures.

3.2.6 Altimeter

The analysis of Section 4 shows that for oceanographic measurements slopes of one part in 10^7 over regions of about 100 km or more need to be measured. This translates into an altimeter performance requirement for a range accuracy of 10-20 cm for a single measurement. Either a laser or a radar altimeter can be considered for this application. The principal advantage of a laser system is that it can provide very fine angular resolution but, for ocean surface measurements, averaging over a fairly large area is required to reduce the effects of local wave structure, so a narrow altimeter beam is of no particular value. Most other considerations, including weight and power requirements, more nearly all-weather capability, and stage of development, favor the radar altimeter. Therefore the radar altimeter has been chosen. The characteristics of the sensor are given in Table 3-8.

Table 3-8. Radar Altimeter

Type:	X-band (9 GHz), single pulse operation
Pulse:	40 nanosec amplitude modulated CN
PRF:	1-100 pulses per sec.
Antenna:	0.9m diameter circular, 37.2 mrad beamwidth
Accuracy:	10 cm
Sensitivity:	Slopes of 10^{-7} over 50-100 km
Data Rate:	One measurement per 10-20 km along track

The purpose of the altimeter is not to make geodetic measurements per se but to obtain data for application to oceanographic requirements for current, tide, and storm measurements. For these purposes the ocean surface slopes can be used rather than absolute surface heights. It is this fact that makes useful measurements feasible, since the slopes can be obtained without knowing precisely the altitude of the spacecraft nor the exact departures of the geoid from the reference ellipsoid.

The transmitter power required for satisfactory imaging is strongly dependent on the incidence angle of the antenn beam. To reduce the required transmitter power over the ocean, the beam should be pointed much nearer the nadir than is customary for side looking radars over land. With the beam starting at about 20° from the vertical reasonable power levels can be used, while observable contrast between rough and moderately smooth seas will be obtained. Ice will produce strong signal returns, so this sensor is particularly useful for mapping sea ice and the polar ice caps.

Sea and polar ice measurements should be made every 1-2 days over latitudes down to 60° or less. To achieve this coverage a swath width of about 600 km is required. Because the highest latitude reached by the satellite is about 81° (north or south) and the radar looks to one side, it is not possible to observe close to both poles with a single fixed antenna configuration. Such observations could be made either with two antennas or with one capable of being pointed to either side of the spacecraft. However, given a single antenna with a swath width of 600 km on a spacecraft at an altitude of 925 km, starting at 20° from the nadir, it is possible to observe to within about 0.5° (63 km) of the north pole and to about 1340 km of the south pole, i. e., to about 78° S latitude. The region never seen near the south pole is entirely over land except for a small portion of the Weddell Sea, so the loss of coverage of this area is not as serious as would be that of the corresponding region near the north pole. It is this configuration that is recommended, since it provides good coverage with minimum weight and complexity.

Performance characteristics of the suggested synthetic aperture radar are summarized in Table 3-6. The power requirement degradation of the maximum achievable resolution in the along track direction, but since the required resolution is very much larger than that obtainable even with the past detection integration, no compromise of mission requirements results.

3.3 SPACECRAFT REQUIREMENTS

The spacecraft requirements are derived from the expected payload capabilities of the EOS spacecraft and from operating characteristics of the chosen sensors. It is, of course, not purely fortuitous that the sensors do not require greater weight or power allotments than those postulated for EOS. The balancing of sensor performance against the spacecraft capability to provide the weight and power required to achieve that performance is probably not evident from the discussions of the individual sensors, but it was nevertheless an important consideration throughout the study.

3.3.1 EOS Payload Limitations

The EOS total payload was taken to be subject to the following limitations:

- | | |
|---------------------------|--------------------------------------|
| ● Maximum payload weight | 315 kg |
| ● Maximum power available | 500 watts average
1500 watts peak |
| ● Maximum data rate | 40 MHz |

The total estimated weight of all six sensors is 292 kg; this falls within the weight limitation with about an eight percent contingency factor. The power presents less of a constraint than the weight. The average power consumption with all sensors operating at once is estimated at 443 watts, about 13 percent less than the allowable average, but since the sensors do not operate all the time the margin is actually considerably greater. The duty cycles of the sensors vary from about 0.2 to no more than about 0.6, on the average, when the relative amount of land and water, and, for the visible sensors, sun angle considerations, are taken into account. With these coverage factors, the average

estimated power requirement is about 200 watts, with a peak, since they will tend frequently to be all operating at once, of about 450 watts. The sensor requirements also fall far short of the maximum data rate.

3.3.2 Orbital Selection

The choice of orbital parameters is discussed in detail in Section 8. The desires for high resolution in the imaging sensor on the one hand, and for complete and frequently repeated coverage on the other, lead to conflicting altitude requirements. The best tradeoff between them occurs at roughly 500 to 1000 km; an altitude of 925 km (500 nmi) has been chosen as nominal for calculating sensor resolutions and coverage. A circular, sun-synchronous orbit is clearly desirable to provide repeated observations under as nearly the same conditions as possible and to regularity in the coverage repetition. The choice of a sun-synchronous orbit establishes a relationship between altitude and inclination; for an altitude of 925 km, the inclination is about 99° . The exact choice of altitude determines the period at which the orbital traces repeat themselves.

Once a sun-synchronous orbit of a given altitude has been chosen, the only significant orbital parameter remaining is that relating the orbit to the local time of day. Choice of this parameter is affected most strongly by the visible imaging spectrometer requirements for suitable sun angles. The image contrast arises almost exclusively from color differences, as opposed, for example, to lunar or Martian imagery, where it comes primarily from shadows associated with terrain relief. A sun angle as high as possible is thus desirable. However, too high a sun angle brings the glitter pattern into the field of view. The very bright specular reflection of the glitter pattern provides almost no information on the specular characteristics of the water itself, while overwhelming the much weaker upwelling scattered sunlight which is affected by the transmission properties of the water. The best available evidence on ocean color contrast relative to sun position is discussed in the section on the visible imaging spectrometer. An orbit for which the local time of the descending node is 1400 appears to be the best, taking into account both sun angles and diurnal cloud and fog trends.

3.3.3 Attitude Control

The spacecraft must obviously be three-axis stabilized and earth-oriented to provide a suitable platform for the global ocean sensors. It should be possible to determine the spacecraft attitude at any instant of time to 0.05° in order to have location accuracy consistent with the resolution of the sensors. The attitude control need not be quite so tight, however, the control should be at least good enough to provide pointing of fixed-mounted sensors to 0.5° in each axis, and preferably to 0.2° or better. Moreover, the control must insure body rates no greater than $0.035^\circ/\text{sec}$ in each axis. These attitude control and determination requirements can be met within the state of the art without unusual cost or capability.

3.4 DATA REQUIREMENTS

The data requirements summarized in this section are based on the use of all six sensors for the maximum amount of time that they could be used. That is, for example, the data acquisition for the visible imaging spectrometer has been based on the times when acceptable sun angles occur, but no allowance has been made for reduced operating time because of cloud cover.

The volume of data acquired by all the sensors is summarized in Table 3-9. The synthetic aperture radar (SAR) acquires about four times as much data as all the rest of the payload together. Thus the SAR data dominate the storage and readout requirements. However, once the standard preprocessing typical for this kind of sensor has been done on the amount of data requiring further processing or analysis becomes much smaller (by over two orders of magnitude).

It is assumed that the ground stations which will receive the global oceanographic data are the NTTF in Maryland, Goldstone, California, and Fairbanks, Alaska. They together provide an average of 16 minutes of readout time per orbit, of which about half is at Fairbanks. The individual orbit times for a typical month vary from zero to 37 minutes. Thus data must be stored on board for over two orbits on occasion, and must be transmitted at a higher than real-time rate.

The storage requirements do not strain the current technology in tape recorders. For example, the tape recorder being developed for ERTS could store about 2.4 orbits worth of radar data, which has been

Table 3-9. Data Acquisition

Sensor	Operating Data Rate (MB/S)		Average Coverage Factor		Average Total Data Per Orbit (MB)
	Instantaneous	Average	Fraction of orbit	Operating time/orbit(sec)	
SLR	8 MB/S	8 MB/S	0.25	1550	1.24×10^4 MB
Multispectral Scanner	1.5	1.0	0.3	1850	} 2.8×10^3
	0.75	0.5	0.3	1850	
Visible Spectrometer	0.3	0.3	0.2	1240	3.7×10^2
Glitter Sensor	0.2	0.04	0.2	1240	50
Microwave Radiometer	0.0002	0.0002	0.6	3700	0.74
Radar Altimeter	0.0001	0.0001	0.6	3700	0.37
					Total 1.56×10^4 MB

seen to have the greatest requirements. It is desired that the readout rates stay within the capabilities established for ERTS, and this can be accomplished. Two 30 megabit/sec channels (i. e., the ERTS Channels) would be used to transmit all the data in an average of 7 minutes per orbit, which is nicely within the available time.

3.5 PAYLOAD GROUPINGS

The final product of the study of global oceanographic requirements for EOS A/B is the recommendation of sensor groupings and their associated orbital requirements for each of the national priorities. Optimum and minimum sensor groupings have been established for each priority as required by the work statement. In the identification of these groupings, iterative analyses were performed which were started almost from the beginning of the study. Thus a set of sensors of configuration and performance within the state-of-the-art, conforming to spacecraft constraints, was evolved to meet the measurement requirements. Because of this guidance of the choice of sensor capabilities and the considerable commonality among the requirements for the different priorities, the optimum grouping established for each priority consists of all six sensors. Minimum sensor groups were selected by identifying those sensors which acquire the most significant information for each priority. The recommendations for optimum and minimum sets of sensors are presented in Tables 3-11 through 3-13, along with the measurements performed and the extent to which relevant information is acquired. The sensors are listed in terms of importance for each grouping.

For the physical processes priority, Table 3-11, the optimum payload capabilities satisfy all the information needs except for two categories under basic geophysical research. With respect to the first, geodesy and dynamic topography, the optimum payload can satisfy only the geostrophic flow measurement requirements using the altimeter. The other information requirements under this category involve a need for daily coverage. The second category, geomagnetism, is not covered because of the operational and physical incompatibility of magnetic measurements with the rest of the payload. The minimum payload provides ocean color, sea surface temperature, and surface roughness (sea ice detection) information and thus emphasizes environmental monitoring and prediction for transportation and hazards.

For the living marine resources priority, Table 3-12, both the optimum payload and the minimum payload possess a positive capability for all information needs, except for weather effects on fishing operations. The minimum payload consists of ocean color, infrared sea surface temperature and all weather microwave sea state and surface temperature measurements. Temperature and color are vital for finding fish and all weather sea state and temperature are important for predicting environmental work conditions and icing conditions. Radar sea ice detection was not selected since the bulk of fishing activities occurs in ice free waters.

The pollution priority mission, Table 3-13, optimum payload and minimum payloads provide positive capabilities for all information needs, except that the minimum payload possesses only marginal capability for detecting and monitoring oil films. The minimum payload provides ocean color and clear weather sea surface temperatures. Positive capability for detecting oil films should also include all weather sea surface temperatures, all weather sea state glitter modifications measurements and surface radar roughness measurements.

3.6 CONCLUSIONS AND RECOMMENDATIONS

The recommended payload groupings, in order of importance for an EOS mission dedicated to global oceanography is contained in Table 3-10. This sensor grouping nearly fulfills all measurement requirements as shown in Section 3.5.

Table 3-10. Summary - Recommended Payload Multi-Priority
MINIMUM PAYLOAD GROUP - ALL PRIORITIES

<u>SENSORS</u>	<u>MEASUREMENTS</u>
I. VISIBLE IMAGER	OCEAN COLOR
II. IR-MULTISPECTRAL SCANNER	SEA SURFACE TEMPERATURE
III. MICROWAVE RADIOMETER	SEA STATE
IV. SYNTHETIC APERTURE RADAR	SURFACE ROUGHNESS

<u>SENSOR</u>	<u>PAYLOAD CHARACTERISTICS</u>			
	<u>SIZE (M³)</u>	<u>WEIGHT (KG)</u>	<u>POWER (WATTS)</u>	<u>DATA RATE (MBS)</u>
I.	0.15	18	18	0.3
II.	1.2	43	45	1.5
III.	0.4	91	175	NILL
IV.	<u>0.3</u>	<u>73</u>	<u>140</u>	<u>8.0</u>
TOTAL	2.0	225	380	9.8

Beyond this, an all encompassing sensor grouping would include, in order of importance the sun glitter sensor and the radar altimeter. It should be noted that the need for altimetry measurements could be fulfilled by GEOS-C and inclusion of the altimeter would impose spacecraft stability requirements during data acquisition.

The recommended payload complement would also include two wide-band tape recorders similar to those under development for ERTS A/B. Additionally, a Data Collection System with tracking capability would be desirable.

In summary, the recommended multi-priority sensor grouping could be developed for the EOS A mission, if appropriate action is taken to develop the payload which would include aircraft flights to finalize design parameters. It should also be noted that the sensors described, except for MOCS, are design concepts and require development.

It should finally be noted that spacecraft oceanography is still in the research and development phase, and there is a lack of sensor hardware experience and software utility.

Table 3-9. Sensor Definition and Relevancy - Physical Processes Priority Mission

SEE SECTION 4 FOR DETAILED INFORMATION NEEDS

PAYLOAD GROUPING

SENSOR DEFINITION		MEASUREMENTS PERFORMED		
OPTIMUM GROUP				
I.	VISIBLE IMAGER	OCEAN COLOR		
II.	IR-MULTISPECTRAL SCANNER	SEA SURFACE TEMPERATURE		
III.	SYNTHETIC APERTURE RADAR	SURFACE ROUGHNESS AND SEA ICE		
IV.	MICROWAVE RADIOMETER	SEA STATE		
V.	GLITTER FRAMING CAMERA	GLITTER PATTERN		
VI.	RADAR ALTIMETER	SEA SLOPE		

PAYLOAD CHARACTERISTICS				
SENSORS	SIZE (M ³)	WEIGHT (KG)	POWER (WATTS)	DATA RATE (MBS)
I.	0.15	18	18	0.3
II.	1.2	43	45	1.5
III.	0.3	73	140	8.0
IV.	0.4	91	175	NILL
V.	0.1	18	45	0.2
VI.	0.05	23	30	NILL
TOTAL	2.2	266	450	10.0

MINIMUM GROUP

SENSOR DEFINITION		MEASUREMENTS PERFORMED		
MINIMUM GROUP				
I.	VISIBLE IMAGER	OCEAN COLOR		
II.	IR-MULTISPECTRAL SCANNER	SEA SURFACE TEMP.		
III.	SYNTHETIC APERTURE RADAR	SURFACE ROUGHNESS AND SEA ICE		

PAYLOAD CHARACTERISTICS				
SENSOR	SIZE (M ³)	WEIGHT (KG)	POWER(WATTS)	DATA RATE (MBS)
I.	0.15	18	18	0.3
II.	1.2	43	45	1.5
III.	0.3	73	140	8.0
TOTAL	1.65	134	200	9.8

RELEVANT INFORMATION ACQUIRED

OPTIMUM GROUP

- I. ENVIRONMENTAL MONITORING AND PREDICTION FOR TRANSPORTATION AND HAZARDS
 - A. SHORT-TERM FORCING FUNCTIONS-INSOLATION
 - B. SHORT-TERM COUPLING MECHANISMS
 - 1) WIND STRESS ON SURFACE WATER
 - 2) HEAT EXCHANGE, EVAPORATION/PRECIPITATION AND FREEZING/MELTING
 - C. SHORT-TERM RESPONSE PATTERNS
 - 1) SEA ICE: PACK AND SHELF ICE FORMATION AND BREAKUP
 - 2) REGIONAL WEATHER CONDITIONS (FOG, SEA STATE, WIND, ETC.)
 - 3) CURRENTS (RESPONSE OF SURFACE WATERS TO WIND AND CORIOLIS FORCES) - CURRENT BOUNDARIES (FRONTS, DIVERGENCES, CONVERGENCES, UPWELLING AREAS)
 - D. SHOAL WATER AREAS (REEFS BANKS, ETC.)
- II. BASIC GEOPHYSICAL RESEARCH
 - A. GEODESY AND DYNAMIC TOPOGRAPHY
 - B. GEOMORPHOLOGY
 - 1) SHALLOW WATER BOTTOM TOPOGRAPHY
 - 2) VOLCANIC ISLANDS, CORAL REEFS, CONTINENTAL AND INSULAR COASTLINES
 - C. CONDITIONS AND PROCESSES IN POLAR REGIONS
 - D. GEOMAGNETISM

MEASUREMENT REQUIREMENTS SATISFIED

- (I.A) REQUIREMENTS SATISFIED FOR OC AND SST. ONE DAY REPETITION RATE POSSIBLE ONLY WITH IR-MULTISPECTRAL CAMERA.
- (I.B.1) REQUIREMENTS SATISFIED FOR OC, SS AND SR. GLITTER PATTERN (GP) ONE DAY FREQUENCY OF COVERAGE POSSIBLE BY UNIQUE GIMBAL GLITTER FRAMING CAMERA, MICROWAVE FREQUENCY OF COVERAGE NOT POSSIBLE
- (I.B.2) SAME AS I.B.1. IN ADDITION SST REQUIREMENTS SATISFIED
- (I.C.1) REQUIREMENTS SATISFIED FOR SST, OC, AND SR. SEA SURFACE SALINITY DATA NOT PROVIDED
- (I.C.2) SAME AS I.B.1. SIDELOOKING RADAR FREQUENCY OF COVERAGE NOT POSSIBLE
- (I.C.3) REQUIREMENTS SATISFIED FOR OC, SST, GP, SS, SSL, AND SR. SEA SURFACE SALINITY DATA NOT PROVIDED. SPECTRAL BANDWIDTH IS 0.015μ INSTEAD OF 0.01μ FOR TURBIDITY.
- (I.D.) REQUIREMENT SATISFIED FOR OC EXCEPT SPECTRAL BANDWIDTH IS 0.015μ INSTEAD OF 0.01μ FOR SHALLOW WATER BATHIMETRY.
- (II.A) REQUIREMENTS SATISFIED FOR SSL FOR GEOSTROPHIC FLOW. ALL OTHER REQUIREMENTS FOR ONE DAY COVERAGE OF SSL NOT MET.
- (II.B.1) REQUIREMENTS SATISFIED FOR OC AND GP EXCEPT SPECTRAL BANDWIDTH IS 0.015μ INSTEAD OF 0.01μ FOR BATHYMETRY
- (II.B.2) REQUIREMENTS SATISFIED FOR OC EXCEPT SPECTRAL BANDWIDTH IS 0.015μ INSTEAD OF 0.01μ
- (II.C) REQUIREMENTS SATISFIED FOR SST AND OC EXCEPT SPECTRAL BANDWIDTH IS 0.015μ INSTEAD OF 0.01 μ
- (II.D) REQUIREMENTS NOT SATISFIED.

MINIMUM GROUP

- I. ENVIRONMENTAL MONITORING AND PREDICTION FOR TRANSPORTATION AND HAZARDS
 - A. SHORT-TERM FORCING FUNCTIONS-INSOLATION
 - B. SHORT-TERM COUPLING MECHANISMS
 - 1) WIND STRESS ON SURFACE WATER
 - 2) HEAT EXCHANGE, EVAPORATION/PRECIPITATION AND FREEZING/MELTING
 - C. SHORT-TERM RESPONSE PATTERNS
 - 1) SEA ICE: PACK AND SHELF ICE FORMATION AND BREAKUP
 - 2) REGIONAL WEATHER CONDITIONS (FOG, SEA STATE, WIND, ETC.)
 - 3) CURRENTS (RESPONSE OF SURFACE WATERS TO WIND AND CORIOLIS FORCES) - CURRENT BOUNDARIES (FRONTS, DIVERGENCES, CONVERGENCES, UPWELLING AREAS)
 - D. SHOAL WATER AREAS (REEFS BANKS, ETC.)
- II. BASIC GEOPHYSICAL RESEARCH
 - A. GEODESY AND DYNAMIC TOPOGRAPHY
 - B. GEOMORPHOLOGY
 - 1) SHALLOW WATER BOTTOM TOPOGRAPHY
 - 2) VOLCANIC ISLANDS, CORAL REEFS, CONTINENTAL AND INSULAR COASTLINES
 - C. CONDITIONS AND PROCESSES IN POLAR REGIONS
 - D. GEOMAGNETISM

- (I.A) REQUIREMENTS SATISFIED FOR OC AND SST.
- (I.B.1) REQUIREMENTS SATISFIED FOR OC. GLITTER PATTERN NOT PROVIDED
- (I.B.2) SAME AS (I.A) GP NOT PROVIDED
- (I.C.1) REQUIREMENTS SATISFIED FOR SR (SEA ICE) AND SST. SEA SURFACE SALINITY DATA NOT PROVIDED.
- (I.C.2) REQUIREMENTS SATISFIED FOR OC AND SST EXCEPT NO SLR DATA
- (I.C.3) REQUIREMENTS SATISFIED FOR OC AND SST. SSL AND GP AND ALL WEATHER SST CAPABILITY NOT PROVIDED.
- (I.D) REQUIREMENTS SATISFIED FOR OC EXCEPT SPECTRAL BANDWIDTH IS 0.015μ INSTEAD OF 0.01μ
- (II.A) REQUIREMENTS NOT SATISFIED
- (II.B.1) SAME AS (I.D)
- (II.B.2) SAME AS (I.D.)
- (II.C) REQUIREMENTS SATISFIED FOR OC AND SST EXCEPT SPECTRAL BANDWIDTH IS 0.015μ INSTEAD OF 0.05μ
- (II.D) REQUIREMENTS NOT SATISFIED

Page intentionally left blank

Table 3-12. Sensor Definition and Relevancy - Living Marine Resources Priority Mission

SEE SECTION 5 FOR DETAILED INFORMATION NEEDS

SENSOR DEFINITION		MEASUREMENT PERFORMED	
OPTIMUM GROUP			
I.	VISIBLE IMAGER	OCEAN COLOR	
II.	IR MULTISPECTRAL SCANNER	SEA SURFACE TEMPERATURE	
III.	MICROWAVE RADIOMETER	SEA STATE	
IV.	GLITTER FRAMING CAMERA	GLITTER PATTERN	
V.	SYNTHETIC APERTURE RADAR	SURFACE ROUGHNESS AND SEA ICE	
VI.	RADAR ALTIMETER	SEA SLOPE	

PAYLOAD CHARACTERISTICS				
SENSOR	SIZE (M ³)	WEIGHT (KG)	POWER (WATTS)	DATA RATE (MBS)
I.	0.15	18	18	0.3
II.	1.2	43	45	1.5
III.	0.4	91	175	NILL
IV.	0.1	18	45	0.2
V.	0.3	73	140	8.0
VI.	0.05	23	30	NILL
TOTAL	2.2	266	450	10.0

SENSOR DEFINITION		MEASUREMENT PERFORMED	
MINIMUM GROUP			
I.	VISIBLE IMAGER	OCEAN COLOR	
II.	IR-MULTISPECTRAL SCANNER	SEA SURFACE TEMPERATURE	
III.	MICROWAVE RADIOMETER	SEA STATE	

PAYLOAD CHARACTERISTICS				
SENSOR	SIZE (M ³)	WEIGHT (KG)	POWER (WATTS)	DATA RATE (MBS)
I.	0.15	18	18	0.3
II.	1.2	43	45	1.5
III.	0.4	91	175	NILL
TOTAL	1.75	152	240	1.8

RELEVANT INFORMATION ACQUIRED

OPTIMUM GROUP

- I. RESOURCE ABUNDANCE/DYNAMICS
 - A. TOTAL GLOBAL RESOURCE ABUNDANCE/YIELD POTENTIAL
 - B. YIELD POTENTIAL OF SPECIFIC OCEAN SECTORS, YEAR-TO-YEAR STOCK SIZE VARIATIONS, MAXIMUM SUSTAINABLE STOCK YIELDS.
 - 1) REGIONAL PRIMARY PRODUCTIVITY
 - 2) ENVIRONMENTAL LETHAL OR SUBLETHAL FACTORS
- II. RESOURCE DISTRIBUTION
 - A. BROAD BIOGEOGRAPHY OF RESOURCES
 - B. ADULT STOCK MIGRATION ROUTES, LOCATION OF SPAWNING GROUNDS/NURSERY AREAS.
 - 1) REGIONAL PRIMARY PRODUCTIVITY
 - 2) MAJOR CURRENT/WATER MASS DISPLACEMENTS
 - 3) CURRENT MEANDERS
 - 4) RIVER PLUMES, ETC.
 - C. CONCENTRATION OF FISH NEAR DISCONTINUITIES
 - 1) OCEANIC FRONTS
 - 2) CURRENT EDDIES
- III. STOCK AVAILABILITY/ACCESSIBILITY
 - A. WEATHER EFFECTS ON FISHING OPERATIONS
 - 1) STORMS
 - 2) CURRENT EDDIES
 - 3) ICING CONDITIONS
 - B. VULNERABILITY OF FISH
 - 1) THERMOCLINE TOPOGRAPHY
 - 2) WATER CLARITY

MEASUREMENT REQUIREMENTS SATISFIED

- (I.A.) REQUIREMENTS SATISFIED FOR OC EXCEPT SPECTRAL BANDWIDTH IS 0.015μ INSTEAD OF 0.01μ
- (I.B.1) REQUIREMENTS SATISFIED FOR OC, SST, SR, GP, AND SS EXCEPT SPECTRAL BANDWIDTH IS 0.015μ INSTEAD OF 0.01μ. SEA SURFACE SALINITY DATA NOT PROVIDED.
- (I.B.2) SAME AS (I.B.1) EXCEPT FOR MAXIMUM FREQUENCY OF COVERAGE FOR OC. MINIMUM FREQUENCY OF COVERAGE PROVIDED.
- (II.A) SAME AS (I.B.1)
- (II.B.1) SAME AS (I.B.1)
- (II.B.2) SAME AS (I.B.1)
- (II.B.3) SAME AS (I.B.1)
- (II.B.4) REQUIREMENTS SATISFIED FOR OC, SST. SURFACE SALINITY DATA NOT PROVIDED. LOWER LIMIT (MAXIMUM ONE DAY) FREQUENCY OF COVERAGE NOT PROVIDED FOR MICROWAVE.
- (II.B.5) REQUIREMENTS SATISFIED FOR SST
- (II.C.1) SAME AS (I.B.1)
- (II.C.2) SAME AS (I.B.1)
- (III.A.1) REQUIREMENTS SATISFIED FOR OC AND SST. ALL WEATHER SST NOT PROVIDED FOR OC ONE DAY FREQUENCY OF COVERAGE.
- (III.A.2) REQUIREMENTS SATISFIED FOR GP, SS AND SR.
- (III.A.3) REQUIREMENT NOT SATISFIED FOR LESS THAN ONE DAY FREQUENCY OF COVERAGE
- (III.A.4) REQUIREMENTS SATISFIED FOR OC AND GP.
- (III.B.1) SAME AS (I.B.1)
- (III.B.2) REQUIREMENTS SATISFIED FOR OC

MINIMUM GROUP

- I. RESOURCE ABUNDANCE/DYNAMICS
 - A. TOTAL GLOBAL RESOURCE ABUNDANCE/YIELD POTENTIAL
 - B. YIELD POTENTIAL OF SPECIFIC OCEAN SECTORS, YEAR-TO-YEAR STOCK SIZE VARIATIONS, MAXIMUM SUSTAINABLE STOCK YIELDS
 - 1) REGIONAL PRIMARY PRODUCTIVITY
 - 2) ENVIRONMENTAL LETHAL OR SUBLETHAL FACTORS
- II. RESOURCE DISTRIBUTION
 - A. BROAD BIOGEOGRAPHY OF RESOURCES
 - B. ADULT STOCK MIGRATION ROUTES, LOCATION OF SPAWNING GROUNDS/NURSERY AREAS.
 - 1) REGIONAL PRIMARY PRODUCTIVITY
 - 2) MAJOR CURRENT/WATER MASS DISPLACEMENTS
 - 3) CURRENT MEANDERS
 - 4) RIVER PLUMES, ETC.
 - 5) SEASONAL MIGRATIONS OF ISOTHERMS
 - C. CONCENTRATION OF FISH NEAR DISCONTINUITIES
 - 1) OCEANIC FRONTS
 - 2) CURRENT EDDIES
- III. STOCK AVAILABILITY/ACCESSIBILITY
 - A. WEATHER EFFECTS ON FISHING OPERATIONS
 - 1) STORMS
 - 2) ENVIRONMENTAL CONDITIONS
 - 3) ICING CONDITIONS
 - 4) LOCATION OF SHOALS
 - B. VULNERABILITY OF FISH
 - 1) THERMOCLINE TOPOGRAPHY
 - 2) WATER CLARITY

- (I.A.) REQUIREMENTS SATISFIED FOR OC EXCEPT SPECTRAL BANDWIDTH IS 0.015μ INSTEAD OF 0.01μ
- (I.B.1) REQUIREMENTS SATISFIED FOR OC AND SST EXCEPT SPECTRAL BANDWIDTH IS 0.015μ INSTEAD OF 0.01μ. GP AND SR REQUIREMENTS NOT PROVIDED. SURFACE SALINITY DATA NOT PROVIDED. SAME AS (I.B.1) - EXCEPT MAXIMUM 1/2 DAY FREQUENCY OF COVERAGE NOT PROVIDED.
- (I.B.2) SAME AS (I.B.1)
- (II.A) SAME AS (I.B.1)
- (II.B.1) SAME AS (I.B.1)
- (II.B.2) SAME AS (I.B.1)
- (II.B.3) SAME AS (I.B.1)
- (II.B.4) SAME AS (I.B.1)
- (II.B.5) REQUIREMENTS SATISFIED FOR SST
- (II.C.1) SAME AS (I.B.1)
- (II.C.2) SAME AS (I.B.1)
- (III.A.1) REQUIREMENTS SATISFIED FOR OC AND SST
- (III.A.2) REQUIREMENTS FOR SS PROVIDED EXCEPT FOR MAXIMUM TWO DAY FREQUENCY OF COVERAGE. GP NOT PROVIDED
- (III.A.3) SAME AS (III.A.1)
- (III.A.4) REQUIREMENTS SATISFIED FOR OC. GP NOT PROVIDED.
- (III.B.1) REQUIREMENTS SATISFIED FOR SST. GP NOT PROVIDED.
- (III.B.2) REQUIREMENTS SATISFIED FOR OC.

Page intentionally left blank

Table 3-13. Sensor Definition and Relevancy - Pollution Priority Mission

SEE SECTION 6 FOR DETAILED INFORMATION NEEDS

PAYLOAD GROUPING					RELEVANT INFORMATION REQUIRED	MEASUREMENT REQUIREMENTS SATISFIED																																									
OPTIMUM GROUP					OPTIMUM GROUP	MEASUREMENT REQUIREMENTS SATISFIED																																									
SENSOR DEFINITION I. VISIBLE IMAGER II. IR-MULTISPECTRAL SCANNER III. GLITTER FRAMING CAMERA IV. MICROWAVE RADIOMETER V. SYNTHETIC APERTURE RADAR VI. RADAR ALTIMETER					MEASUREMENTS PERFORMED OCEAN COLOR SEA SURFACE TEMPERATURE GLITTER PATTERN SEA STATE SURFACE ROUGHNESS SEA SLOPE																																										
PAYLOAD CHARACTERISTICS <table border="1"> <thead> <tr> <th>SENSOR</th> <th>SIZE (M³)</th> <th>WEIGHT (KG)</th> <th>POWER (WATTS)</th> <th>DATA RATE (MBS)</th> </tr> </thead> <tbody> <tr> <td>I.</td> <td>0.15</td> <td>18</td> <td>18</td> <td>0.3</td> </tr> <tr> <td>II.</td> <td>1.2</td> <td>43</td> <td>45</td> <td>1.5</td> </tr> <tr> <td>III.</td> <td>0.1</td> <td>18</td> <td>45</td> <td>0.2</td> </tr> <tr> <td>IV.</td> <td>0.4</td> <td>91</td> <td>175</td> <td>NILL</td> </tr> <tr> <td>V.</td> <td>0.3</td> <td>73</td> <td>140</td> <td>8.0</td> </tr> <tr> <td>VI.</td> <td>0.05</td> <td>23</td> <td>30</td> <td>NILL</td> </tr> <tr> <td>TOTAL</td> <td>2.2</td> <td>266</td> <td>450</td> <td>10.0</td> </tr> </tbody> </table>					SENSOR	SIZE (M ³)	WEIGHT (KG)	POWER (WATTS)	DATA RATE (MBS)	I.	0.15	18	18	0.3	II.	1.2	43	45	1.5	III.	0.1	18	45	0.2	IV.	0.4	91	175	NILL	V.	0.3	73	140	8.0	VI.	0.05	23	30	NILL	TOTAL	2.2	266	450	10.0	1. THERMAL POLLUTION A. POWER PLANT LOCATION AND POWER PLANT EFFECTS 1) CURRENT LOCATION AND BOUNDARIES 2) UPWELLINGS 3) RIVER PLUMES 4) PHYTOPLANKTON STANDING CROP DYNAMICS B. GLOBAL MEAN TEMPERATURE ALTERATION II. HEAVY METALS AND RADIONUCLIDES A. PHYTOPLANKTON STANDING CROP DYNAMICS - SPECTRAL SIGNATURES B. GENERAL SURFACE CONDITIONS 1) GENERAL OCEAN SURFACE 2) CONVERGENCES 3) RIVER PLUMES III. CHLORINATED HYDROCARBONS A. PHYTOPLANKTON STANDING CROP DYNAMICS - SPECTRAL SIGNATURES B. GENERAL SURFACE CONDITIONS 1) GENERAL OCEAN SURFACE CIRCULATION 2) CONVERGENCES 3) RIVER PLUMES 4) OIL FILMS		(I.A.1) REQUIREMENTS SATISFIED FOR OC AND SST. SEA SURFACE SALINITY DATA NOT PROVIDED. (I.A.2) SAME AS (I.A.1) (I.A.3) SAME AS (I.A.1) (I.A.4) REQUIREMENTS SATISFIED FOR OC EXCEPT SPECTRAL BANDWIDTH IS 0.015 INSTEAD OF 0.01 (I.B) ICE CAP SIZE MEASUREMENT REQUIREMENTS SATISFIED FOR VISIBLE IMAGER AND SYNTHETIC APERTURE RADAR IMAGER. WINDING TEND MEASUREMENT REQUIREMENTS SATISFIED FOR SST. (II.A) SAME AS (I.A.4) (II.B.1) SAME AS (I.A.1) PLUS DYNAMIC TOPOGRAPHY MEASUREMENTS SATISFIED TO SLOPES OF 10° (II.B.2) SAME AS (I.A.1) (II.B.3) SAME AS (I.A.1) (III.A) SAME AS (I.A.4) (III.B.1) SAME AS (II.B.1) (III.B.2) SAME AS (I.A.1) (III.B.3) SAME AS (I.A.1) (III.B.4) REQUIREMENTS SATISFIED FOR OC, GP, SST, AND SR. ULTRAVIOLET DATA NOT PROVIDED.
SENSOR	SIZE (M ³)	WEIGHT (KG)	POWER (WATTS)	DATA RATE (MBS)																																											
I.	0.15	18	18	0.3																																											
II.	1.2	43	45	1.5																																											
III.	0.1	18	45	0.2																																											
IV.	0.4	91	175	NILL																																											
V.	0.3	73	140	8.0																																											
VI.	0.05	23	30	NILL																																											
TOTAL	2.2	266	450	10.0																																											
MINIMUM GROUP I. VISIBLE IMAGER II. IR-MULTISPECTRAL SCANNER					MINIMUM GROUP 1. THERMAL POLLUTION A. POWER PLANT LOCATION AND POWER PLANT EFFECTS 1) CURRENT LOCATION AND BOUNDARIES 2) UPWELLINGS 3) RIVER PLUMES 4) PHYTOPLANKTON STANDING CROP DYNAMICS B. GLOBAL MEAN TEMPERATURE ALTERATION II. HEAVY METALS AND RADIONUCLIDES A. PHYTOPLANKTON STANDING CROP DYNAMICS - SPECTRAL SIGNATURES B. GENERAL SURFACE CONDITIONS 1) GENERAL OCEAN SURFACE CIRCULATION 2) CONVERGENCES 3) RIVER PLUMES III. CHLORINATED HYDROCARBONS A. PHYTOPLANKTON STANDING CROP DYNAMICS - SPECTRAL SIGNATURES B. GENERAL SURFACE CONDITIONS 1) GENERAL OCEAN SURFACE CIRCULATION 2) CONVERGENCES 3) RIVER PLUMES 4) OIL FILMS		(I.A.1) REQUIREMENTS SATISFIED FOR OC AND SST EXCEPT ALL WEATHER SST NOT PROVIDED. SEA SURFACE SALINITY DATA NOT PROVIDED. (I.A.2) SAME AS (I.A.1) (I.A.3) SAME AS (I.A.1) (I.A.4) REQUIREMENTS SATISFIED FOR OC EXCEPT SPECTRAL BANDWIDTH IS 0.015 INSTEAD OF 0.01 (I.B) SAME AS (I.A.1) EXCEPT RADAR SR DATA NOT PROVIDED FOR ICE CAPS. (II.A) SAME AS (I.A.4) (II.B.1) SAME AS (I.A.1). DYNAMIC TOPOGRAPHY SEA SLOPE MEASUREMENTS NOT PROVIDED. (II.B.2) SAME AS (I.A.1) (II.B.3) SAME AS (I.A.1) (III.A) SAME AS (I.A.4) (III.B.1) SAME AS (II.B.1) (III.B.2) SAME AS (I.A.1) (III.B.3) SAME AS (I.A.1) (III.B.4) REQUIREMENTS SATISFIED FOR OC AND SST EXCEPT ALL WEATHER SST DATA NOT PROVIDED. GLITTER PATTERN, SEA STATE, SURFACE ROUGHNESS AND ULTRAVIOLET DATA NOT PROVIDED.																																								
PAYLOAD CHARACTERISTICS <table border="1"> <thead> <tr> <th>SENSOR</th> <th>SIZE (M³)</th> <th>WEIGHT (KG)</th> <th>POWER (WATTS)</th> <th>DATA RATE (MBS)</th> </tr> </thead> <tbody> <tr> <td>I.</td> <td>0.15</td> <td>18</td> <td>18</td> <td>0.3</td> </tr> <tr> <td>II.</td> <td>1.2</td> <td>43</td> <td>45</td> <td>1.5</td> </tr> <tr> <td>TOTAL</td> <td>1.35</td> <td>60</td> <td>63</td> <td>1.8</td> </tr> </tbody> </table>					SENSOR	SIZE (M ³)	WEIGHT (KG)	POWER (WATTS)	DATA RATE (MBS)	I.	0.15	18	18	0.3	II.	1.2	43	45	1.5	TOTAL	1.35	60	63	1.8																							
SENSOR	SIZE (M ³)	WEIGHT (KG)	POWER (WATTS)	DATA RATE (MBS)																																											
I.	0.15	18	18	0.3																																											
II.	1.2	43	45	1.5																																											
TOTAL	1.35	60	63	1.8																																											

Page intentionally left blank

REFERENCES FOR SECTION 3

1. P. G. White, "High Altitude Remote Spectroscopy of the Ocean," presented at the SPIE Symposium on Remote Sensing of Earth Resources and the Environment, November 12, 1971, Palo Alto, California.
2. D. Anding, R. Kauth and R. Turner, "Atmospheric Effects on Infrared Multispectral Sensing of Sea Surface Temperature from Space," Willow Run Laboratories, University of Michigan, prepared under Contract NAS12-2117 for NASA Ames Research Center, December 1970.
3. C. Cox and W. Munk, "Slopes of the Sea Surface Deduced from Photographs of Sun Glitter," Bulletin from Scripps Institution of Oceanography 6, 401, 1965.

4. MONITORING AND PREDICTION OF PHYSICAL PHENOMENA

From the point of view of the observer attempting to understand the fundamental processes that affect the physical environment, the global ocean and the atmosphere serve as the link between the basic source, or forcing function, for all environmental changes (the sun) and the specific local response patterns known, from the short-term point of view, as weather, and in the long-term as climate.

The input of solar energy per unit area is, of course, greater in the equatorial region than at the poles, where ice forms and melts (according to season) and so provides a pair of large heat sinks. The basic conditions therefore exist for the transfer of solar energy around the globe.

The oceans and the atmosphere provide the means for this transfer through such coupling mechanisms as evaporation, condensation, precipitation, freezing and melting, (see Figure 4-1). Logically, the global distribution of temperature, pressure, and motion (along with the resulting transport of heat and moisture) should be predictable by the equations of motion and thermodynamics. Although, in principle, such an analytical approach should be straightforward, in practice there are enormous difficulties.

The first of these difficulties is a general lack of the kind of detailed and comprehensive information that is needed for a better understanding of how the system works. Man's knowledge of the ocean atmosphere system is limited in both space and time. Scientists have only recently begun to obtain a synoptic view of even the surface manifestations of its dynamics, through the weather satellites that have been launched during the past decade.

The second difficulty lies in the complexity of the system. The continental land masses, the coriolis force, seasonal changes, and various other factors so complicate the dynamics of the basic energy transfer that it defies analysis by classical methods. Computer technology, however, provides an increasingly promising means of analyzing even these formidably complicated interactions, if comprehensive data can be provided.

This brings us directly to consideration of what a global oceanographic satellite can do. Specifically, it can:

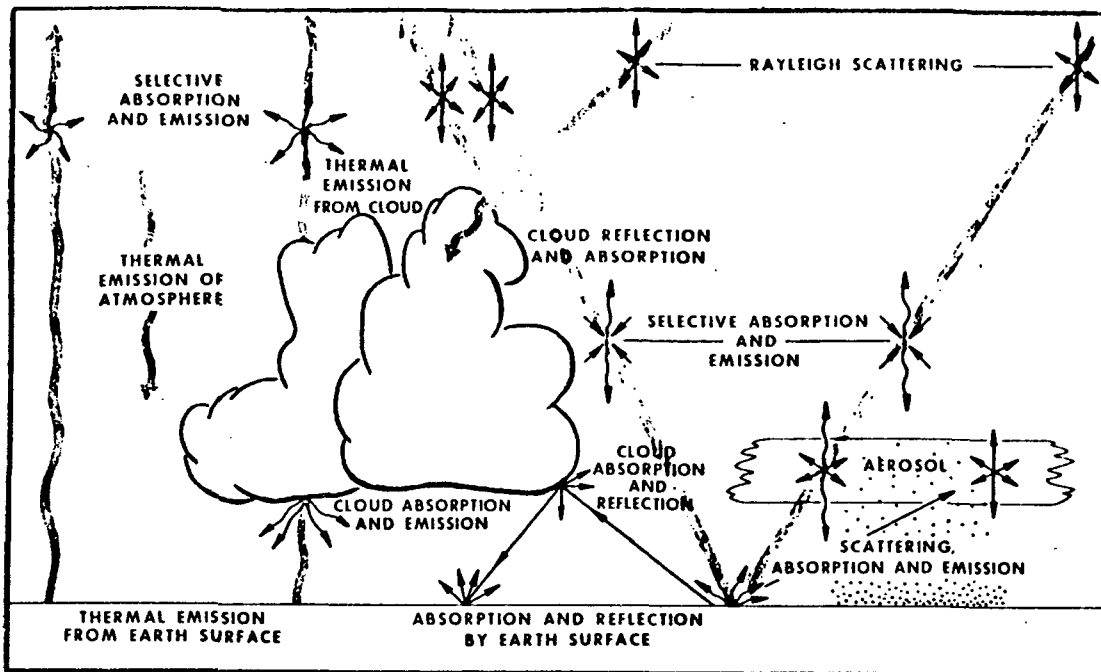


Figure 4-1. Factors Affecting Transfer of Solar Energy Absorbed and Re-emitted by Global Ocean and the Atmosphere Above it

- 1) Continuously map cloud cover in order to measure the amount of solar energy that reaches the surface of the ocean so that the amount of heat that is absorbed can be roughly calculated as an indication of the strength at any given time of the fundamental forcing function. This extremely basic kind of energy estimate may eventually be applicable to long-range weather forecasting and might have more immediate application to the prediction of such factors as the depth of the thermocline, which is of interest not only to naval and research submarines but also to fishing fleets.
- 2) Map and monitor the extent of the polar ice caps in order to estimate what might be called their heat-sink capacity, thereby their effect on global temperature changes. This would also provide part of the basis for long-range weather forecasting and would be immediately useful for predicting ice boundaries for shipping in extremely northerly or southerly waters.
- 3) Continuously map ocean surface temperature patterns as an indication of the rate of insolation, which is the fundamental energizer of all ocean currents and weather phenomena.
- 4) Continuously map wind and ocean current patterns for prediction of short-term (2-5 days) and longer-term (5-14 days) weather.

- 5) Monitor sea state as an indication of locally existing and broadly developing weather conditions.
- 6) Continuously map fixed and slowly evolving phenomena, such as shoals and coral formations, as an aid to charting services.

It is also possible that such a satellite might provide data useful to geodesists and geomorphologists for their fundamental studies of the planetary configuration.

The remainder of this section discusses the interactions between solar heat and polar cold and the responses to those interactions and the extent to which they can be observed by satellite-borne sensors. If the discussion seems oversimplified, it is so partly because experts do not agree entirely upon what the true and precise interrelationships are and partly because a certain amount of deliberate oversimplification can help to clarify the overall argument, which is that more information is needed for a clear understanding of the global ocean system.

4.1 SOLAR-POLAR INTERACTIONS

4.1.1 Insolation

Since the sun is the basic source of energy for all oceanic processes (and more than half the heat that drives atmospheric processes comes from the ocean's surface), measurement of the amount of heat that reaches the surface of the ocean is of fundamental importance. While a satellite system can measure ocean surface temperature by means of infrared radiometry, insolation is a complicated phenomenon which depends upon a wide variety of factors, as shown in Figure 4-1. Far more significant than surface temperature is the amount of input energy that is absorbed by the ocean for, by absorbing heat during the day, the ocean stores solar energy so that the forcing effect of the sun on atmospheric processes is continued during the night.

The rate at which energy is absorbed is a function of atmospheric transparency as well as time and solar radiance and the following equation offers a crude means of calculating in units of gram calories per square centimeter per 24 hours, the solar energy (Q_s) that arrives at the ocean surface.

$$Q_s = 0.014 A_n t_d (1 - 0.0006 C^3)$$

where A_n = Noon altitude of the sun (degrees)

t_d = Length of daylight (minutes)

C = Cloud cover (total, in tenths)

A somewhat more refined, though still only grossly useful, calculation can be made if atmospheric transparency can be measured in terms of low, medium, and high-altitude layers of cloud. This permits a more detailed calculation, as follows:

$$Q_s = Q_{os} (1 - 0.0075 C_L^2)$$

$$Q_s = Q_{os} (1 - 0.006 C_M^2)$$

$$Q_s = Q_{os} (1 - 0.0035 C_H^2)$$

where Q_{os} = Insolation with a clear sky and C_L , C_M , and C_H are the values for cloud cover at low, medium and high altitudes. The minimum Q_s for any cloud layer is the value used for sea surface insolation.

Given solar input, a calculation can be made of albedo (Q_r) which, when subtracted from the input figure, should provide an approximation of the energy absorbed by the ocean.

Albedo (Q_r) for the sea surface can be expressed in terms of Q_s :

$$Q_r = 0.15 Q_s - (0.01 Q_s)^2$$

Relevant measurables for determining insolation are those that deal with atmospheric transparency, i. e., cloud cover, haze, fog, other aerosols, etc. Visible imagery along with measurements made in the IR and microwave portions of the spectrum can be used to determine atmospheric transparency.

The value of the satellite system would, of course, be its ability to provide the data for calculations of cloud cover on a synoptic scale, while airborne and surface-based observations would be used, as they are now, to provide more detailed, local measurements.

While the results, in terms of determining the quantity of heat actually absorbed by the ocean, would inevitably be more akin to estimates than to measurements in the strict sense of the word, the gradual

accumulation of historical data would contribute substantially to the overall objectives of the EOS mission, which is to provide just this kind of baseline information.

4.1.2 The Polar Ice Caps

Though the general atmospheric circulation is forced by uneven distribution of heating between the equator and the poles, variations in equatorial heating and polar cooling are poorly understood and little studied, largely because of the paucity of relevant data over the oceans. Yet it has been discovered that significant anomalies in the exchange of heat and moisture between the ocean and atmosphere do occur* and that these anomalies are closely related to variations in the dynamic behavior of the atmosphere or, in a word, the weather.

For the Arctic region, anomalies of heat exchange and related variations in atmospheric circulation have been investigated in great detail by Soviet scientists, and are receiving increased attention elsewhere. For the Antarctic regions, however, such studies have not yet gotten underway, largely because adequate data have been lacking. It is here that a large contribution can be made by a satellite. The problem, simply stated, is to gather data on the seasonal variations in the extent of the ice caps (which satellite-borne imaging systems can do synoptically and, for all practical purposes, continuously) with a view to roughly measuring their effect as regulators of the heat exchange between ocean and atmosphere.

It has been suggested that such variations may be an important factor in amplifying the climatic effects of small changes in global insolation. Fletcher⁽¹⁾ has investigated this hypothesis and has shown that variations in the extent of polar ice should have a considerably greater influence on thermal forcing of the atmosphere during the fall and winter than during the summer. Bjerknes⁽²⁾ has indicated that monitoring the extent of the ice in the Southern Ocean on a continuing basis is an essential task in the development of extended-range forecasting and in understanding air-sea interactions.

*The North Atlantic was the first ocean area to be studied, followed by the whole Atlantic; in recent years, emphasis has shifted to the Pacific, where even larger anomalies of ocean/atmospheric heat exchange have been found to occur, in both the equatorial zone and the mid-latitudes.

Annual variations in the area covered by pack ice are about five times larger in the Antarctic than they are in the Arctic and range from about 8 percent of the Southern hemisphere to less than 1 percent.

While the overall problem is to record the major variations in heat exchange over the oceanic regions, the specific contributing factors that a satellite system can measure over the polar regions are:

- Location and extent of pack ice, open leads, and polynyas, especially in winter
- The distribution of ice and open water in both space and time
- Variations in mean albedo.

These observations of thermal forcing patterns should be part of a continuous program that will yield reliable and permanent data on year-to-year variations of the Arctic and Antarctic heat budgets and the interactions between the polar oceans and their peripheral areas.

In addition to this basic information, satellite surveillance of the polar regions can, of course, provide meteorologists with data that are of more immediate interest for short-term and long-range forecasts as well as with specific indications of the movement of ice toward warmer latitudes and therefore into the shipping lanes, where they become hazards to navigation.

4.2 THE RESPONSE PATTERNS

In their most obvious manifestations, the response of the global ocean and atmosphere to the forcing functions of heat and cold are simply those that have been repeatedly observed by existing weather satellites. The present and planned sensing capabilities of these satellites are shown in Appendix D. For example, imagery in the visible spectrum can show in time the rate at which evaporation and condensation are operating in a given area to form clouds. With an indication of wind direction (which can be deduced from the movement of the clouds) and the temperature of downwind areas (mapped by infrared spectrometry) precipitation forecasts can be made. In areas where temperatures are low enough, predictions can be made of snow and hail precipitation.

With the EOS sensors, discussed in Sections 3 and 7, some refinements of weather forecasting techniques should be possible. The microwave spectrometer and glitter sensors, for example, can provide an indication of sea state, from which wind velocity can be deduced, and this could improve the accuracy of weather forecasts with respect to time. The Synthetic Aperture Radar would also provide substantial improvements in ice-mapping, as compared with any instruments that are available or planned for purely meteorological satellites.

An oceanographic-dedicated satellite would provide one unique additional capability in the ocean color sensor and this, taken in conjunction with the refinements discussed above, appears to justify such a specialized system. Further justification lies in the very real advantages to oceanographers of having a complete observation platform and data-processing system in one coordinated package. For, instead of having to search for relevant atmospheric profile data in other, unrelated systems, they would have their own data, all generated simultaneously by their own system so that correlation would be virtually automatic and the entire data management problem would be substantially reduced.

Apart from weather (which in its extreme form as major storms can, of course, endanger shipping and coastal life and alter the configuration of vulnerable shorelines, shoals, and similar features), the oceanographic satellite would provide a record of such long-term geophysical changes as the evolution of coral formations and of islands or coastal features created by volcanic activity. This information would be immediately applicable to the drawing of new charts and the revision of existing ones as well as to the relocation of aids to navigation.

The system would also, by means of the ocean color sensor, record the changes in course and configuration of the ocean currents and the divergences, convergences, and other features which affect upwellings and overturns. These phenomena are more relevant in their practical effects, however, to the management of living marine resources than they are to basic research on physical ocean phenomena. They are, therefore, discussed in the next section.

GENERAL INFORMATION NEEDS

OBSERVABLE PHENOMENA

PARAMETER

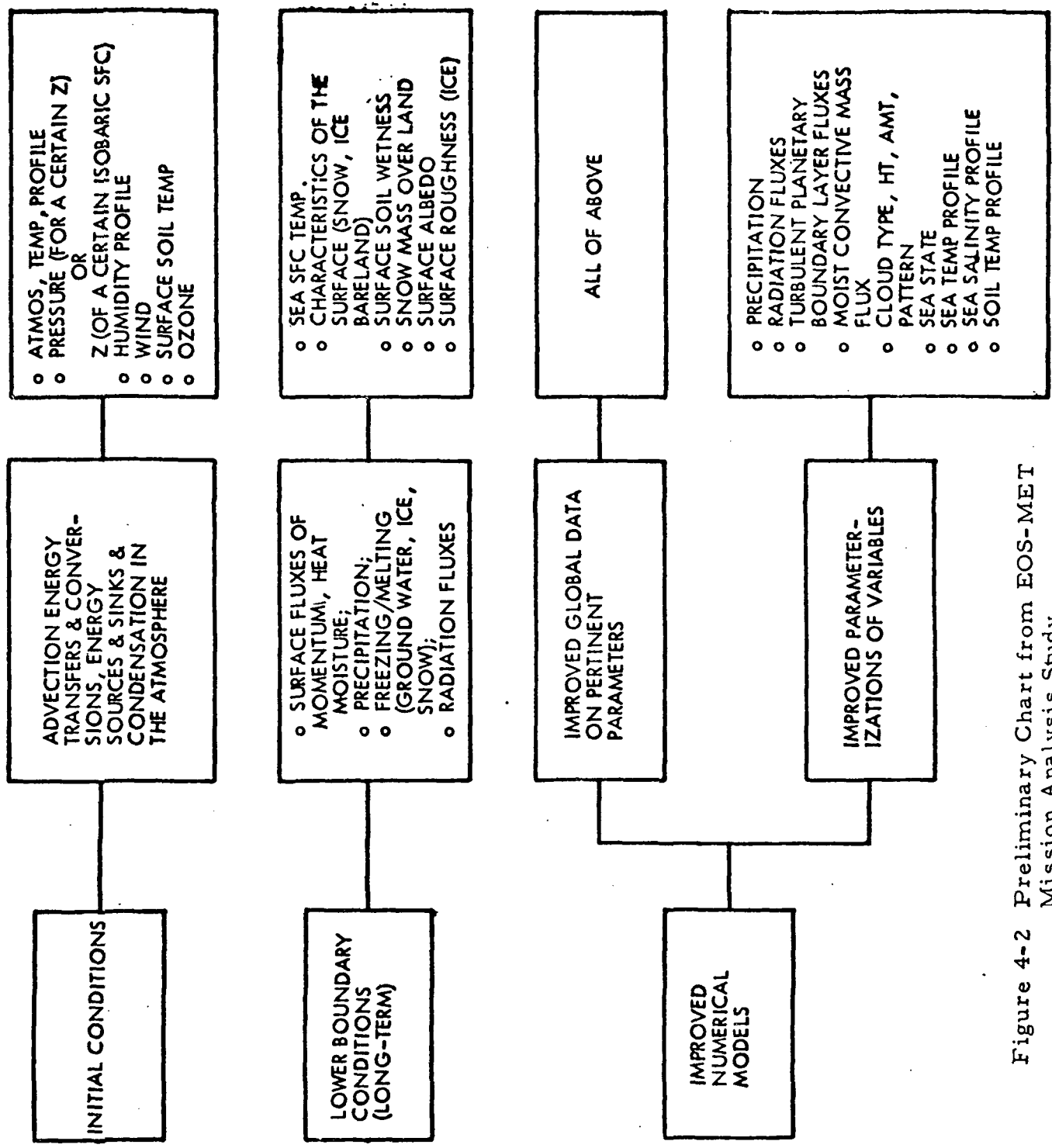


Figure 4-2 Preliminary Chart from EOS-MET Mission Analysis Study

REFERENCES FOR SECTION 4

- 1) J. O. Fletcher, Personal Communication, National Science Foundation, Washington, D. C., November 1971.
- 2) J. Bjerknes, Personal Communication, UCLA, November 1971.

5. MANAGEMENT OF LIVING MARINE RESOURCES

Most experts agree that agriculture is approaching the limits of its ability to meet the nutritional needs of the present world population. Even with the advances in agricultural efficiency that have been made in recent years, the majority of the present population is still grossly undernourished. Further increases in production appear to be limited not only from the technological point of view but also by the amount of additional land that can be made arable. So, in order to meet the needs of the populations projected for the remainder of this century, it is estimated that world food supplies will have to be approximately doubled by 1980 and tripled by the year 2000. If, as seems inevitable, agriculture is unable to sustain anything like so large an increase, the oceans will have to be exploited to the greatest possible extent in an attempt to meet the need.

Ryther⁽¹⁾ states that the world's fisheries produced some 60-million metric tons of food in 1967 (though this figure has since been questioned) or between two and three percent of the world's total food production.

Estimates of the amount of food the oceans may be capable of producing vary widely, as shown in Table 5-1. Whatever one's estimate of the total resources may be, however, it is obvious that huge increases in the efficiency of seafood harvesting (particularly of underutilized* marine organisms) are absolutely necessary.

Russia and Japan are well aware of this need and are aggressively developing their fishing capabilities. Russia, alone, for example, budgeted nearly \$3-billion a few years ago to provide the new capital equipment required to double their production over a five-year period.⁽²⁾ In contrast to this active expansion, the fishing fleets of the United States (which is the world's largest importer of fish) are actually shrinking and the U. S. catch is declining.

*The already dangerous over-exploitation of such species as tuna underlines the need to go down the food chain to organisms which are capable of providing high nutritional values with greater efficiency than the more complex organisms, such as large fin-fish.

Table 5-1. Estimates of Total Ocean Yields of Aquatic Animals (2)

Author	Forecast (Million Metric Tons)	Year	Method
Thompson	21.6	1949	Ext.
FAO	55.4	1955	Ext.
Finn	50 to 60	1960	Ext.
Graham and Edwards	55 (bony fishes)	1962	Ext.
Meseck	55 (by 1970)	1962	Ext.
Graham and Edwards	60 (bony fishes)	1962	Ext. f.
Schaefer	66 (by 1970)	1965	Ext.
Meseck	70 (by 1980)	1962	Ext.
Alverson	80	1965	Ext.
Bogdanov	70 to 80	1965	Ext. f.
Graham and Edwards	115 (bony fishes)	1962	f.
Schaefer	160	1965	Ext.
Schaefer	200	1965	f.
Pike and Spilhaus	200	1965	f.
Chapman	1000	1966	f.
Pike and Spilhaus	180 to 1400	1962	f.
Chapman	2000	1965	f.

Ext. - Extrapolated from catch trends or existing knowledge of world fish resources.

f. - Flow of material through food chain.

From a purely nationalistic point of view, therefore, there is an urgent need to encourage the building and manning of new and much larger U. S. fishing fleets. There is an equally urgent need to increase the efficiency of our fishing operations by guiding the fleets to the most productive fishing grounds (with a minimum of time spent hunting for schools*) and to provide greatly improved information on weather and other hazards that reduce operating efficiency and endanger lives.

*A high-seas tuna boat, to cite only one example, normally spends more than 85 percent of its on-ground time in searching for schools.

Beyond these immediate needs, however, there is an evident long-term need for international cooperation in the management of worldwide marine food resources to ensure that the ocean's maximum sustainable yield is both attained and maintained instead of being diminished by uncontrolled exploitation. The legal agreements and technical methods of ensuring effective management can only be developed if solidly factual information (on the size of harvestable fish stocks and the factors that increase or decrease them) is both available and kept constantly up to date.

As indicated in Section 3, no presently feasible satellite system can provide information that is directly usable for this purpose. But it is well within the capabilities of current technology to provide indirect data (on wind and current patterns, water color, sea state, etc.) which show where harvestable stocks are likely to be and indicate the dynamic phenomena that affect their size, well-being and harvestability. Only by judicious use of such data, in combination with more precise surface and airborne measurements, can mankind hope to plan for intelligent use of these desperately needed food resources and to control their exploitation effectively.

The information that is required to provide a basis for improved management breaks down into three categories: The dynamics of abundance and scarcity of the various resources, the measurement (or inventorying of the size and distribution of specific stocks, and the factors which affect the harvestability of those stocks that are nutritionally (either directly or as organic agricultural fertilizers) valuable to man.

5.1 DYNAMICS OF RESOURCE ABUNDANCE

The factor that most obviously indicates the abundance or scarcity of all other marine organisms is the fundamental element in the food chain, phytoplankton. While various types of planktonic plants are found at various depths in the ocean, most of them are either at the surface or near enough to it to be visible to a spaceborne water color imaging system. And, where plankton blooms, the higher marine organisms all the way up the chain are bound to congregate.

By calculating the chlorophyll concentration in plankton beds on the basis of water color imagery, it is possible to make useful rough estimates of the bio-mass in areas of interest because the top-to-bottom depth

of a given aggregation of algae can be assumed to be quite limited (since their well-being depends upon sunlight from above as well as on inorganic nutrients from below) and reasonably uniform in a given area of uniform color.

With accumulated records of such data on a worldwide basis, it should be possible in time (and with the support of additional data from detailed terrestrial observations) to make useful estimates of fish populations, at least of those species that school and feed at or near the surface.

5.1.1 Global Primary Productivity

Lack of synoptic observation of important sectors of the ocean -- areas where dynamic physical processes of variable intensity are responsible for conveyance of nutrient-rich water into sunlit upper strata to support photosynthesis -- is the primary reason knowledge of global primary productivity is so limited at present.

Some of the most productive waters in the world may lie off the continent of Antarctica, yet the extent of this area has never been defined. Experts differ, in fact, as to whether the high productivity that takes place in Antarctic circumpolar waters occurs uniformly over the vast area south of the Antarctic Convergence, or is confined to irregular, discontinuous areas of upwelling close to shore, as is the case in most other parts of the world. The Indian Ocean has also been relatively neglected. While this ocean comprises approximately one fifth of the area of the world ocean, it now produces only about 1/25 of the world catch.

Once the patterns of primary productivity are documented on a global basis, it should be possible to better estimate the global marine food potential. Allowing for energy losses from one level to the next as the food chain is ascended, primary productivity data may be applied to arrive at rough estimates of productivity (maximum sustainable yield) at trophic levels occupied by easily harvested organisms.

Changes in the quantity of phytoplankton pigments in near-surface waters may offer a valuable mesoscale index of variations in the intensity of primary productivity. Much of the world ocean is relatively monotonous insofar as variation in productivity is concerned. Thus, only a fraction -- upwelling zones and coastal water masses -- would require intensive monitoring. These water masses comprise only about ten percent of

the area of the global ocean. It is also in these regions that the level of productivity is extremely high. Annual productivity (grams of carbon/m²) in coastal waters (not counting upwelling areas) is twice the level in the open ocean, according to calculations by Ryther.⁽¹⁾ It is not surprising in view of this that about 90 percent of the U. S. catch is comprised of species that spend at least part of their lives in estuaries or shallow coastal waters nearshore. (The fact that coastal stocks are more easily accessible to fishermen also has something to do with this, however.) Convective overturn of surface waters and wind mixing over shallow thermoclines are agents responsible for high nutrient levels and correspondingly high productivity levels during certain times of the year in higher latitudes. The most intensely productive conditions, however, are associated with upwelling areas.

Annual productivity in upwelling areas is conservatively six times the level in the open ocean province.⁽¹⁾ Additional significance of upwellings to world fisheries derives from the fact that food chains tend to be short here. Harvestable stocks such as Peruvian anchovy and Antarctic krill (a shrimp) feed directly upon phytoplankton. Fishing these stocks minimizes the energy losses (roughly 90 percent at each step along a food chain) that would otherwise occur over the additional steps necessary to produce an organism of harvestable size in other ocean provinces.

Upwellings occur in a variety of ocean situations, e. g., along western coasts of continents, in the turbulence downstream from islands and shoals, and in equatorial areas, where parallel currents diverge in response to coriolis force. Much of what is known about upwellings has been summarized by Cushing.⁽³⁾ Table 5-2 presents some of this information.

5. 1. 2 Variation in Abundance of Specific Stocks

Efficient exploitation and management of living resources requires information to aid prediction of changes in population size. Generally speaking, factors which influence stock size in marine species may be divided into two categories: density-dependent factors and density-independent factors. The former include such factors as size of the parent stock and intraspecific competition for a common limited food supply or for attachment space, in the case of sedentary forms. The latter include extrinsic environmental influences, such as water mass conditions.

Table 5-2. Characteristics of Known Upwelling Areas
(from Cushing³)

MAIN UPWELLINGS

	<u>Season</u>	<u>Length (Km)</u>	<u>Width (Km)</u>	<u>Area (Km²)</u>
West Coast of North America (California Current)				
1. Baja California to Point Conception	<u>FMAMJJ</u>	880	190	169. 10 ³
2. Point Conception to Cape Mendocino	<u>AMJJAS</u>	560	190	106. 10 ³
3. Cape Mendocino to Cape Flattery	<u>MJJASO</u>	800	290	230. 10 ³
West Coast of South America (Peru Current)				
1. Cape Blanco to 10°S	<u>FMAMJJASO</u>	720	400	288. 10 ³
2. 10°S to Arica	<u>FMAMJJASO</u>	1300	170	191. 10 ³
3. Antofagasta to Cape Carranza	<u>DJFMAMJJ</u>	1500	250	375. 10 ³
4. Cape Carranza to 45°S	<u>ASONDJFM</u>	1000	150	150. 10 ³
West Coast of North Africa (Canaries Current)				
1. Freetown to Dakar	<u>ONDJF</u>	800	50	40. 10 ³
2. Dakar to Cap Blanc	<u>ONDJFMA</u>	700	150	105. 10 ³
3. Cap Blanc to Canaries	<u>AMJJAS</u>	1020	300	306. 10 ³
4. Canaries to Casablanca	<u>AMJJAS</u>	1000	150	150. 10 ³
5. Cap St. Vincent to Vigo	<u>JJASO</u>	600	150	90. 10 ³
West Coast of South Africa (Benguela Current)				
1. Pointe Noire to Porto Amboin	<u>FMA</u>	700	50	35. 10 ³
2. Baía dos Tigros to Walvis Bay	<u>DJFMAMJJ</u>	800	300	240. 10 ³
3. Walvis Bay to Orange River	<u>SONDJFMAMJJA</u>	700	300	210. 10 ³
4. Orange River to Cape of Good Hope	<u>SONDJFMA</u>	700	220	144. 10 ³

Table 5-2. Characteristics of Known Upwelling Areas (Continued)
(from Cushing⁽³⁾)

EQUATORIAL UPWELLINGS

<u>Season</u>	<u>North Equatorial Current</u>	<u>Counter Current</u>	<u>South Equatorial Current</u>
September - January	Weak	Weak	Strong
February - April	Strong	None	Weak
May - July	Strong	Strong	Weak
July - August	Weak	Strong	Strong

DOMES

<u>Location</u>	<u>Probable Area (km²)</u>
off Costa Rica	1.5×10^5
off Java	3.0×10^5
off Angola Southwest of Dakar	Possibly a little larger than Java Dome

UPWELLINGS IN THE INDIAN OCEAN AND INDONESIAN REGION, INCLUDING THE SOUTH CHINA SEA

<u>Season</u>	<u>Location</u>	<u>Area (km²)</u>
May	375 km from Cape Guardafui	94×10^3
June and July	625 km from Cape Guardafui	112×10^3
August and September	375 km from Cape Guardafui	94×10^3
October	200 km from Cape Guardafui	61×10^3
May and June	As Salala - Ras al Hadd	126×10^3
July	Ras Fartak - Ras al Hadd	161×10^3
August	Mukalla - Ras al Hadd	217×10^3
September	As Salala - Ras al Hadd	126×10^3
October	Marbat - Al Khalaf	32×10^3
September - October	Alleppey - Guilon	-
?	Trivandrum - Panjin	-
February - March	Off Walthair	-
December - February	Burma Coast	-
August	West Coast of Thailand	-
October - January	Northeast Coast of Thailand	-
April - September	South Vietnam Coast	-

MINOR UPWELLINGS

<u>Location</u>
Gulf of Panama
Gulf of Venezuela
Off Cape Reinga
Off Northeast Coast of South Island of New Zealand

It may be possible, with extremely high-resolution spaceborne sensors, to estimate the sizes of specific surface-schooling fish populations and get some indication of the food and habitat available so that density-dependent factors can be roughly measured. But this takes no account of bottom-feeding species and, even for surface-schooling species, the resolution requirement eliminates density-dependent factors from consideration as observables for an EOS satellite.

Observation of density-independent factors, on the other hand, is very much within the scope of the EOS concept and can provide information for estimates of the likelihood that various species will increase or decrease in a given time period. Thus, adverse environmental conditions are primarily responsible for the prodigious egg and larval mortality rates of most marine organisms, while reduction in size of the adult stock -- especially in heavily exploited (stable) populations -- can result in the release of so few eggs that the population suffers.

Many density-independent environmental factors are broad-scale synoptic influences and, as such, are of interest for remote sensing. The importance of ocean currents to the survival of sardines off the west coast of North America has been explained by Sette.⁽⁵⁾ Sardine larval survival is very low and year classes are weak when the south-flowing California Current is strong and steady, because larvae are prevented from reaching coastal nursery grounds. When the flow is sluggish on the other hand, nursery grounds are accessible, and the corresponding year classes are strong. Cumulative wind data are valuable in predicting circulation patterns of surface waters, and would similarly be useful in predicting the drift of eggs and larvae. Projections of future year class strength of various stocks may then be made on the basis of whether the eggs and larvae are conveyed into favorable or unfavorable areas. Pollution conditions which occur over wide areas may have profound effects on marine resource population dynamics, although the exact nature of such effects has yet to be documented for the most part.

In summary, it may be said that the information most needed for understanding and predicting resource abundance (and controlling the exploitation of key resources so as to maintain the maximum sustainable

yield) is of two basic types. First, the dependence of resource population dynamics upon environmental factors must be better understood. Second, information is needed that will enhance our ability to understand and predict synoptic influences, which give rise to anomalous physical environmental conditions. The major contribution of remote sensing will lie in synoptic coverage of physical environmental processes, in particular:

- Conditions leading to high primary productivity
 - upwellings
 - seasonal convective overturn of high latitude water masses
 - estuarine and terrestrial run-off influences in coastal waters
- Current and water mass displacements
- Variation in location and intensity of oceanic fronts
- Distribution of polluted water

5.2 DISTRIBUTION OF LIVING MARINE RESOURCES

It is axiomatic that the need for improved knowledge of the potential of the global ocean in terms of abundance and sustainable yield of living resources implies the need for knowledge of the macroscale spatial disposition (biogeography) of these resources. This is not enough from the standpoint of practical exploitation, however, as most resource populations are not stationary. What may appear to be fluctuations in abundance of marine resources may in reality be changes in distribution of otherwise stable populations. As a result of evolution and physiological adjustment, marine organisms are adapted to a range of environmental conditions. The range is peculiar to a given species and may be narrow or wide, depending upon the condition and the organism.

In the case of marine organisms with sufficient mobility to achieve a degree of independence of ocean currents (mature stages of most species which are subject to harvest fit this description), suboptimal or lethal environmental conditions often can be avoided. On the other hand, when organisms with limited mobility encounter unfavorable conditions, lethal or sublethal effects may impair reproductive ability or cause death and their population dynamics are correspondingly affected as discussed

above. It follows that the logical places to search for itinerant resources are those parts of the ocean where optimal conditions obtain. The suitability of a given condition is tempered by other conditions; moreover, whether a condition is optimal or not may depend upon the life history stage of the species in question.

Broadly speaking, the biogeography of a species is controlled by the distribution of tolerable environmental conditions. Outside that range, they will not be expected to occur -- within the range, highest probability of occurrence will be over a narrower optimum range of conditions. Evidence is accumulating which suggests that within broad areas of suitable temperature, salinity, transparency, and oxygen conditions, many species (especially pelagic schooling species) concentrate in the neighborhood of discontinuities and aggregate upon concentrations of organisms that serve as forage. It is generally acknowledged that the large-scale distribution of small animals which serve as forage for schooling fish roughly resembles the contemporaneous spatial distribution of surface chlorophyll, and that the latter may thus provide a valuable index of the former. For tuna, at least, the distribution of such biological properties may be the only useful basis for distinguishing areas of probable abundance from areas of probable scarcity within vast areas over which temperatures are suitable.⁽⁶⁾ Thus, it is important to monitor conditions indirectly indicative of the presence of fish.

Our knowledge of conditions and interactions among conditions which determine stock distribution, while limited at present, is the key to reduction of the search time that plagues many fisheries. As a single factor, temperature is the most useful environmental parameter for delineation of fishing grounds. Temperature ranges for tuna species are illustrated in Figure 5-1.⁽⁷⁾ Sea surface temperature happens to be one of the most time-variant fishery-oceanography parameters. Figure 5-2, showing displacements of isotherms during a six day period, illustrates this.⁽⁸⁾

Study of stock migration is fundamental to fisheries research. Many pelagic fish species make use of ocean-wide circulation features for purposes of spawning, feeding and providing nursery grounds for

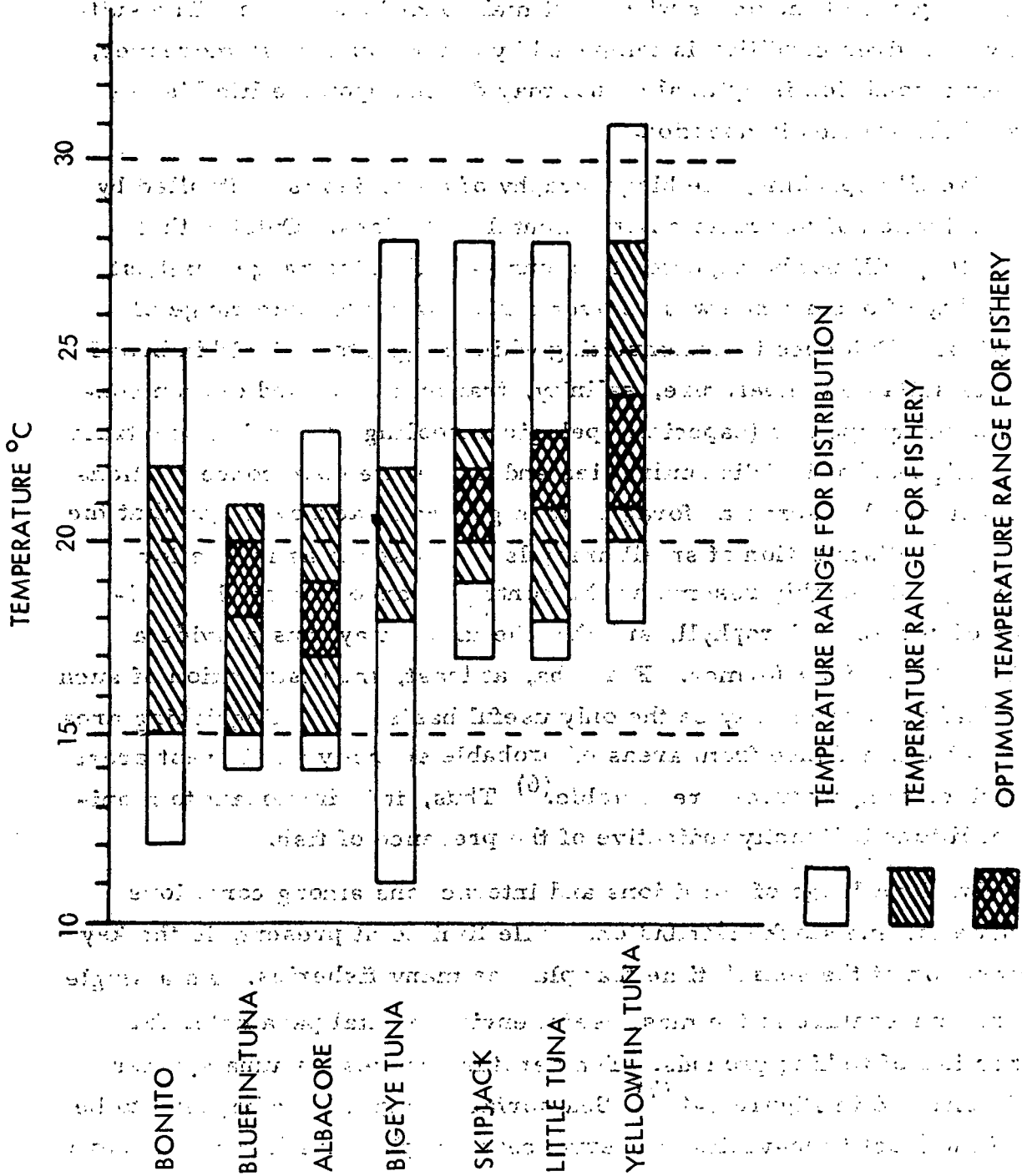


Figure 5-1. Temperature Range for Distribution and Fishing of Tuna Species (from Uda (7))

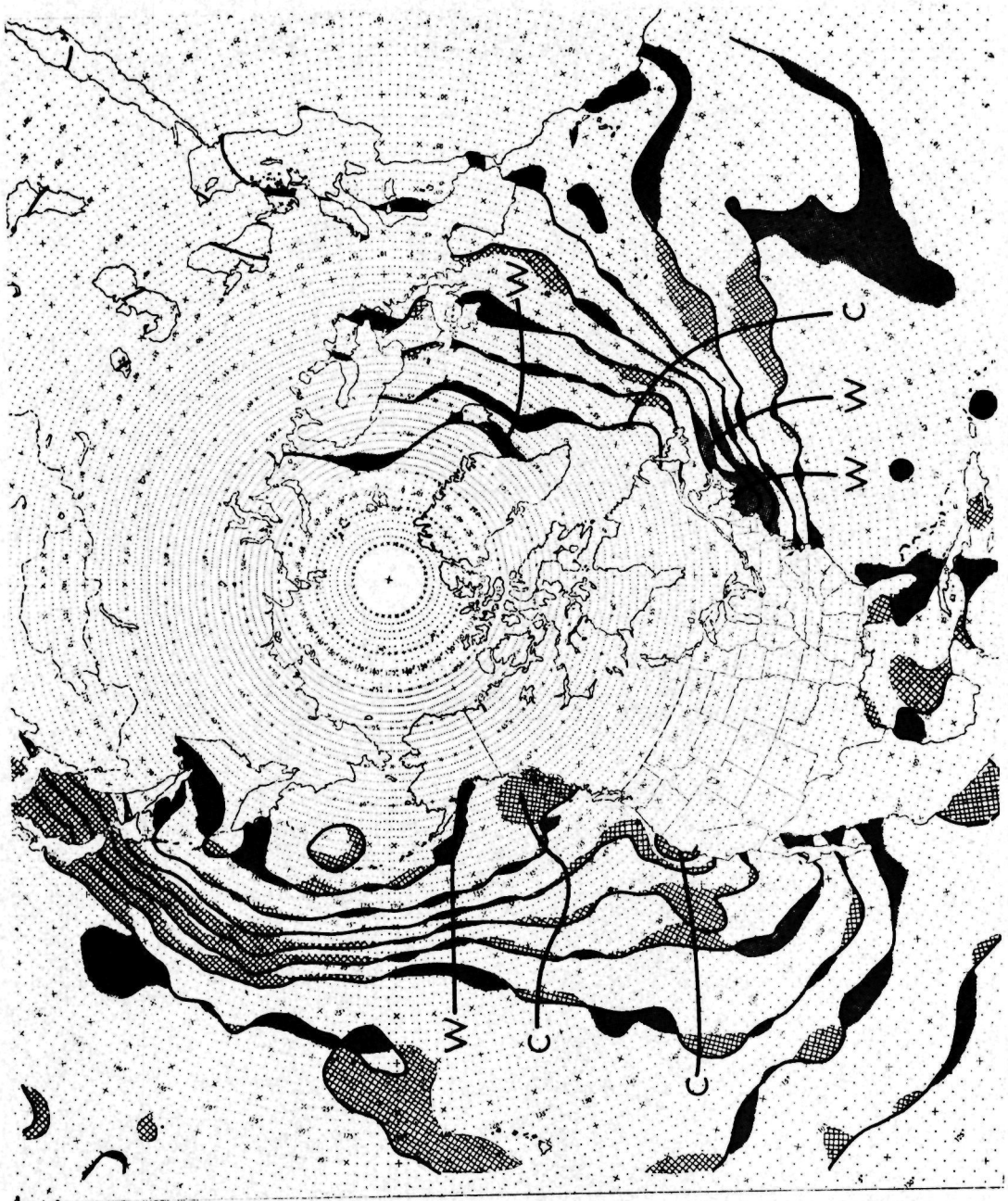


Figure 5-2. Sea Surface Temperature Change from 25 to 31 August 1964
 (from Laevastu and Hubert (8))

their progeny. An example is the albacore (*Thunnus alalunga*), specimens of which have been caught off Japan after having been tagged near California.⁽⁹⁾ Other populations or subpopulations accomplish these functions over a much smaller geographical area. In any case, the basic pattern is illustrated in Figure 5-3.

Eggs and larvae of substantially all marine organisms that represent actual or potential resources are planktonic - they drift with the ocean currents from spawning areas into biologically-rich nursery grounds. The latter are usually upwelling areas or otherwise fertile coastal or nearshore water masses. Larval and juvenile growth takes place in nursery grounds, and, after a period of time, mature individuals arrive in adult feeding areas as new recruits to the particular fishery in question. Active swimming against ocean currents is usually required for adults to reach spawning grounds. Adult migration, consequently, is roughly of the same range as the drift of juveniles. The exact routes taken, time of arrival, and even the location of spawning grounds or feeding areas is subject to the vagaries of ocean water mass conditions. Figure 5-4 illustrates the effect that anomalous temperature conditions may have on the geographical location of fishing grounds, in this case for albacore. The optimum temperature range for albacore fishing is between 17°C and 19°C. The shaded area in the figure shows the area normally bounded by these isotherms during August (long-term average). The cross-hatching shows the area bounded by the same isotherms during the period August 20-25, 1967. It may be seen that the optimum fishing grounds were displaced much closer to the coast during this unusual year. To predict such changes, synoptic monitoring of water mass and current displacements and the factors responsible for them is necessary.

Oceanic fronts are features important to the distribution of certain fish, especially tuna. According to Blackburn,⁽¹²⁾ ocean fronts are "probably best considered as boundaries (lines of convergence) between surface waters of different densities, recognizable by strong horizontal gradients of temperature and/or salinity, and accompanied by some sinking of one or both types of water involved". Fishermen seek fronts because fish tend to be associated with these features. The reasons for the association are not well understood. While data does not exist to

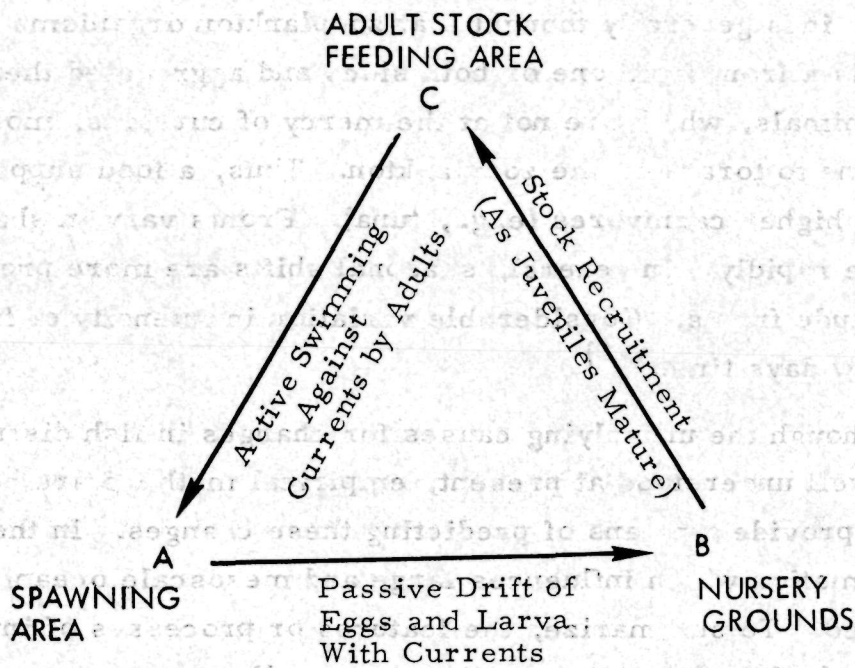


Figure 5-3. Diagrammatic Migration Circuit Used by Fish (After Cushing) (10)



Figure 5-4. Optimum Fishing Areas for Albacore (Cross Hatched) for 20 to 25 August 1967 and for an Average August (from Hela and Laevastu (11))

confirm this, it is generally thought that zooplankton organisms are conveyed towards a front from one or both sides and aggregated there. Larger nekton animals, which are not at the mercy of currents, move into frontal regions to forage on the zooplankton. Thus, a food supply may be available for higher carnivores (e. g., tuna). Fronts vary in sharpness and can move rapidly. In general, seasonal shifts are more pronounced in lower latitude fronts. Considerable variation in intensity of fronts may occur in a few days time. (11)

Even though the underlying causes for changes in fish distribution may not be well understood at present, empirical methods are being devised that provide a means of predicting these changes. In the broadest sense, information which influences large and mesoscale oceanic circulation is needed. To summarize, the features or processes of interest from the standpoint of remote sensing are as follows:

- Location and dynamics of fertile water masses (upwellings, nutrient-rich coastal and nearshore waters)
- Distribution of surface isotherms and isohalines
- Oceanic fronts
- Estuarine and terrestrial run-off effects on coastal water masses
- Water mass and current displacements

5.3 ACCESSIBILITY OF FISHING GROUNDS AND STOCK CATCHABILITY

The kind of information most needed by the harvesting sector of the fishing industry is improved weather forecasts. Weather not only affects a fisherman's comfort and safety enroute to and from fishing grounds, it also affects his ability to find fish and deploy gear once he is on the fishing grounds.

Fishermen ply sectors of the ocean that merchant and military ships seldom traverse. Because of the sparsity of weather reports, vast areas, especially in the southern hemisphere, receive virtually no coverage by existing data assimilation and predictive services.

Reliable reports on existing conditions and near-term (few days) and long-term (weeks) prognoses are most needed by fishermen. Information on wind conditions and sea state is the most important. A great

need exists for improved information on the location, intensity, direction of travel and probable duration of storms and squalls -- especially in isolated fishing areas. Modern high-sea fishing vessels are usually forced to stop fishing when sea conditions reach seven to eight Beaufort (25-40 knot winds). Smaller vessels operating in coastal and nearshore waters are forced to stop much earlier, especially where swell waves resonate with locally-generated wind waves to produce "outsized waves" which can subject gear to enormous stresses.

In high latitudes, icing conditions represent a severe hazard to smaller vessels. This phenomenon occurs where air temperature drops below the freezing point of sea water. Sea spray, driven by wind from wave crests or emanating from bow splashes as the ship encounters large waves, accretes to the hull, rigging, and superstructure of the vessel. Reduction of freeboard and stability may be great enough to cause capsizing. Icing conditions occur typically under the following circumstances -- air temperature between -4 and -7°C , sea water temperature between -2 and 2°C , and wind force of Beaufort 6 or more. (11)

Weather, sea state, and current information is needed to permit effective least-time route planning. In this regard, the most important cause for overall loss of ship's speed is waves. This was discussed above in the section on physical phenomena. Knowledge of current and wind speed and direction is critical to fishing operations. For example, direction of trawling and setting of purse seines is highly dependent upon the ability of crew members to visually spot fish schools. Under heavy sea conditions, fish that normally school at or near the surface may be driven to deeper water. Even under moderate sea conditions, schools at the surface may be very difficult to spot relative to the situation under calmer conditions.

Finally, updated and refined bathymetric charts are in continual demand by fishermen. Accurate charts are important for avoidance of navigational hazards and for location of optimal fishing grounds (e. g., in the vicinity of banks, islands, reefs, and seamounts).

In addition to environmental factors which bear directly upon the fisherman and his ability to locate and catch fish, a number of environmental factors influence the vulnerability of fish to the strategies and gear employed in fishing operations.

According to Murphy and Shomura, ⁽¹³⁾ tightness of schooling in deep-swimming yellowfin tuna -- a factor which affects the number of fish caught by longlines -- depends on the temperature structure of the water. Schools are tightly packed and easily fished in narrow divergence zones. However, when the cool water of a divergence is spread over a wide area, there is little aggregation.

Thermocline topography is particularly important to high seas tuna fisheries. Where the thermocline is shallow, tuna are more easily caught by purse seines, the reason being that the fish are prevented from escape through the bottom of the net because of the cold water directly below the thermocline.

Visibility (water turbidity) may also be an important factor. If a fish is able to see a net in the water, its chances for escape may be enhanced. Water turbidity is especially important in gillnet fisheries.

In summary, the features or processes important in determining stock catchability and accessibility of fishing grounds are:

- Current vector
- Wind vector
- Storms and squalls
- Icing conditions
- Sea state and swell
- Water clarity
- Thermocline topography
- Bottom topography

REFERENCES FOR SECTION 5

1. J. H. Ryther, "Photosynthesis and Fish Production in the Sea," 1970 Science 166 (3901), pp 72-76.
2. M. D. Schaeffer and D. L. Alverson, "World Fish Potentials," in The Future of the Fishing Industry of the United States, University of Washington, Publications in Fisheries - New Series, 1968, Volume IV, pp 81-85.
3. D. H. Cushing, "Upwelling and Fish Production," FAO Fisheries Technical Paper No. 84, 1969, pp 40.
4. K. E. F. Watt, Ecology and Resource Management, McGraw-Hill, New York, 1968, 450 pp.
5. O. E. Sette, "The Long-Term Historical Record of Meteorological Oceanographic and Biological Data," California Cooperative Oceanic Fisheries Investigations Report, VII, 1960, pp 181-194.
6. "Useful Applications of Earth-Oriented Satellites," 1969. Prepared by Panel 5 of the Summer Study on Space Applications for NASA, National Academy of Sciences, Washington, D. C., 104 pp.
7. M. Uda, (from Laevastu, T. and I. Hela, 1970), Fisheries Oceanography, Fishing News, Ltd., 1959, 238 pp.
8. T. Laevastu and W. E. Hubert, "The Nature of Sea Surface Temperature Anomalies and their Possible Effects on Weather," f. N. W. C. Technical Note 55, 1970, 13 pp.
9. T. Otsu, "Albacore Migration and Growth in the North Pacific Ocean as Estimated from Tag Recoveries," Pacific Science 14 (3), 1960, pp 257-266.
10. D. H. Cushing, Fisheries Biology, University of Wisconsin Press, Madison, 1968, 200 pp.
11. T. Laevastu and I. Hela, Fisheries Oceanography, Fishing News, Ltd. London, 1970, 238 pp.
12. M. Blackburn, "Oceanography and the Ecology of Tunas," Oceanography, Marine Biology, Ann Rev. 3, 1965, pp 299-322.
13. G. I. Murphy and R. S. Shomura, "Longline Fishing for Deep-Swimming Tunas in the Central Pacific, August-November, 1952" U. S. Fish and Wildlife Service Special Science Report - Fish No. 137, 1955, 42 pp.

6. MONITORING OCEAN POLLUTION

The principal contribution that a satellite system can make to the eventual control of ocean pollution is indirect. By monitoring areas of upwelling and ocean currents (particularly the zones of convergence and divergence) and similar phenomena, it can provide information of the basis of which terrestrial platforms can be more effectively directed in their efforts to make direct measurements of pollution effects.

Our investigation of all the identified sources of pollution on a global scale indicate that two principal types of pollutants are of major significance:

- 1) Industrial and agricultural chemicals, which are transported to the oceans by the atmosphere, by rivers, and by direct discharge from coastal plants
- 2) Thermal effects produced by (a) industrial waste heat, which is also transported by the atmosphere, rivers and direct outfalls, and (b) atmospheric haze*.

In addition to these main causes of ocean pollution, the study team investigated herbicides, "soft" pesticides, municipal and industrial sewage and other forms of dumping, and petroleum spills. These were deemed to be the domain of fine scale and/or local investigators, however, because they are relatively short-lived and local in their effects.

Oil spills have, of course, received wide publicity and have done much to alert the public to the dangers of pollution in general. Their effects are locally lethal to wildlife, temporarily ruinous to beaches and dramatically useful as a stimulus to public awareness of the larger problem, but they cannot, at present, be considered as long-term global threats.

*The major causes of deleterious atmospheric haze are industrial and agricultural smokes, aircraft contrails, and volcanic dusts. These phenomena can affect the temperature of the oceans by altering the radiation balance of the ocean/atmosphere system as a whole. Variations in solar activity also affect the radiation balance, of course, but are better observed by other means than the satellite system conceived for EOS.

Sewage, soft pesticides, and herbicides are similarly short-lived in effect (according to presently available information) and, though unquestionably dangerous on a local scale, are also best monitored by other means.

The most dangerous pollutants by a considerable margin are the "hard" agricultural and industrial chemicals, that is heavy metals, chlorinated hydrocarbons, and radionuclides. The first two of these are widely distributed in huge quantities and all three are both highly toxic and long-lived. They enter the marine food chain at the primary level and become increasingly concentrated as they rise through the hierarchy of marine organisms. The result is that some stocks of large edible fish have already become too contaminated for human consumption. The effects at the primary level, however, are of greatest interest to this study because by monitoring standing stocks of phytoplankton (particularly in areas of high plankton concentration), a satellite system should be able to provide an indirect but valuable global assessment of damage caused by such contaminants.

Thermal effects, due to either industrial or natural causes, do not appear to be an immediate threat to the ecology of the global ocean but do call for monitoring with a view to establishing control levels for industrial and agricultural sources and applying controls in the event that they do become dangerous.

The remainder of this section treats the two main categories of pollution in somewhat greater detail.

6.1 "HARD" CHEMICALS

This group of pollutants includes heavy metals, radionuclides, and chlorinated hydrocarbons that are used both as agricultural pesticides and in various industrial processes.

The principal sources of the majority of the heavy metals (mercury, arsenic, cadmium, chromium, nickel, potassium, etc.) are industrial plants. One of the most dangerous and widely distributed metal pollutants, however, is lead which emanates principally from automobile exhausts.

It is estimated that some 350,000 metric tons of lead are burned annually in internal combustion engines and that this has increased the lead content of the surface waters of the northern hemisphere by 5-6 parts per billion (ppb) in the past 45 years. The present annual rate of pollution from this source is estimated to be equal to the amount of lead that reaches the oceans as a result of natural weathering. It therefore, in effect, doubles the natural rate. Continued pollution and biological concentration at the current rate will ultimately kill an increasing range of marine organisms.

Mercury is an even more dangerous metabolic poison because its effects are more severe and immediate. It occurs ionically and in such organic compounds as methyl and ethyl mercury, which are more toxic and readily absorbed than the ionic form. Ten ppb of the organic compounds are sufficient to reduce photosynthesis in a representative marine diatom to practically zero, while the currently tolerable limit for humans of 0.5 ppb, has already been exceeded in swordfish. In spite of its high cost, only 48 percent of the mercury used in the U.S. in 1968 was recovered and some 1400 metric tons entered the environment. Worldwide, the quantity at least equals the amount entering from natural sources.

Both common and exotic radioactive elements have been released to the environment as a result of man's nuclear experimentation. To date, none have results in severe global environmental problems. Airborne radionuclides arise primarily from nuclear weapons testing, whereas those from nuclear power plants are primarily waterborne. The incidence of the former is decreasing at present while the latter is increasing.

The chlorinated hydrocarbons include such pesticides as DDT, DDE, aldrin and dieldrin, and a variety of polychlorinated biphenyls used in plastics and rubber manufacturing.

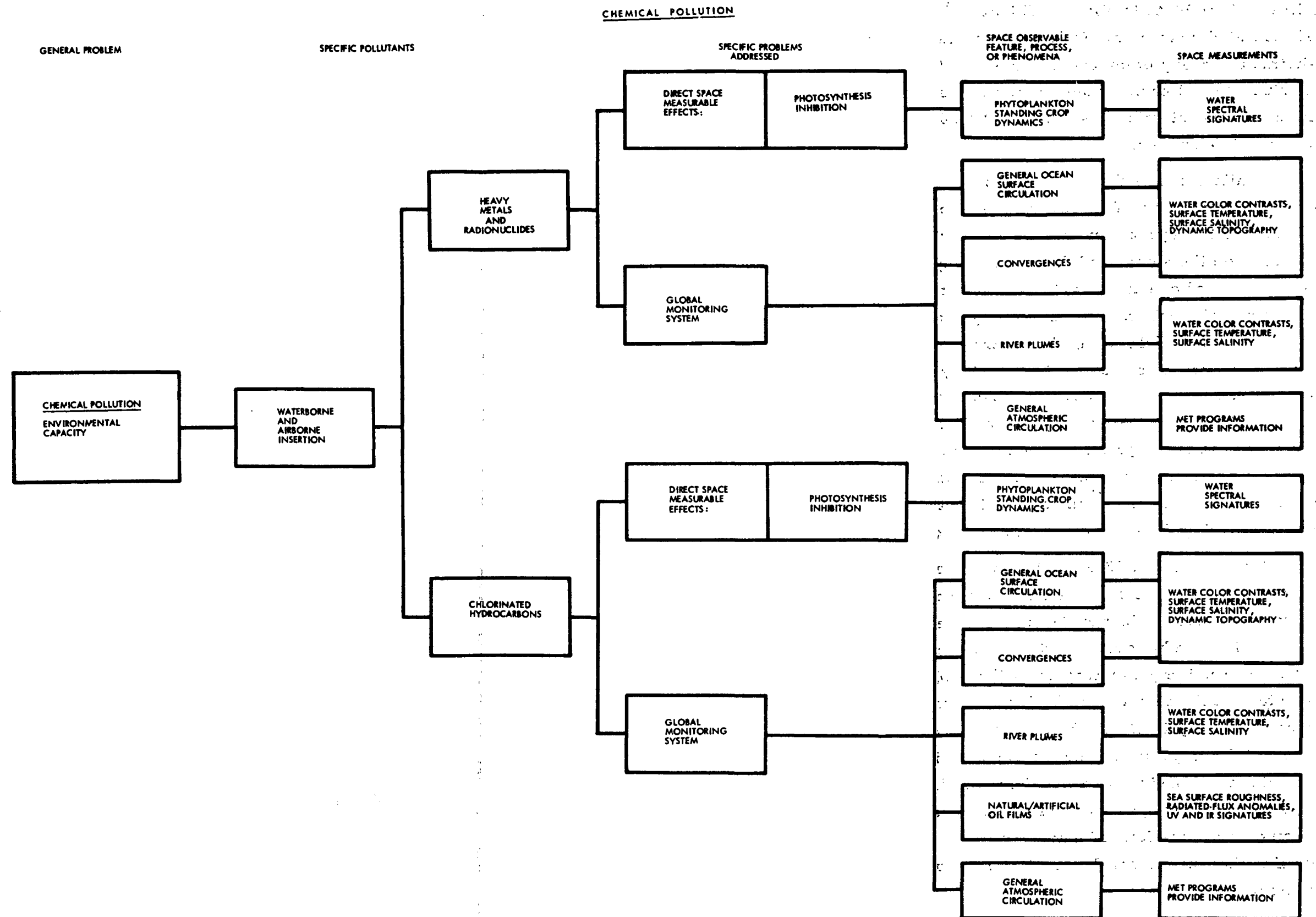
To take DDT as a typical example, it is estimated that some 1,200,000 metric tons have been produced since it was introduced more than 25 years ago. Since it has a half-life of 10-20 years, most of this quantity is still actively dangerous and it is estimated that 25 percent has reached the oceans. Although the mixed layer (that part of the ocean that lies above the thermocline and is subject to turbulent mixing) can probably dissolve ten times the total quantity produced, the danger lies in the ability of oil

films and the biota to absorb DDT at 10^4 to 10^5 times the concentration of saturated sea water. Only a few parts per billion are sufficient to kill shrimp and many other crustaceans and fin-fish. The higher orders of marine life and carnivorous mammals, such as man, accumulate pesticides in concentrations as much as 100,000 times greater than that of saturated sea water.

While some of these pollutants are distributed atmospherically in the vapor state or as dust (or by being absorbed into dust particles), others are transported by water runoff from the land. As they run into or settle on the surface of the ocean, they are further distributed by surface winds and ocean currents. In regions of upwelling (off the coast of Southern California to cite only one typical area), where there are heavy concentrations of plankton, they start to concentrate immediately. Off the eastern coasts of the continents, they are transported by surface winds and ocean currents to the areas of upwelling off the western continental shores. Consequently, there is some delay (and therefore some time for part of the pollutants to settle to the bottom) before concentration begins. Where gyres meet in current convergences, transfers are effected from one major current system to another so that pollution produced by highly developed countries is unquestionably a global problem.

The function of EOS, as the study team sees it, is therefore to map atmospheric and ocean circulation patterns (See Table 6-1) (as discussed in greater detail in Section 4) so that gyres, convergence zones, and areas of upwelling can be located and tracked as they vary in intensity and position. The principal indicators of these phenomena are cloud patterns, sea state, and ocean color which, as shown in Sections 3 and 7, can be measured synoptically by the sensors recommended for EOS. The purpose of this mapping and monitoring activity would be to provide a specific and factual basis for more effective planning and direction of the use of standard oceanographic techniques to gather detailed and precise pollution data at locations of major interest. It is on the basis of these detailed measurements that control measures could be developed and applied.

Table 6-1. Detection, Monitoring and Control of Global Ocean Pollution -
- Space Measurement Requirements



Page intentionally left blank

6.2 THERMAL EFFECTS

While many different types of industrial plants discharge waste heat to the atmosphere, into rivers, and directly into coastal waters, the most readily measurable sources are electric power plants. Recent figures show that world expenditure of energy in 1970 was about 5 million megawatts. This figure is expected to rise to about 10 million MW in 1980 and 30 million by the year 2000. About 80 percent of the waste heat from today's power plants reaches the ocean through river runoff or through direct outfalls. The effects of such runoffs can be measured locally (e. g., the Columbia River plume can be traced thermally to a distance of about 300 kilometers from the river's mouth) but then rapidly disappear in the mass of ocean water. They cannot, therefore, be said to contribute measurably to temperature changes in the global ocean.

A major problem, in enforcement of water quality standards, is the specification of tolerable temperature limits. This requires understanding of the extent of undesirable effects as a function of the level of alteration from the natural thermal environment and an understanding of what the baseline natural thermal environment should be. For example it may be accepted that a 0.5°C change from natural conditions is detrimental to a certain ecological community that we are attempting to preserve but, if we do not know what the natural temperature levels should be, we are unable to prescribe absolute temperature limits above which enforcement of regulations would be necessary. To complicate matters, the natural levels are highly variable with season, current directions, and local weather phenomena. A satellite system dedicated to global mesoscale ocean phenomena may be ideal for determining what natural conditions should be as a function of season, currents and weather. Periodic mapping of large scale temperature changes along coastlines either before or after installation of a power station would provide knowledge of reference levels against which alterations of natural conditions could be measured. It would be desirable to perform mapping on a weekly basis with 0.2°C accuracy and a spatial resolution on the order of 1/2 mile (high sensitivity, low resolution measurements).

The most significant argument against the immediacy of the danger of thermal pollution by industry, however, is the fact that there has been a general atmospheric cooling trend since 1940, which has resulted in a mean global air temperature decrease of nearly 0.3°C. Hubbs⁽¹⁾ shows that changes in the sea surface and air temperature track each other closely so it is reasonable to assume that a slight general cooling of the oceans has also occurred. This is in spite of the rapid increase in industrial output of waste heat since the beginning of the industrial revolution.

Mechanisms which could contribute to such slight but large scale climate changes include:

- Modifications of solar energy input to the global system due to variations in solar activity
- Changes in atmospheric reflectivity (i. e., albedo) due to clouds and suspended particles
- Changes in upper atmosphere emissivity due to contaminants such as CO₂ (greenhouse effect)
- Direct thermal addition due to human activity (combustion, fusion, and fission).

The effects are related by the simplified global energy balance equation:

$$I_o (1-r) A_e + E_e - 4A_e \epsilon \sigma T^4 = 0 \quad (1)$$

where

I_o = solar energy input

r = albedo

A_e = cross-sectional area of the earth

E_e = non-radiative energy due to natural phenomena such as tidal (gravitational) energy and energy contributed by man's activities

ϵ = effective emissivity

σ = Stefan Boltzmann Constant

T = temperature

Substituting knowns into the first term of Equation (1), $I_o = 0.135 \text{ watts/cm}^2$; $r = 0.037$ results in approximately 10^{17} watts for the first term of the equation. Current estimates for E_e are 3×10^{13} watts (man contributes about

one-third of that amount). Thus, man is currently contributing less than 0.01 percent of the solar energy input.

It is interesting to note that some meteorologists feel a one percent change in climate is critical. Such a change would require the contribution through man's activities to be increased 100 times. At double the current rate of power generation, it would take nearly 70 years to bring E_e to one percent of the first term of the equation. The effect of man's activities on global climate seems, therefore, unlikely to constitute a near-term danger. Thermal addition due to other mechanisms, however, should be considered.

From 1860 to 1960, CO_2 has increased from 305 ppm to 345 ppm, a 14 percent increase. Figure 6-1 attempts to correlate sun spot activity, CO_2 and dust-albedo effects. It shows that CO_2 and sun-spot number might account for world mean temperature change up to 1940. Beyond 1940, controversy exists as to the cause of the cooling trend. Most agree that an increase in reflectivity due to dust is the most probable factor. Figure 6-2 implies that dust contribution due to volcanic activity is not

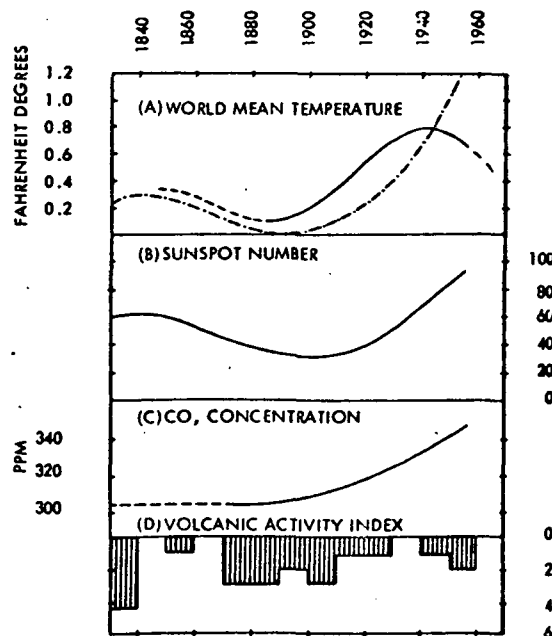


Figure 6-1. Estimated Chronology of World Wide Atmospheric Particulate Load by Volcanic Activity (stratospheric loading only, dotted curve) and by Human Activity (heavy solid curve). (3)

A - COTOPAX
 B - MAJKAN
 C - ASKJA
 D - KRAKATOA
 E - TARAWERA
 F - BANDAI SAN
 G - AWU
 H - SANTA MARIA
 I - SHTYBELYA
 J - KATMAI
 K - SO. ANDES
 L - HEKLA
 M - MT. SPURR
 N - BEZMYANNAYA
 O - AGUNG
 P - AWU
 Q - GALAPAGOS

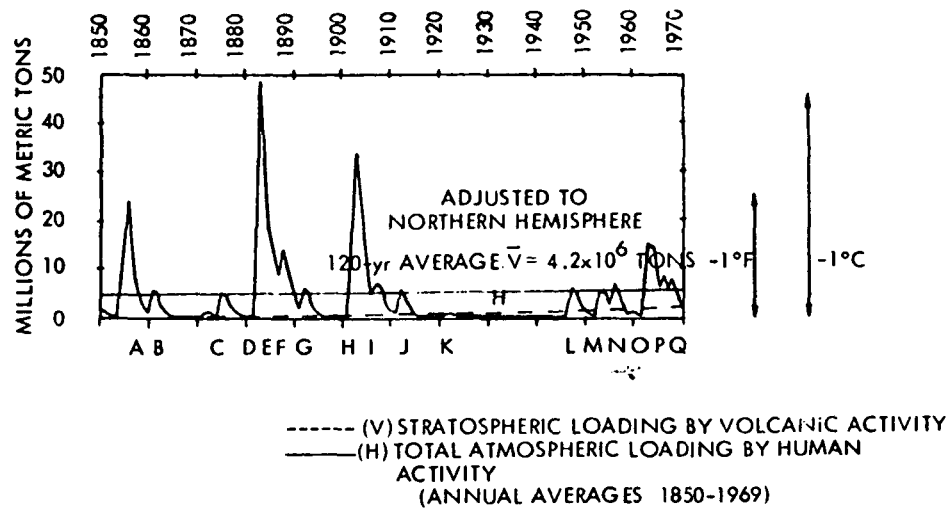


Figure 6-2. Trends of World Mean Temperature, Sun Spot Index, Carbon Dioxide, and Volcanic Activity. (2)

sufficient to account for the cooling trend. If this is the case, other mechanisms that might contribute to climate change include:

- Industrial smoke
- "Blue" haze due to agricultural burning (most of the CO_2 increase noted above has been shown to be linked to agricultural burning and not to fossil fuel burning)
- Increase in cloudiness due to jet contrails (current projections based upon 1500 subsonic jets making 1/2 mile contrails lasting for 2 hours result in an estimate of a 5-10 percent increase in cirrus clouds over the North American-Atlantic-Europe area)

The postulated EOS satellite system (See Table 6-2) would not be capable of measuring the direct effects of these contaminants on the atmosphere since their global effects (as opposed to their readily observable local effects) are still too slight to be detected. This very fact, however, reinforces the vital role of the satellite system as a means of establishing a body of data as a baseline against which future measurements can be made in order to determine the need for control measures.

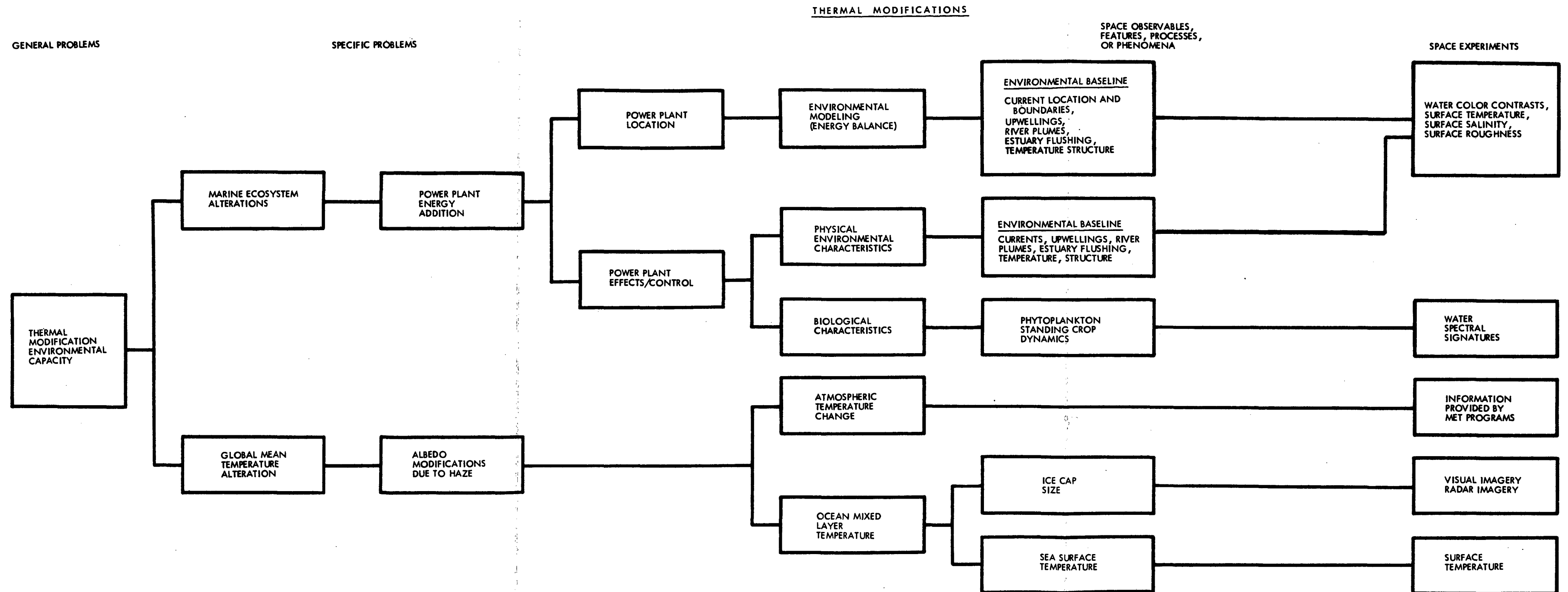
The principal means of acquiring this baseline information would, of course, be the infrared radiometer, which would be used to produce

global maps of sea-surface temperature patterns so that even slight changes could be noted from year to year and more discriminating methods could be developed to determine their specific causes.

Monthly average sea-surface temperatures (that is the temperature of the upper few centimeters of the water) correspond closely to monthly average air temperatures. Based upon the magnitudes of the global temperature changes shown in Figures 6-1 and 6-2, a satellite sensor with 0.1°C accuracy and 1° longitude/latitude spatial resolution is recommended. This would provide spatial averaging of large areas impossible with terrestrial sea-surface measuring techniques. Data should be gathered at least monthly so that an accurate annual average distribution can be assembled for comparison with data gathered by future satellite systems and for comparison with current attempts at averaging of sea-surface measurements.

Page intentionally left blank

Table 6-2. Detection, Monitoring and Control of Global Ocean Pollution -
- Space Measurement Requirements



Page intentionally left blank

REFERENCES FOR SECTION 6

1. Carl Hubbs, "Changes in Fish Fauna," *Journal of Marine Research* VII (3), 1948.
2. Reed A. Bryson, "All Other Factors Being Constant . . . , -A Reconciliation of Several Theories of Climatic Change," *Global Ecology - Readings Toward a Rational Strategy for Man*, Harcourt Brace Jovanovich, Mc, New York 1971, pp 78-84.
3. J. Murray Mitchell, Jr., "A Preliminary Evaluation of Atmospheric Pollution as a Cause of the Global Temperature Fluctuation of the Past Century", *Global Effects of Environmental Pollution*, S. Fred Singer, Editor, Springer-Verlag, New York, 1970, pp 139-155.

7. SENSORS

This section is concerned with the means by which remote measurement of oceanographic phenomena is accomplished. To the layman, it is often difficult to perceive how a spacecraft orbiting the earth at some 500 miles above the sea surface can be even moderately successful in analyzing conditions which, as many oceanographers will attest, are difficult to detect IN SITU. The fact is that state of the art techniques in remote sensing, orbital selection, and data processing combine to satisfy a majority of the requirements delineated in previous sections. Further, new methodology developed as a result of EOS A/B flights combined with instrumentation improvements will provide information even more profound than is now possible.

Perhaps the most significant contribution of the oceanographic emphasis of EOS A/B missions will be the first opportunity for rapid and complete overviews of world ocean conditions. Previously, data collected from ships at sea, buoy systems and aircraft have attempted to observe and measure oceanographic phenomena. However, because many of the phenomena are physically large in scale, an orbiting platform is, in fact, the only practical means for examining the complete picture of oceanic conditions and interactions. However, aircraft, ships, and buoy systems will continue to contribute to global ocean knowledge by providing the necessary confirmation and calibration of EOS A/B data.

In examining the requirements for remote measurement sensors, the data needs in terms of electromagnetic spectral region, spatial resolution, sensitivity, temporal requirements and other requirements defined in Sections 4-6 are converted to conceptual sensor specifications. The means for this synthesis, that is, the physical relationships, hardware capabilities, and practical considerations have been rigorously reviewed in a previous ⁽¹⁾ study as well as in many texts and are well known to the sensor systems design engineer. This section will, therefore, select particular sensor configurations and present specifications with discussions of particular advantages and disadvantages in each case. Analysis is, however, emphasized in areas which were less thoroughly reviewed in the previous study. (Thus, apparent emphasis on particular sensors in this

section is not an indication of mission priorities; the weighted value of the contribution each sensor has to the overall mission is treated in the mission relevancy section.) Each class of sensor (visible imagery, glitter, IR, microwave radiometer, SAR, altimeter) is individually presented. In some cases, such as infrared radiometry, more than one instrument is proposed providing a choice during the payload definition phase of a minimum or maximum emphasis experiment. Presently there are a number of sensors which exist or are currently being developed which closely satisfy the EOS A/B requirements. These are mentioned in the sensor discussion and Section 7.7 Specification Sheets where applicable.

The sensors have been synthesized for a circular orbit having an altitude of 925 km (500 nmi). Increasing altitude generally greatly increases size and weight for a given sensor performance, which is discussed further in detail below. Increasing altitude, of course, allows a greater swath width for a fixed angular field of view. Section 7.7 is a collection of instrument specification sheets describing the proposed sensors. Appendix B consists of requirement summary sheets from which sensor design goals were formulated.

7.1 VISIBLE IMAGING SPECTROMETRY

7.1.1 Sensor Description

The instrument configuration selected for ocean-color measurements is an electronically scanned imaging spectrometer. Energy collected by an objective lens is focused on a slit which determines the instrument field of view. A collimating lens directs the light to a transmission diffraction grating where it is disbursed into a spectrum. A re-imaging lens focuses the energy onto the face of an image tube or detector array. On the face of the tube then, is a two dimensional matrix consisting of spatial elements in one direction and spectral information in the other. The image tube (array) provides both spectral and spatial (line) scans by scanning in a conventional raster. The result is a compact, no-moving-part instrument capable of high spectral resolution and sensitivity for each of several hundred picture elements (pixels) across track. The data output is the

spectral signature of each pixel in a strip map.* An important feature of this configuration is the inherent registration of the spectral energy from each pixel. Figure 7-1 is an optical schematic of this instrument.

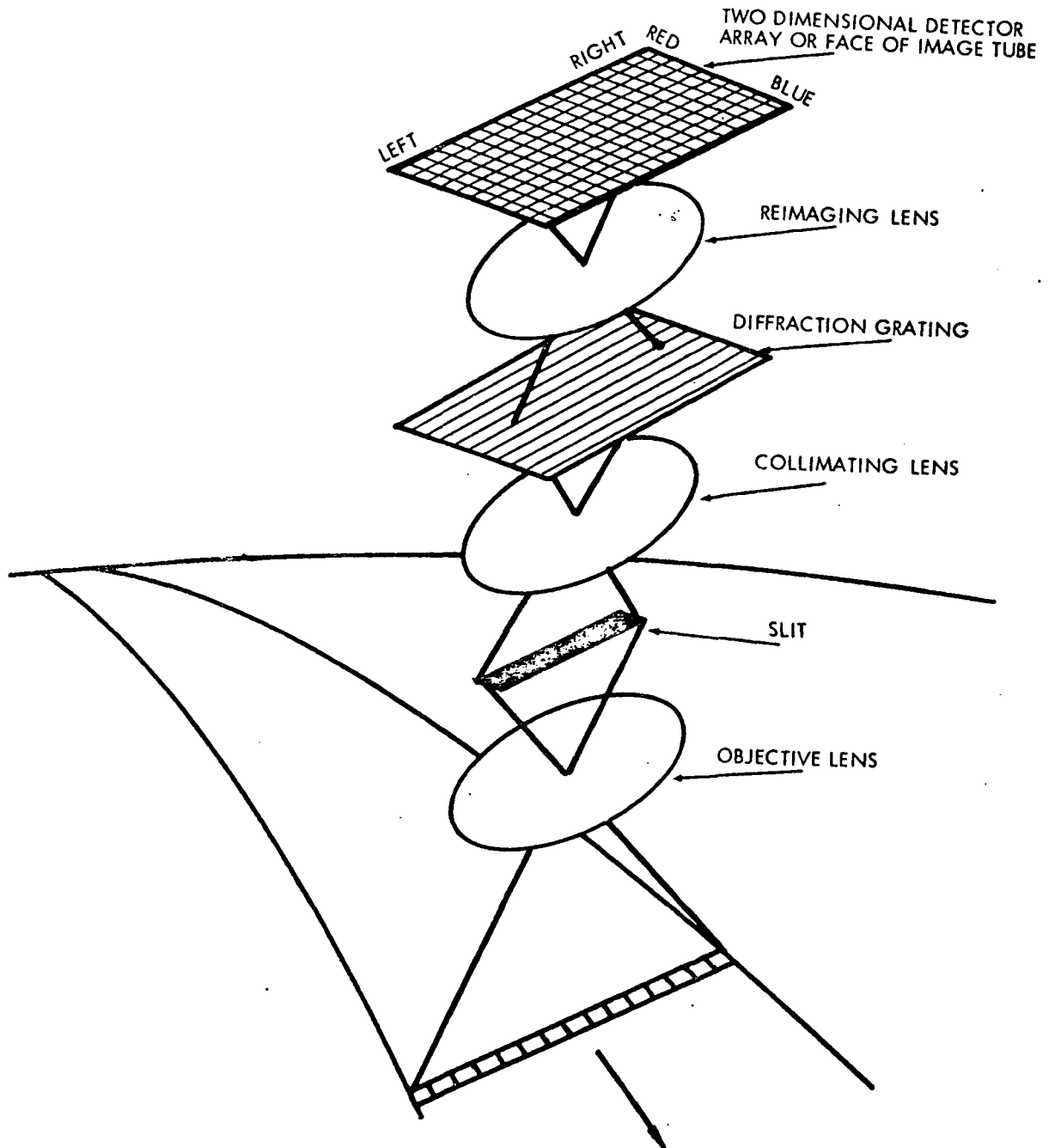


Figure 7-1. Imaging Spectrometer

*Appendix F is a description of ocean color data reduction techniques which obviates the requirement for a complete spectral scan as opposed to selected bands. The work described in this paper was performed under Contract No. N62306-72-C-0037 for the U. S. Naval Oceanographic Office.

Presently there is under development a spaceborne model of this device which very closely satisfies the EOS A/B global ocean requirements. The Multi-Channel Ocean Color (MOCS) experiment of the NASA Langley Advanced Applications Flight Experiments (AAFE) program, principle investigator Peter G. White, TRW Systems, is summarized in Table 7-1 and depicted in Figure 7-2. Figure 7-3 illustrates MOCS sensitivity.

In order to achieve the coverage necessary for global mapping applications, three MOCS sensors could be mounted with their fields of view adjacent providing a swath of 925 km (500 nmi) at 925 km altitude. Other than the obvious reason of redundancy, three sensors are preferred to one because of sun glitter. On occasion, the glitter pattern may contaminate part of the field of view due to high sea state. By having three discrete instruments, any one having glitter in its field of view will isolate saturation or flare effects from the other two.

Table 7-1. Characteristics of MOCS (Multichannel Ocean Color Spectrometer)

	<u>SPACECRAFT</u>
SPECTRAL RANGE	4000 - 7000 Å
SPECTRAL RESOLUTION	150 Å (20 CHANNELS)
FIELD OF VIEW	17.1°
ANGULAR RESOLUTION	2 x 2 mr
GROUND RESOLUTION	1.8 x 1.8 km (925 km ALT.)
S/N	110:1 (5000Å - 45° SUN)
POWER	6 W
WEIGHT	6 KG (13 LBS)
SIZE	19" x 8" x 5"
DETECTOR	F4012 IDT
OPTICS (OBJECTIVE)	F/O.95: 50 MM

An alternate approach to providing the required performance with a single instrument is to employ one or two image intensifier stages ahead of the image dissector tube. This combination, referred to as a "smoothing dissector," would provide an advanced MOCS sensor the increased signal to noise necessary for a single sensor to satisfy the performance requirements (Figure 7-4).

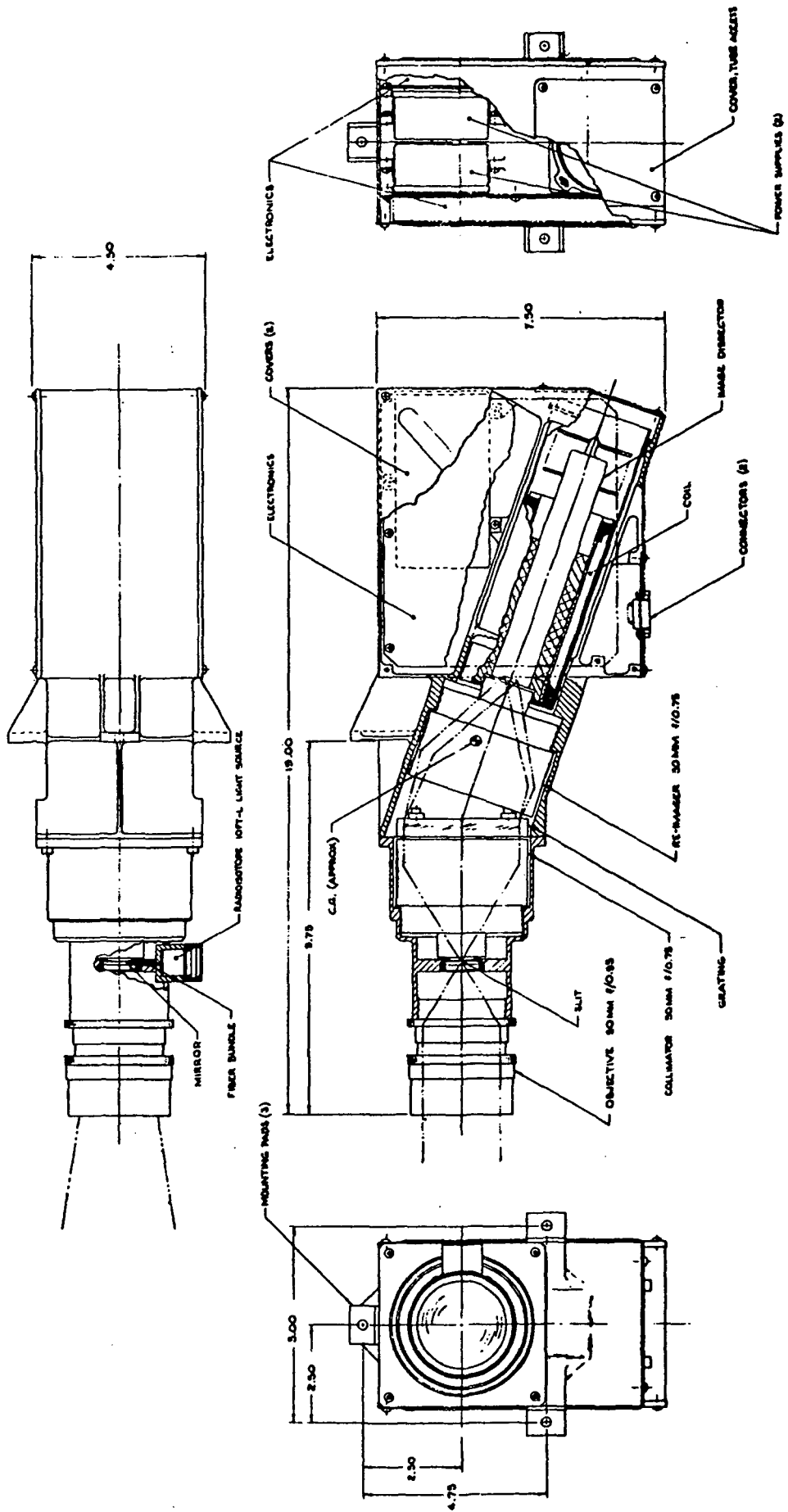


Figure 7-2. MOCS Mechanical Configuration (Dimensions in inches, 1 inch = 2.54 cm)

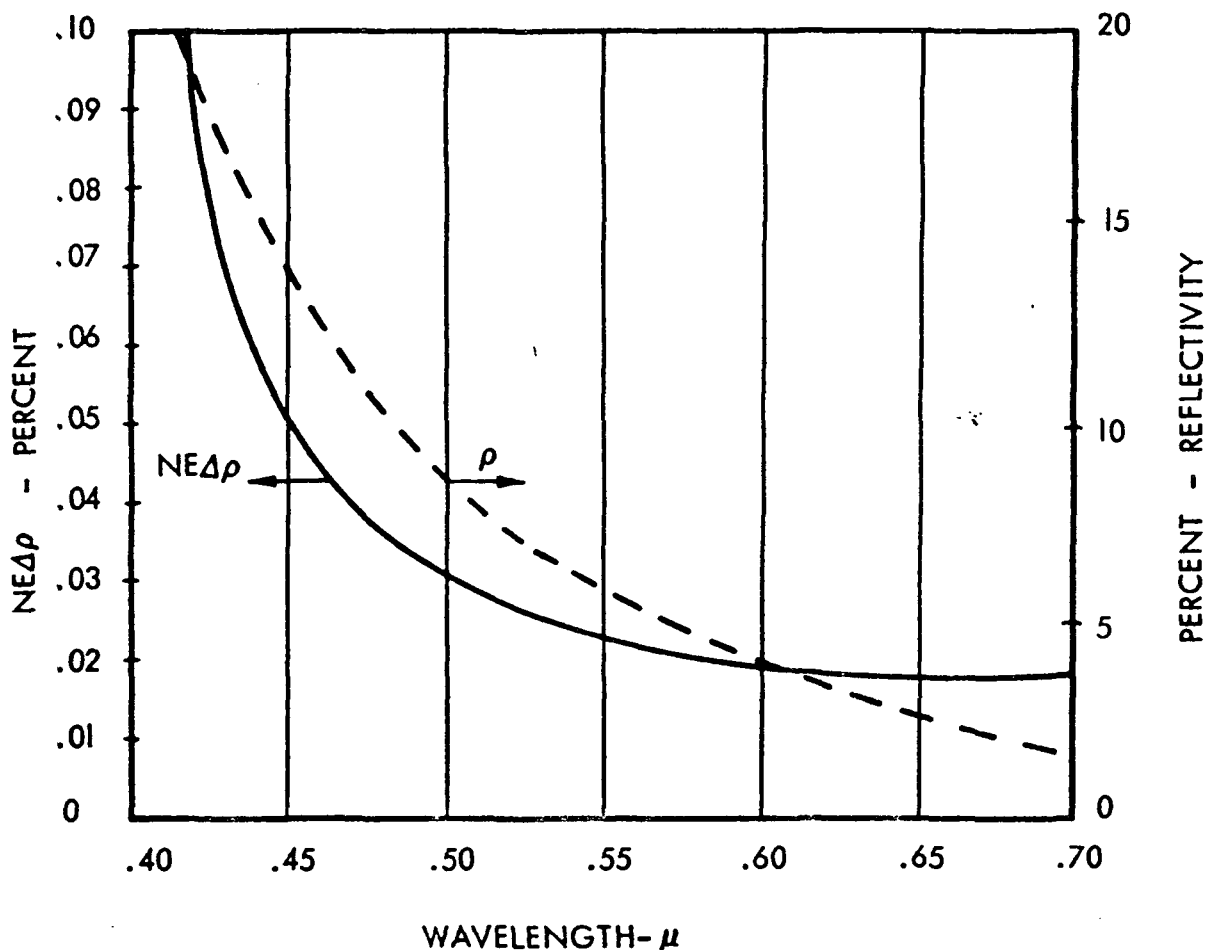
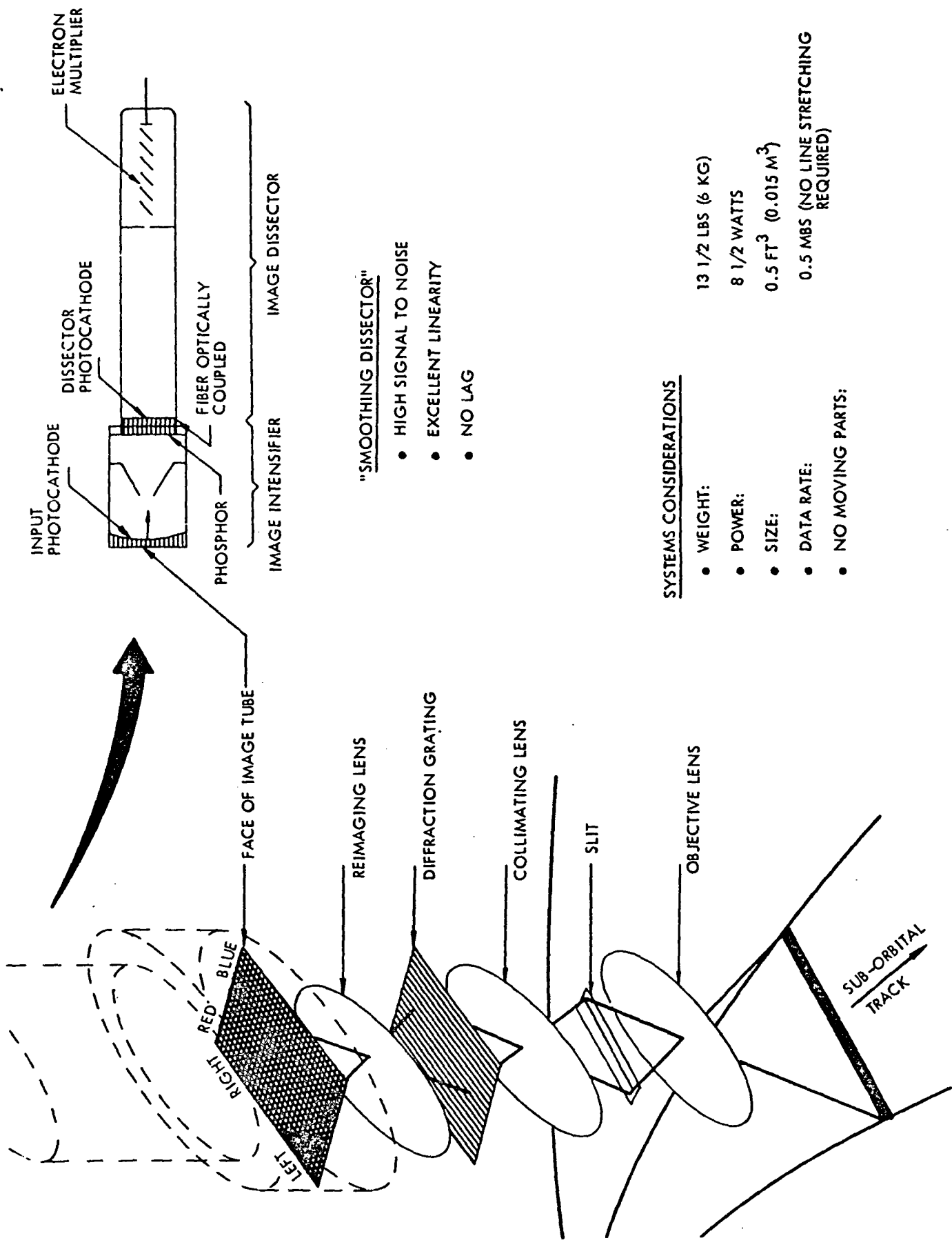


Figure 7-3. Electronically Scanned Oceanographic Imaging Spectroradiometer Performance

The orbit selected for the EOS A/B missions will be 2 pm sun-synchronous. As the spacecraft crosses the equator region, the sun will be at 60° elevation. This produces a glitter pattern to the side of the satellite sub-orbital track. As the spacecraft progresses north or south, the glitter pattern will appear to shift fore or aft. To avoid the glitter pattern a pointing mirror will aim the MOCS sensors field of view to the side perhaps 20° at the equator depending on which position in the orbit data is being collected.

The 2 pm orbit was selected for maximum global coverage taking into account scene contract, haze, glitter and obliquity constraints. Appendix G is an analysis of considerations leading to the choice of a 2 pm orbit. Instrument specification sheets 7.1.1 and 7.1.2 summarize the performance and specifications of the tri-MOCS and advanced ("smoothing dissector") sensor.



"SMOOTHING DISSECTOR"

- HIGH SIGNAL TO NOISE
- EXCELLENT LINEARITY
- NO LAG

SYSTEMS CONSIDERATIONS

- WEIGHT: 13 1/2 LBS (6 KG)
- POWER: 8 1/2 WATTS
- SIZE: 0.5 FT³ (0.015 M³)
- DATA RATE: 0.5 MBS (NO LINE STRETCHING REQUIRED)
- NO MOVING PARTS:

Figure 7-4. "Smoothing Dissector" Version of Imaging Spectroradiometer

7.1.2 Visible Imaging Spectrometry - Rationale for Design Parameters

7.1.2.1 Calculation of Open Ocean Radiances from Satellite Altitudes

Essentially no measurements of the radiances from the open oceans are presently available. The presence of the large particles found in the haze of the maritime atmosphere is expected to reduce the contrast, as seen from a satellite, for the small differences in ocean color which indicate areas of ocean productivity.

Reference 2 gives some measured visible spectral data taken at altitudes up to ten thousand feet over two different water masses. One set is of the sterile Gulf Stream water and the other of a more productive nearby area, as determined by the "ground truth" data showing average chlorophyll content. The Gulf Stream water showed a mean chlorophyll value of 0.07 mg/m^3 , the other water had a mean value of 0.22 mg/M^3 . Values up to 10 or 15 mg/M^3 of chlorophyll may be found at times, but the ability to measure the difference, 0.15 mg/M^3 of chlorophyll may be found at relatively low areas of productivity would be considered a meaningful accomplishment from space.

Figures 7-5 and 7-6 are taken directly from Reference 2 and they show a spectral difference in measured radiance between the two water bodies at the 10K ft altitude. Using these data calculations were made of the reflectivity, and radiance, to be expected from the top of the atmosphere, based upon the following assumptions:

- The measured spectral reflectivities for the 500 foot altitude cases were assumed to be the signals to be measured - in other words, the contribution from the atmosphere below the the altitude is assumed to be negligible.
- The contribution to the total signal from that part of the atmosphere above 10K feet was determined assuming that the atmosphere above 5K feet, over the oceans, was the standard clear atmosphere of Reference 3. This atmosphere, includes haze and ozone as well as the molecular (Rayleigh) component.

Reference 3 lists values of the optical thickness of each kilometer layer of the atmosphere from 0 to 50 km. The amount of solar radiation scattered upward by a layer, i , of the atmosphere is assumed proportional to $(1 - e^{-\tau_i \sec \theta})$, where τ_i is the optical thickness for the layer i and θ is the solar zenith angle. Thus the percentage of the total airlight at the nadir

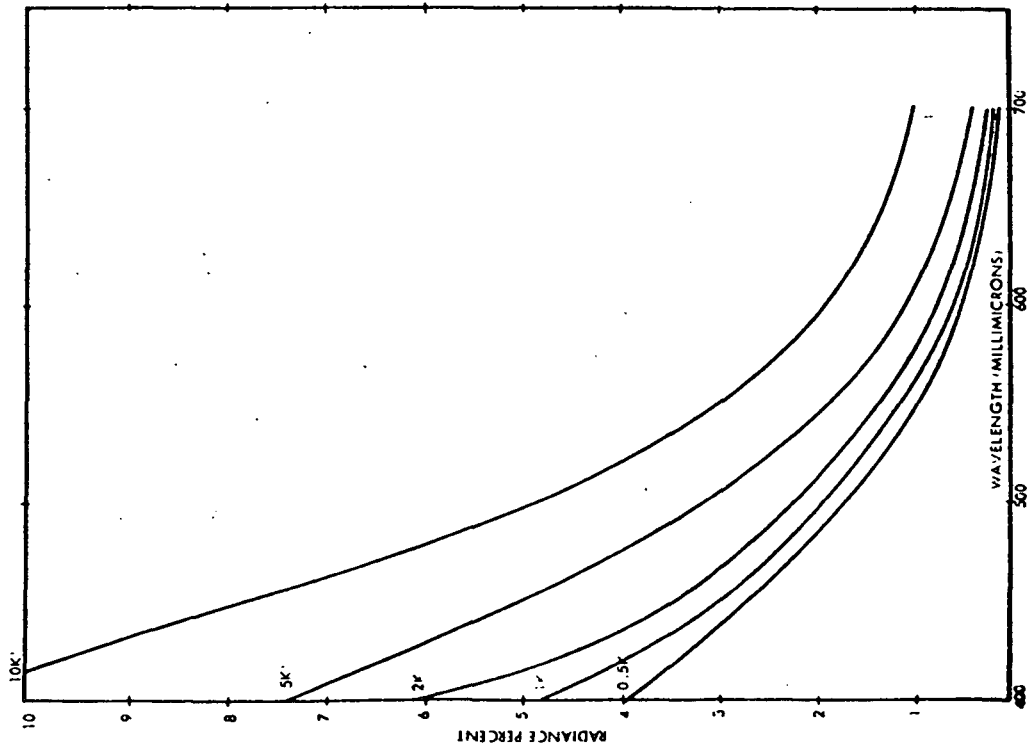


Figure 7-5. Taken from Ref. 1; Spectra Measured over Area with Mean Chlorophyll Value of 0.07 mg/M³

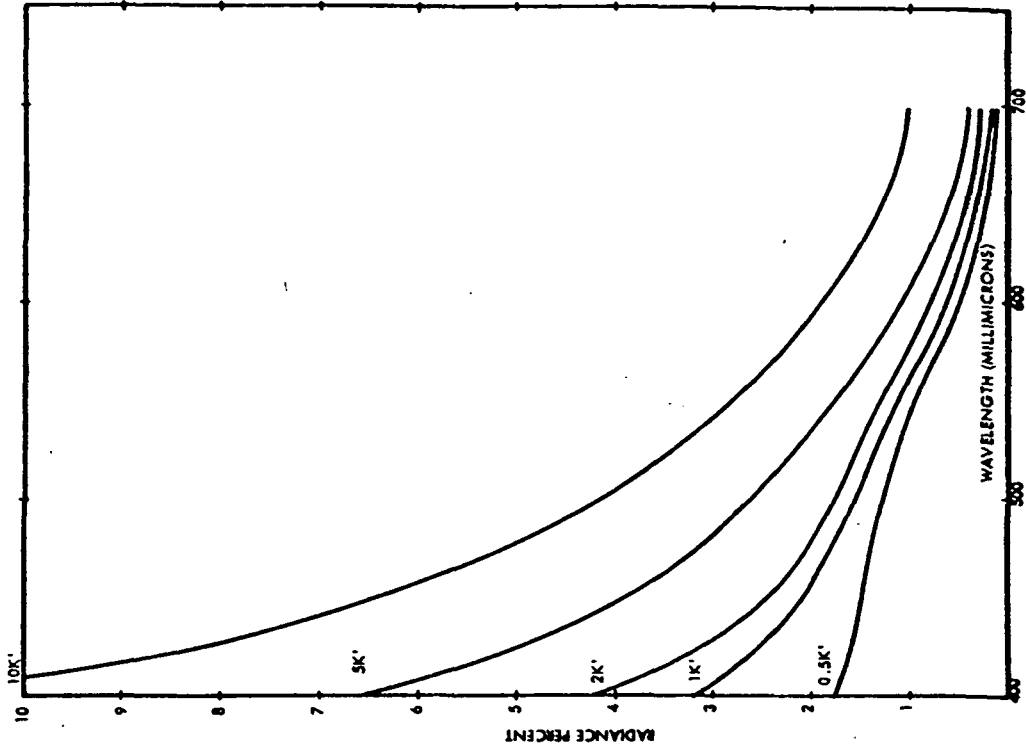


Figure 7-6. Taken from Ref. 1; Spectra Measured over Area with Mean Chlorophyll Value of 0.22 mg/M³

for any altitude H, is

$$100 \sum_{i=0}^H (1 - e^{-\tau_i \sec \theta}) / \sum_{i=0}^{\infty} (1 - e^{-\tau_i \sec \theta})$$

Figure 7-7 is a plot of this percentage for the Elterman standard atmosphere for various visible wavelengths. The ordinate is plotted in units of kilometers, since the data is given in one kilometer layers. * Table 7-2 indicates the procedure followed. The reflectance differences between 5,000 and 10,000 feet altitudes are listed as taken from Figures 7-5 and 7-6 (from Reference 2) and from Figure 7-7, the corresponding percentage contribution to the airlight from the layer between 5,000 and 10,000 is listed as well as that to be expected from above 10,000 feet (all from Figure 7-7). Using the ΔR_L values for the low chlorophyll case (0.07 mg/M^3), somewhat arbitrarily, an example of the procedure used is as follows. At 400 m μ , a value of ΔR_L of 5.2 corresponds to 15.7 percent of the total airlight. Therefore, an additional amount of ΔR (46.7 percent or 15.7) is to be added to the data of Figures 7-5 and 7-6 to obtain the total radiance as seen from above the atmosphere. The last three columns of Table 7-2 show the extrapolated radiances and their difference. These are plotted in Figure 7-8 as the upper two curves.

The bottom two curves were obtained from a series of curves plotted in Reference 4. These curves are plots of nadir spectral radiance from the earth and atmosphere for various values of earth reflectivity. These curves are based upon various authors calculations using the continental air mass models. The earth reflectivities used were the value from Figures 7-6 and 7-6 for the 500 foot altitudes. It is obvious that a much better contrast exists for the continental measurements from space and those from the oceans. It can be shown, however, that these noted differences for the open ocean case should be measurable with present state-of-the-art equipment.

*A Value of 45° solar zenith was used for the cases. These curves remain essentially unchanged for solar zenith angles down to 60° .

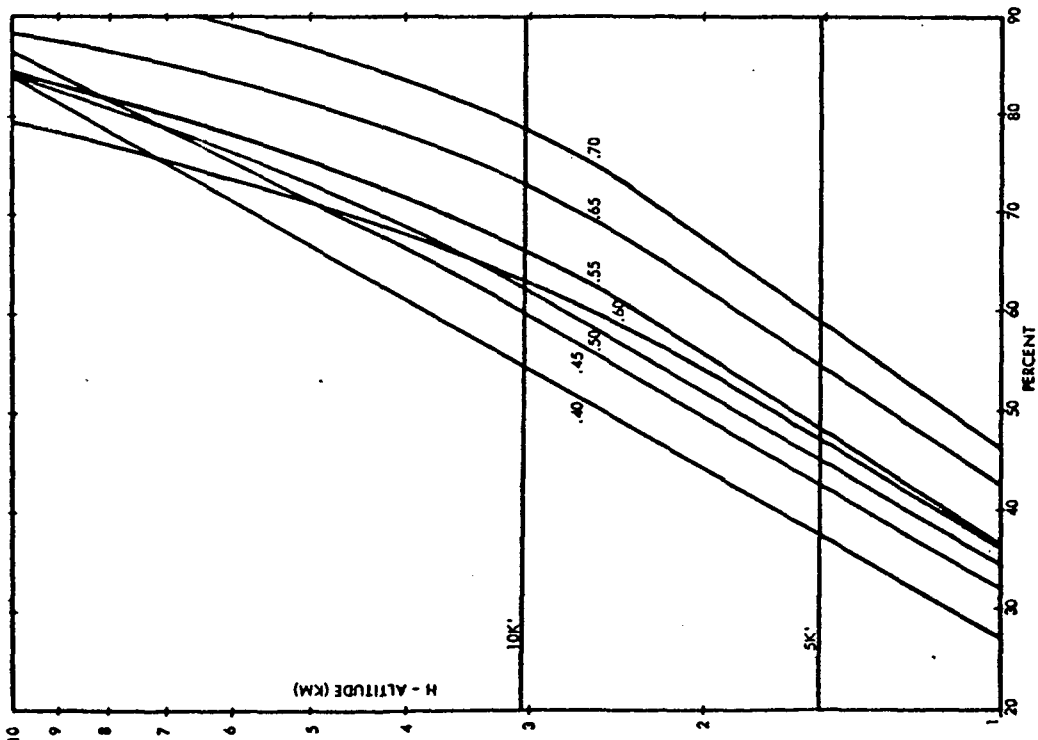


Figure 7-7. Percentage of Airlight versus Altitude at Various Wavelengths

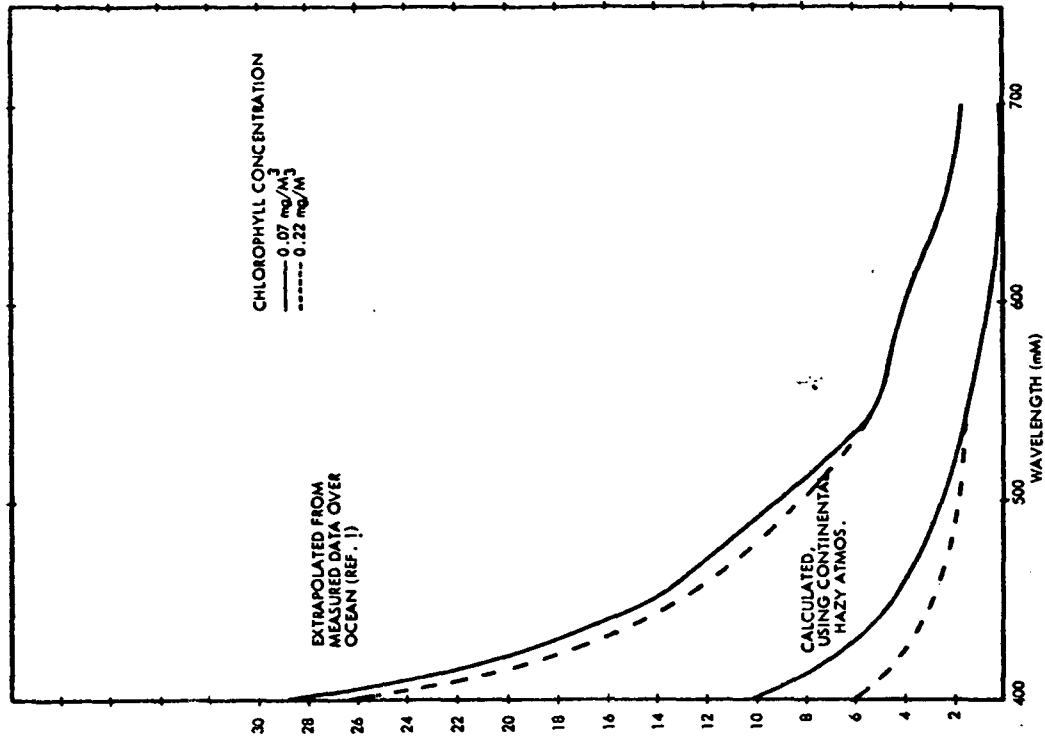


Figure 7-8. Calculated Reflectivity from Ocean and Atmosphere for Two Low Chlorophyll Concentrations Found in Open Oceans

Table 7-2. Calculations of Airlight At Top of Atmosphere by Extrapolating Measured Data of Reference 2

λ (m μ)	Reflectance Diff. Between 5K' and 10K' altitudes (From Fig 1)(From Fig 2)		Percentage Contribution to airlight between 5K' and 10K' (From Fig 3)	Percentage of Airlight from above 10K' alt. (From Fig 3)	Amount of Airlight in Terms of R to be added to that measured at 10K'	Airlight Measured from top of atmosphere (Plotted in Figure 4) (%)		
	ΔR_L	High Ch.				R_L	R_H	ΔR
.400	5.2	4.6	15.7	46.7	15.7	28.4	26.7	1.7
.425	3.7	3.0	16.0	43.3	10.0	19.8	18.0	1.8
.450	2.6	2.4	16.3	40.0	6.4	14.0	12.7	1.3
.500	1.8	1.5	17.0	37.4	4.0	9.0	8.2	0.8
.550	1.1	1.1	18.1	33.4	2.0	4.9	4.9	0.0
.600	0.82	0.82	15.0	36.8	2.0	3.9	3.9	0.0
.650	0.65	0.65	18.2	26.9	1.0	2.3	2.3	0.0
.700	0.54	0.54	19.7	21.2	0.6	1.6	1.6	0.0

Reference 5 gives values of spectral solar irradiance for air masses, $m=0$ and $m=2$, or $\theta=0$ and 60° respectively. These values were interpolated to obtain the solar irradiance, at the earth's surface, for $\theta=45^\circ$. (The reflectivity values of Reference 2 are referenced to solar irradiance reaching the earth's surface.)

Multiplying the values by $\cos\theta$ (since the reference gives values of irradiance on a surface normal to the sun) and dividing by π yields the solar radiance of the earth (or ocean) surface for the solar zenith angles of 45° and 60° . Modifying these solar radiance values by the upper curves of Figure 7-8 results in the curves of Figure 7-9, the expected spectral radiance, or seen from above the atmosphere, for the two cases of 0.07 and 0.22 mg/M^3 of chlorophyll concentration. The radiance differences for the two solar zenith angles are given in the following Table 7-3.

Table 7-3. Calculated Radiance Differences as Seen from Space for 0.07 and 0.22 mg/M^3 of Chlorophyll (units of watts/ M^2 - μ -ster)

Wavelength (millimicrons)	$\theta = 45^\circ$ ΔN_γ	$\theta = 60^\circ$ ΔN_γ
400	2.4	1.4
425	4.0	2.2
450	3.7	2.1
500	2.6	1.6
550	0	
600	0	
650	0	
700	0	

Since the data of Reference 2 was obtained using a nadir viewing angle of 40° , the calculated reflectivities and radiances of Figures 7-8 and 7-9 can be assumed to apply to off-nadir viewing of 40° . In any case, these are "worst case" conditions and these radiances, radiance differences, reflectivities and reflectivity difference values can be used in the design of a system viewing the open oceans from a satellite in the visible region. In addition, it may be noted that there are no differences beyond about

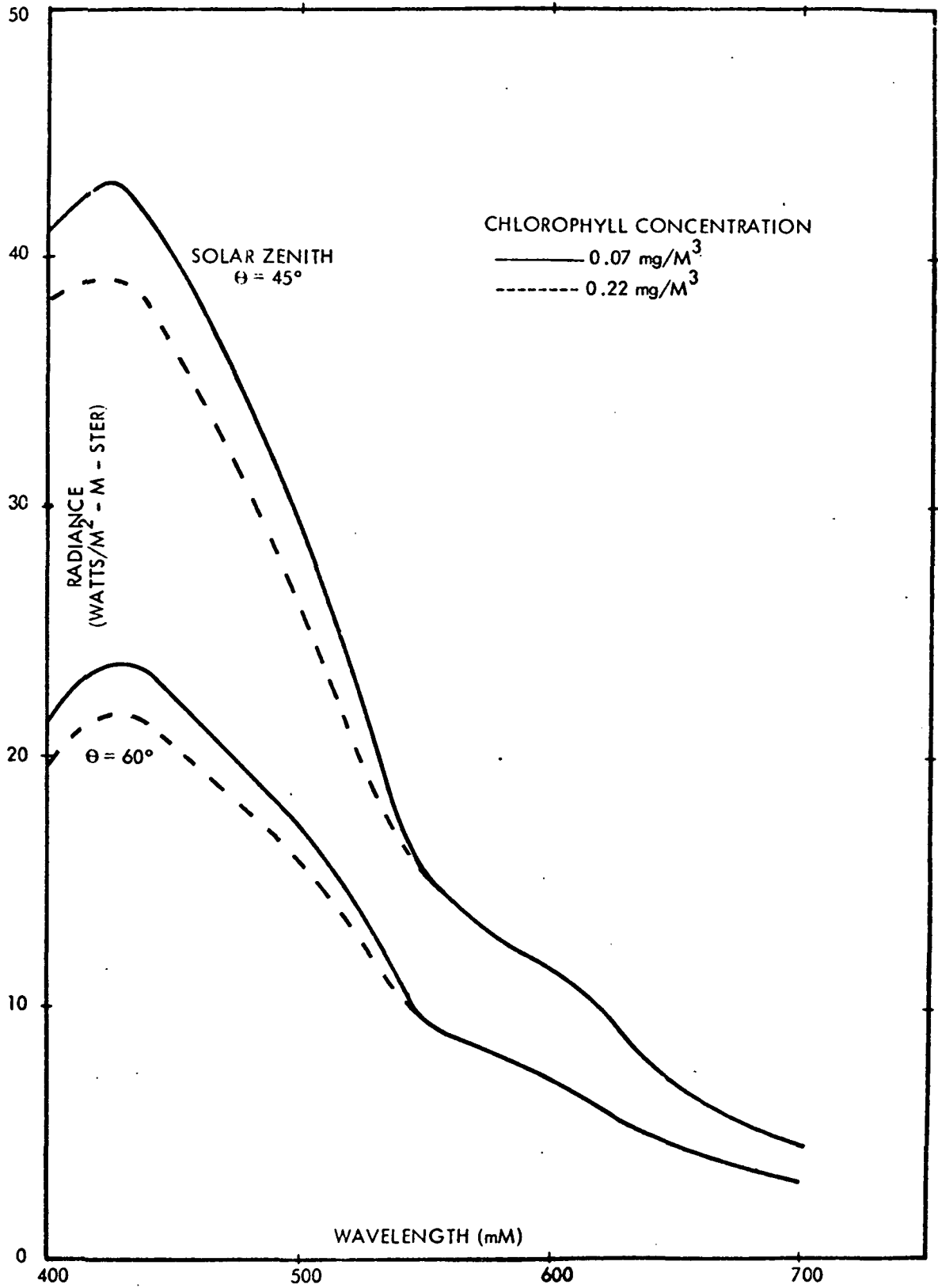


Figure 7-9. Calculated Radiance from Ocean and Atmosphere for Two Low Chlorophyll Concentrations Found in Open Oceans

550 m μ . For the higher values of chlorophyll content, sometimes found in the open oceans, the reflectivity should increase out to about 600 m μ , over the values shown. The contrast, however, should always be higher for the longer wavelengths because the molecular scattering from the atmosphere (Rayleigh) increases with decreasing wavelength. Thus a system designed to meet the wavelength requirements for small chlorophyll changes at low concentrations should be adequate for the larger concentrations.

Reference 2 indicates that a threshold sensitivity to concentrations as low as 0.10 mg/M³ would be meaningful as an index of biological activity. Since the measured data used in this report was for an average difference of 0.15 mg/M³ the reflectance and radiance difference expected from space should be decreased by a factor of a third. Thus a reflectance difference of less than one percent (a value of 0.00087), for the 450 millimicron part of the spectrum is a conservative design criteria.

7.1.2.2 Required Spectral Range for Open-Ocean Color Measurements

In the previous discussion emphasis was placed upon the calculation of the difference to be expected in the radiances from the ocean for areas of low productivity (as indicated by low values of chlorophyll concentration). It was seen that no measurable radiance differences existed beyond 550 nanometers. There are good reasons however for measurements out to 700 nanometers. These are:

- Areas of high productivity (indicated by chlorophyll concentration up to 15 mg/M³) do occur in the open oceans. The upwelling energy from beneath the water in these cases shows a large increase in the green up to about 600 nanometers and beyond. In addition, the narrow chlorophyll absorption band due to chlorophyll a, which is centered at 670 nanometers (Reference 6) may be measurable from space when these high concentrations do occur.
- Shoal areas exist in certain parts of the open oceans which will show the effect of sedimentation and bottom reflectance. Reference 7 shows the effect of increasing reflectance to 600 nanometers as the sandy bottom is observed in shallow waters.
- Although pollution, and various other organisms are more often seen near shore. They can be found in the open oceans, such organism as the "red tide."

Figure 7-10 is a sampling of reflectance curves obtained from low-flying aircraft over waters showing a great diversity of signatures. The information contained in these signatures would be seriously compromised if only portions of them were available.

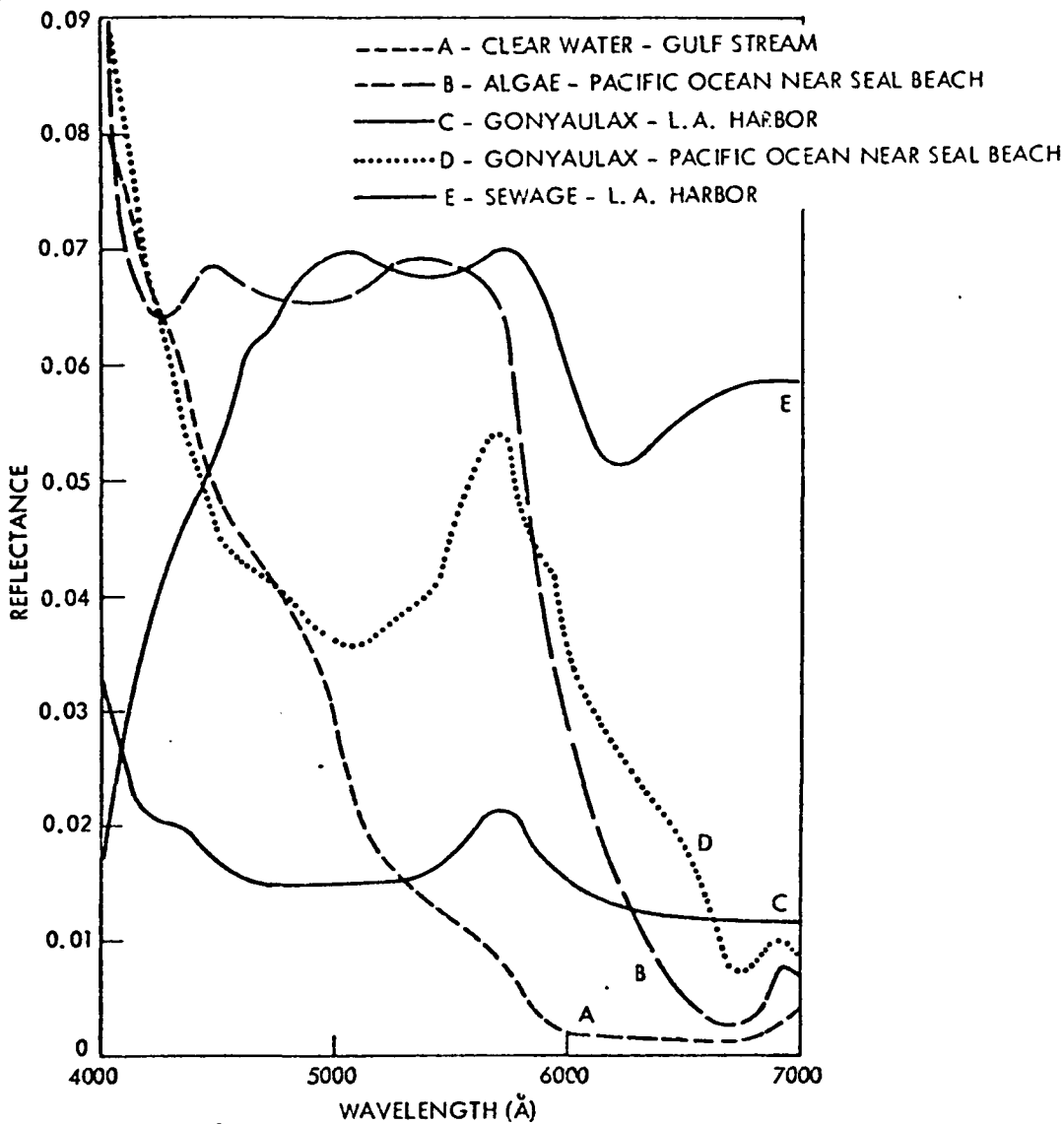


Figure 7-10. Reflectance Curves Obtained from Low-flying Aircraft

Figure 7-11 is a map of the Los Angeles Harbor showing the track followed by an aircraft and the location over which spectrometer scans (rectangles) and ground truth stations (dots) were taken. Figures 7-12 thru 7-17 show the reflectances from each of the 28 scans. Particulate matter from sewage and cannery outfalls affected the first few curves and the red tide (a type known as gonyaulax) is evident by the hump at about 575 manometers. The shape of the curves from 550 to about 700 manometers correlated well with ground the truth taken (organism count and Secchi depth). A more detailed discussion of these data correlations can be found in Reference 8.

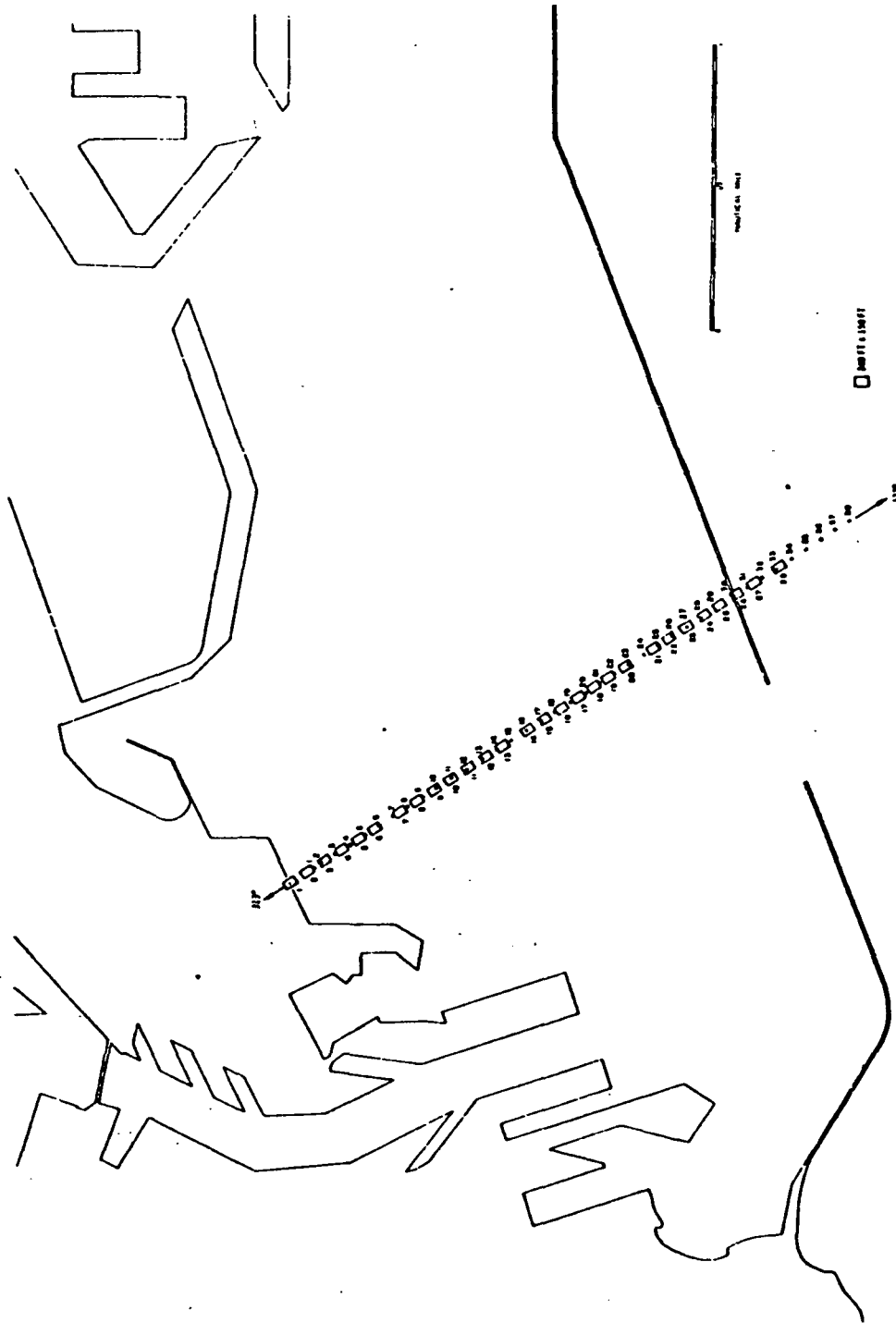


Figure 7-11. Map Showing Locations of Spectrometer Scans & Surface Test Stations

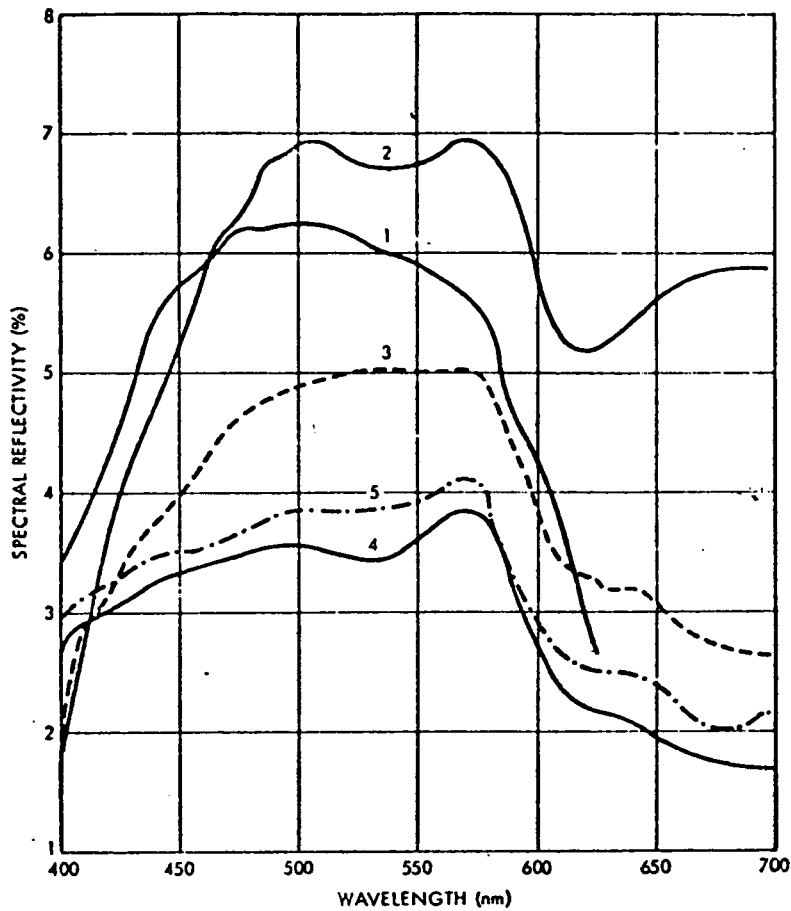


Figure 6-12. Spectral Reflectance Along Airplane Track over Los Angeles Harbor for Spectra 1-5

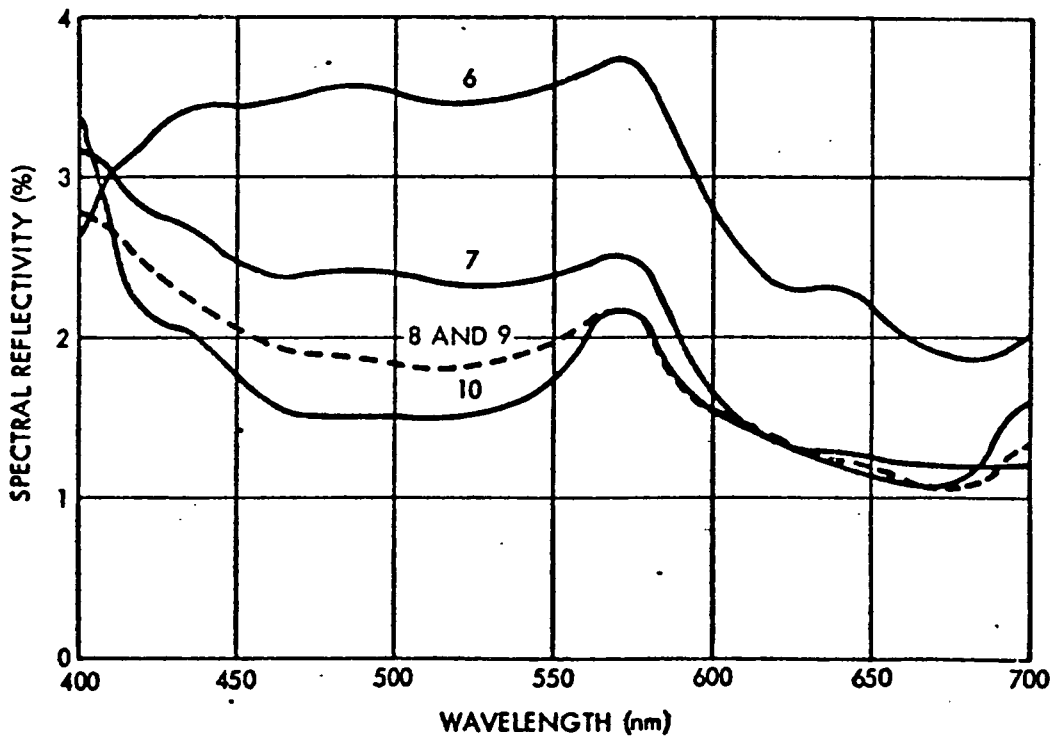


Figure 7-13. Spectral Reflectance Along Airplane Track over Los Angeles Harbor for Spectra 6-10

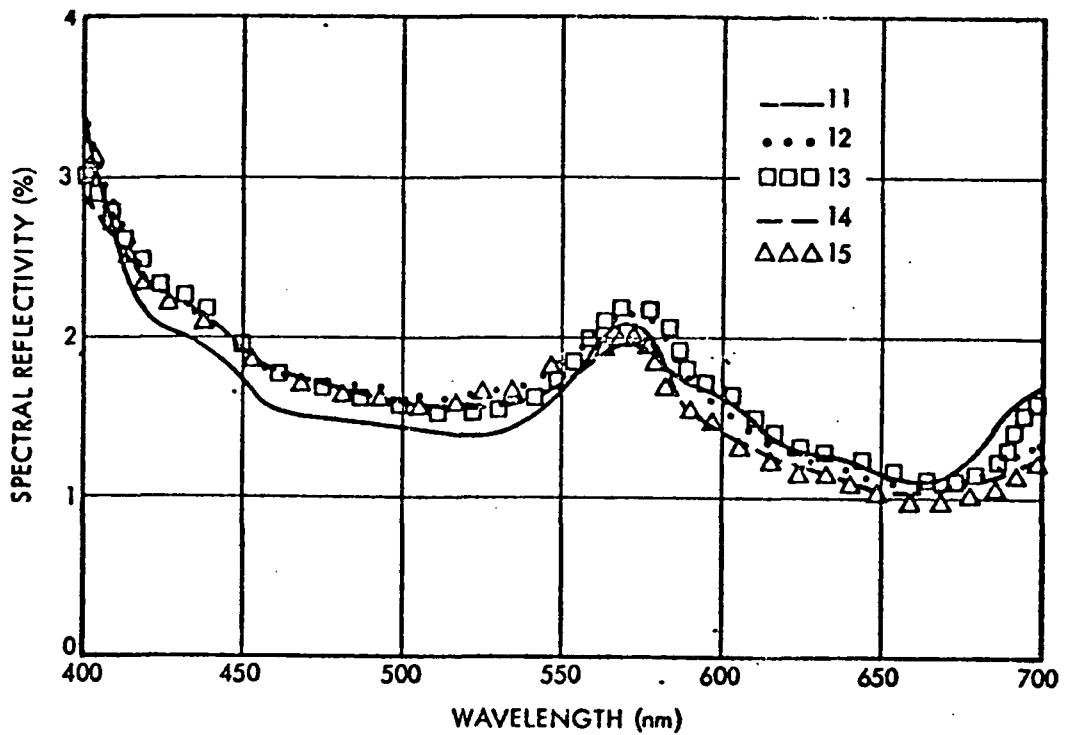


Figure 7-14. Spectral Reflectance Along Airplane Track over Los Angeles Harbor for Spectra 11-15

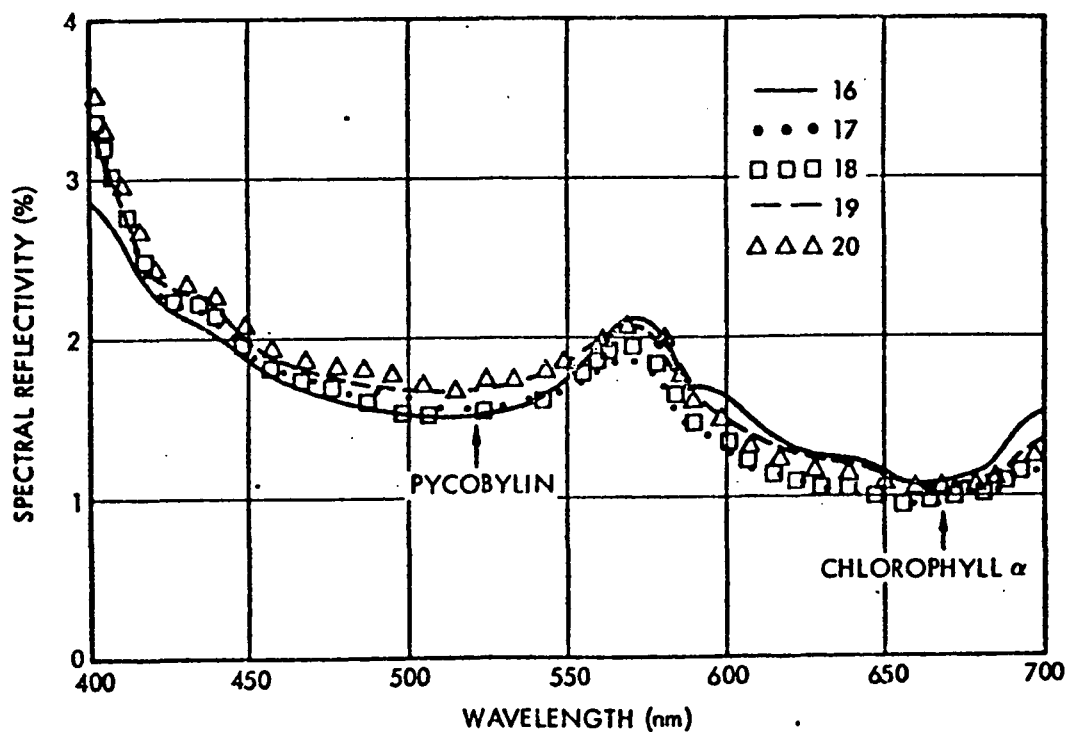


Figure 7-15. Spectral Reflectance Along Airplane Track over Los Angeles Harbor for Spectra 16-20

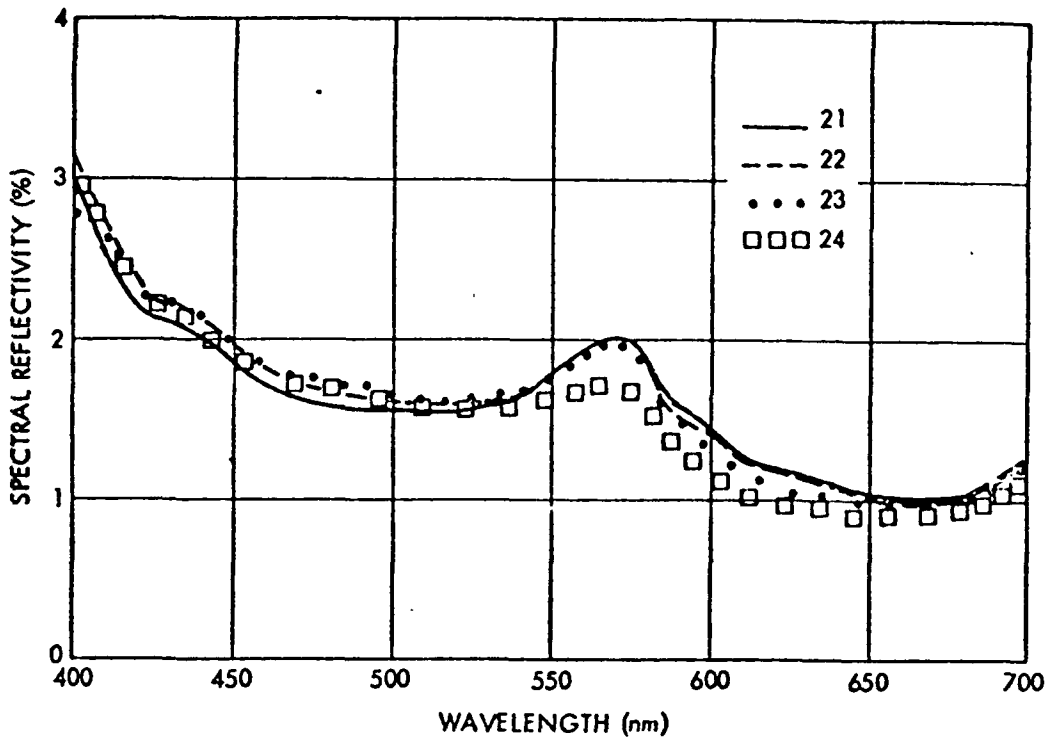


Figure 7-16. Spectral Reflectance Along Airplane Track over Los Angeles Harbor for Spectra 21-24

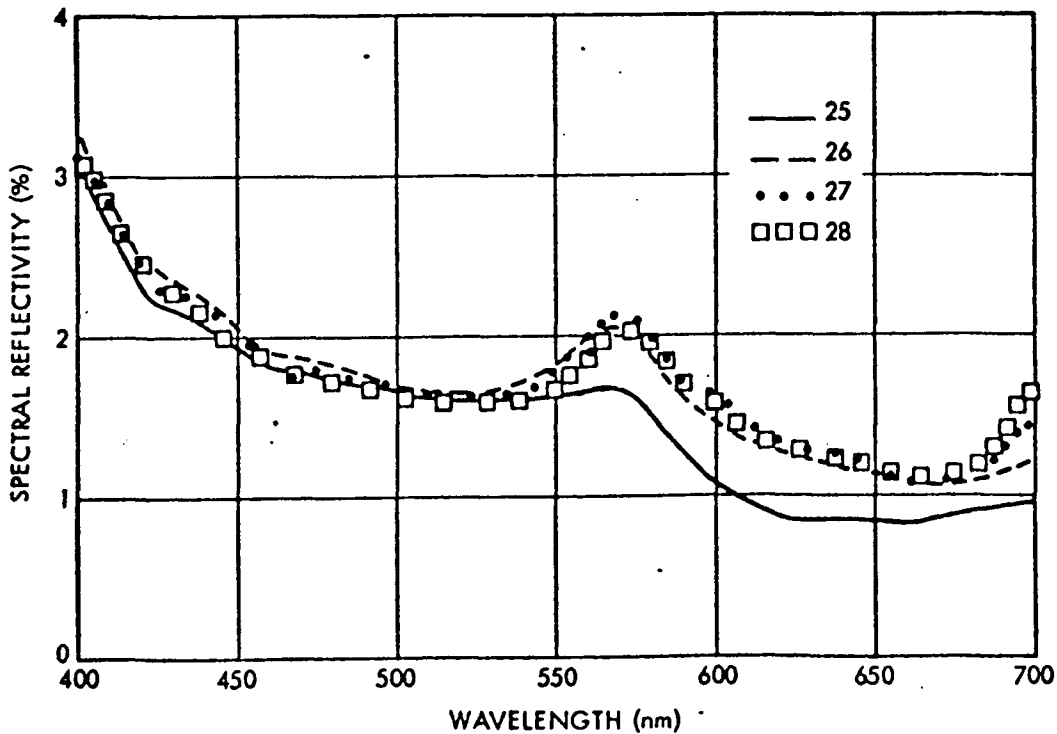


Figure 7-17. Spectral Reflectance Along Airplane Track over Los Angeles Harbor for Spectra 25-28

7. 1. 2. 3 Calculation of Minimum Signal-to-Noise

From the above discussion the following criteria, for a satellite-borne ocean color sensor are: (450 millimicrons).

Spectral Radiance of Scene (60° solar zenith angle)	22 watts/M ² -M-ster
Minimum Detectable Radiance Diff .	1. 4 watts/M ² -M-ster
Minimum Detectable Reflectivity Diff.	0. 0009
Minimum Spectral Bandwidth	150°

This last specification is somewhat arbitrary, but an inspection of Figure 7-6 would indicate a value less than this is not needed to characterize the shape of the curves.

To achieve the accuracy and precision necessary let it be required that

$$S/N = \frac{2N\lambda}{\Delta N\lambda}$$

So at 450 mμ the minimum required S/N is 31, at 450 mμ.

7. 1. 2. 4 Effect of Viewing off the Nadir

Assuming that no part of the field of view sees any of the glitter pattern a visible sensor will still suffer some degradation in contrast as the viewing angle increases from the nadir. A simple approximation to this loss of contrast can be calculated based upon the following assumptions.

- The radiance, due to upwelling light from beneath the water, which is the signal to be measured passes through a longer path length and the transmission is proportional to $e^{-\tau \sec \alpha}$, where τ is the optical thickness (a function of wavelength) and α is the viewing angle off the nadir.
- The airlight (the sunlight backscattered toward the instrument) will increase with viewing angle also because of the effective longer path length. The amount of airlights can be assumed proportional to $1 - e^{-\tau \sec \Theta \sec \alpha}$, where Θ is the solar zenith angle. This is only an approximation, but is probably valid for small changes in α , particularly for the scattering angle in the background direction.

The ratio of increase in airlight to the decrease in signal can then be calculated from the following relationship (as a function of α).

$$\text{Ratio} = \frac{1 - e^{-\tau \sec \theta \sec \alpha}}{1 - e^{-\tau \sec \theta}} \times \frac{e^{-\tau}}{e^{-\tau \sec \alpha}}$$

This ratio is shown plotted in Figure 7-18 for a wavelength of 0.45 microns ($\tau = .454$ from the Ettermann Standard Atmosphere) a worst case for the visible spectrum and solar zenith angles of $\theta = 60^\circ$ and 45° . It can be seen that this ratio increases to a value of 20 percent. Only beyond 30° off the nadir and therefore viewing angle off the nadir up to about 25° or 30° do not seriously degrade the contrast.

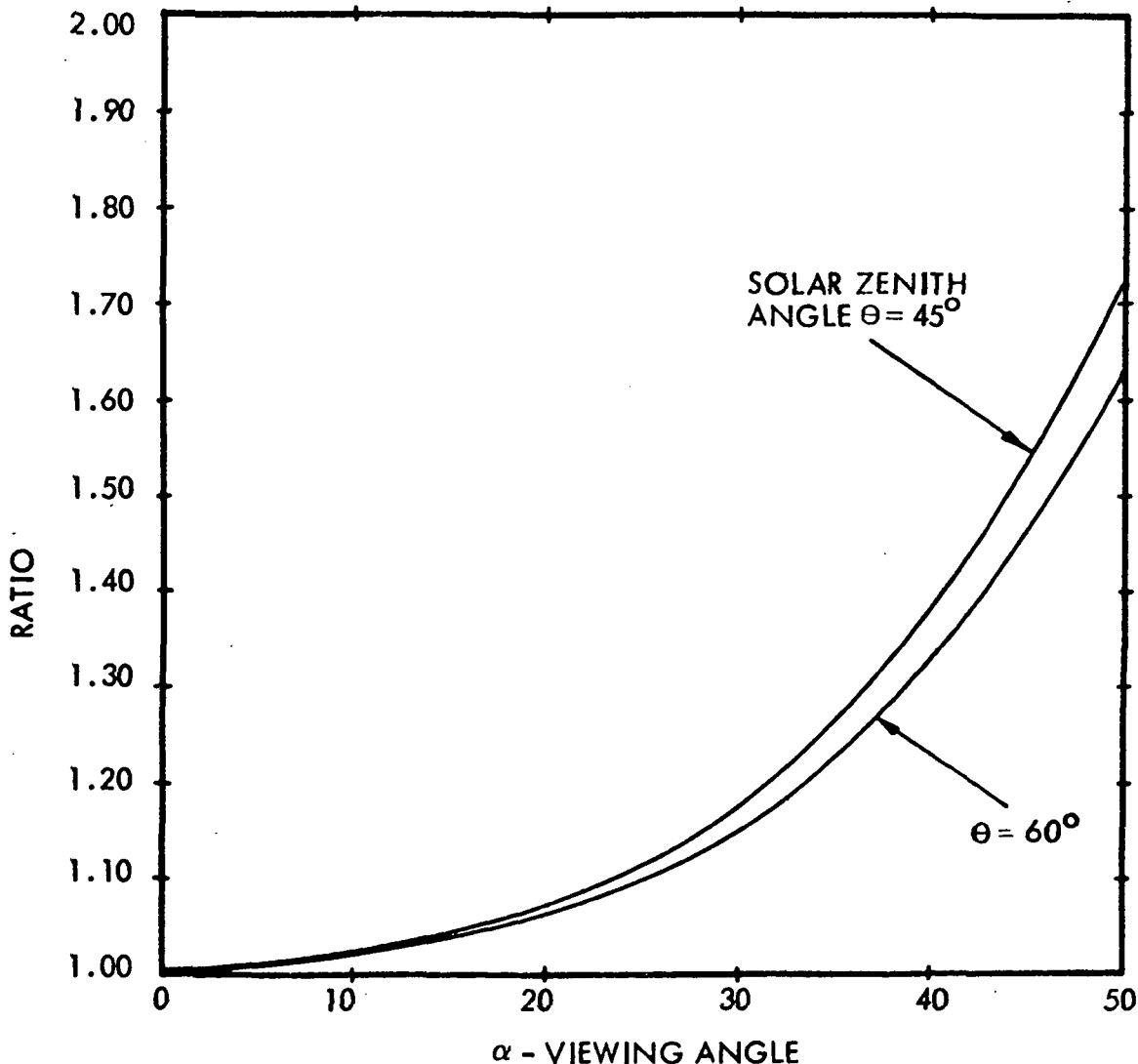


Figure 7-18. Ratio of Increase in Airlight to Decrease in Signal from Water versus View Angle off Nadir (0.45 microns)

7.2 GLITTER PATTERN SENSOR

7.2.1 Objective

The glitter pattern sensor is included in the payload for the determination of wind speed and direction over the open ocean and for the detection and measurement of the extent of areas of reduced sea state, such as might arise from areas of upwelling or natural or manmade slicks. Secondly, it can be used outside of sun glint areas for obtaining medium resolution black and white imagery over fairly large areas.

7.2.2 Theory

If the surface of the ocean were perfectly smooth, it would provide a specular image of the sun about 13 km across,* as seen from an appropriate sensor in the spacecraft. Since the surface is in fact roughened, primarily because of the action of wind, the specular reflection is broken up into many small facets, each of which reflects according to the law of reflection. As seen from a distant sensor, this means that locations removed from the nominal position of specular reflection (the "horizontal specular point") will have local surface slopes such as to reflect into the field of view of the sensor. Clearly the rougher the surface, the higher the probability that points farther removed from the horizontal specular point will have local slopes great enough to reflect sunlight into the sensor. At the distance of the spacecraft, the specularly reflecting facets, which may be only a few millimeters across, will not be individually resolved. The observed glitter pattern will thus appear as a bright center, with the radiance decreasing smoothly at increasing distances from the center. Since the total flux from the sun is independent of the ocean surface roughness, the broadening of the pattern with higher sea states results in a corresponding decrease in the radiance at the center. The observed average radiance at any point will be proportional to the fraction of the total area covered by the specularly reflecting facets, and this, in turn, will be a function of the roughness and of the distance from the center of the pattern. Thus a measurement either of the absolute radiance of the center of the glitter pattern, or some suitable measurement of the pattern size, will give an indication of the sea state. Moreover, since the surface roughness is caused by the wind, it is to be expected that such measurements

*925 km (500 nm) altitude

could give an indication of wind velocity as well. It turns out that the broadening of the glittering patterns is caused primarily by the very small, high-frequency components of the waves, i. e., the capillary waves, which are in fact most sensitive to the local wind, further justifying this expectation. Modern investigations of the correlation of glitter patterns with wind speed include those of Hulbert (1934) and Shuleikin (1941). These measurements involved determining "maximum" slopes occurring at different wind speeds from the size of the glitter patterns, and thus were dependent on the criteria implied in the definition of the pattern boundaries. In 1951, Cox and Munk undertook to compute the distribution of slopes from the measured variation of radiance within the glitter pattern and to relate these to the prevailing wind velocities. The measurements were taken near the island of Maui with wind speeds up to 14 m/sec. The results were reported in abbreviated form in 1954 and fully in 1956. They found that the frequency distribution of the occurrence of slopes could be represented by a Gram-Charlier series, which to a first approximation is a two dimensional Gaussian distribution. This may be written:

$$P(Z_x, Z_y) = (2\pi\sigma_c\sigma_u)^{-1} \exp\left\{-\frac{1}{2}\left[\left(\frac{Z_x}{\sigma_c}\right)^2 + \left(\frac{Z_y}{\sigma_u}\right)^2\right]\right\} \left[1 + \sum_{i=0}^{\infty} \sum_{j=0}^{\infty} C_{ij} H_i\left(\frac{Z_x}{\sigma_c}\right) H_j\left(\frac{Z_y}{\sigma_u}\right)\right] \quad (7-1)$$

where Z_x and Z_y are the slope components crosswind and upwind, respectively, and σ_c and σ_u are the corresponding rms values of the slope components. σ_c and σ_u are linearly related to the wind speed. H_i and H_j are Hermite polynomials and the C_{ij} are coefficients determined from the data. Eight of these terms are enough to give the accuracy justified by the data.

Rosenberg and Mullamaa (1965), Levanon (1968) and Strong and Ruff (1970) have investigated the feasibility of determination of sea state and near-surface wind speeds from satellites using the Cox and Munk wave-slope statistics. Rosenberg and Mullamaa, and Levanon primarily considered the use of geosynchronous satellites while Strong and Ruff considered a satellite altitude of 700 km. In addition to the determination of average winds, glitter patterns can provide data for the detection and measurement of slicks or other areas of reduced sea state, since these

show up as darker when near the edges of the pattern and brighter when at or near the center. This application of glitter pattern measurements has been studied by McClain and Strong (1969), Bowley, Greaves, and Spiegel (1969) and Soules (1970).

The Gaussian approximation to the Cox and Munk expression for surface slope statistics (i. e., the first term in the Gram-Charlier series) is adequate for discussing the application of glitter pattern measurements from a satellite. The relationships between rms slope components and wind speeds found by Cox and Munk are:

$$\begin{aligned}\sigma_c^2 &= .003 + .00192 W \pm .002 \\ \sigma_u^2 &= .000 + .00316 W \pm .004 \\ \sigma_c^2 + \sigma_u^2 &= .003 + .00512 W \pm .004\end{aligned}\tag{7-2}$$

where the wind speed is given in m/sec. They observe that the sum $\sigma_c^2 + \sigma_u^2$ is independent of variations in wind direction, and thus its use gives a better determination of wind speed than either separately. (Note that this sum, computed as a single quantity, is not quite equal to the sum of σ_c^2 and σ_u^2 determined separately.) Moreover, the use of this quantity greatly simplifies the data processing. Therefore we use the slope frequency statistics for the determination of wind speed in the form:

$$P(Z_x, Z_y) = (\pi\sigma^2)^{-1} \exp \left\{ -\frac{Z_x^2 + Z_y^2}{\sigma^2} \right\} \text{ where } \sigma^2 = \sigma_c^2 + \sigma_u^2.\tag{7-3}$$

The wind direction can be determined independently, by identifying the direction of the glitter pattern ellipse after corrections have been made for geometric factors. Any errors in the determination of the direction of the major axis of the ellipse, and thus in the identification of the wind direction, do not affect the wind speed measurement.

7.2.3 Glitter Sensor Description

The glitter pattern sensor consists of a 1000 line TV camera with a slow scan capability, f/4 optics with a mechanical shutter and an iris diaphragm adjustable from f/4 to f/16, and two-axis gimbaling so that

that any area from horizon to horizon can be observed. The camera tube requirements are well within the state of the art; a 1 1/2-inch vidicon (such as the RCA 8051) with ASOS target could be used, or a return-beam vidicon or SEC vidicon might be appropriate. While the absolute photometric capability of vidicons leaves much to be desired, relative measurements within a single frame of imagery can be made with acceptable accuracy, as will be shown in the discussion of expected results. Wavelength requirements are not critical, but it is desirable to operate in the long wavelength portion of the visible spectrum to reduce the background effects of scattered sunlight, reflected skylight, and diffuse scattering from the ocean surface layers. The sensor characteristics are summarized in Table 7-4. A conceptual drawing of the sensor is shown in Figure 7-19.

Table 7-4. Sun Glitter Sensor Characteristics

Sensor Type	1.5-inch vidicon
Wavelength Range	0.58 - 0.7 μ
Field of View	40 $^{\circ}$ x40 $^{\circ}$; ca 780 km across the field @ 30 $^{\circ}$ from nadir
Resolution	1000 TV lines; 0.78 km per TV line.
Dynamic Range	64:1 within a frame
Exposure Time	12 to 48 msec
Exposure Control	4:1 with exposure time; 16:1 with iris diaphragm
Pointing Range	0-45 $^{\circ}$ from nadir, 360 $^{\circ}$ in azimuth

7.2.4 Mode of Operation

In theory, the sea-state at the horizontal specular point can be determined by a measurement of the radiance at that point. In practice, however, this method would incur large errors from errors in the absolute photometric calibration of the sensor and from imperfect compensation for atmospheric effects. Moreover, this measurement gives no information

CAMERA ELECTRONICS
15 x 15 x 32 CM 6 kg

CONTROLLER
15 x 15 x 32 CM 6 kg

POWER
cs 45 W AVE
52 W PEAK

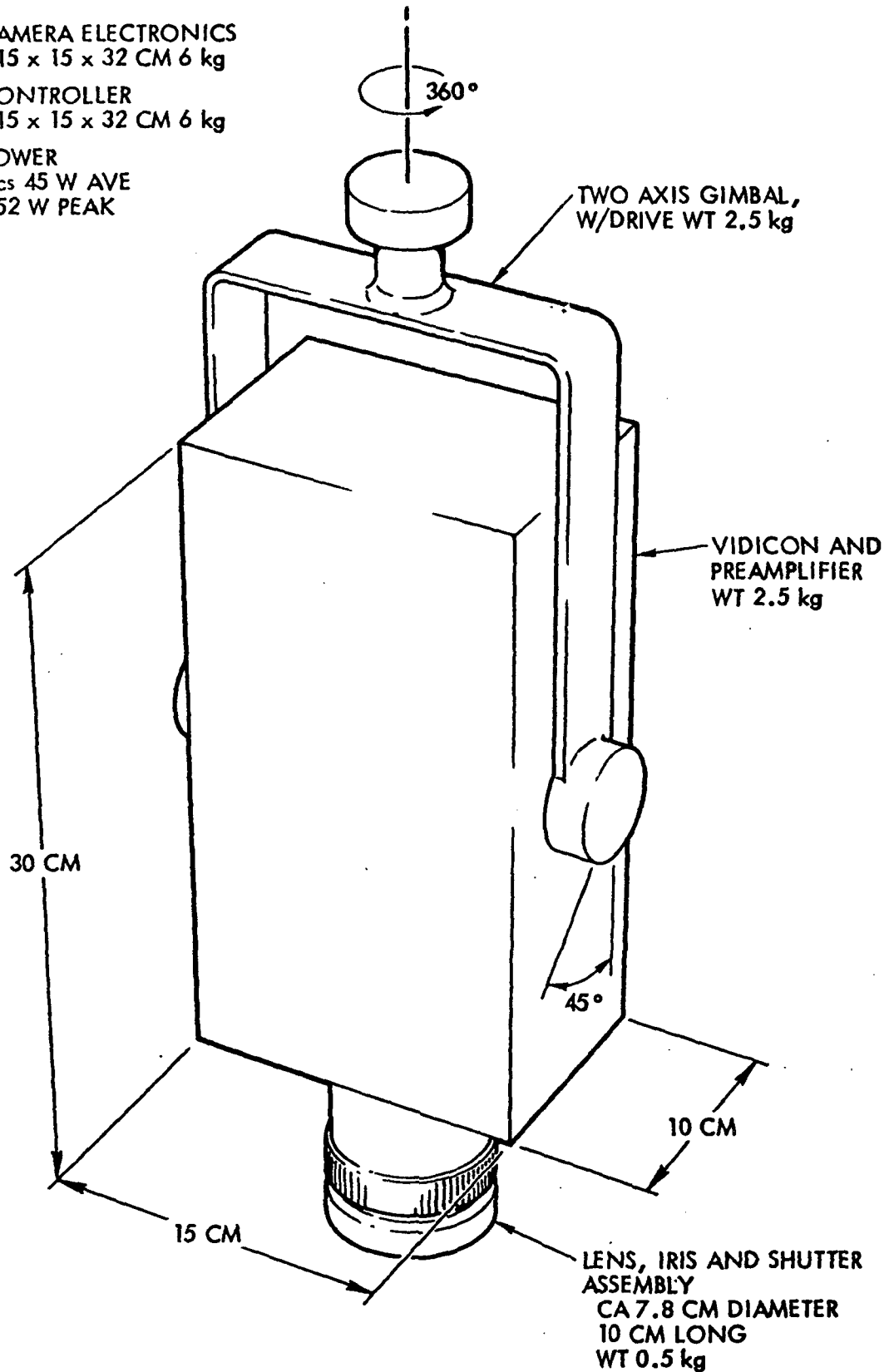


Figure 7-19. Glitter Sensor

on wind direction. For these reasons it is preferable to use a relative method in which the angular distance from the center to some relative radiance contour is measured. Such a method is less sensitive to instrumental and atmospheric effects and permits a determination of wind direction. The primary disadvantage of measuring the "size" of the glitter pattern is that the measurement is necessarily that of the average sea state over a considerable area. Figure 7-20 shows the distance from the center of the pattern of three equal radiance contours (B/B_c is the ratio of radiance at the contour to that at the center) both in degrees at the image plane and in kilometers on the surface as functions of wind speed. The surface distances assume a spacecraft altitude of 925 km and a nadir angle of 30° .

Using a contour at which the radiance is considerably less than that at the center (smaller radiance ratio) clearly reduces the effects of measurement errors, but at the cost of obtaining a wind velocity value averaged over an uncomfortably large area, as can be seen from Figure 7-20. This is objectionable primarily because it is unlikely that substantially constant wind conditions will prevail over areas as great as 900 km in diameter (for the worst case shown, wind speed 15 m/sec and the 0.6 brightness contour). It will be seen that at least in most cases, measurement of the size of the 0.9 contour provides a good compromise between measurement accuracy and area over which the wind velocity is averaged.

The pointing of the sensor will be commandable, either by stored commands on a precomputed schedule, or by operator-generated commands for special observations. For wind velocity determination, the pointing will normally be determined by a program taking into account the known location of the horizontal specular point and whether it occurs over an ocean area of interest. The sensor is pointed to put the horizontal specular point at the center of the frame in azimuth, and generally at or near the center in nadir angle. With image scanning in the azimuth direction of the frame, this provides considerable simplification in data processing because of symmetry about the frame center line, as well as insuring maximum coverage of the glitter pattern.

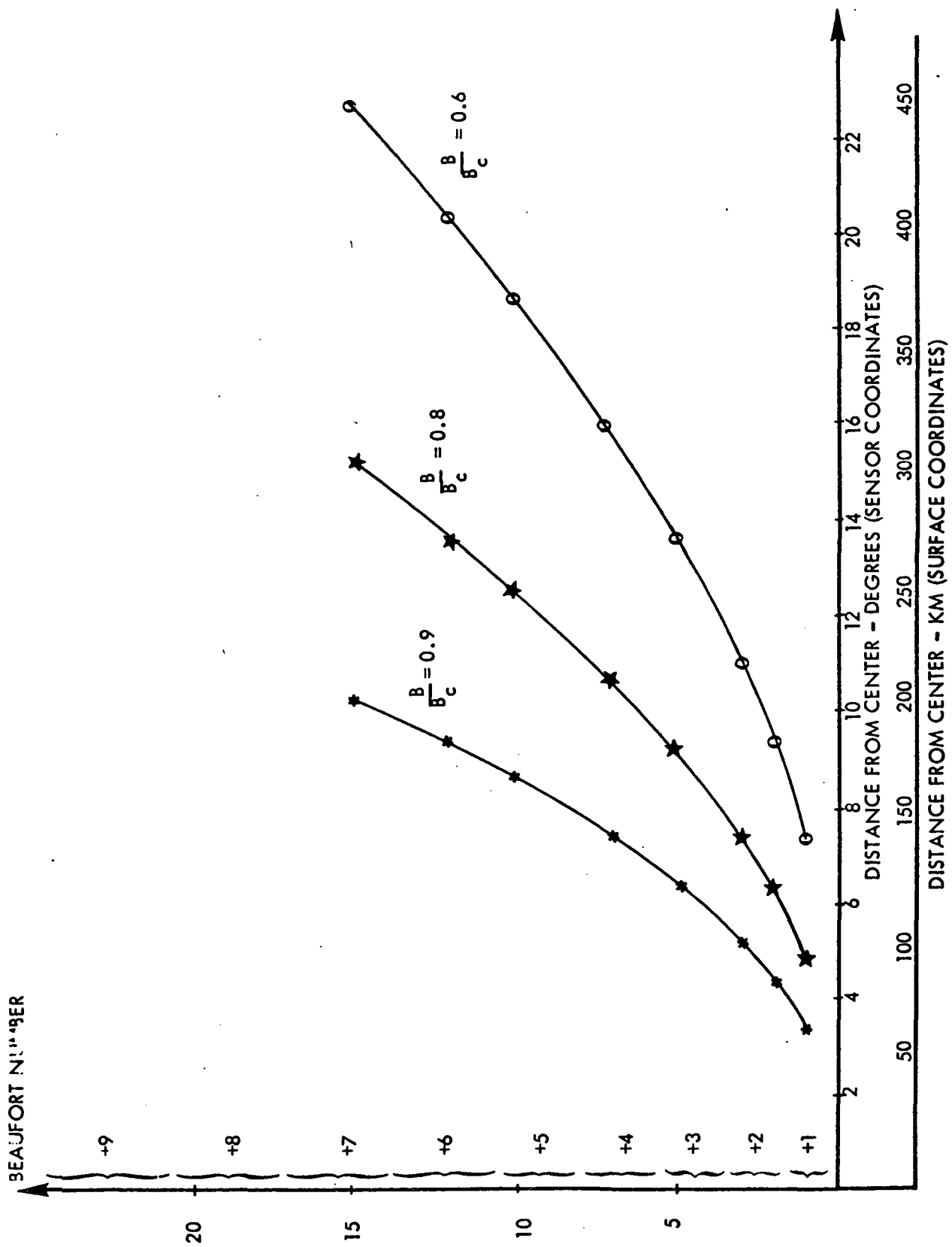


Figure 7-20. Distance of Radiance Contours from Center of Glitter Pattern

The center radiance will be about $270 \text{ lum/m}^2 / \text{ster}$ for a wind of 2 m/sec and could be even much higher for unusually calm conditions. On the other hand, the center radiance for a wind speed of 15 m/sec is about $27 \text{ lum/m}^2 / \text{ster}$. Therefore exposure control must be exercised, using an auxiliary sensor to get the appropriate center brightness and adjusting the exposure time and/or the iris diaphragm setting, in order to keep the dynamic range within a frame within reasonable limits.

To determine wind speed, the normal procedure would be first to measure the apparent radiance at the center of the pattern. The vidicon pixel size is about $.025^\circ$, while the sun subtends about $.5^\circ$, so the central region of essentially constant brightness is about 20 pixels across, and in the absence of cloud interference, about 300 pixels can be averaged to get this value. Corrections for geometric factors can be applied, and at least some nominal corrections for background luminance can be made if necessary; the latter will be increasingly important for higher wind speeds and hence lower luminance values. The contour representing 0.9 of this central value can then be measured, and the wind speed deduced from the Cox and Munk statistics.

The measured contour, corrected for viewing geometry, can be fitted to an ellipse centered on the horizontal specular point. The direction of the major axis of this ellipse gives the average direction of the wind with an ambiguity in sign which can readily be resolved from knowledge of the general circulation pattern. Cox and Munk did find a small upwind-downwind asymmetry in the slope statistics, but it is extremely doubtful that it would be large enough to resolve the ambiguity in the presence of expected measurement errors as well as real variations in the synoptic situation.

The foregoing discussion has implied the absence of cloud cover or sea state anomalies (e. g., slicks) of sufficient amount to affect the measurement accuracy; however, both these phenomena are likely to occur, particularly clouds with the higher sea states. Fortunately, there are methods to obtain good wind and sea state data even in the presence of such interference. If the center of the pattern is observable, but some of the contour is not, one can have the computer iteratively reject all values which lie too far from the mean, the tolerance being based on the

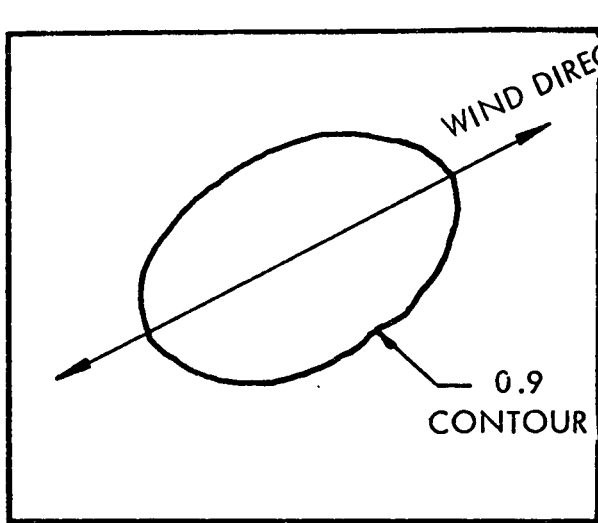
expected range of real values, and thus automatically end up using only points which are probably valid. Alternatively, one could have an operator look at a displayed image, and indicate to the computer, say via a light pen, those areas which are to be excluded from use in the determinations. If the center of the pattern is obscured, the determination could be made from sections of two different contours; from their separation and the location of the center (known from spacecraft and astronomical data) the average wind speed over the area bounded by the sections of the contours used could be deduced. This second method could be used at any time for determination of wind speeds over areas within the measurable glitter pattern but not centered on the pattern center. In this method, however, an estimate of wind direction probably could not be obtained. The various possibilities are illustrated in Figure 7-21 a, b, and c.

In addition to its use for determining sea states and wind velocities, the glitter pattern sensor could be pointed at any area of interest outside the glitter pattern for broad area, medium resolution, black and white imagery in support of other sensors. For example, it could provide cloud cover information for areas covered by the infrared or microwave radiometers.

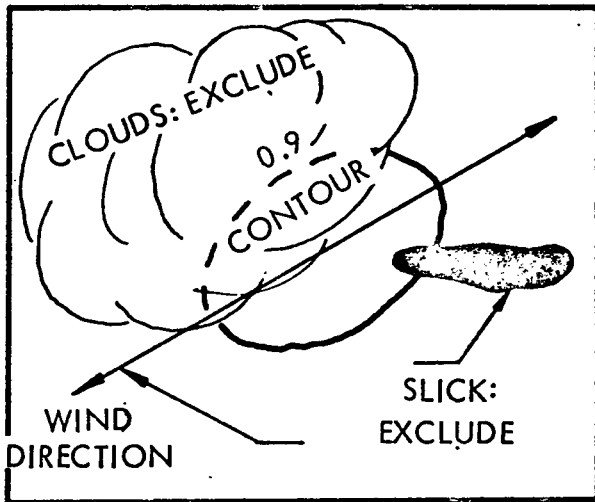
7.2.5 Coverage

7.2.5.1 Orbital Considerations

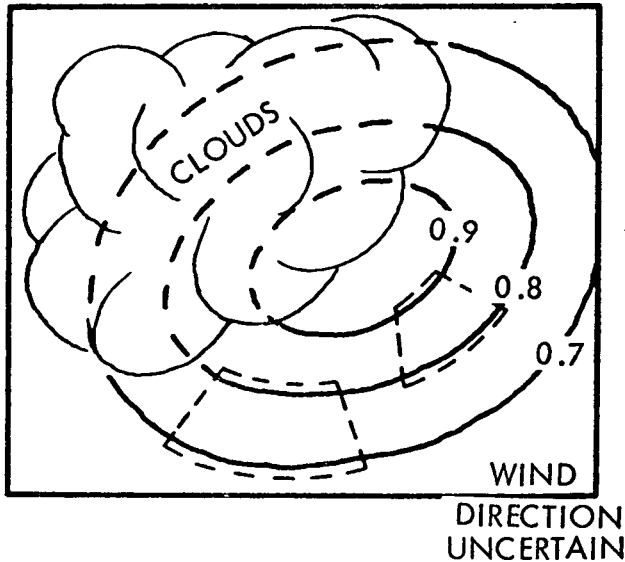
Computer runs of the location of the horizontal specular point (i. e., the center of the glitter pattern) relative to the orbit trace have been made for sun-synchronous orbits with an altitude of 913 km and an inclination of 99.085° . Runs were made for three sun declinations, $+23.5^\circ$, 0° , and -23.5° , corresponding to the summer solstice, either equinox, and the winter solstice respectively. The local time at the descending node was taken at 9:30, noon, and 14:30 for each of these cases. The horizontal specular point is visible (the sun is at or above the spacecraft's horizon) from 65 to 71 percent of the time, depending on the orbit. However, if the local angle of incidence of the sun's rays at the specular point exceeds about 60° , it is difficult to make accurate sea-state measurements, because the center of the pattern is very near the horizon, the resolution is poor, and the brightness relationships become complicated and variable with atmospheric conditions. If the angle of incidence is restricted to $\leq 60^\circ$, usable sun glitter patterns can be seen over ranges of about 101°



CASE A: NO CLOUD OR SLICK INTERFERENCE



CASE B: INTERFERENCE FROM CLOUDS AND/OR SLICKS BUT CENTER IS NOT OBSCURED.



CASE C: CENTER OF PATTERN OBSCURED; USE AN AREA LIKE ONE OF THOSE ENCLOSED IN DASHED LINES.

Figure 7-21. (a, b, c)

to 118° of latitude. Over these ranges the trace of the horizontal specular points roughly parallels the orbital trace. The characteristics of the nine orbit cases are summarized in Table 7-5. Plots of the orbit and glitter pattern traces for noon orbits at summer solstice, equinox, and winter solstice are shown in Figures 7-22, 7-23, and 7-24, respectively. The absolute values of longitude are of course quite arbitrary in these plots; they can be adjusted to fit the longitude of the ascending node of any desired particular orbit. The points shown on the plots are 125.4 seconds apart, so the separation is 810 km. Values of the local angles of incidence are shown beside the points at the extremes of the ranges over which these angles are $\leq 60^\circ$.

7.2.5.2 Range of Wind Speeds

A number of considerations lead to the conclusion that the highest wind speeds which can be deduced with any degree of confidence from surface roughness (glitter pattern) measurements are about 15 m/sec. Wu (1969) has found that the high frequency wave components which are primarily responsible for the size of the glitter pattern saturate beyond this value. The maximum radiance of the pattern (approximately at its center) decreases with increasing size of the pattern, with corresponding decreases at the fractional radiance contours, so the background radiance from reflected skylight, sunlight refracted into the water and then out again by scattering, and scattering from the atmosphere becomes a

Table 7-5. Glitter Pattern Characteristics for Nine Orbits

Time of Year	Local time of Descending Node	Fraction of orbit with sun at or above Horizon	Latitude Range for angle of incidence 60°	Minimum angle of incidence
Summer Solstice	0930	0.69	75N - 27S	25.8°
	1200	0.65	79N - 35S	3.2°
	1430	0.71	80N - 33S	33.3°
Equinox	0930	0.71	60N - 51S	32.5°
	1200	0.67	59N - 59S	0°
	1430	0.71	51N - 60S	32.5°
Winter Solstice	0930	0.71	32N - 80S	33.3°
	1200	0.67	36N - 79S	3.2°
	1430	0.69	26N - 75S	25.8°

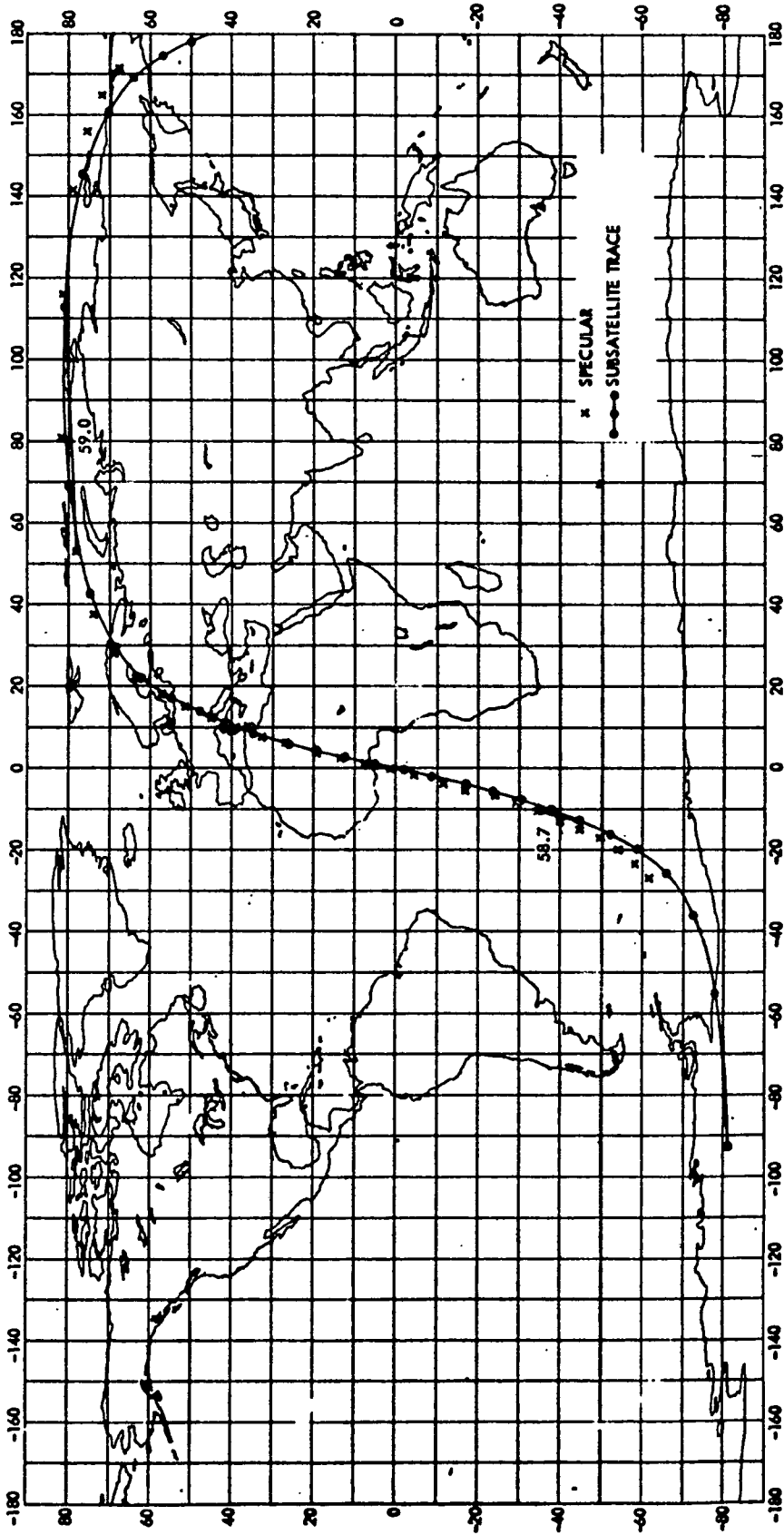


Figure 7-22. Specular Point Locations (Summer Solstice)

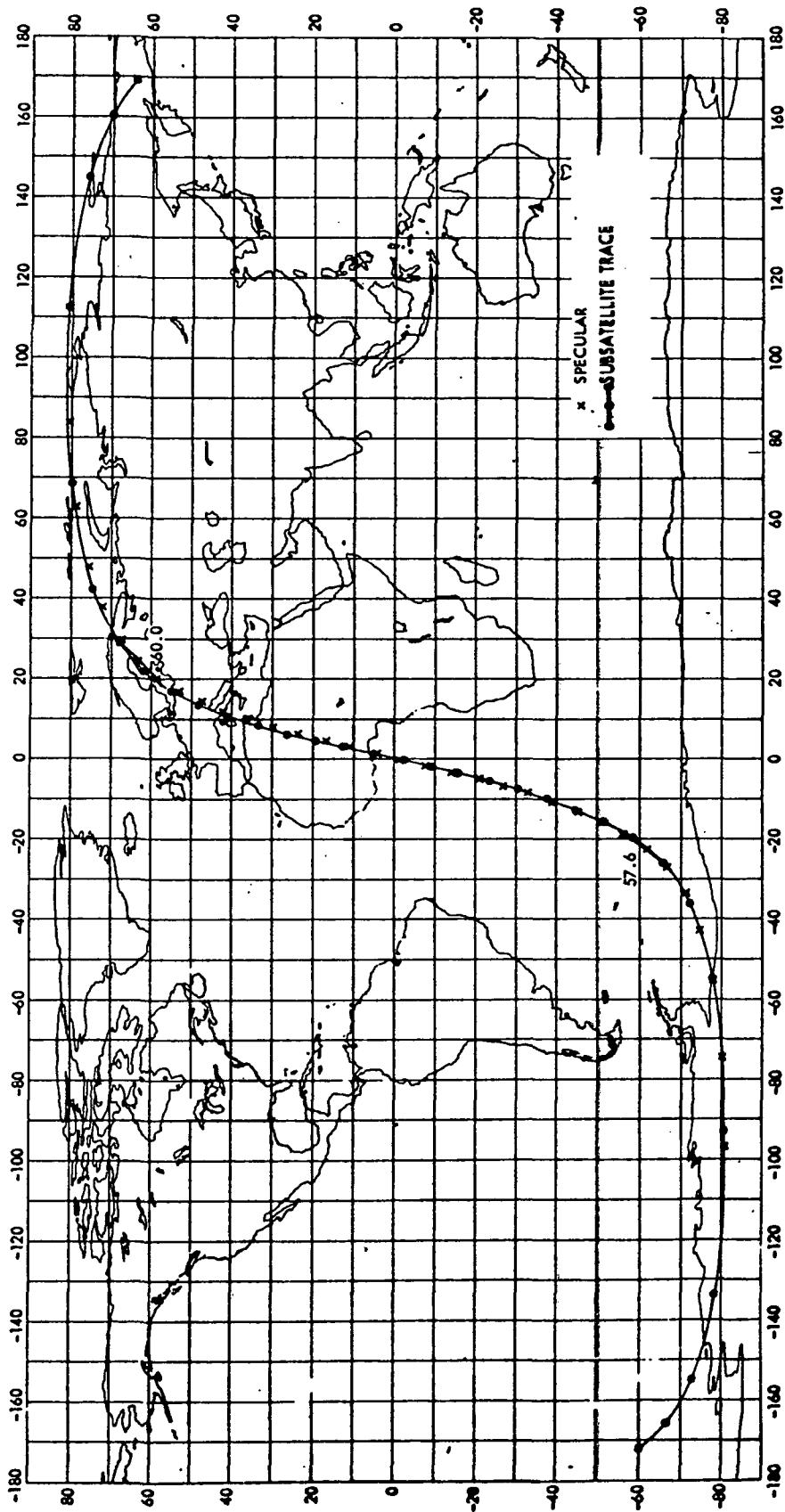


Figure 7-23. Specular Point Locations (Equinox)

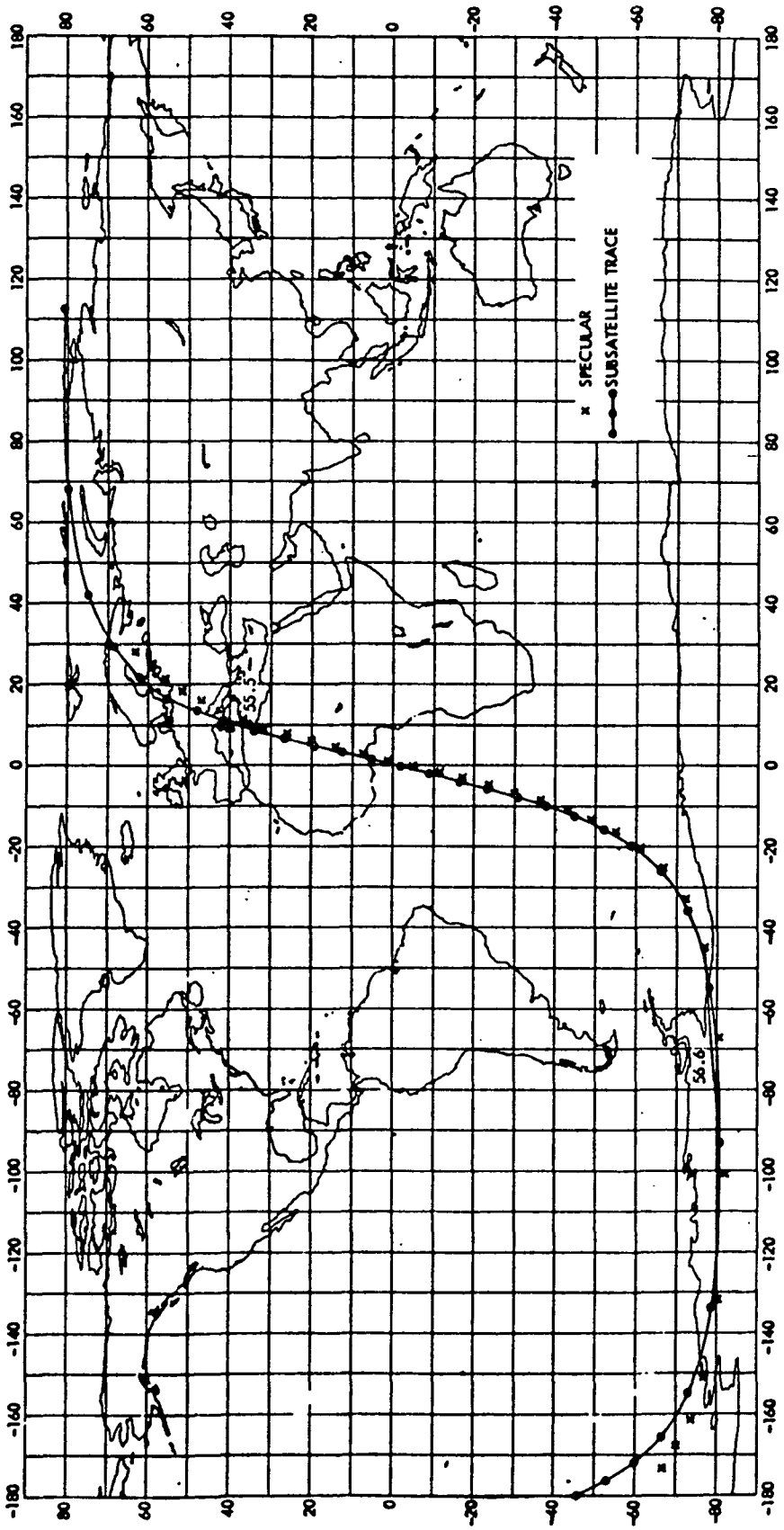


Figure 7-24. Specular Point Variation (Winter Solstice)

greater fraction of the glitter radiance, making accurate measurements more difficult. The increased incidence of foam (from white caps) with high winds also introduces errors into the model. Finally, winds in excess of 15 m/sec are likely to have considerable cloud cover associated with them.

At the other extreme, the statistical model itself is subject to large relative errors at low wind speeds. Moreover, it is unlikely that average winds of extremely low velocities will occur over large open ocean areas. Therefore a lower limit of 1 to 2 m/sec is to be expected.

The relationships among various units used for wind speeds and the Beaufort Number designations are given in Table 7-6. Thus, the range of measurements covers Beaufort Numbers 1 through 7.

7.2.5.3 Area Coverage

For sea state and wind velocity measurements, *per se*, the concept of continuous area coverage is not particularly applicable. In normal operation, the data obtained will be the wind velocities at a series of points roughly paralleling the orbit trace. The density of these points can be made whatever is desired; about one every 200 km seems appropriate. If desired, measurements can be made somewhat away from the glitter pattern center, as indicated in Section 7.2.4, so wind measurements over a swath some 200 to 700 km wide, depending on sea state and cloud interference, are possible. The range of latitudes over which the line or swath of measurements can be made is shown in Table 7-5.

Areas of reduced sea state can be detected anywhere within the sensor field of view in which the glitter pattern is strong enough to make them observable. The glitter pattern moves with the spacecraft, though at a slightly slower rate (see Figures 7-22, 7-23, 7-24) so if sensor frames are taken every 200 km, there is a chance to see any reduced sea state area in about 4 frames (each is about 800 km across) and thus the chance of observing it in a favorable position relative to the glitter pattern is increased. Roughly, then, reduced sea state areas can be observed over a swath up to 800 km wide, covering about the same latitude range as the primary wind measurements.

For general black and white imagery, a usable swath perhaps 3800 km across is accessible to the sensor, since the total distance horizon to horizon is about 6700 km, but areas near the horizon must be excluded both because of severe obliquities and unsatisfactory lighting conditions.

Table 7-6. Modern Beaufort Scale

WIND SPEED				
BEAUFORT NUMBER	KNOTS	MPH	METERS PER SECOND	KM PER HOUR
0	UNDER 1	UNDER 1	0.0 - 0.2	UNDER 1
1	1 - 3	1 - 3	0.3 - 1.5	1 - 5
2	4 - 6	4 - 7	1.6 - 3.3	6 - 11
3	7 - 10	8 - 12	3.4 - 5.4	12 - 19
4	11 - 16	13 - 18	5.5 - 7.9	20 - 28
5	17 - 21	19 - 24	8.0 - 10.7	29 - 38
6	22 - 27	25 - 31	10.8 - 13.8	39 - 49
7	28 - 33	32 - 38	13.9 - 17.1	50 - 61
8	34 - 40	39 - 46	17.2 - 20.7	62 - 74
9	41 - 47	47 - 54	20.8 - 24.4	75 - 88
10	48 - 55	55 - 63	24.5 - 28.4	89 - 102
11	56 - 63	64 - 72	28.5 - 32.6	103 - 117
12	64 - 71	73 - 82	32.7 - 36.9	118 - 133
13	72 - 80	83 - 92	37.0 - 41.4	134 - 149
14	81 - 89	93 - 103	41.5 - 46.1	150 - 166
15	90 - 99	104 - 114	46.2 - 50.9	167 - 183
16	100 - 108	115 - 125	51.0 - 56.0	184 - 201
17	109 - 118	126 - 136	56.1 - 61.2	202 - 220

7.2.6 Expected Results

The radiance at the center of the glitter pattern is given by

$$B = L_s \frac{\omega_s}{4} \cos \theta_i R(\theta_i) P(Z_x, Z_y) \quad (7-4)$$

where B = radiance related to sensor coordinates
 L_s = Luminance of the surface of the sun
 Θ_i = Angle of incidence at the horizontal specular point
 $R(\Theta_i)$ = Fresnel coefficient of reflection for Θ_i
 ω_s = Solid angle subtended by the sun; it must be divided by 4 because of the doubling of angles in the sensor coordinate system.
 $P(Z_x, Z_y)$ is given by Equation 6-3

At points away from the center, this equation is only approximate, since the local angle of incidence differs from Θ_i , but for the purpose of estimating errors this variation can be neglected. We can put $Z^2 = Z_x^2 + Z_y^2$, so for a contour of radiance B , the ratio of its radiance to that of the center is given by

$$\frac{B}{B_c} = \frac{e^{-\frac{Z^2}{\sigma^2}}}{e^{-0}} = e^{-\frac{Z^2}{\sigma^2}} \quad (7-5)$$

$Z = \tan \varphi$, where φ is the surface slope necessary to reflect the sunlight onto the chosen contour, so

$$\frac{\tan^2 \varphi}{\sigma^2} = \log \left(\frac{B_c}{B} \right), \text{ or } \tan^2 \varphi = c \sigma^2 \quad (7-6)$$

$$\text{where } c = \log \left(\frac{B_c}{B} \right)$$

From Equations 7-2 and 7-6,

$$W = \frac{\tan^2 \varphi - .003c}{.00512c} \quad (7-7)$$

The actual measurements are made in sensor coordinates, in which

$$\Theta = 2 \varphi \quad (7-8)$$

where Θ is the angle in sensor coordinates, which is twice that of the slope, since an image moves through twice the angle that a mirror moves.

The errors incurred in measuring the wind speed will result from geometrical errors in the vidicon, radiance errors in the vidicon, and errors in the model, so that

$$\begin{aligned} [E(W)]^2 &= \left(\frac{\partial W}{\partial \tan \varphi} \frac{\partial \tan \varphi}{\partial \tan \Theta} \right)^2 [E(\tan \Theta)]^2 + \\ &\left(\frac{\partial W}{\partial \tan \varphi} \frac{\partial \tan \varphi}{\partial B} \right)^2 [E(B)]^2 + \left(\frac{\partial W}{\partial (\sigma^2)} \right)^2 [E(\sigma^2)]^2 \quad (7-9) \\ &= GE^2 + BE^2 + ME^2 \end{aligned}$$

The details of the calculation of the partial derivatives and the estimates of the basic errors leading to values of GE, BE, and ME are given in Appendix C. The results are summarized in Table 7-7.

Table 7-7. Summary of Expected Wind Speed Measurements

Radiance Ratio	c	Wind Speed (m/sec)	Radius of Contour	GE (m/sec)	BE (m/sec)	ME (m/sec)	RMS Error	Percent of Wind Speed
0.6	0.5	1	137 km	.016	.023	.782	.785	79
		10	360	.106	.155	.782	.835	8.4
		15	445	.150	.230	.782	.860	5.8
0.8	0.22	1	89	.016	.050	.782	.815	82
		10	230	.106	.345	.782	.890	8.9
		15	270	.150	.510	.782	.990	6.6
0.9	0.105	1	63	.016	.107	.782	.820	82
		10	160	.106	.710	.782	1.08	10.8
		15	187	.150	1.05	.782	1.34	8.9

The model error (ME), according to Cox and Munk, is constant in absolute value, regardless of wind speed or conditions of measurement. It not only dominates the total error at low wind speeds; it also produces very large relative errors. It may be expected that the accumulation of data may permit some refinement of the model, but this is not really important because the absolute error is already less than 1 m/sec.

The error arising from geometrical non-linearities in the sensor (GE) is independent of the contour used but it increases with increasing wind speed. However, it never makes a significant contribution to the total error.

As might be expected, the error in measuring radiance values (BE), increases with wind speed, since lower values are measured, and increases as the radiance ratio increases, since the difference being measured decreases. However, it only becomes equal to the model error for about 12 m/sec and use of the 0.9 contour.

The rms error expected for a 15 m/sec wind, measuring the 0.9 contour, the worst case shown, is 1.34 m/sec, still less than one half a Beaufort number at this level. Thus measurements made on the 0.9 contour give satisfactory accuracies for wind speeds averaged over fairly reasonable areas; it is proposed to use this contour for normal measurements. However, the sensor field of view permits the use of contours nearer to or farther from the center, if this should prove to be advisable.

The accuracy which can be obtained in the wind direction determination is difficult to assess. For very low winds the model predicts a nearly circular pattern; only for winds in excess of about 4 m/sec is the ellipticity of the pattern enough for detection of the wind direction. In addition, the real variability of the wind direction over areas 100 to 400 km across will degrade the accuracy of the determination. However, one can estimate that for a steady wind of 10 m/sec, with the assumptions outlined in Appendix C, the wind direction should be obtained to about $\pm 24^\circ$.

7.2.7 Data Rates

The field of view of the sensor is 1000 by 1000 TV lines, or 10^6 pixels per frame, with 6 bits per pixel required to give the necessary radiance resolution. Thus about 6×10^6 bits, plus a few for pointing and housekeeping information are needed for the raw data for a frame. If a frame is taken every 180 km, this means about one frame every 28 seconds, and a total of about 70 frames per orbit if the trace of the horizontal specular point is entirely over water. Thus a maximum of about 420 Megabits of data might be accrued per orbit.

Each frame must be exposed in about 48 msec or less to preserve the inherent resolution capability of the 1000 line vidicon and thus to be able to locate slicks or other features of interest. (Since the glitter pattern moves along with the spacecraft, there is very little smearing of the pattern itself for exposure times corresponding to spacecraft travel long compared with a pixel but short compared with changes in the average wind). However, with 28 seconds between frames available, slow readout can be used to reduce the instantaneous data rate if this is desired. About five seconds can be used for frame readout before the inevitable degradation of the image with time becomes too great to compensate for with sufficient accuracy. Thus the readout video signal can be kept down to about 200 KHz, or about 1.2 Megabits/sec if digitized.

7.3 INFRARED IMAGING/RADIOMETER

Two versions of IR sensors have been synthesized. Both utilize a conical scan technique. The instantaneous field of view (I. F. O. V.) of a telescope is scanned in a conical motion by a rotating mirror, the axis of the cone coinciding with the nadir. A circular motion on the ground of the I. F. O. V. is thus produced. As the spacecraft moves along its orbital path (Figure 7-25), a strip, or swath is scanned in a raster comprised of curved lines. This geometry was selected because of its several unique advantages:

- Resolution element size and velocity on the ground are constant. This is particularly important for the wide fields of view necessary for global ocean monitoring.
- The obliquity angle remains constant throughout the scan as well as the atmospheric path length. Because of this and the aforementioned spot size and velocity considerations, the desired sea surface temperature accuracies (0.2 to 0.5°K absolute) will more readily be achieved since less variables are involved.
- Scan efficiency is an honest 33 percent regardless of the field of view required. In fact, conical scanning affords the opportunity to view the same scene on the ground in a single orbital pass from different directions by looking both forward and aft in which case the scan efficiency is 66 percent.
- Image reconstruction without distortions is greatly facilitated.

- Since the mechanical motion is purely rotational, scan rate is constant (neglecting "hunting," as later discussed) and mirror distortions eliminated. The latter feature is important because little degradation of the optical performance can be tolerated without sacrificing resolution. Further, rotary motion is energy conserving and thus requires little power for operation.

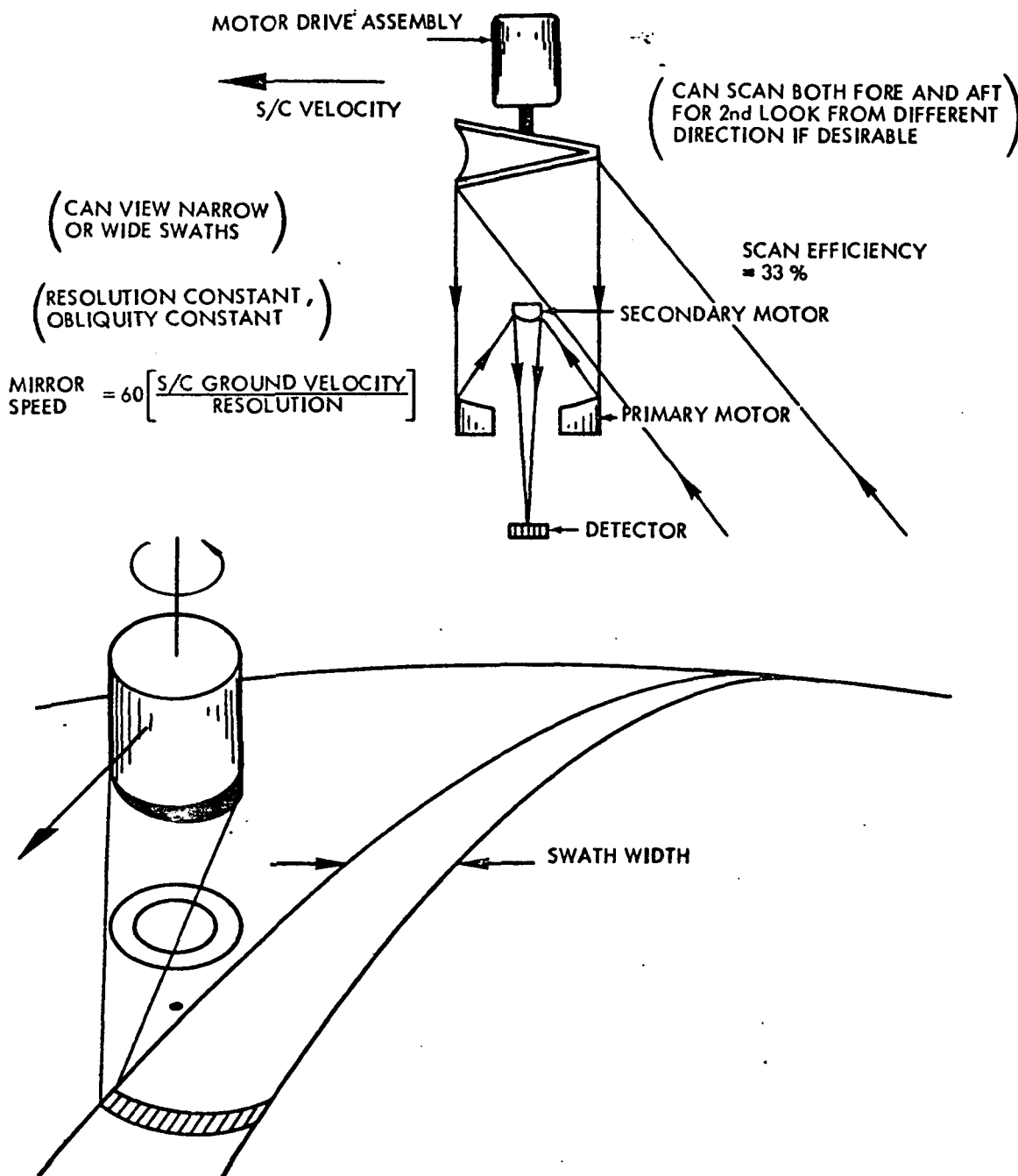


Figure 7-25. Conical Scan

The first candidate IR sensor (instrument specification sheet 6.3.2) might be considered a minimum experiment in that it is single channel (8-13 μ) and fixed swath width (1000 km). A 12 cm (4.7 inch) diameter f/1 reflecting telescope consisting of a primary and secondary mirror focuses the earth's thermal radiance on a single Hg Cd Te detector ($D^* \sim 2 \times 10^{10}$). A filter is required to block the lower wavelengths to avoid daytime specular solar reflectance. The detector will be radiatively cooled by a horn viewing deep space similar to the M. S. P. S. scheduled for flight on ERTS A/B. This technique, although rather bulky in size, requires no power for operation and should provide sufficient cooling for one or a few detectors. The scan mirror will rotate at 420 rpm, probably being driven by a hysteresis-synchronous A. C. motor and supported on ball bearings. This speed should pose no problem for ball bearings even in a space environment. Class 9 or better bearings, "dry" lubricated with specially designed labyrinth seals, will provide sufficient accuracy (less than 10 percent of the one milliradian I. F. O. V. due to precession or out-of-roundness) and reliability. Fluid (gas or liquid) bearings, both hydrodynamic (self generating) and hydrostatic (external pressure supply) have been successfully applied to rotating mirror scanners in applications requiring ultra-precision and/or high rotational speed. However, the extra peripheral equipment necessary (supply pumps or artificial atmospheric environment) makes their use unjustified in this application. One item, always of concern in spaceborne optical devices, is the possibility of foreign material depositing on optical surfaces over a period of time, degrading their performance. However, recent developments in lubricants and seal design have eliminated the possibility of lubricant outgassing contaminating the optics.

The hysteresis-synchronous motor is used because it "locks" onto its driving signal and is very efficient (80 percent or better when momentarily over-magnetized upon reaching scan speed). Although the motor runs at the same average speed as the driving frequency, a phenomena known as "hunting" occurs. Depending on driving torque and shaft supported moment of inertia, sinusoidal ripple in scan velocity (perhaps 4-5 Hz for this application) develops. There are two schools of thought concerning this slight advance and retard of the scan mirror (thus the

I. F. O. V. spot on the ground). The first is to compare shaft position, indicated by a shaft mounted optical encoder, with the driving signal. Any lead or lag is corrected by phase-lock-loop circuitry. Digital techniques have been particularly successful, being able to maintain true scan position within 5-10 arc seconds. The second is to allow the scanner to hunt and use the encoder to trigger the A/D address or telemeter position data to the ground and remove pixel position error from the data there. Selection of the technique will be made in final design of the sensor.

This minimum experiment IR radiometer/imager (depicted in Figure 7-26), although requiring some design effort, is well within demonstrated state of the art in performance and component development.

The maximum IR experiment recommended is similar in configuration utilizing a conical scan configuration. However, it is a much more flexible and capable instrument in that it is multispectral, having several spectral channels including some in the visible spectrum and has a variable field of view.

In a recent study,⁽⁹⁾ Anding et al have described a technique for removing atmospheric effects on temperature measurements by performing simultaneous radiometric measurements in three narrow spectral intervals centered at 4.9, 9.1 and 11.0 μ . The effects of non-cloudy atmospheres on the observed radiance can be nearly completely compensated for and estimates of sea temperature to an accuracy of 0.15°K can be obtained. For fields of view which contain clouds, the three-channel radiometric data also provide the necessary information to indicate the presence of semitransparent or opaque clouds within the field of view and, if opaque, the fractional amount of cloud obscuration to an accuracy of approximately 10 percent for any field of view size. A model signature typical of those developed by Anding et al is illustrated in Figure 7-27.

In addition to the thermal channels, it is recommended that a broadband visible channel be included. This is to aid cloud cover determination and provide panchromatic imagery precisely registered with the IR data. Additionally, a near IR and/or an ultra-violet band (low sensitivity due to transmission of atmosphere) may aid in recognizing oil slick and other targets. It is not practical, however, to attempt detailed visible spectral

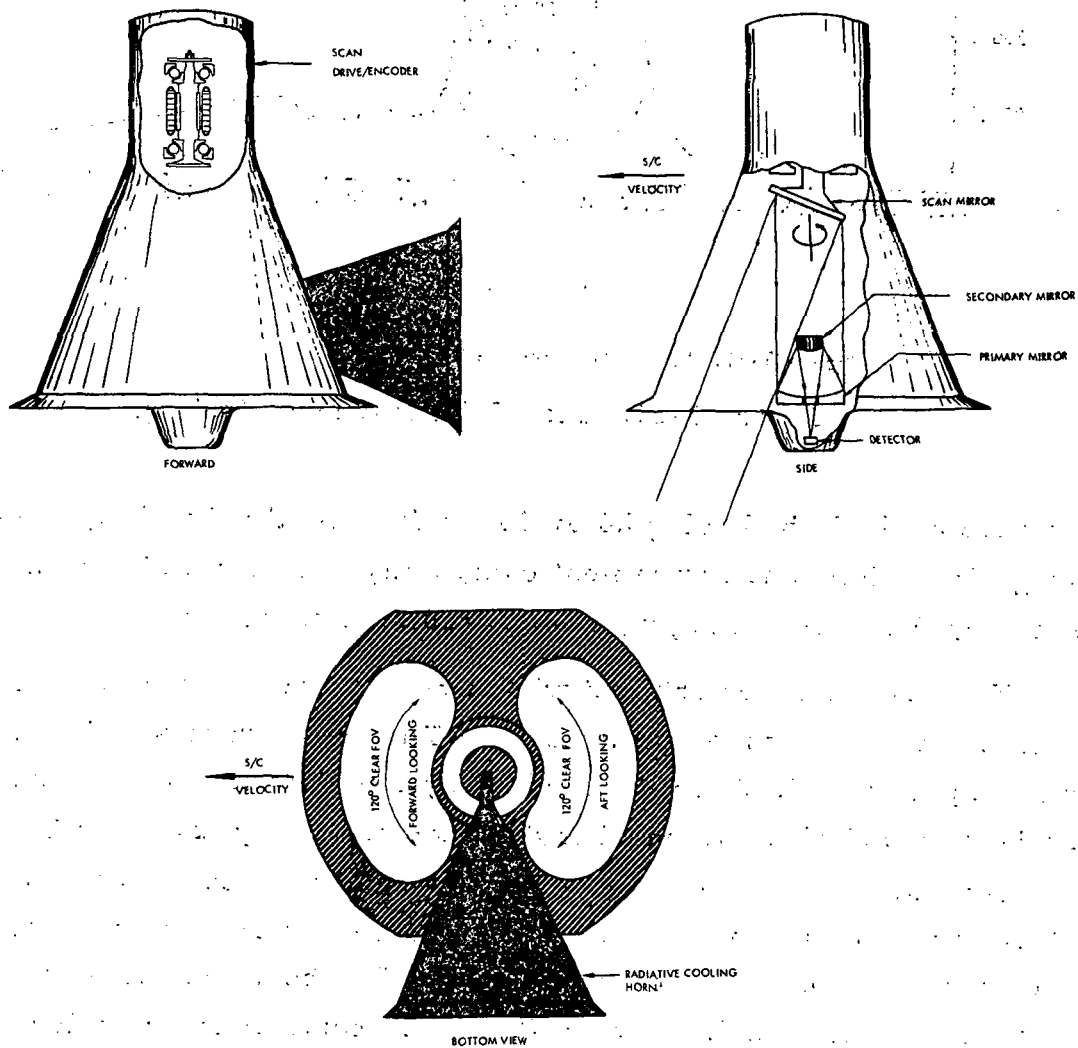


Figure 7-26. Conical Scan Infrared Imager (Minimum Experiment)

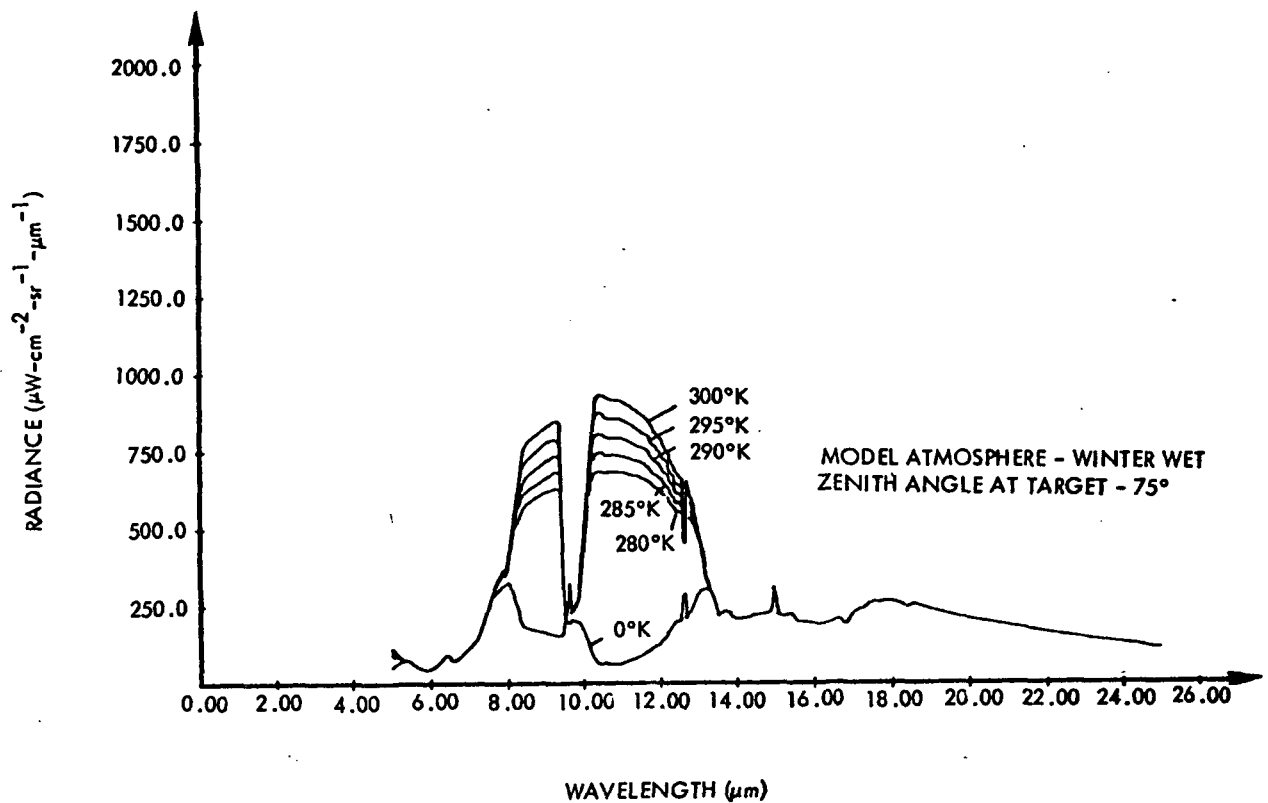


Figure 7-27. Model Atmosphere (Anding)

Figure 7-27. Model Atmosphere (Anding)

signature analysis by having 20 or 30 highly sensitive bands because of energy limitations and instrument complexity. This task is better performed by the visible imaging spectroradiometer elsewhere described.

The maximum experiment will have a feature unique to spaceborne (or aircraft, for that matter) sensors. The swath width will be adjustable from very narrow (100 km) to essentially complete horizon to horizon coverage. This is accomplished without changing scan efficiency or the number of resolution elements. This capability will allow concentrated viewing of a local feature, medium swaths for general coverage, or broad observation of large phenomena in a single orbital pass. Further, the same area on the ground may be viewed from two different or continuously varying incident angles for the atmospheric and emissivity studies. The means of implementing the variable field of view is to articulate the scan mirror at the fixation to its supporting shaft (Figure 7-28) thus allowing different cone angles to be selected. Adjustment of the angle would be made by a slip-ringed stepper, mechanically, or other means. This feature is quite practical for the 25 cm aperture optics since the rotational speed is low (7 revolutions per second) for this application.

The size and weight of a 25 cm aperture sensor are fairly significant in terms of payload percentage. For this reason it is anticipated that beryllium metal will be used in its construction allowing a 30 to 40 percent weight savings. From Table 7-8, which illustrates typical mirror and structural materials, the stiffness to weight advantage of beryllium is apparent. Also, one material can be used for both optics and supporting structure simplifying design (thermal expansion compatibility, etc.). The weight estimate to 43 kg on instrument specification sheet 6.3.1 was made assuming the extensive use of beryllium.

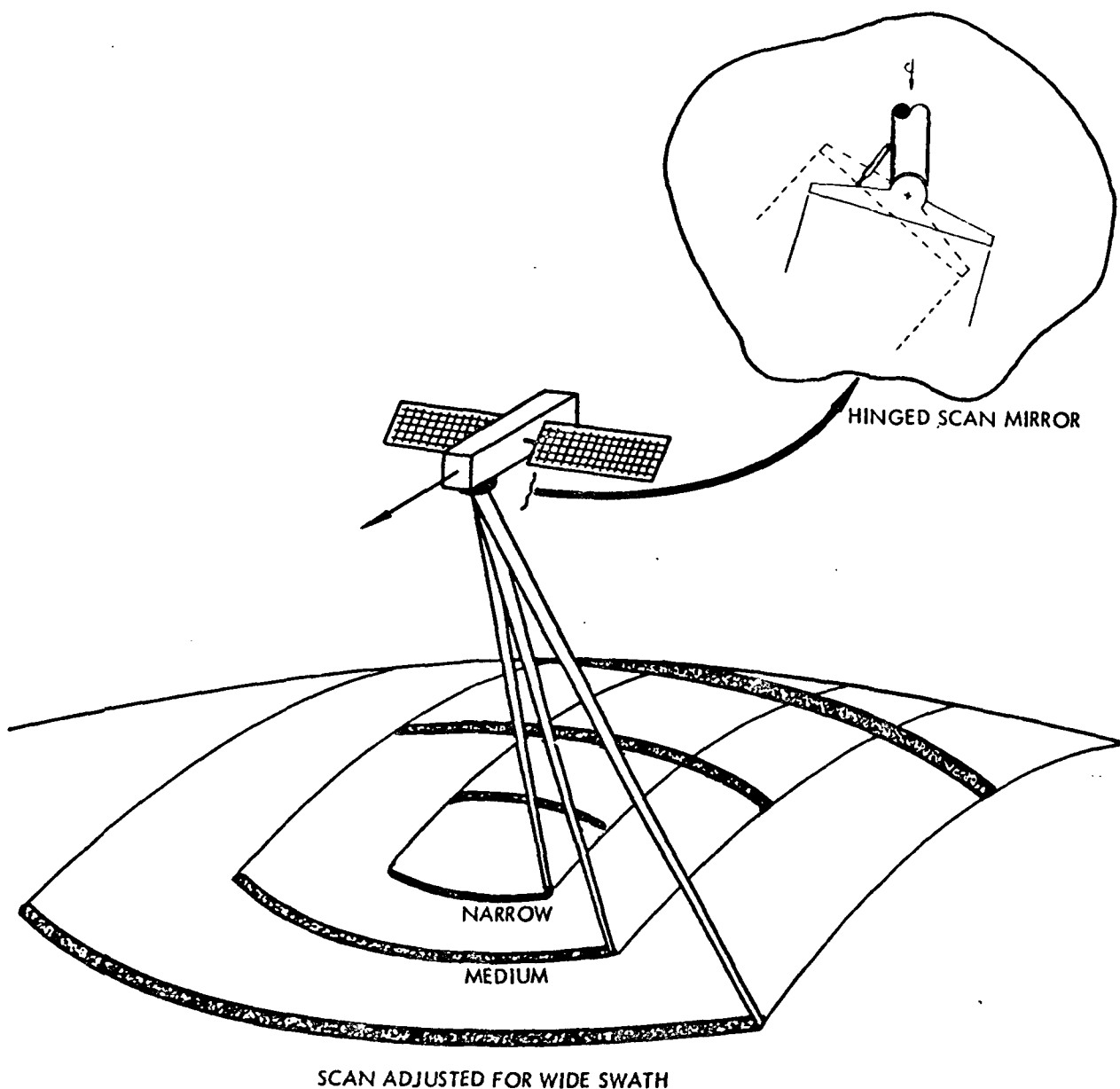


Figure 7-28. Multispectral/Adjustable FOV Scanner

Table 7-8. Comparison of Materials Used for Mirror Substrates and Supporting Structure

PROPERTY	MATERIAL							
	BERYLLIUM (S-350)	FUSED SILICA	CERVIT	ALUMINIUM 2024-T86	STAINLESS 410	MAGNESIUM ZK514	INVAR	TITANIUM GAL-4V
DENSITY (LBS/IN ³)	.0677	.0795	.0905	.10	.29	.0656	.291	.164
COEFFICIENT OF THERMAL EXPANSION IN/IN/°F	6.5x10 ⁻⁶	.33x10 ⁻⁶	+1x10 ⁻⁷	12.6x10 ⁻⁶	5.5x10 ⁻⁶	14.5x10 ⁻⁶	.7x10 ⁻⁶	5.0x10 ⁻⁶
THERMAL CONDUCTIVITY, BTU/HR/FT ² /FT/°F	104.	0.83	0.96	70.	14.4	63.	7.8	4.5
MODULUS OF ELASTICITY LB/IN ²	44x10 ⁶	10.5x10 ⁶	13.4x10 ⁶	10.6x10 ⁶	29x10 ⁶	6.5x10 ⁶	21x10 ⁶	16x10 ⁶
MODULUS TO DENSITY RATIO	657x10 ⁶	132x10 ⁶	148x10 ⁶	106x10 ⁶	100x10 ⁶	99x10 ⁶	72x10 ⁶	98x10 ⁶
POISSON'S RATIO	.03	.16	.25	.33	.3	.35	.29	.322
APPLICATION	MIRROR SUBSTRATES AND STRUCTURE	SUBSTRATE	SUBSTRATE	SUBSTRATE/STRUCTURE	STRUCTURE	SUBSTRATE/STRUCTURE	STRUCTURE	STRUCTURE

Calibration of each channel will be performed between each active part of the scan by including known radiance standards in the sensor package, i. e., blackbody sources for the IR channels and diode emitters for the visible. Since part (66 or 33 percent depending on whether one or both fore/aft views are active) of the scan cycle is "deadtime," the data rate can be reduced by "line stretching." That is, expanding the data during active scanning to fill the time taken for one scan. This can be accomplished by a buffer storage or a more recently developed technique requiring no storage external to the sensor proprietary to TRW.

7.4 LASER AND RADAR INSTRUMENTATION FOR PRECISION OCEAN ALTIMETRY

This and the following sections describe conceptual sensor designs and specific hardware configurations suitable for application to oceanographic missions. These missions include ocean current, tide, and storm measurements, and require precise determination of the mean ocean height profile over extended ocean areas. This section first considers the applicability of laser versus radar altimetry systems, and decides in favor of the radar system for all missions on the basis of hardware size, weight, and power considerations. A baseline radar system is then described, and subsystem configurations are detailed for the major components. It is concluded that reliable system performance can be obtained with virtually off-the-shelf components requiring neither excessive development time, technical risk nor cost. Next this section considers geodetic factors in altimetry measurements. Irregularities in the geopotential produce two effects in altimetry measurements:

1. The mean sea surface (neglecting various oceanographic phenomena) follows an equipotential surface called the geoid, which differs from an ellipsoid by amounts up to ± 80 meters (see Figure 7-30)
2. The satellite carrying the altimeter follows a trajectory disturbed by the geopotential field.

Because the gross magnitude of these effects far exceeds the desired precision for oceanographic measurements, the following questions will be addressed:

1. Spectrum. What are the magnitudes of the disturbances of the geopotential over long distances (orbit or earth scale), moderate distances (2000 km), and short distances (100 km); or what is the spectrum of geopotential effects?
2. Predictability. To what accuracy can the effects of the geopotential on the orbit and the sea surface be predicted?
3. Elimination Through Differencing. To what extent can the effects of the geopotential be ignored because they will be eliminated by differencing the observed altitudes on different passes?

It is necessary to define for reference the desired accuracy in altimetry for oceanographic measurements: changes in slope of the mean sea surface of from one part in 10^5 to one part in 10^7 over regions of 100 km or more are to be measured. These slopes correspond to an altitude change of 100 cm down to 1 cm over 100 km.

It was concluded that interference from unknown short wavelength slopes in the geoid enters at slopes of order 2.5×10^{-7} . However, these effects are the same on different passes over the same region, and hence can be subtracted out in determining changes in slope of the mean sea surface. Short wavelength slopes (1000 km) in the orbit resulting from geopotential disturbances are of order 10^{-7} or less. These slopes vary from orbit to orbit, and are not well known for short wavelengths.

7.4.1 Instrumentation Characteristics for Altimetry

The following altimeter performance requirements have been developed.

Range Accuracy	10-20 cm, 1σ
Pointing Accuracy	$.3^\circ$ 1σ each axis
Area Averaging	Accuracy specification applies to relative mean ocean height over 5-10 km diameter areas
Data Rate:	One measurement per 10-20 km along track
Sensor Altitude	925 km (500 nmi)
Viewing Geometry	Nadir
Duty Cycle	≤ 100 percent
Availability	All weather
Reliability	1 year MTBF
Weight	≤ 90 kg (≤ 200 lb)
Power Input	≤ 150 watts

7.4.1.1 Laser versus Radar Tradeoff

The relative applicability of laser and radar altimeters for spaceborne ocean ranging has been examined on several occasions.⁽¹⁰⁾ The results depend strongly on the specific mission chosen and generally favor the laser system when fine angular beamwidths or angular resolution are required, and otherwise favor the radar. In the present application, extensive area averaging over the ocean surface is required to reduce the undesired effects of local wave structure, and consequently narrow altimeter beams are of little use. The radar can then be expected to be the preferred configuration, as borne out in the following tradeoff analysis.

For purposes of comparison, a pulsed X-band radar and a Nd:YAG Q-switched laser have been selected. The X-band system is recommended on the basis of a tradeoff between component miniaturization and all-weather capability, and the Nd:YAG system represents a suitable choice of high efficiency power source and sensitive receiver. While neither system represents the results of an exhaustive tradeoff optimization, both are thought to satisfactorily represent typical operational systems.

Table 7-9 presents the results of the laser/radar tradeoff in terms of the parameters which must strongly impact the spacecraft platform and overall mission feasibility: sensor size, weight, and power. It is clear from the table that the laser system is both larger and heavier than the radar, and requires more than four orders of magnitude more power. The laser power requirement is sufficient to exclude the system on this basis alone, while the radar transmitter power requirement is so modest as to be negligible compared to peripheral electronic power requirements and filament supplies. The overall radar power requirement is estimated to be less than 30 watts.

Table 7-9. Tradeoffs Between Laser and Radar Altimeters for Equal Performance (10 pulses per second)

	<u>Laser Altimeter</u>	<u>Radar Altimeter</u>
Power	5 kw	30 watts (0.17 watts transmitter)
Weight	45 kg (100 lb)	23 kg (50 lb)
Volume	.085 m ³ (3 cu ft)	.014 m ³ (0.5 cu ft)

Further advantages of the radar system are:

- The radar altimeter is more nearly capable of all-weather performance than the laser altimeter.
- The radar system measurement rate can be significantly higher than that of the laser system.
- Radar systems are generally better developed than laser systems. As a result most of the radar altimeter components can be obtained off-the-shelf, while some of the components assumed in the laser analysis are still in the developmental stage (e. g., detectors with high quantum efficiency at 1.06 microns and narrow spectral filters with high transmission at 1.06 microns).

7.4.1.2 Radar Altimeter

Table 7-10 lists the characteristics and performance capabilities of the recommended radar altimeter. Operation at 9 GHz ensures satisfactory measurement accuracy through all but the heaviest weather and yet allows operation with only a 0.9 meter (3 ft) diameter antenna structure. Receiver sensitivities remain good at X-band and a maximum of off-the-shelf hardware is available for across the board component selection.

A 43 kw peak power transmitter is recommended which is capable of achieving the required ranging accuracy with a single 40 nanosec amplitude modulated CW pulse. The required sampling rate can be satisfied with this system with a pulse repetition rate of less than one per second. Much higher data rates can be achieved for increased range accuracy, or can be traded off against peak transmitted power. Transmitter size and weight requirements are not directly related to peak power however (but to average power), and the savings will not be first order. Conversely, a significant increment in receiver complexity will be required to perform multiple pulse integration. On balance it appears that the single pulse system is the most attractive for this application.

At 925 km range the antenna illuminates an ocean surface area of approximately 34.5 km diameter (half power). Of this area a 40 nanosec pulse instantaneously illuminates a footprint equivalent to an 8.8 km diameter spot. The illuminated area originates at the nadir point, builds up to 8.8 km diameter, and then sweeps out to 34.5 km in an essentially constant area ring. Relative range measurements are made on the basis of the inflection point of the pulse rise waveform, or the null point of the

Table 7-10. Radar Altimeter

System:

Source power required	30 watts
Overall system weight	23 kg (50 lb)
Overall system volume	.014 m ³ (.5 ft ³ = 864 in ³)
Accuracy	10 cm
Attitude stabilization accuracy	0.3°

Antenna:

Diameter	0.9 m (3 ft)
Thickness	1 cm
Aperture shape	Circular
Aperture illumination	Uniform
Beamwidth	2.13° (37.2 mr)
Gain	38 dB
Weight	3.2 kb (7 lb)

Transmitter:

Frequency	X-band (9 GHz)
Pulse peak power	43 kw
Pulse length	40 ns
Pulse repetition frequency	1-100 ppS

Receiver:

Noise figure	8 dB
Bandwidth	25 MHz
Bandpass characteristic	Synchronous single tuned
Receiver delay	150 ns

Processor:

Type	Two-stage delay differencing
Processor delay	75 ns
Output waveform	Ramp doublet (ideal)
Timing sensor	Pulse-time discriminator

Altitude Tracking Circuit:

Type	Phase (altitude) locked prf oscillator
Tracking bandwidth	.157 Hz
Tracking time constant	1 second

Altitude Counting Circuit:

Type	Digital frequency meter (prf count)
Reference oscillator stability	10 ⁻⁸
Reference oscillator frequency	10 MHz

Data Storage:

Altitude counts	
Time signals	
Temperature	(Diagnostics)
Voltage	(Diagnostics)
Signal strength	(Sea-state indication)
Bias delay altitude	(Bias error correction)
Radiometer Signal	(Refractivity correction)

second derivative of range return. Each measurement represents an average over approximately 60 km² of ocean and thus averages over local wave structures very well. A signal to noise ratio of 900 is provided to allow location of the inflection point to the required accuracy.

7.4.2 Geoid Effects in Altimetry

Kaula⁽¹¹⁾ has derived from statistical analysis of surface gravity anomalies a set of power series representations of the spectrum of geopotential effects. The preferred representation of the earth's potential for geodetic and satellite applications is a summation of spherical harmonics with empirically derived coefficients

$$\bar{C}_{lm}, \bar{S}_{lm}$$

where the order l corresponds to terms of wavelength $\frac{2\pi R}{l}$ in the potential expansion (R is radius of the earth and m varies from 0 to l). Kaula's spectral representation formula was first applied to terms of order $l \leq 15$. Present determinations of the coefficients for the geopotential such as by Gaposchkin and Lambeck⁽¹²⁾ are complete to order $l = 16$. In addition, there are a few higher order terms evaluated from resonant orbits of periods 12, 13, and 14 revolutions per day.

For terms of order $l \leq 15$, the spectrum of variations of order l is represented by

$$\delta_l(V^*) = \sigma \left\{ \bar{C}_{lm}, \bar{S}_{lm} \right\} \approx \pm 10^{-5} / l^2$$

Estimates of higher order spectra were computed assuming a different value of k for l 's between 15, 36, 90 and 180:

$$\delta_l(V^*) \approx k / l^2$$

These terms were derived by fitting to mean free air gravity anomalies at the earth's surface.

7.4.2.1 Spectrum of Variations at the Geoid

Figure 7-29 gives Kaula's results for the spectrum of the geoid surface which is directly proportional to the above:

$$\delta_l(h) = R \delta_l(V^*)$$

Comments about which wavelengths are well known and predictable were added on the basis that 16th order terms are only recently determined, 8th order terms have long been known and higher order terms are still unknown.

To summarize Figure 7-29 note that well known geoidal effects are of wavelength 5000 km or more, and of rms amplitude 1 to 20 meters. Recently determined terms are of wavelength 3600 km to 5000 km and rms amplitude 50 to 100 cm. Unknown terms are of wavelength 2500 km or less and amplitude 50 cm or less. Terms of rms amplitude 10 cm are of wavelength 1600 km.

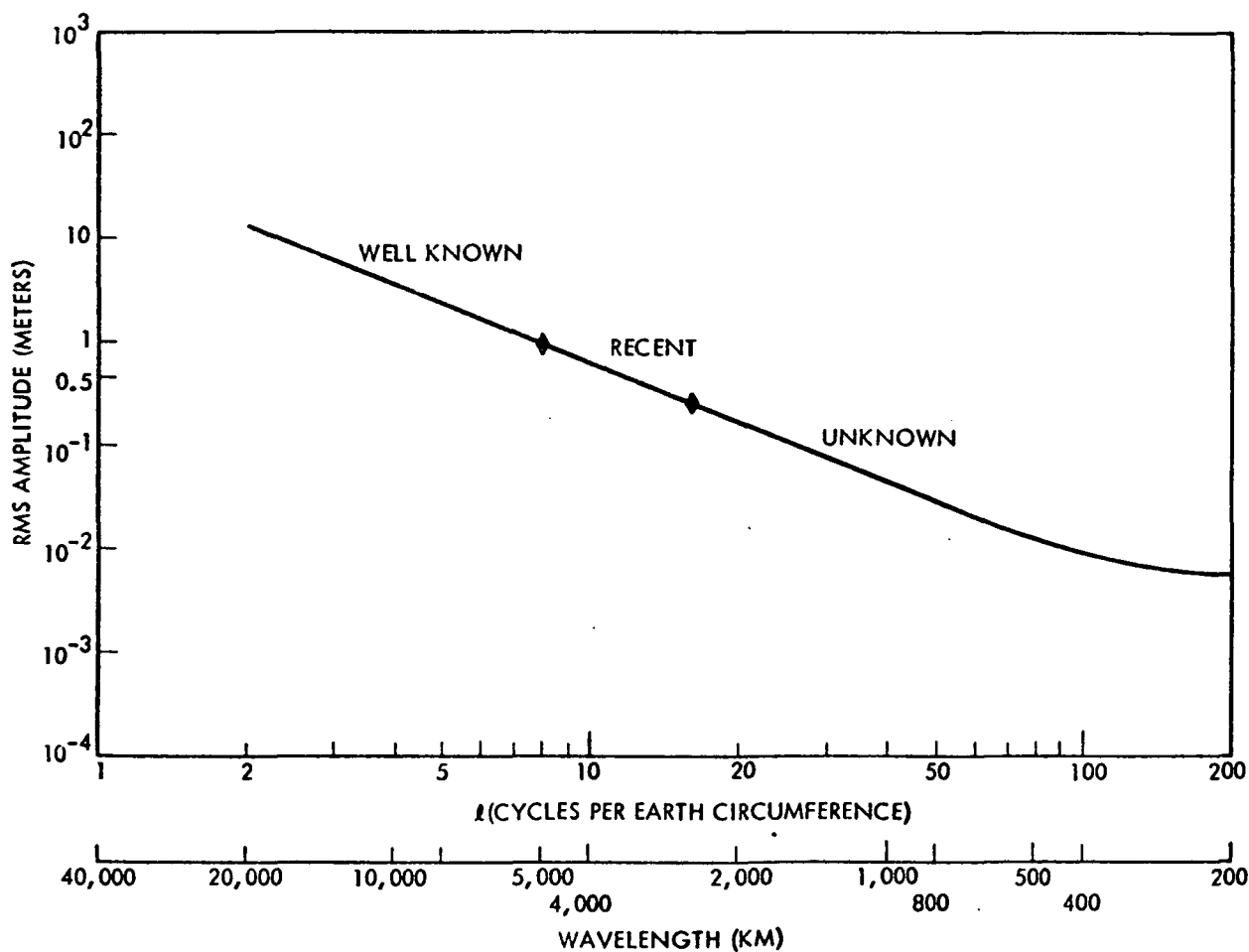
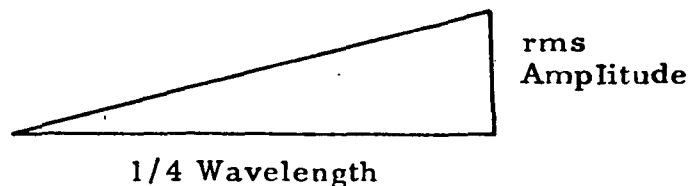


Figure 7-29. Spectrum of Geoid Undulations, RMS Amplitude Versus Number of Cycles, l , or Wavelength (from Kaula)

Translating to mean sea surface slope reference, the various terms can be compared to slopes of 1/4 wavelength as abscissa, and rms amplitude as ordinate.

Table 7-11. Slope of Geoid



<u>Amplitude</u>	<u>Wavelength</u>	<u>Slope = $\frac{\text{Amplitude}}{1/4 \text{ Wavelength}}$</u>
100 cm	5000 km	$.80 \times 10^{-6}$
50 cm	3600 km	$.55 \times 10^{-6}$
10 cm	1600 km	$.25 \times 10^{-6}$

Hence geoid undulations of unknown form produce mean sea slopes of the order 10^{-6} (Table 7-11).

7.4.2.2 Predictability of Geoid Effects

Figures 7-30 and 7-31 are reproduced from the work of Richard H. Rapp,⁽¹³⁾ and indicate the shape of the geoid and its uncertainty, respectively. A figure similar to Figure 7-30 from the Smithsonian Standard Earth is shown in Figure 7-32. Note that while the two geoid figures have the same major features, the variations between them exceed in most cases the internal accuracy of the solution represented by Figure 7-31.

In ocean areas, the internal errors for Rapp's solution are of the order of 4 meters. Differences between Rapp's and the Smithsonian solution are as much as 50 meters in the worst cases, (e. g., near New Zealand 60 meter maximum versus 114 meter maximum). Because spherical harmonics determined from satellite do a poor job of representing abrupt geodetic features such as trenches and peaks, discrepancies near such features will be large. If detail is needed near such features, it is usually taken from surface gravimetry (land or submarine). Predictability of the geoid in ocean areas is therefore poor. Where tracking stations are scarce, the worst discrepancies will occur. With the advent of satellite-to-satellite tracking, an order of magnitude improvement will be made in remote area geoid modeling.

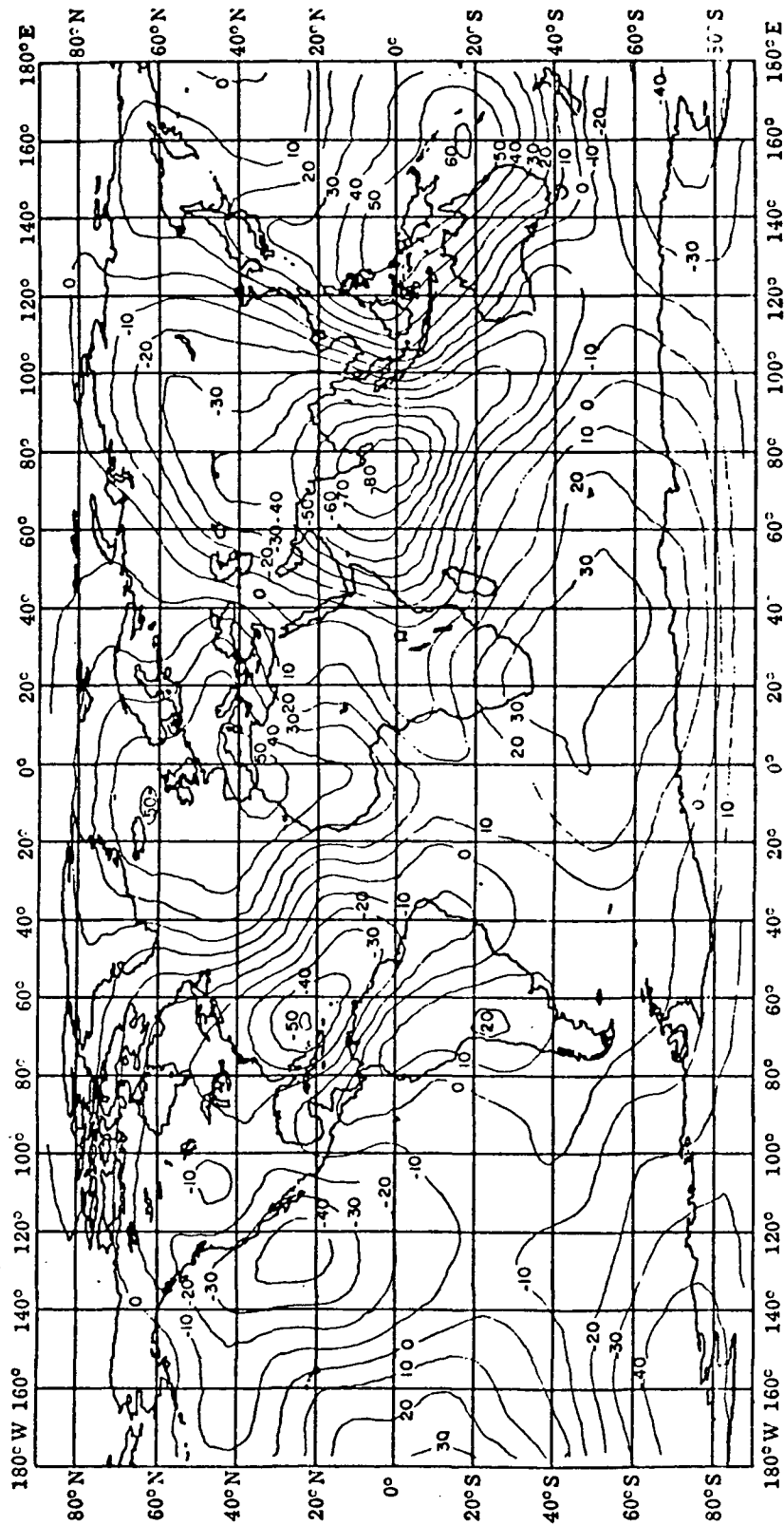


Figure 7-30. Geoid Undulations from (14, 14) Solution Reference Flattening = 1/298.25, Values in Meters (R.H. Rapp)

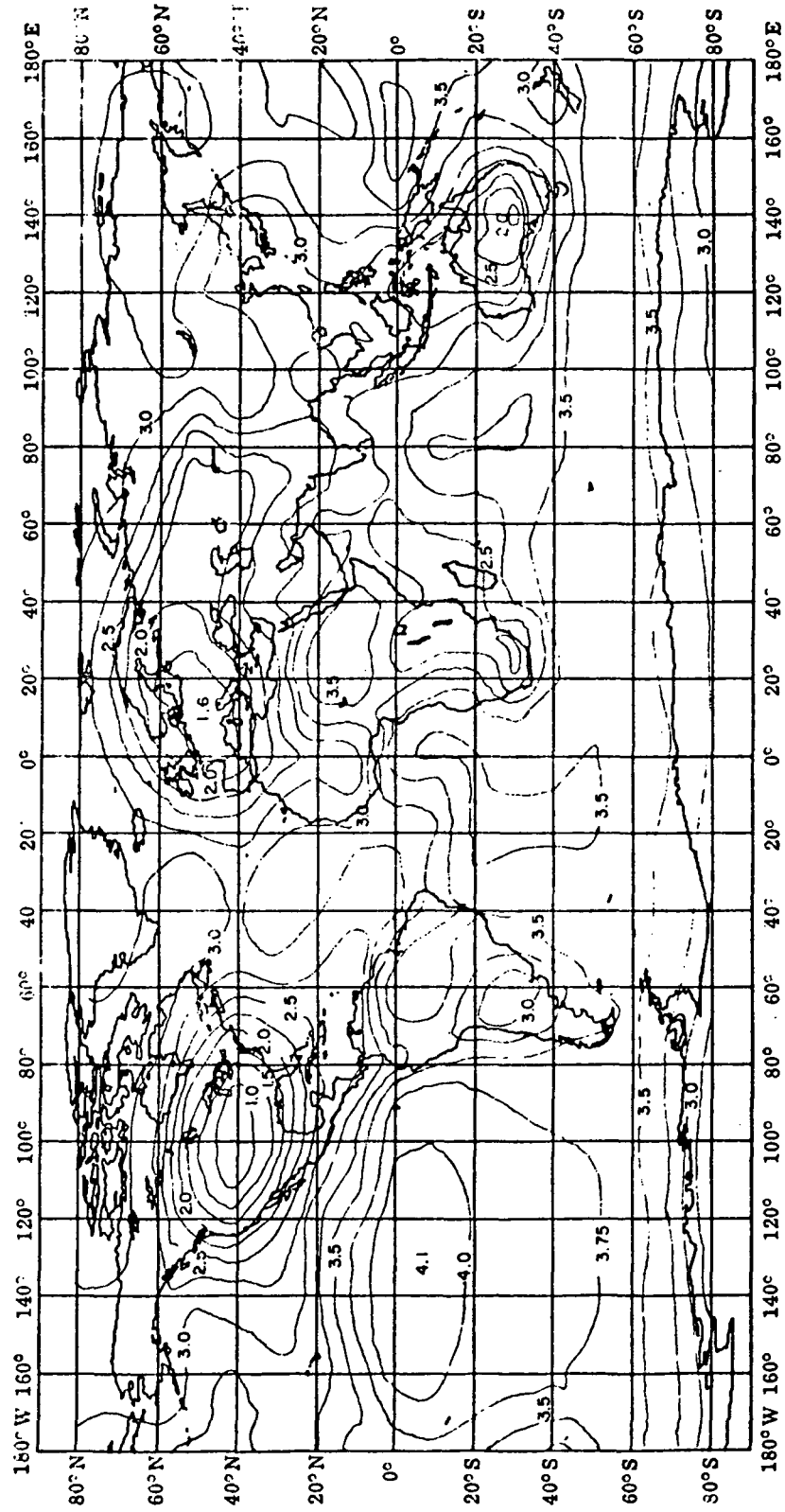


Figure 7-31. Internal Standard Error of Geoid Undulation in Meters (R. H. Rapp)

7.4.2.3 Differencing of Geoid Effects

The saving grace for the proposed oceanographic application of altimeter measurements is that it is changes in mean sea surface that are of interest. The geoid fortunately remains fixed, and for observations made in the same geographic area, the effects of the geoid will subtract out.

7.4.3 Perturbations of the Satellite

The geopotential field produces accelerations on the satellite which cause the trajectory to vary from orbit to orbit. The largest effects are those caused by features represented by zonal harmonics, which vary with latitude only. In the notation mentioned for coefficient C_{lm} , S_{lm} , $m = 0$ for zonal harmonics. These effects, as well as lunar-solar perturbations and solar radiation pressure, cause long term gradual changes in the orbit which may be ignored in studying short baseline oceanographic changes of slope. The absolute determination of orbital parameters -- in particular, the altitude above the ellipsoid, or the geocentric distance -- is also unimportant in noting short baseline slope variations.

The features in the geopotential which vary with longitude and latitude are represented by tesseral harmonics with coefficients C_{lm} , S_{lm} , where $m \neq 0$. In general these effects average out over 24 hour intervals because of the rotation of the earth. Their orbital perturbations are traditionally separated into two groups: long period effects which have a period more than one orbital period, and short period effects, which are of period less than one orbit. The long period effects are not of interest, again because they are easily distinguished from short baseline slope changes.

7.4.3.1 Spectrum of Short-Period Geopotential Perturbations in Orbit

The spectrum of short-period variations resulting from the tesseral harmonics are plotted in Figure 6-32 for an orbit of inclination 60° and small eccentricity, at altitude 886 km, and for $m = 0$. The formulation of Kaula from which this figure was taken gives the following representation of the short period spectrum:

$$\Delta_{lm} = \frac{m}{kN} \left(\frac{a_e}{a} \right)^{l+1} \frac{l+m(\sin I - 1)}{l^3 m} \left[1 - 2(.25 - e) \cdot \left\{ l \pmod{2} \right\} \right] 3000 \text{ meters}$$

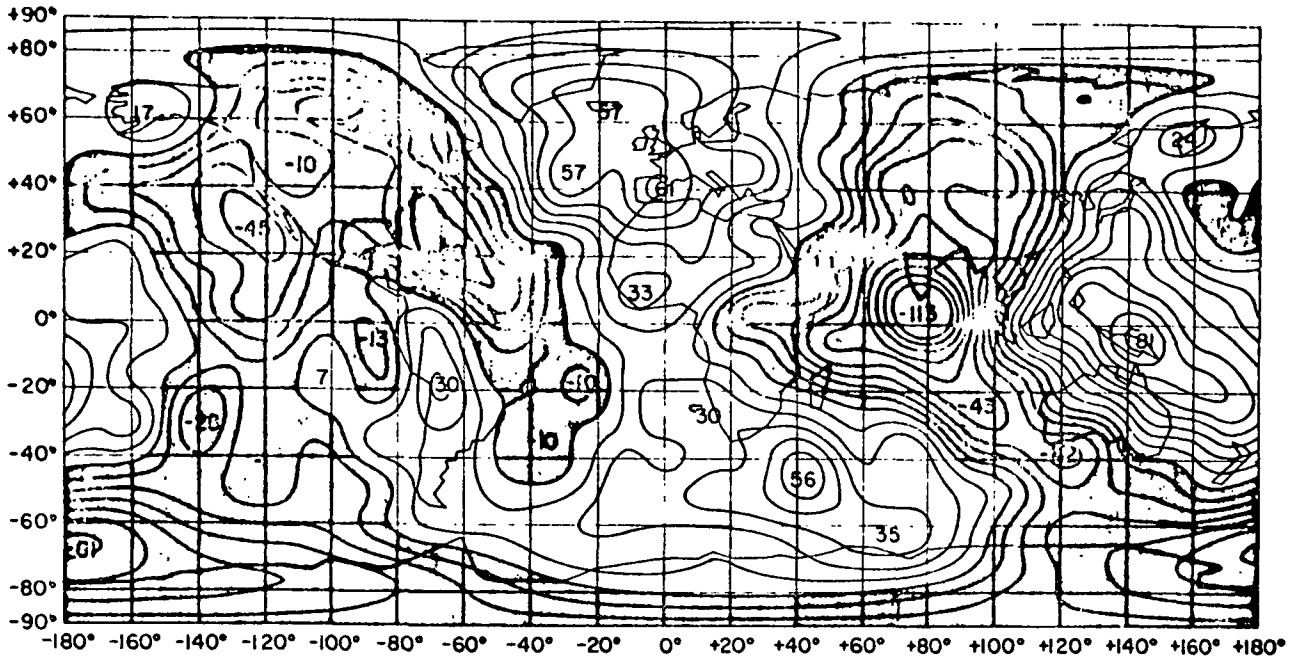


Figure 7-32. Geoid Heights in Meters of the New Combination Solution Corresponding to a Reference Ellipsoid of Flattening $f = 1/298.255$ (Gaposchkin)

Table 7-12 summarizes the slopes that would be typical for the spectrum represented in Figure 7-33. Slope is approximated by dividing the rms amplitude by one quarter wavelength.

Table 7-12. Slopes of Short-Period Orbital Variations Attributed to Tesseral Harmonics in Geopotential (from Figure 7-32)

RMS Aplitude	Wavelength (km)	ℓ	Slope = $\frac{\text{RMS Amplitude}}{1/4 \text{ Wavelength}}$
15 m	22,800	2	$.2 \times 10^{-5}$
1 m	10,000	4	$.4 \times 10^{-6}$
10 cm	5,000	8	$.8 \times 10^{-7}$
1 cm	3,300	14	$.1 \times 10^{-7}$

The slopes which approach the baseline scale of 1000 km or less of interest in this application are of order 10^{-7} or less.

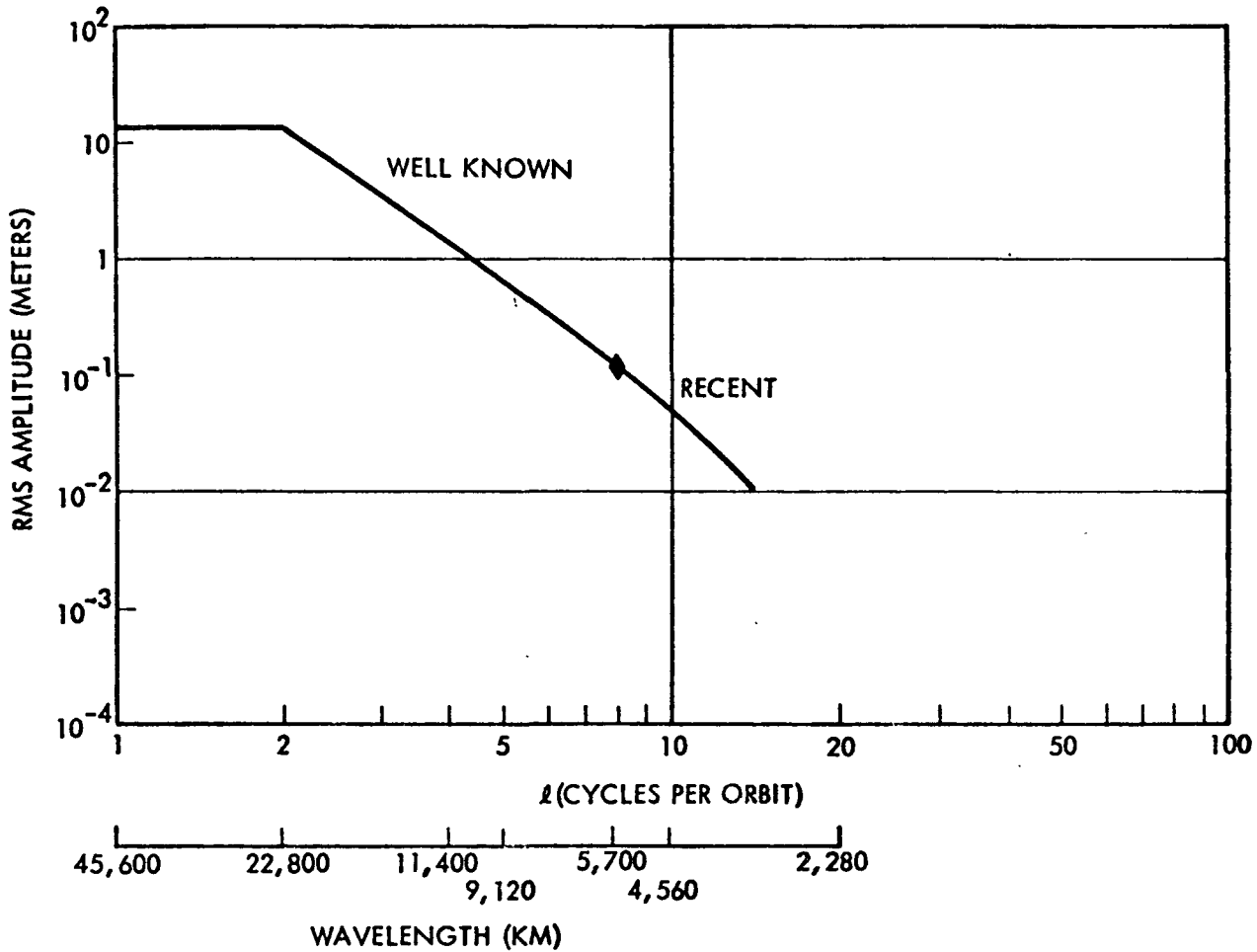


Figure 7-33. Spectrum of Short Periodic Perturbations of Orbit at Altitude 886 km (480 nmi) for Terms of l Cycles per Orbit in Geopotential

7.4.3.2 Predictability of Geopotential Effects

Because the features in the geopotential represented by terms up to order $l = 8$ have been well known for some time, they are predictable. Terms of order $8 < l < 16$ are recently determined, and can be predicted with some uncertainty. These are the terms of rms amplitude between 1 and 10 cm. Unknown terms ($l > 16$) produce disturbances of less than 1 cm rms amplitude.

7. 4. 4 Interaction of Oceanographic and Geopotential Effects in Altimetry

In a document entitled "Oceans from Space: Proceedings of a Symposium on the Status of Knowledge, Critical Research Needs, and Potential Research Facilities Relating to the Study of the Oceans from Space, Houston, Texas", Peter C. Badgley et alia made the following statement about the measurement of ocean currents using satellite altimetry:

"There is one feature, though, of the western boundary currents; they are long narrow features. This change of 100 centimeters, or so, takes place over a relatively small distance normal to the current of about 100 kilometers. Figure 7-34 is a section roughly normal to the Gulf Stream near Cape Hatteras. We see that there is a dip as one goes away from shore and a rise as one goes out to the Gulf Stream. Other sections yield substantially the same results, and one can say that the change in elevation relative to the geoid across the Gulf Stream over a distance of, say, 100 kilometers is of the order of a meter. We have added the contours to the Gulf Stream to the contours of the geoid as shown in Figure 7-35, and one can see the Gulf Stream as a characteristic perturbation. If we consider a section normal to the Gulf Stream as in Figure 7-36, the Gulf Stream is still visible. The dashed line is from Guier and Newton assuming that their geoid is correct. The solid line is what an altimeter would measure, if it happened to follow this particular track. If the line for the geoid was a little bit more jiggly than shown, the curve for the sea surface would also trace those jiggles, and one might still be able to see the Gulf Stream. The limitation is that the geoid must not have scales in it comparable to the width of the Gulf Stream.

If the geoid is not too bumpy, and no one really knows, then one can detect western boundary currents. This concept will extend to all the other important western boundary currents of the earth. One of the properties of these western boundary currents is they do vary in position with time very slowly, and a spacecraft is a good way to keep track of this time variation on a global scale. We believe that the gradient approximation will hold quasi-instantaneously, but after the course of a few days, as Dr. Ewing points out in Chapter 4, the Gulf Stream is someplace else. This might be one way to find it. "

The statement, "If the geoid is not too bumpy, and no one really knows, then one can detect western boundary currents," may be considered further in the light of William Kaula's results as discussed in the preceding sections. Because surface gravity measurements on land and by submarine at sea have yielded detailed information about the geoid over limited areas, it has been possible for Kaula to describe that bumpiness using spectral analysis. Estimates by Kaula of the amplitude of geoid and orbit undulations of various wavelengths are reproduced in Figures 7-29 and 7-33. These results of Kaula led to the conclusion by us that geopotential disturbances of the orbit over 1000 km intervals are of order less than one part in 10^7 (See Table 7-12). The geoid undulations over intervals of 1000 km produce slopes of order one part in 10^6 or less (See Table 7-11), and are invariant with time. Hence, they can be subtracted out when tracking currents over various orbital passes. For oceanographic features as large as one part in 10^5 , these short wavelength geoid undulations will cause little interference even on a single pass. The Gulf Stream example illustrated by the figures of Badgley is of this order.

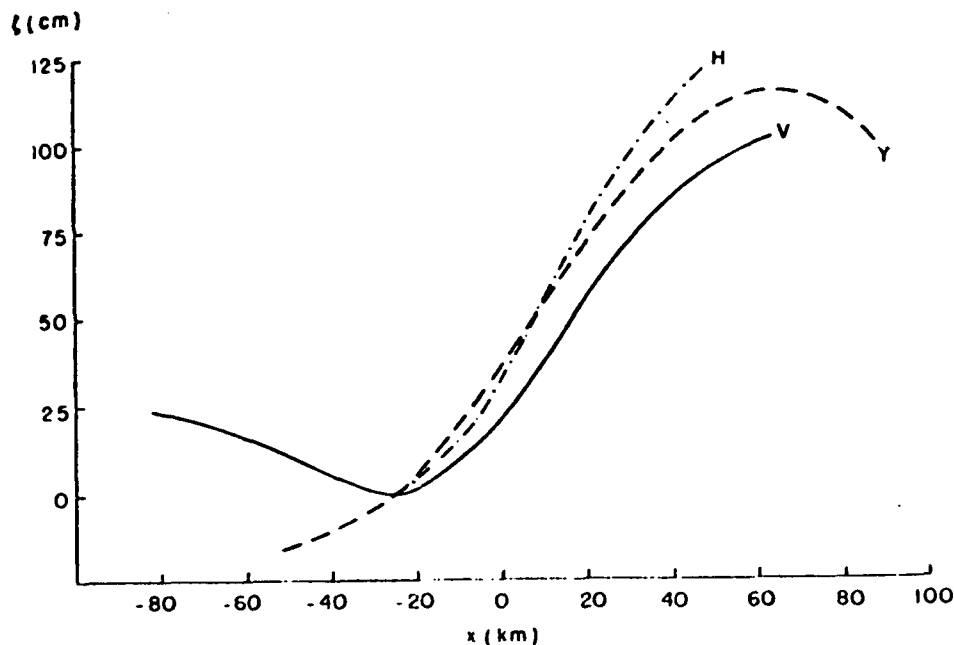


Figure 7-34. Sections Normal to the Gulf Near Cape Hatteras

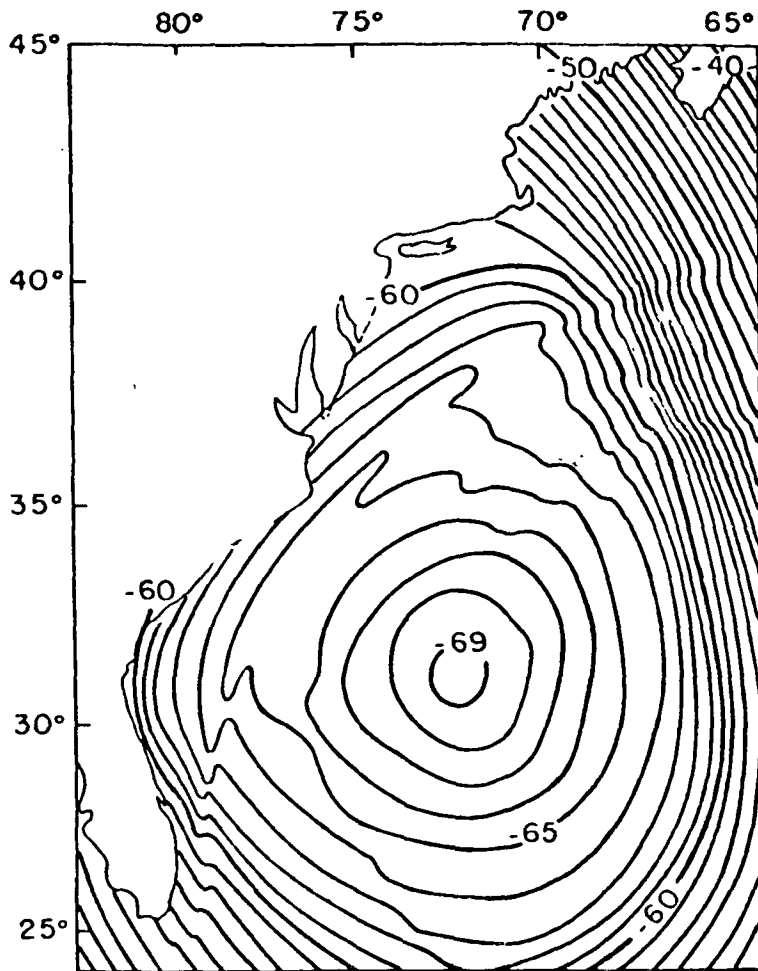


Figure 7-35. Superposition of Guier-Newton Geoid and Sea Surface Topography for Gulf Stream Region

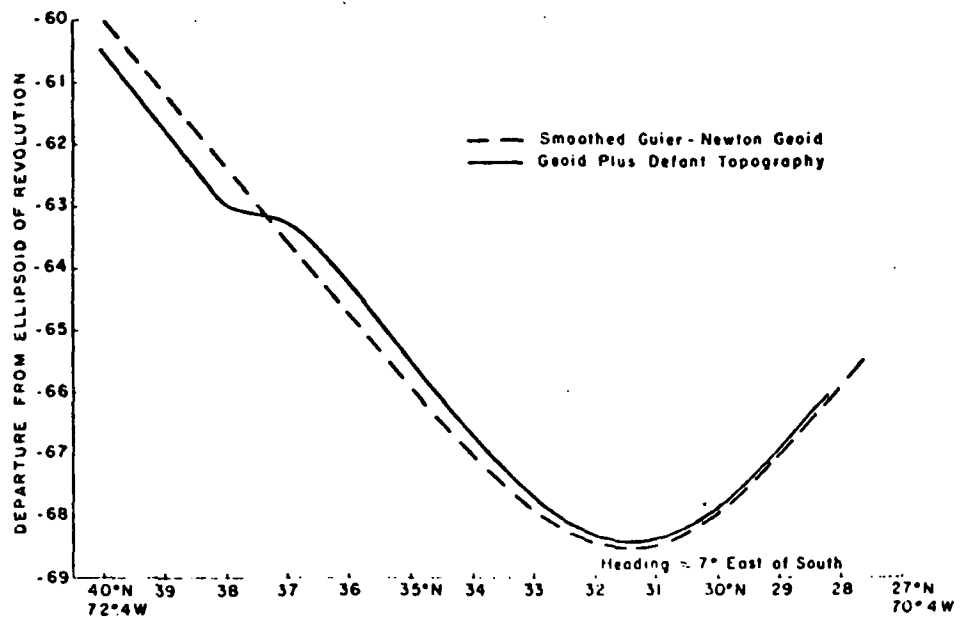


Figure 7-36. Superposition of Geoid Plus Sea Surface Topography Along a Section Normal to the Gulf Stream

7.5 MICROWAVE RADIOMETRY, IMAGING

Although radiometric measurements are only slightly affected by attenuation due to clouds at frequencies sufficiently below the water absorption band, thermal emission from clouds and the whole atmosphere in the field of view will contribute to the apparent temperature. Furthermore, the emissivity of water is a complicated function of variables such as salinity, wavelength and surface roughness, as well as temperature, so that a single measurement of apparent temperature by the microwave radiometer is useless as a means of determining the true water temperature. However, true water temperature can be derived from apparent temperatures measured at several angles and frequencies.

Microwave radiometers require large aperture antennas to achieve useful spatial resolution. Although large paraboloidal reflector antennas are feasible for space use, mechanical scanning is impractical. Fixed planar arrays, electrically scanned, can provide equivalent resolution and high scanning speeds. Conical scanning is even more desirable for microwave radiometry than for IR radiometry because of the variability of the emissivity of water with angle.

The basic microwave radiometer consists of an antenna and a calibrated wide band receiver, with a narrow bandpass filter. For practical reasons the Dicke type is almost universally used. In the Dicke radiometer, the receiver is alternately switched between the antenna and a calibrated temperature reference source. The sensitivity of the radiometer is improved by increasing the input bandwidth, decreasing the noise figure or increasing the observation dwell time. Practical configurations now in use, such as the superhetrodyne receiver, have bandwidths of 200-400 MHz, noise figures of 5-6 db and dwell times of the order of 25-50 milliseconds to achieve a sensitivity of $.5^{\circ}$ to 1° C, and absolute accuracy of 1° to 2° C. A cooled parametric amplifier input to the receiver would allow an improvement of about a factor of 2 in sensitivity, but none in absolute accuracy.

7.5.1 Microwave Radiometer

The microwave radiometer system recommended for the broad ocean requirements is similar to the dual frequency dual angle radiometer system recommended for the coastal zone requirements.

The theoretical background, a full description and a design procedure for the system are given in the final report on Coastal Zone Requirements for EOS A/B (Ref. 1). For convenience, a brief description is given here. A block diagram of the system is shown in Figure 7-37.

As shown in Figure 7-38, the composite antenna for the system, produces four separate pencil beams, each with the same beamwidth. Two of the beams are formed at 10 GHz; one at 40° and the other at 60° incidence angle. The other two

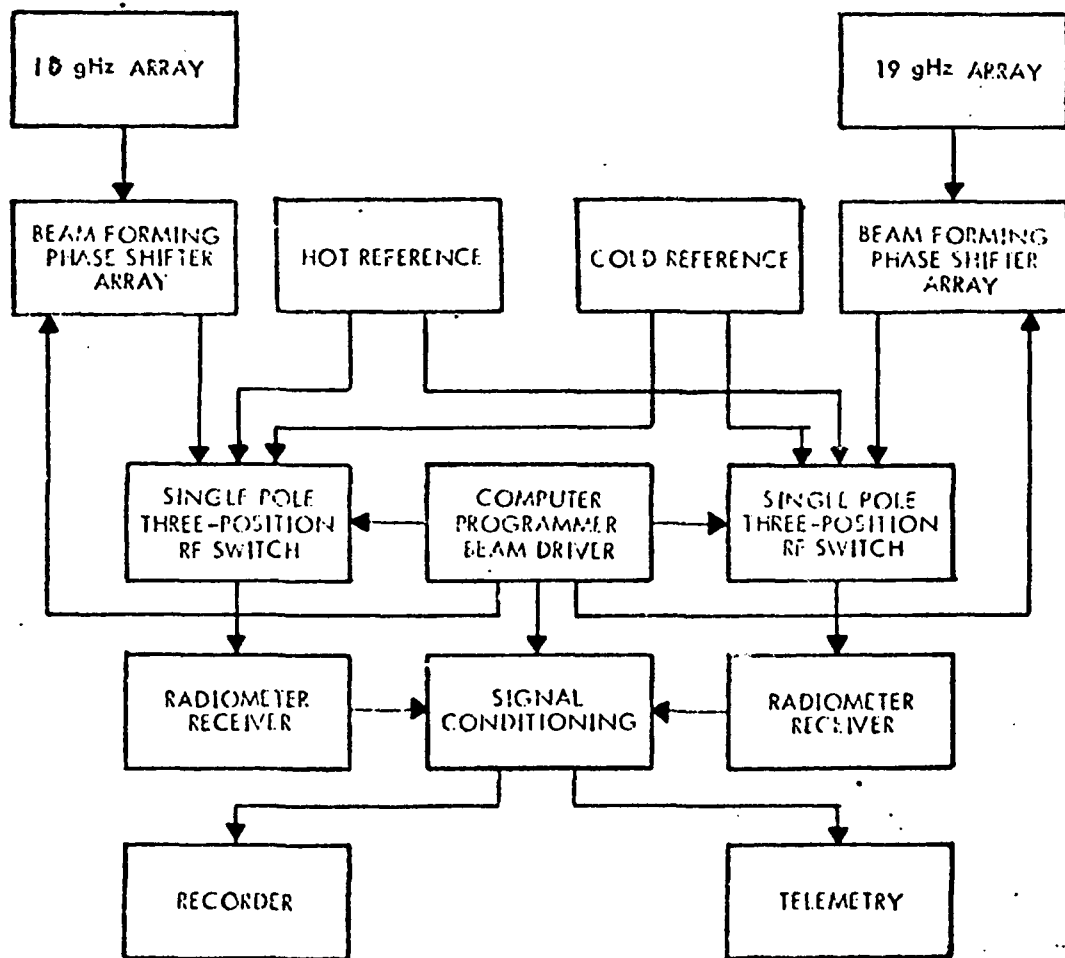


Figure 7-37. Block Diagram of Dual Frequency Dual Angle Radiometer System

beams are formed at 19 GHz, also at 40° and 60° incidence angles. All beams conically scan over a swath centered on the subsatellite track. The 40° incidence angle beams see the same surface areas as the 60° incidence angle beams, but with a time delay dependent on the orbit altitude (about 75 seconds for the 300-500 nmi altitude range).

For greatest sensitivity, each antenna beam would feed a separate radiometer, but in order to minimize errors due to receiver gain drifts, it is preferable to time share a single receiver at each frequency, switching alternately to the 60° and 40° antenna beams. This method eliminates long term drifts from the measured temperature difference but does require gain stability of about one part in a thousand for the time between the observations by the 40° and 60° beams (about 75 seconds).

The switching sequence is shown in Figure 7-39. The antenna is assumed to be step scanned across the swath, and at each position apparent temperature data is readout sequentially from the four antenna beams. In addition, each receiver is switched to a hot reference and cold reference once per scan. This not only provides absolute temperature calibrations, but also ensures that any drift during the measurement delay period can be compensated for in forming the temperature differences.

As shown in Figure 7-38 the composite antenna includes 10 GHz and 19 GHz phased array sections. The 10 GHz sections would be approximately twice as large in linear dimensions as the 19 GHz sections in order to provide the same beamwidth at both frequencies. Although it is possible that an integrated, interlaced element, dual frequency dual angle antenna could be developed, it is assumed here that for practical reasons the two frequency and two angle sections are essentially separate antennas, each controlled by the computer programmer.

The system makes simultaneous observations of the vertically polarized energy received at approximately 10 and 19 GHz, each at incidence angles of 60° and 40° with respect to the local vertical, resulting in four measurements of apparent surface temperature from each resolution element of the surface. The true water temperature, surface roughness and atmospheric water vapor density can be derived from the four measurements using a computerized model which includes multiple scattering

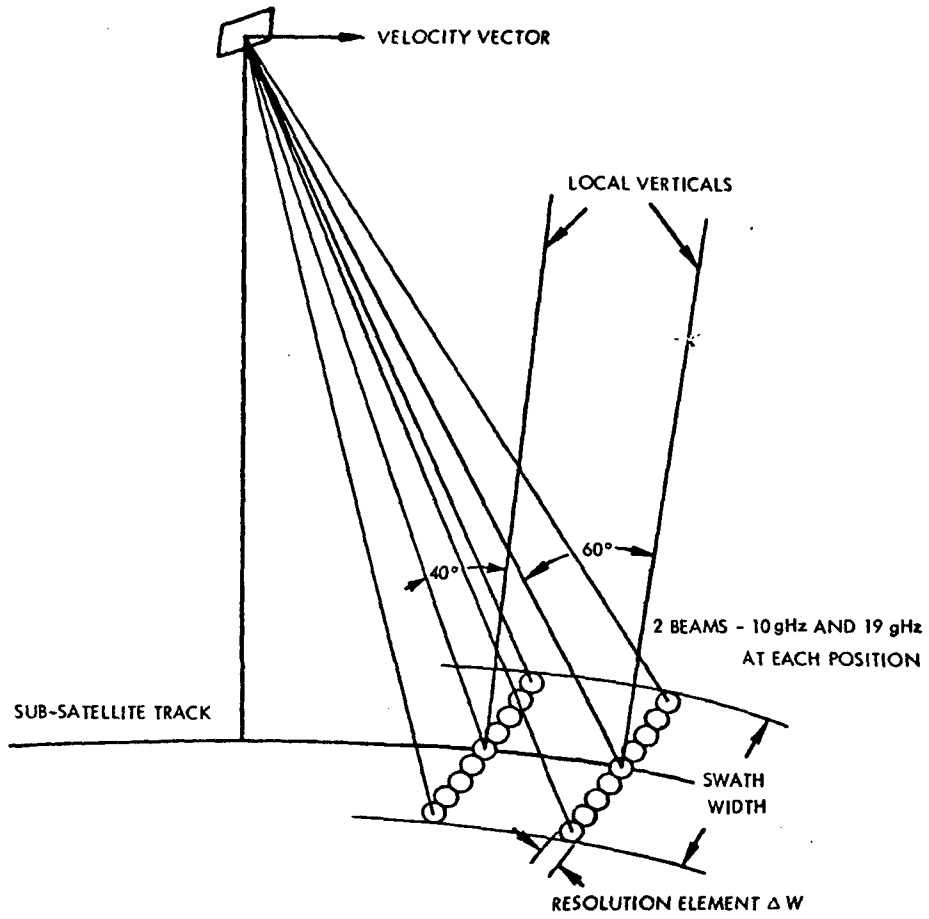


Figure 7-38. Antenna Beam Geometry

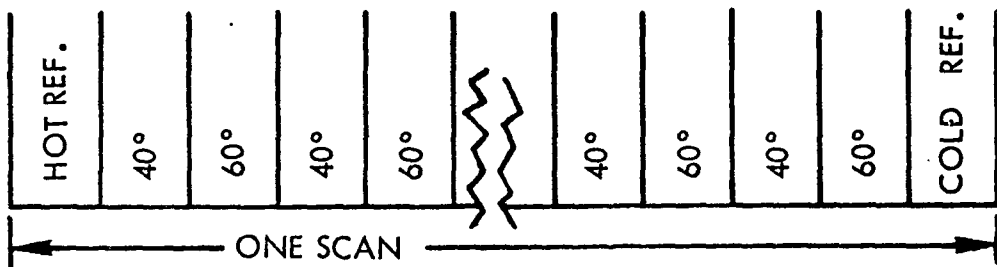


Figure 7-39. Switching Sequence

and shadowing effects, and which takes into account the atmosphere, salinity, sea spray and foam (Ref (14)). The general procedure is as follows:

- (1) The vertically polarized brightness temperatures at 19 GHz and 10 GHz are measured at angles of 60° and 40° ; for each frequency the difference of the temperatures, $T_{60,40} = T(60^\circ) - T(40^\circ)$, is formed.
- (2) A "guess" is made of the lowest, T' , and the highest, T'' , water temperatures likely to occur in the region of ocean being observed.
- (3) The value of $T_{60,40}$ at 10 GHz and the pair of temperatures T' , T'' then determine a corresponding pair of values of rms surface slope s' , s'' . The values of s' , s'' may be shown to be independent of atmospheric water vapor content and the presence of wind-driven spray layer.
- (4) From the measurement of $T_{60,40}$ at 19 GHz and the two sets of values (T', s') , (T'', s'') so far determined, one can deduce a corresponding pair of values p' , p'' of atmospheric water vapor content.
- (5) Using the 10 GHz measurement of either $T(40^\circ)$ or $(T_{60,40})$ and the two sets of values (T', s', p') , (T'', s'', p'') , two new values of water temperature T_w' , T_w'' can be determined. The smaller of these values is then a new minimum and the larger a new maximum water temperature; according to our numerical results they will lie much closer together than the original estimates T', T'' . If they differ by a sufficiently small amount, then the true water temperature has been determined; in addition, the surface roughness (or wind speed) and atmospheric water vapor content are also bracketed by the values of (s', s'') and (p', p'') .
- (6) If $T_w'' - T_w'$ is not sufficiently small, then T_w' and T_w'' are taken to be new estimates of the minimum and maximum water temperatures, and steps (1) through (5) are repeated.

In an illustrative example using assumed measurements of $\Delta T_{60,40}$ of 40°K and $T(40^\circ)$ of 138°K at 9.3 GHz, and assumed water temperature known to be between 10°C and 20°C (283°K to 293°K) a single use of the above procedure results in determination of the water temperature to be $286.9 \pm .75^\circ\text{K}$, and the rms surface slope angle to be $10.5 \pm 0.5^\circ$. In addition, the water vapor density of the atmosphere at the surface is determined to be $16.45 \pm 0.30 \text{ g/m}^3$. If more accurate values are desired,

the procedure can be repeated with the extremes of the first temperature determination as the new estimates of maximum and minimum temperatures. The procedure rapidly converges, thus in the illustrative example one iteration would determine temperature well within the uncertainty of the basic radiometer.

The uncertainty of the temperature measurement of the basic radiometer is given by the following equation.

$$\Delta T \Delta W = K \frac{VWN \phi/2}{\sin \phi/2}^{1/2} \quad (7-10)$$

$$\text{where } K = \frac{177 (\overline{NF} - 0.5)}{(K_1 B_R)^{1/2}} \quad (7-11)$$

- and \overline{NF} is the noise figure of the receiver
 K_1 is a constant determined by the circuit configuration and type of modulation
 B_R is the predetection equivalent noise bandwidth
 B_F is the post-detection equivalent noise bandwidth
 V is the orbital velocity of the satellite
 W is the swath width scanned
 ϕ is the scan angle of the conical sector
 ΔW is the spatial resolution
 N is the number of measurement pairs

The expression in the brackets of Equation 7-10 contains the parameters relating to the observational requirements, such as orbital velocity, swath width, number of observations at each point and scan angle. These values are in turn dependent on the orbit altitude and incidence angle of the beam with respect to the local vertical.

The constant K given by Equation 7-11 may be considered a figure of merit for the radiometer, as it consists of factors solely determined by the type of radiometer and its parameters.

Typical values are; \overline{NF} , 5-6 db at 10 to 19 GHz; K from .125, for the Dicke comparison type radiometer with square wave modulation/demodulation to .5 for the unmodulated absolute reading radiometer; B_R from 200 to 400 MHz for systems with electrically scanned antennas.

The swath width is approximately (flat earth approximation) given by

$$W = \frac{2h}{\cot \Theta} \sin \frac{\phi}{2} \quad (\text{nmi}) \quad (7-12)$$

where h is the orbit altitude
 Θ is the angle of the antenna beam with respect to the local vertical
 ϕ is the conical scan angle

The conical scan angle for the desired swath width may be determined from Figure 7-40 for 300 and 500 nmi orbits at 40° and 60° angles of incidence.

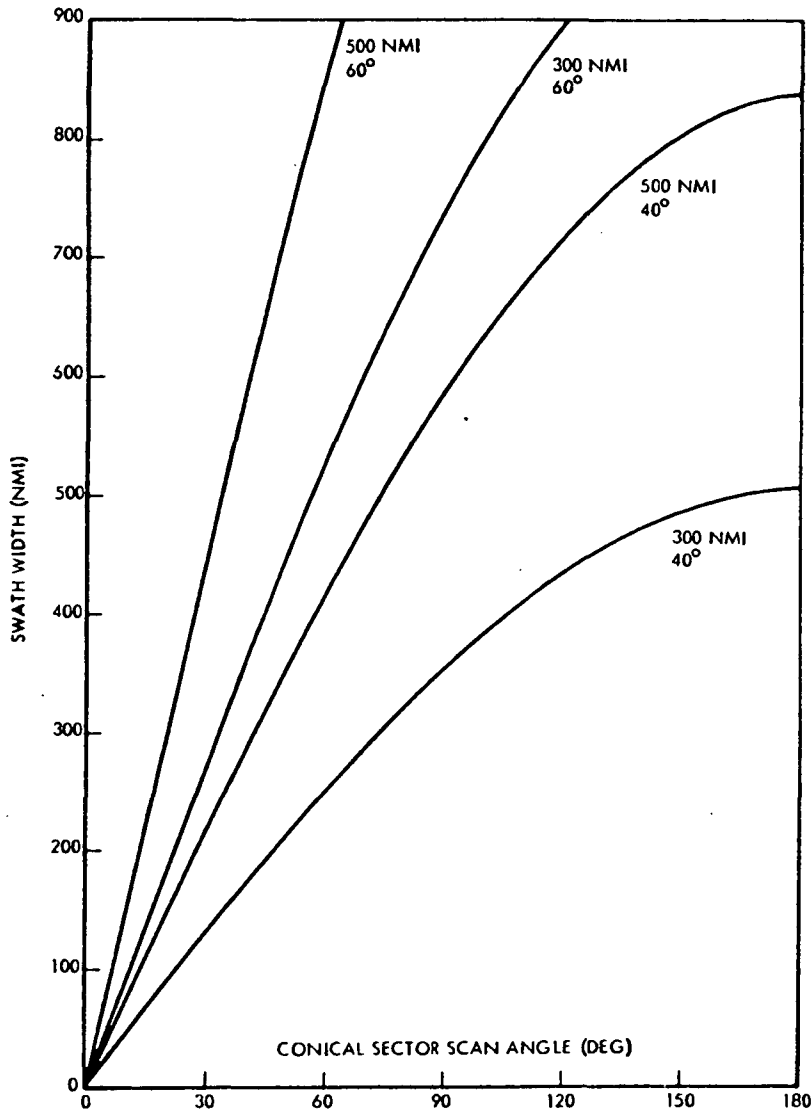


Figure 7-40. Swath Width versus Scan Angle

The specification for the microwave radiometer system, (Instrument Specification Sheet 6.5), was derived from the preceding equations, assuming that the satellite altitude is about 500 nmi and that the antenna must fit within the shroud of the Delta, limiting it to about 7 feet across. The size, weight and power of the radiometer systems are primarily determined by the sizes of the antennas required, which are inversely proportional to the resolution. For electrically scanned, planar array antennas, the weight is approximately proportional to the area of the aperture. The power required for electrically scanned planar array antennas is proportional to the length for antennas of the Nimbus E radiometer type. The weight and power for the recommended radiometer system was estimated by extrapolating from the weight and power of the Nimbus E radiometer system.

7.6 SYNTHETIC APERTURE RADAR

7.6.1 General Considerations

In contrast to the situation in the visible and infrared regions of the spectrum, at frequencies below about 10 GHz there is little attenuation due to the atmosphere, even with heavy moisture-laden clouds. Consequently side-looking imaging radar operating below 10 GHz can provide all weather imaging of the surface. The synthetic aperture technique may be used to achieve high resolution with a feasible antenna size. As shown in Figure 7-41 the antenna pattern required is a fan beam tilted to one side of the orbit plane so that the antenna is very long compared to its height. Scanning is provided in the along track direction by the spacecraft motion, and in the across track direction by time delay of the signal backscattered from the surface, so that the antenna can be rigidly attached to the platform. However, it may be desirable to provide for some tilt adjustment in order to optimize the imaging performance for different purposes.

The transmitter power required for satisfactory imaging is very dependent on the incidence angle of the antenna beam. Contrary to the usual practice with side looking radars looking at land, in order to decrease the transmitter power the antenna beam should be pointed only 10 to 20 degrees from the vertical when looking at the sea surface. This will provide contrast between rough and moderately rough seas and slicks. Float-

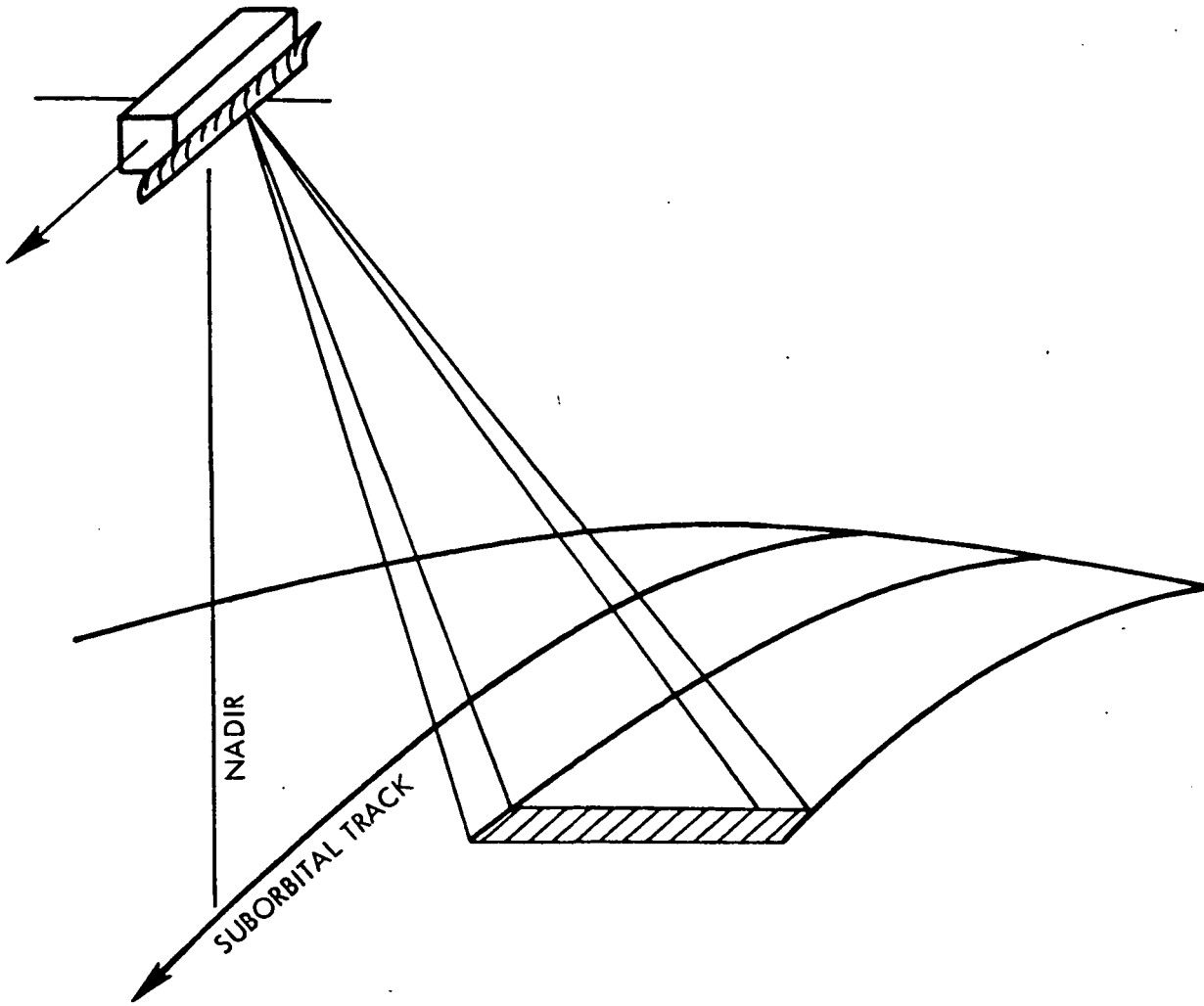


Figure 7-41. Synthetic Aperture Radar

ing objects such as ships and ice will have strong returns and will stand out as bright spots. Shorelines should be outlined by the contrast in reflectivity between land and sea.

7.6.2 Transmitter Average Power

The synthetic aperture radar (SAR) recommended for the broad ocean observation is similar to that recommended for the coastal zone. However, the difference in the mission allows the resolution requirement to be relaxed, permitting a significant decrease in the power required.

The power requirement can be further reduced by using post detection integration to improve the signal to noise ratio of the SAR. This power reduction is obtained at the expense of an increase in the size of the along track resolution. However, since the theoretical along track

resolution is about one half antenna length ($L/2$), for any practical antenna length the along track resolution would be several orders of magnitude smaller than the desired resolution. Thus, for this mission resolution can be traded for reduced power.

The transmitter average power required is given by the following equation, which includes post detection integration.

$$PAV = 5.6 \times 10^{-19} \left[\frac{W^2}{\Delta W (K_A L/2\Delta A)^{1/2}} \right] \left(\frac{S/N_o}{\sigma_o} \right) \left(\overline{NF} L_V L_M \right) \left(\frac{hV}{\lambda L} \right)$$

where

W	is the swath width
ΔW	is the resolution
L	is the antenna length
ΔA	is the along track resolution
K_A	is the ratio of the distance moved between pulses, to one half antenna length
S/N	is the minimum signal to noise ratio
σ_o	is the minimum backscattering coefficient
\overline{NF}	is the noise figure of the receiver
L_V	is the two-way attenuation of the vertical path
L_M	is a miscellaneous loss factor
h	is the orbit altitude (assumed 500 nmi)
V	is the spacecraft velocity
λ	is the wavelength

7.6.3 Parameter Values

The specification for the SAR (Instrument Spec Sheet No. 6.6) was derived using the following parameter values:

Altitude	925 km (500 nmi)
Swath width	600 km
Resolution	1 km (both directions)
Antenna Length	6.5 m (20 ft)
Signal to noise ratio	3 db
Minimum radar back scattering coefficient	-20 db
Wavelength	10 cm (3 GHz)
Noise figure	1.5 (uncooled paramp)
Atmospheric attenuation	1 db
Miscellaneous losses	1.5 db

The 3 GHz frequency was selected in order to provide all weather capability on a global basis. At that frequency the two-way attenuation of the vertical path through the atmosphere is less than 1 db even if the path includes an intense thunderstorm in the tropics.

7.7 INSTRUMENT SPECIFICATION SHEETS

The following pages summarize performance and physical characteristics of the proposed sensors.

INSTRUMENT SPECIFICATION

Sensor: Visible Imaging Spectrometer

Reference No.
7.1.1

<u>General Description</u>	
Function	To measure the spectra of reflected sunlight in an imaging mode
Configuration, Major Elements	Imaging spectrometer: objective lens, collimating lens, diffraction grating, re-imaging lens, image dissector
Developmental Status	Presently under development by TRW Systems for AAFE: MOCS (Multichannel Ocean Color Sensor)
<u>Performance Characteristics</u>	
Wavelength Range	.4-.7 μ
Spectral Resolution	.015 μ
Field of View	51 $^{\circ}$ (3 MOCS sensors, 17.1 $^{\circ}$ each) (925 km swath @ 925 km alt.)
Spatial Resolution	1.8 km
Sensitivity	NE $\Delta\rho$ = .001 or better
Absolute Accuracy	\pm .003
<u>Physical Characteristics</u>	
Size	.035 cubic meters (total of 3)
Weight	18 kg (6 kg, each of 3 sensors)
Power	18 watts total
<u>Platform/Data Considerations</u>	
Pointing Accuracy	.07 $^{\circ}$ (1 pixel)
Line of Sight Rate	.05 $^{\circ}$ /sec
Data Output	0.3 MBS (all 3 sensors)
<u>Comments</u>	
	No moving parts
	3 MOCS sensors sweep adjacent swaths providing 925 km swath (3 day coverage)

INSTRUMENT SPECIFICATION

Sensor: Visible Imaging Spectrometer
("Smoothing Dissector" Version)

Reference No.
7.1.2

<u>General Description</u>	
Function	To measure the spectra of reflected sunlight in an imaging mode
Configuration, Major Elements	Imaging spectrometer: objective lens, collimating lens, diffraction grating, re-imaging lens, image dissector/intensifier
Developmental Status	Presently under study by TRW Systems for AAFE: MOCS (Multichannel Ocean Color Sensor)
<u>Performance Characteristics</u>	
Wavelength Range	.4-.7 μ
Spectral Resolution	.015 μ
Field of View	51 $^{\circ}$ (925 km swath at 925 km alt.)
Spatial Resolution	1.8 km
Sensitivity	NE $\Delta\rho$ = .001 or better
Absolute Accuracy	\pm .003
<u>Physical Characteristics</u>	
Size	.01 cubic meters
Weight	6 kg
Power	8.5 watts
<u>Platform/Data Considerations</u>	
Pointing Accuracy	.07 $^{\circ}$ (1 pixel)
Line of Sight Rate	.05 $^{\circ}$ /sec
Data Output	0.3 MBS
<u>Comments</u>	No moving parts Advanced version of MOCS (under study)

INSTRUMENT SPECIFICATION

Sensor: Glitter Framing Camera

Reference No.
7.2

<p><u>General Description</u></p> <p>Function</p> <p>Configuration, Major Elements</p> <p>Developmental Status</p>	<p>Primary: To obtain images of glitter pattern from which to deduce average sea state and detect and locate areas of reduced sea state.</p> <p>Secondary: To obtain moderate resolution images of areas outside glitter pattern</p> <p>1000 TV line camera (RBV or Sec Vidicon); f/4 optics with adjustable iris diaphragm f/4 to f/16; two axis gimbaling or 2 axis pointing mirror</p> <p>State-of-the-art</p>
<p><u>Performance Characteristics</u></p> <p>Wavelength Range</p> <p>Spectral Resolution</p> <p>Field of View</p> <p>Spatial Resolution</p> <p>Sensitivity</p> <p>Absolute Accuracy</p>	<p>0.58-0.7μ - not critical but should be at red end of visible spectrum</p> <p>Broadband - one band only</p> <p>40$^{\circ}$ x 40$^{\circ}$; 777 km across at 30$^{\circ}$ from nadir</p> <p>2500 feet; 0.78 km (per TV line) (925 km altitude)</p> <p>64:1 dynamic range at any given exposure, additional 16:1 by varying exposure</p> <p>20 percent photometric</p>
<p><u>Physical Characteristics</u></p> <p>Size</p> <p>Weight</p> <p>Power</p>	<p>.03 cu. meters</p> <p>18 kg</p> <p>45 watts average, 52 watts peak</p>
<p><u>Platform/Data Considerations</u></p> <p>Pointing Accuracy</p> <p>Line of Sight Rate</p> <p>Data Output</p>	<p>0.5$^{\circ}$ (+ 5 nmi)</p> <p>0.35$^{\circ}$/sec</p> <p>100 KHz video, 10 sec/frame, 1 frame/30 sec</p>
<p><u>Comments</u></p>	<p>Brightness at center of glitter pattern varies from about 200 Lum/ft²/ster to 2500 Lum/ft²/ster.</p> <p>2 frames/min give about 4 images of any point on surface.</p> <p>Pointing required 0 to 40$^{\circ}$ from nadir, 360$^{\circ}$ in azimuth</p>

INSTRUMENT SPECIFICATION

Sensor: IR - Multispectral Mechanical Scanner
(Maximum Requirement)

Reference No.
7.3.1

<p><u>General Description</u></p> <p>Function</p> <p>Configuration, Major Elements</p> <p>Developmental Status</p>	<p>Thermal mapping of sea surface, effect of atmospheric constituents removed from data by comparing 3 or more spectral bands. Additional channels included to measure cloud cover, etc.</p> <p>Variable FOV con scan, 25 cm dia. f/2 optics, HgCdTe detector for IR, Radiatively cooled to 77° K</p> <p>Within SOA, new instrument development</p>
<p><u>Performance Characteristics</u></p> <p>Wavelength Range</p> <p>Spectral Resolution</p> <p>Field of View</p> <p>Spatial Resolution</p> <p>Sensitivity</p> <p>Absolute Accuracy</p>	<p>9.1, 11.0, 4.7μ, + BB visible, UV, and near IR channels</p> <p>$\Delta\lambda = 0.5, 1.0, 0.5$ respectively + (.4-.7), (.3-.4) and (.7 to 1.0) μ</p> <p>Adjustable: 100 km to horizon to horizon (sensitivity given for 360 km swath)</p> <p>1 km</p> <p>NEΔT = .07, .05, .16° K and NEΔρ = .01 and .01</p> <p>0.2° or better</p>
<p><u>Physical Characteristics</u></p> <p>Size</p> <p>Weight</p> <p>Power</p>	<p>0.3 cubic meters</p> <p>43 kg (95 lbs)</p> <p>45 watts</p>
<p><u>Platform/Data Considerations</u></p> <p>Pointing Accuracy</p> <p>Line of Sight Rate</p> <p>Data Output</p>	<p>.05° (1 pixel)</p> <p>.035°/sec (10 percent overlap)</p> <p>1.25 MBS rate, 450 KBS good (33 percent scan efficiency) (10 bit quantizing)</p>
<p><u>Comments</u></p>	<p>Spectral channels may be added or changed with little effect on size/weight/power</p>

INSTRUMENT SPECIFICATION

Sensor: IR Radiometer (Imager)
(Minimum Requirement)

Reference No.
7.3.2

<u>General Description</u>	
Function	To measure sea surface temperature in a continuous swath creating a stripmap
Configuration, Major Elements	12 cm (4 1/2" dia.) f/1 telescope, conically scanned, 33 percent efficient, HgCdTe detector, radiatively cooled to 100° K
Developmental Status	New instrument but well within state-of-the-art
<u>Performance Characteristics</u>	
Wavelength Range	8-13μ (one band)
Spectral Resolution	Same
Field of View	1000 km swath width @ 925 km = h (500 nmi)
Spatial Resolution	1 km (constant across swath)
Sensitivity	NEΔT = 0.03°C
Absolute Accuracy	~0.1°C (discounting atmospheric effects)
<u>Physical Characteristics</u>	
Size	0.2 cubic meters (mostly radiation cooling horn)
Weight	18 kg (40 lbs)
Power	20 watts
<u>Platform/Data Considerations</u>	
Pointing Accuracy	.05° (1 pixel)
Line of Sight Rate	.035°/sec (10 percent overlap)
Data Output	250 KBS rate, 85 KBS good (33 percent efficiency scan) (10 bit quantizing)
<u>Comments</u>	<ol style="list-style-type: none"> 1. Scan mirror speed = 420 rpm 2. No atmospheric calibration 3. Day/night operation

INSTRUMENT SPECIFICATION

Sensor: Radar Altimeter

Reference No.
7.4

<u>General Description</u>	
Function	To measure distance from spacecraft to mean sea surface for determination of changes of slope of mean sea surface.
Configuration, Major Elements	90 cm dia. antenna, X-band, Transmitter, Receiver, Processor, Altitude tracking circuit, Altitude counting circuit.
Developmental Status	A maximum of off-the-shelf hardware is available for components
<u>Performance Characteristics</u>	
Wavelength Range	X-band
Spectral Resolution	----
Field of View	2.13° beamwidth, grid sampling every 50 km along track
Spatial Resolution	Footprint of 8.8 km at 925 km altitude
Sensitivity	Slopes of 10 ⁻⁷ over 50-100 km
Absolute Accuracy	10 cm
<u>Physical Characteristics</u>	
Size	.014m ³ (864 in ³)
Weight	23 kg (50 lb)
Power	<30 watts
<u>Platform/Data Considerations</u>	
Pointing Accuracy	0.3° 1σ each axis
Line of Sight Rate	NA
Data Output	<100 BPS
<u>Comments</u>	

INSTRUMENT SPECIFICATION

Sensor: Microwave Radiometer

Reference No.
7.5

<u>General Description</u>	
Function	Measurement of sea surface temperature and roughness.
Configuration, Major Elements	19 GHz antenna, 40 and 60 degree conical sector scan, V polarization. 10 GHz antenna, 40 and 60 degree conical sector scan, V and H - polarization. Receiver, temperature references, switching and scanning electronics.
Developmental Status	Partially developed by Aerojet.
<u>Performance Characteristics</u>	
Wavelength Range	10 GHz, 19 GHz
Spectral Resolution	300 MHz bandwidth
Field of View	1350 km swath width
Spatial Resolution	50 km
Sensitivity	0.5° K
Absolute Accuracy	1.5° K
<u>Physical Characteristics</u>	
Size	10 GHz antennas; 3.5' x 7', 2.5' x 3.5' 19 GHz antennas; 2' x 4', 1.5' x 2'
Weight	90 kg (200 lbs)
Power	175 watts
<u>Platform/Data Considerations</u>	
Pointing Accuracy	0.2°
Line of Sight Rate	0.2°/sec
Data Output	200 B/sec
<u>Comments</u>	

INSTRUMENT SPECIFICATION

Sensor: Synthetic Aperture Radar

Reference No.
7.6

<u>General Description</u>	
Function	Radar images of ocean surface
Configuration, Major Elements	Antenna, transmitter, receiver
Developmental Status	Production for aircraft -- not space qualified
<u>Performance Characteristics</u>	
Wavelength Range	3 GHZ
Spectral Resolution	Bandwidth 0.5 MHZ
Field of View	Swath width 600 km
Spatial Resolution	1 km
Sensitivity	Good image above σ_0 of -20 db
Absolute Accuracy	
<u>Physical Characteristics</u>	
Size	Antenna 20' x 1' x 3'' unfurled, transmitter/receiver 200 cubic inches
Weight	73 kg (160 lbs)
Power	130 watts
<u>Platform/Data Considerations</u>	
Pointing Accuracy	1 MR
Line of Sight Rate	10 MR/sec
Data Output	Analog signal bandwidth 0.5 MHZ Digital data rate: 8 MB/sec (8 Bit encoding)
<u>Comments</u>	

REFERENCES FOR SECTION 7.

1. "Coastal Zone Requirements for EOS A/B," Final Report, prepared under Contract No. NAS1-10280 by TRW Systems for NASA Langley Research Center, 4 February 1971.
2. Clarke, G. L. Ewing, G. C. and Lorenzen, C. J., "Remote Measurement of Ocean Color as an Index of Biological Productivity." Contribution No. 2411 of the Woods Hole Oceanographic Institution.
3. Elterman, L., "Atmospheric Attenuation Model, 1964, in the Ultraviolet, Visible, and Infrared Regions for Altitudes to 50 km." AFCRL Report 04-740, September 1964.
4. Fraser, R. S. and Ramsey, R. C. "Nadir Spectral Radiance of the Sunlit Earth as Viewed from Above the Atmosphere." TRW Systems IOC, March 1968.
5. Moon, P. "Proposed Standard Solar-Radiation Curves for Engineering Use." Journal of Franklin Institute, Volume 30 pp 583-619, 1940.
6. Yentock, Charles S. "The Influence of Phytoplankton Pigments on the Color of Sea Water," Deep-Sea Res., Volume 7, pp 1-9, 1960.
7. Duntley, Seibert Q., "Light In the Sea." Journal of the Optical Society of America, Volume 53, pp 214-233, February 1963.
8. Jenkin, K., and Ramsey, R., "The Development of a WISP Information System." TRW Final Report, Contract No. N-62306-70-C-0274, Prepared for SPOC, Naval Oceanographic Office, February 1971.
9. Anding, D., Kauth, R., and Turner, R., "Atmospheric Effects on Infrared Multispectral Sensing of Sea Surface Temperature from Space," Willow Run Laboratories, University of Michigan, prepared under Contract NAS12-2117 for NASA Ames Research Center, December 1970.
10. Kolker, Myer and Weiss, Ephram, "Space Geodesy Altimetry Study," NASA Report CR-1298, March 1969.
11. Kaula, W. M., "The Appropriate Representation of the Gravity Field for Satellite Geodesy," Bulletin Geodesique, 1969 (Proc. IAG).

REFERENCES FOR SECTION 7

12. Gaposchkin, E. M., and Lanbeck, K., 1969 Smithsonian Standard Earth, Smithsonian Astrophysical Observatory Special Report 315, May 1970.
13. Rapp, Richard H., "Gravitational Potential of the Earth Determined from a Combination of Satellite, Observed and Model Anomalies," Journal of Geophysical Research, 73, October 1968, pp 6555-6562.
14. Wagner, R. J., "Recent Developments in the Earth Resources Study Program," TRW 999000-7240-T0-000, 13 March 1970.

BIBLIOGRAPHY FOR SECTION 7

- Bowley, C. J., J. R. Greaves, and S. L. Spiegel, "Sunlint Patterns: Unusual Dark Patches," *Science* 165, 1360 (1969).
- Cox, C. and W. Munk, "Measurement of the Roughness of the Sea Surface from Photographs of Sun's Glitter," *J. Opt. Soc. Am.* 44, 838 (1954).
- Cox, C. and W. Munk, "Slopes of the Sea Surface Deduced from Photographs of Sun Glitter," *Bull. Scripps Inst. Ocean.* 6, 401 (1956).
- Levanon, N., "Determination of the Sea Surface Slopes Distribution and Wind Velocity Using Sun Glitter Viewed from a Synchronous Satellite," *Final Scientific Report on NASw-65* (1968).
- McClain, E. P., and A. E. Strong, "On Anomalous Dark Patches in Satellite Viewed Sunlint Areas," *Mon. Wea. Rev.* 97, 875 (1969).
- Rosenberg, G. V., Yu. - A. R. Mullamaa, "Some Possibilities of Determining Wind Speed Over an Ocean Surface Using Observations from Artificial Earth Satellites," *IZV Atmospheric and Oceanic Physics Theory* 1 (1965).
- Strong, A. E., and I. S. Ruff, "Utilizing Satellite-Observed Solar Reflections from the Sea Surface as an Indicator of Surface Wind Speeds," *Remote Sensing of Envir.* 1, 181 (1970).
- Soules, S. D., "Sun Glitter Viewed from Space," *Deep Sea Research* 17, 191 (1970).
- Wu, J., "Froude Number of Wind Stress Coefficients," *J. Atmos. Sci.* 26, (1969).

8.0 ORBITAL ANALYSIS

8.1 STATEMENT OF THE PROBLEM AND SUMMARY OF THE REQUIREMENTS

The phenomena being observed and the sensor subsystem are of prime concern in choosing an orbit for a remote spacecraft mission dedicated to global oceanography. Disregarding any difficulties in data handling, an ideal EOS orbit would acquire high resolution data with a daily revisit time and a near vertical view of all oceanic regions of interest. The relationships of orbital mechanics preclude achievement of the ideal orbit with a single spacecraft and thus orbital analysis for global oceanographic missions involves the study of possible compromise situations, and a series of prioritized tradeoffs must be made to blend these relationships into a comprehensive mission.

Two of the more important phenomenological categories of interest are World Ocean Productivity and World Ocean Fisheries and Proposed MARMAP* Area. Figures 8-1 and 8-2 show the geographical location of the phenomena associated with these categories. To accomplish the missions' objectives from a phenomenological standpoint, the essential regions must be covered by the chosen orbit.

Comparing sensor performance characteristics and requirements with the quantized measurements associated with the phenomena in each problem area bounds the observation frequency and field of view (See Table 8-1). The sun angle constraints imposed by the sensor subsystem are shown in Table 8-2.

* Marine Resources Monitoring, Assessment and Prediction Program

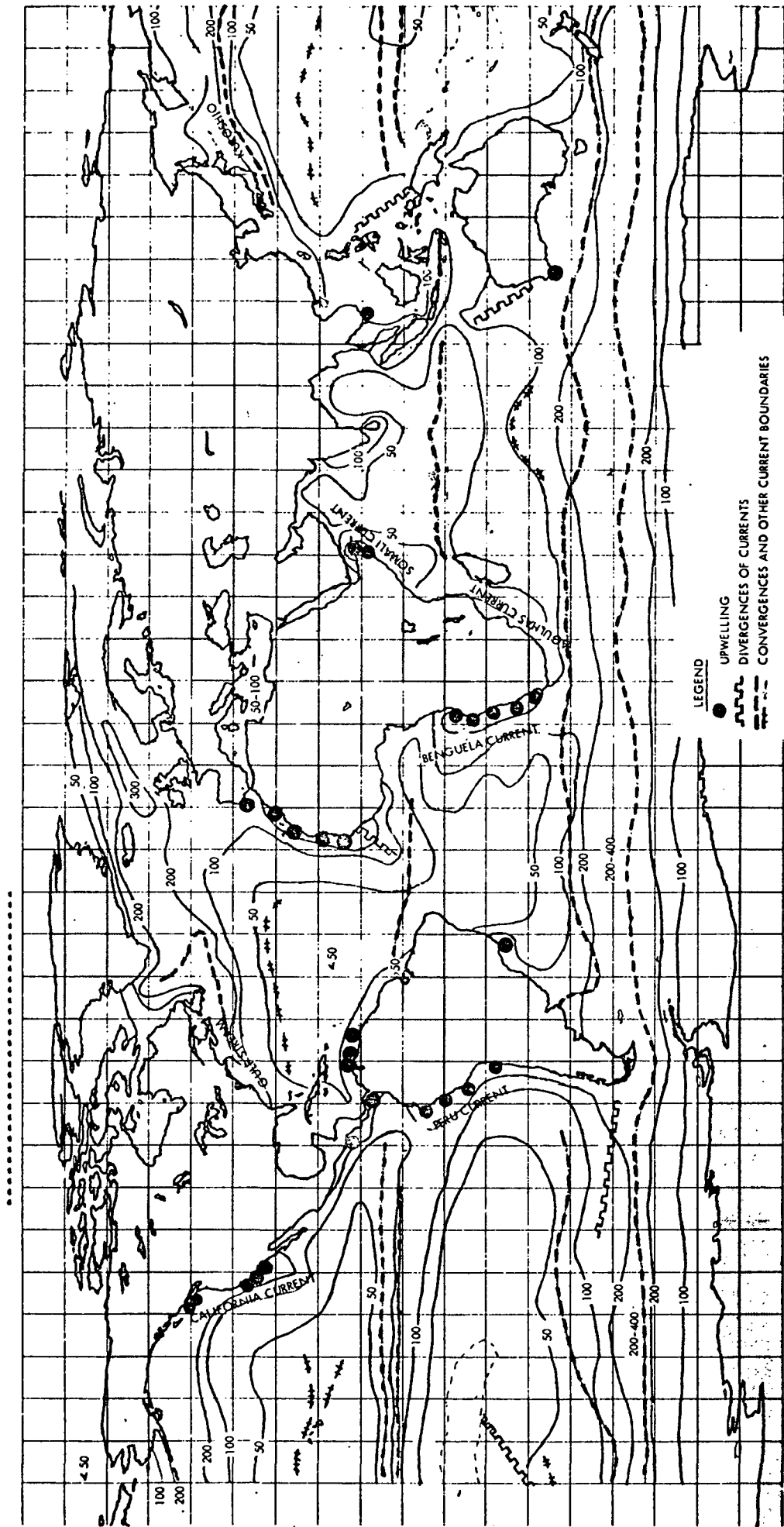
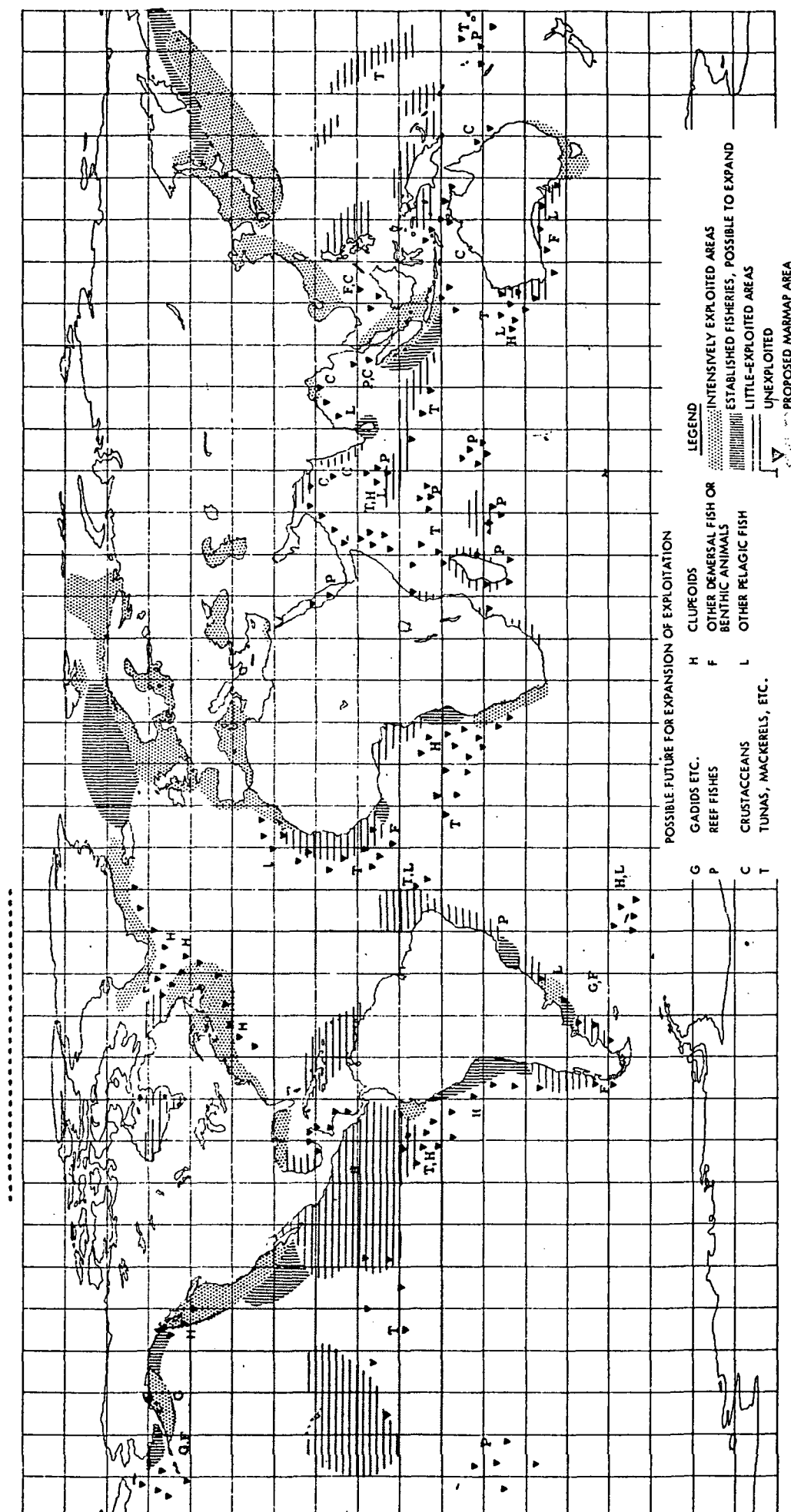


Figure 8-1. World Ocean Productivity (1)



POSSIBLE FUTURE FOR EXPANSION OF EXPLOITATION

G GADIDS ETC.
 P OTHER DEMERSAL FISH OR BENTHIC ANIMALS
 C CRUSTACEANS
 T TUNAS, MACKERELS, ETC.

H CLUPEOIDS
 F OTHER DEMERSAL FISH OR BENTHIC ANIMALS
 L OTHER PELAGIC FISH

LEGEND

INTENSIVELY EXPLOITED AREAS
 ESTABLISHED FISHERIES, POSSIBLE TO EXPAND
 LITTLE-EXPLOITED AREAS
 UNEXPLOITED
 PROPOSED MARMAP AREA

Figure 8-2. World Ocean Fisheries and Proposed Marmap Area (1)

Table 8-1. Constraints Imposed by Quantized Measurements

SENSOR CLASS	Detection, Monitor, and Control of Global Ocean Pollution		Management of Living Marine Resources		Monitor and Predict Physical Phenomena	
	OBS FREQ (days)	F. O. V. (km)	OBS FREQ (days)	F. O. V. (km)	OBS FREQ (days)	F. O. V. (km)
IR Radiometry	3-30	200-500	1/2-14	100-1000	1-5	1000
Visible Imaging	3-30	200-500	1/2-14	100-1000	1-5	100
Microwave Radiometry	3-30	200-500	1/2-14	100-1000	1-5	100-1000
Side Looking Radar	3-30	100	3-14	Full	30	—
Glitter	3-30	100	1/2-14	1000	1-5	1000
Altimetry	3-30	Full	7-14	1000 grid spacing	1-5	1000 grid spacing

Table 8-2. Sensor Sun Angle Constraints

SENSOR	SUN ANGLE RANGE DEGREES OFF LOCAL VERTICAL
<u>VISIBLE SENSORS</u>	
SEA STATE SENSOR	0-80
SPECTROMETER	0-50
<u>INFRARED SENSORS</u>	0-90
<u>MICROWAVE SENSORS</u>	
RADIOMETER	0-90
<u>ALTIMETER</u>	0-90
<u>SYNTHETIC APERTURE RADAR</u>	0-90

8.2 THEORY

8.2.1 Parametric Development

Completely describing the motion of a spacecraft about the earth requires a knowledge of factors not accurately known or too complex to include in a closed form analysis. The mass distribution of the earth and the effects of solar and lunar gravitation are examples of these factors. Neglecting them and applying Newton's Laws provide a basis for establishing the orbital equations and show that the satellite follows an elliptic path with the earth as a focus.

To fully describe this path six parameters must be examined: inclination, i , altitude, h , eccentricity, e , right ascension of the ascending node, Ω , argument of perigee, ω , and the time of nodal passage. TRW has considered circular orbits because of the constant sensor range and the uniformity of ground station visibility times. Thus the eccentricity becomes zero and the argument of perigee drops out. By setting $\omega = 0$, the position of the satellite is then referred to the ascending node (See Figure 8-3).

In fulfilling the visible sensor requirements, illumination of objects beneath the spacecraft should remain essentially constant throughout the year. This can be accomplished by imposing the condition of sun-synchronism which exists when the orbit-plane nodal regression rate is one revolution per year. This nodal regression rate is obtained by setting the altitude and inclination in accordance with equation (1). The advantages and disadvantages of this condition are shown in Table 8-3.

Specifying the time of nodal passage (relative to the earth's rotation), an initial right ascension of the ascending node Ω , and h or i establishes the circular orbit as follows:

$$\dot{\Omega} = .985647 = -9.98 \left(\frac{a}{a_e} \right)^{-7/2} \cos i \text{ degrees/day} \quad (1)$$

where a_e = radius of the earth

$$a = a_e + h \quad (\text{See Figure 8-4})$$

For moderately high altitude circular orbits the condition of sun-synchronism results in an inclination between 95 and 105 degrees. (See Figure 8-4).

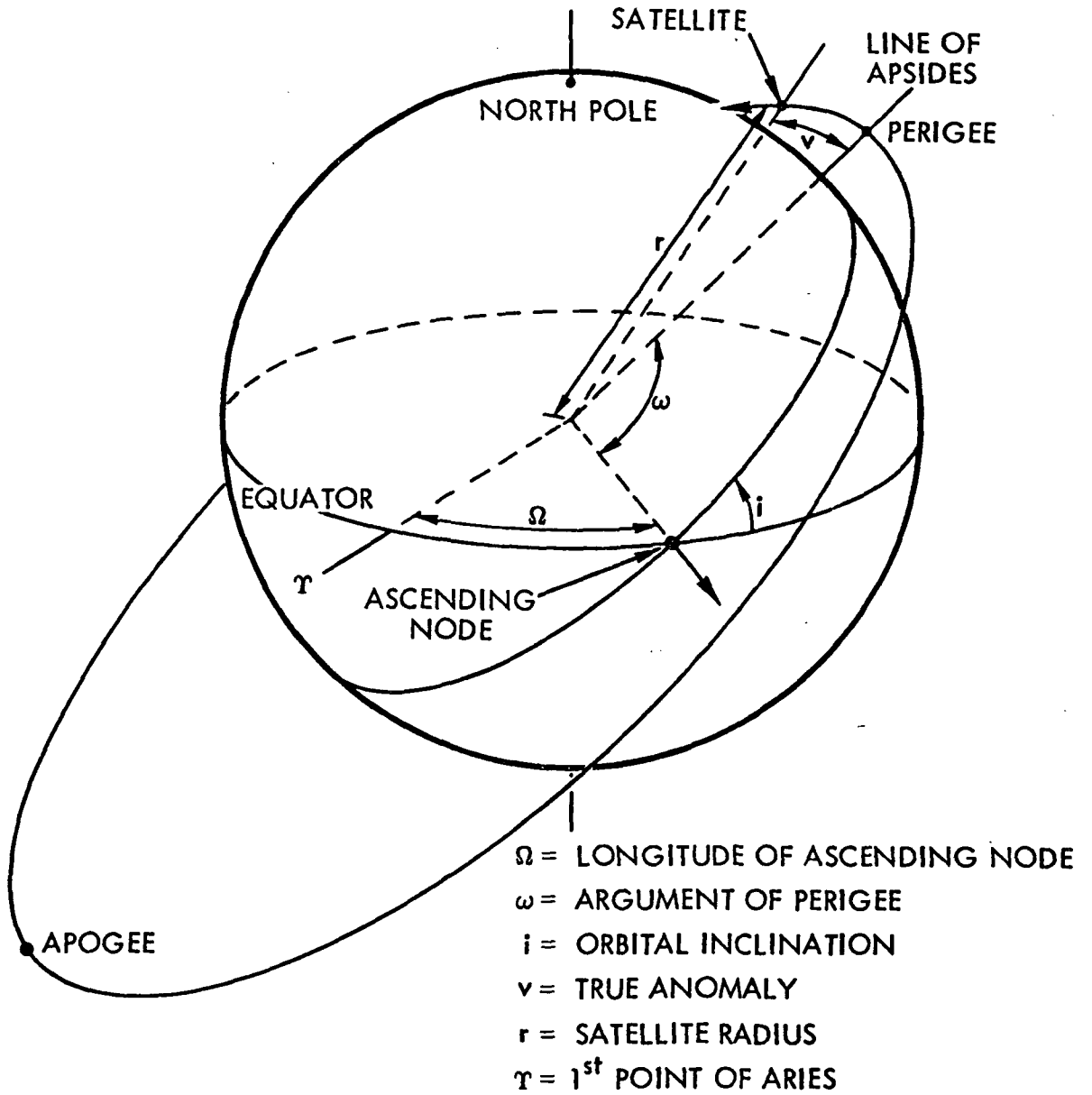


Figure 8-3. Orbital Geometry

Table 8-3. Advantages and Disadvantages of a Sun-Synchronous Orbit

<u>ADVANTAGES</u>	<u>DISADVANTAGES</u>
<p>THE SPACECRAFT PASSES OVER THE SAME GROUND POINT AT THE SAME LOCAL TIME EACH DAY ENABLING "STANDARD" DATA TO BE TAKEN.</p>	<p>DIURNAL EFFECTS AT ANY SINGLE POINT ARE MISSED.</p>
<p>DURING THE COURSE OF A YEAR THE SUN ANGLE VARIATION IS BOUNDED FOR A SPECIFIC LATITUDE.</p>	
<p>MANY POINTS ON THE GLOBE RECEIVE COVERAGE TWICE DURING A CYCLE; ONCE ON THE ILLUMINATED SIDE AND ONCE ON THE DARK SIDE.</p>	
<p>SPACECRAFT DATA "FILLS IN THE GAPS" ASSOCIATED WITH STANDARD OCEANOGRAPHIC AND METEOROLOGICAL DATA TAKEN BY CONVENTIONAL STATIONS AT 0600, 1200, 1800, 000 G.M.T.</p>	<p>INCLINATION IS ELIMINATED AS A DEGREE OF FREEDOM.</p>
<p>NEAR GLOBAL COVERAGE</p>	
<p>TRAJECTORY IS SIMPLIFIED</p>	

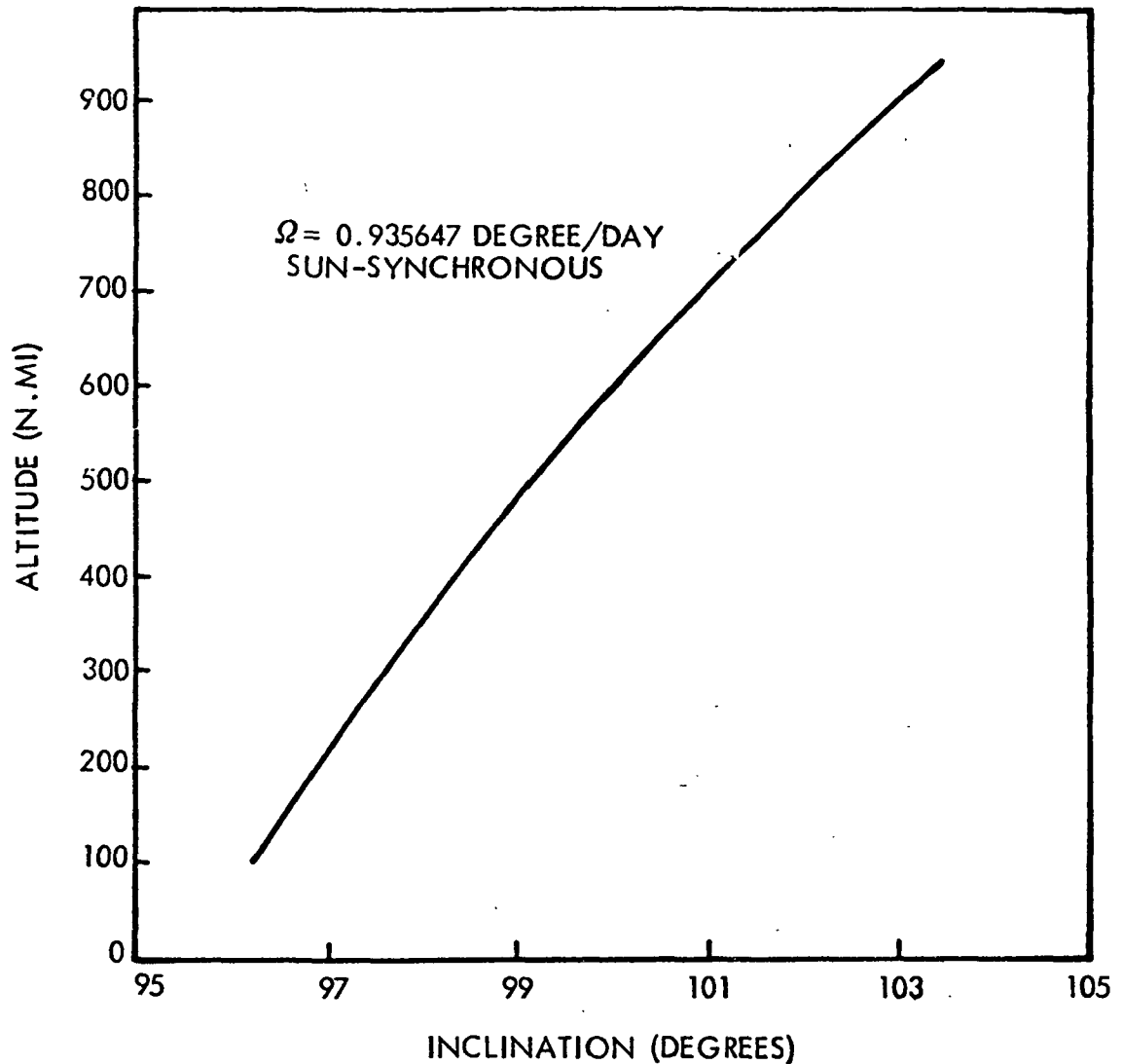


Figure 8-4. The Interdependence of Altitude and Inclination Resulting from Sun-Synchronism

8.2.2 Trace Pattern

Perhaps the most important factor in sizing an orbit is the spacecraft's trace pattern, where the term "trace" refers to the collection of subsatellite points generated on the surface of a rotating earth by the spacecraft in its orbital progression.

To facilitate the discussion the parameter Q is introduced as follows:

$$Q = 360^\circ/S^{(2)} \quad (3)$$

where Q = trace repetition parameter

from this we get

$$S = 360^\circ/Q \quad (4)$$

where

S = Longitudinal separation of northern equatorial crossings between two successive satellite revolutions (trace shift)

S can be further defined as:

$$S = \dot{\theta}P_N - \Delta\Omega = (\dot{\theta} - \dot{\Omega})P_N \quad (5)$$

where

$\dot{\theta}$ = inertial rotational velocity of the earth

P_N = nodal period of the spacecraft about the earth

The ground trace advance (i. e., the trace shift at various latitudes) can also be related to latitude and spacecraft altitude as shown in Figure 8-5.

By substituting Equation 5 into Equation 3, and using Equation 1 for the nodal regression rate, Q is shown to be a function of inclination and altitude:

$$Q = \frac{360}{(\dot{\theta} + 9.98(a/a_e)^{-7/2} \cos i)P_N} \quad (6)^*$$

where

$$P_N \cong 84.4857(a/a_e)^{3/2}$$

For sun-synchronous orbits, where there is an interdependence of h and i, Q can be considered a function of h.

$$Q = 17.044(ae/a)^{3/2} \quad (7)$$

*See Figure 8-6.

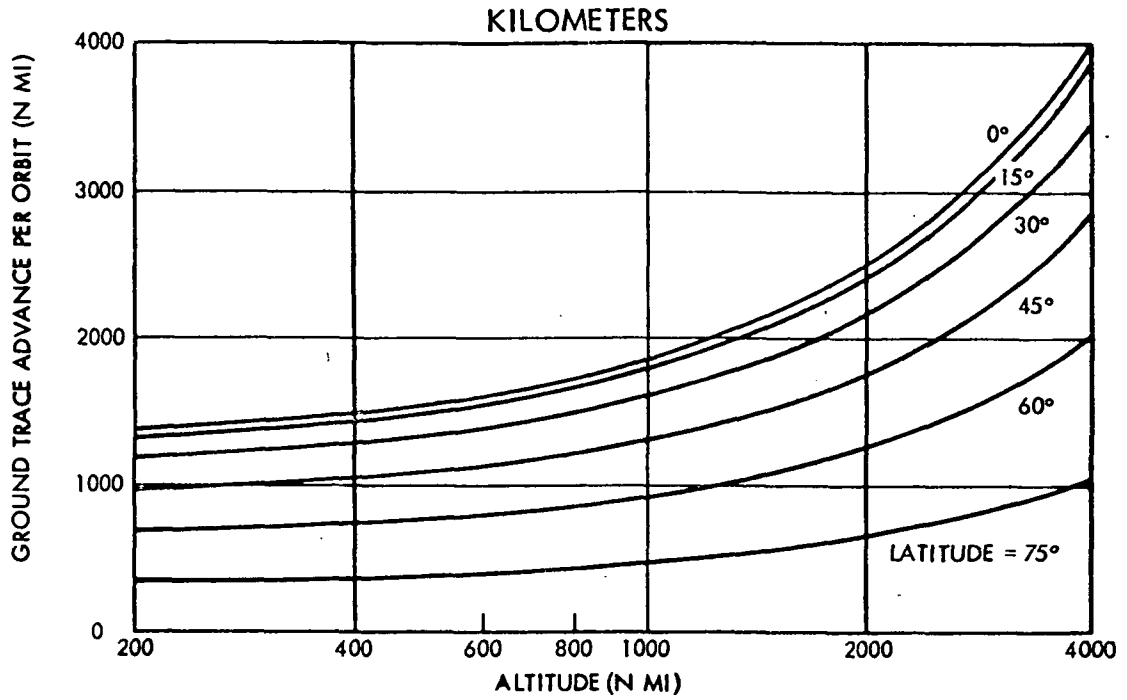


Figure 8-5. Ground Trace Advance as a Function of Altitude for Various Latitudes

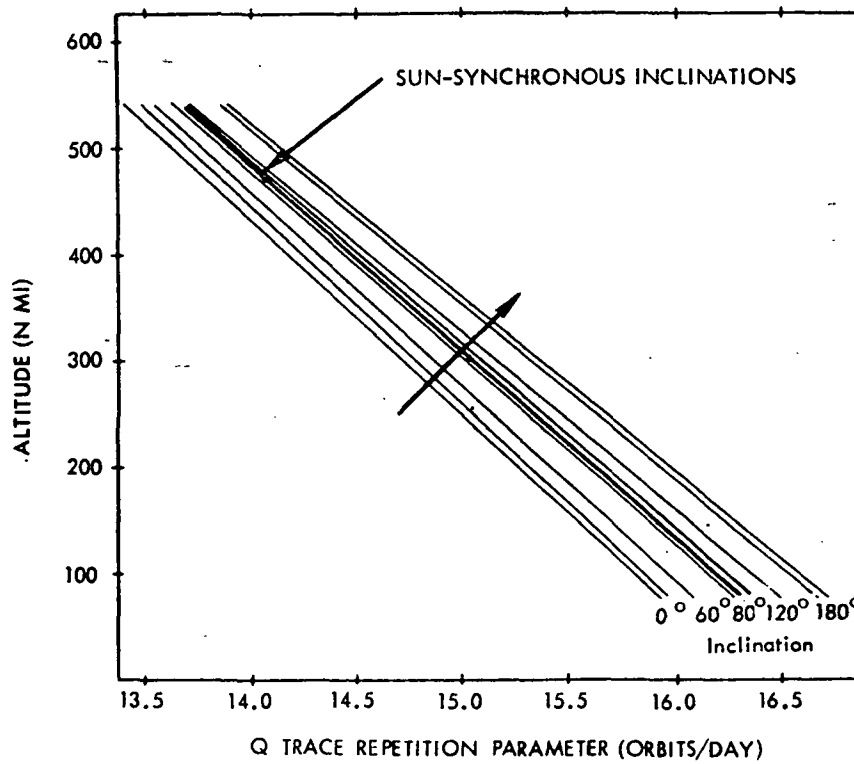


Figure 8-6. Variations in Altitude with the Trace Repetition Parameter for Increasing Inclination⁽²⁾

In general, Q can have the form, $Q = I + \frac{n}{d}$ (8)

where

I = an integer

$\frac{n}{d}$ = a rational fraction reduced to lowest terms

Choosing an integer for Q results in a trace pattern which repeats itself every day. Otherwise, the denominator of the fraction, d , defines the number of days it takes the ground trace to repeat itself (i. e., cyclic frequency). The numerator n is related to the number p where p is the number of integral segments between trace branches laid down on successive days. Each trace shift S is divided into d integral segments: if $n/d \leq 1/2$, $p = n$; but if $n/d > 1/2$, $p = d - n$ (see Figure 8-7). (2)

As shown in the requirements summary, the dynamic nature of many of the global oceanographic phenomena suggests viewing be repeated at intervals of not more than several days. This implies a high cyclic frequency.

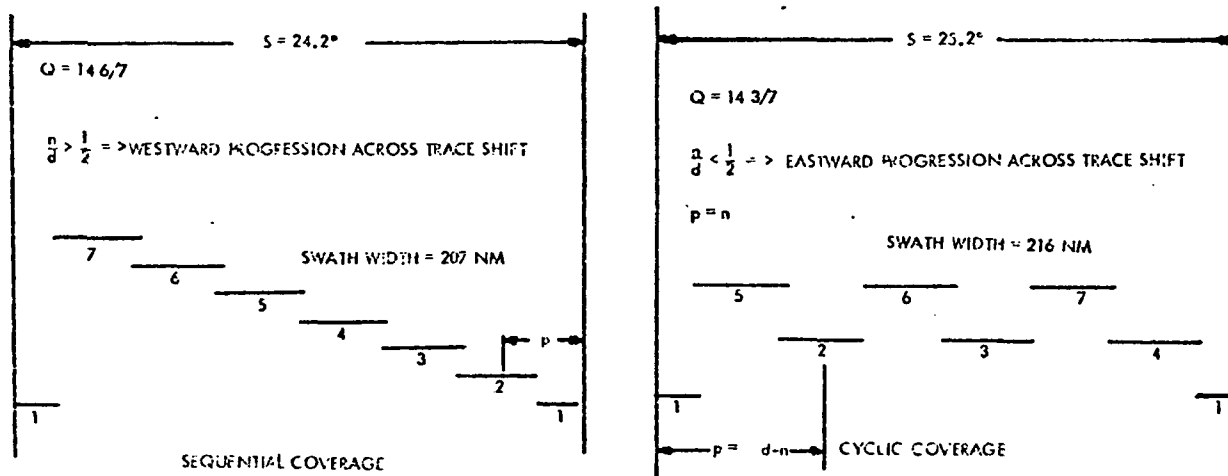


Figure 8-7. Coverage Schemes for a Cyclic Frequency of Seven Days

8.3 ORBIT SELECTION CRITERION

8.3.1 Orbit Considerations

A choice of a representative range for Q (and therefore a representative range of h for sun-synchronous orbits) is related to a choice of the orbital altitude, and is influenced by: sensor requirements, image distortion or viewing obliquity, illumination conditions, ground station visibility times, cloud cover, and atmospheric drag.

8.3.1.1 Sensor Requirements

Resolution Requirements. The moderate spatial and spectral resolution requirements for remote observation of global phenomena seem to imply the use of fairly high altitudes (an upper limit of approximately 1482 km (800 n mi). For instance, an infrared radiometer can attain a 1 km spatial resolution and a sensitivity of 0.5°C , NE ΔT $0.1 - 0.2^{\circ}\text{C}$ for a 1156 km (625 n mi) swath width by employing optics 11.4 cm (4.5-inches) in diameter. At an altitude of 2778 km (1500 n mi) with the same sensitivity and spatial resolution the radiometer can cover a 3463 km (1870 n mi) swath width by employing an optic's diameter of 30.48 cm (12 inches). The same resolution can be acquired for a swath width three times as large by using 30.48 cm optics instead of 11.4 cm. The microwave radiometer, on the other hand, at 926 km (500 n mi) can obtain a 44.4 km (24 n mi) spatial resolution and a sensitivity of 1°C with a 127 x 127 cm (50 x 50 inches) 159 kg (350-pound) antenna ; this just meets the fringe of the requirements listed in Sections 3-5. To meet this resolution and sensitivity requirement at 2778 km (1500 n mi) the antenna must be 381 x 381 cm (150 x 150 inches) and 429 kg (3150 pounds) which is a considerable change. Because of the significant change in antenna size and weight as the altitude is increased and the overall system limitations, 1482 km (800 n mi) was chosen as an upper bound on the altitude.

A lower limit on orbital altitude is imposed by the visible spectrometer. Table 8-1 seems to indicate that an observation frequency between one and five days is needed to satisfy the global oceanographic requirements. For three synchronized MOCS or a smoothing dissector visible imaging spectrometer positioned along the nadir, the field of view

would be 51.3 degrees. (See Section 7.1.) To obtain complete global coverage using this view angle the highest observation frequency that can be obtained is three days. This occurs at altitudes greater than 100 km (540 n mi). The sensor requirements, therefore, dictate an orbital altitude between 1000 km (540 n mi) and 1482 km (800 n mi).

Sun Glitter. Solar specular reflection (sun glitter) is avoided in remote ocean color sensing because it masks the data (subsurface upwelling light in the visible and near infrared spectral regions) desired for ocean surveys. On the other hand, there are many observations which require looking directly into the sun glitter pattern: wind speed and direction, surface debris and slicks, and the wave spectrum of internal waves. To accommodate both the glitter sensor and the ocean color sensor (the visible imaging spectrometer) consideration should be given to the motion of the glitter pattern, the importance of the phenomena being observed and the pointing capabilities of each sensor.

Surface reflection varies as a function of the angle formed between the sensor, target, and the sun, as well as the sea state (i. e., surface wind velocity). Figure 8-8 shows these variations for a solar illumination angle of 45 degrees. Field-of-view half angles for an earth-oriented sensor give increasing contributions of surface reflection to the total radiance on the sunward side of the subsatellite trace, particularly at higher wind velocities where the edge of the glitter pattern begins to encroach on the field of view. On the other side of the trace the radiance asymptotically approaches a minimum which is primarily caused by upwellings. For a solar illumination angle of zero degrees, the sea radiance forms a gaussian distribution with the peak radiance being at the intersection of the local vertical and the surface as shown in Figure 8-9.

To avoid the glitter pattern in an afternoon or morning orbit in which the sun is to one side of the orbit plane the spectrometer must have a gimbaling capability. As the spacecraft travels about the earth, the glitter pattern shifts relative to the local vertical. To account for this shift the spectrometer should either be positioned in such a way that glitter interference is at a minimum or have a dynamic pointing capability.

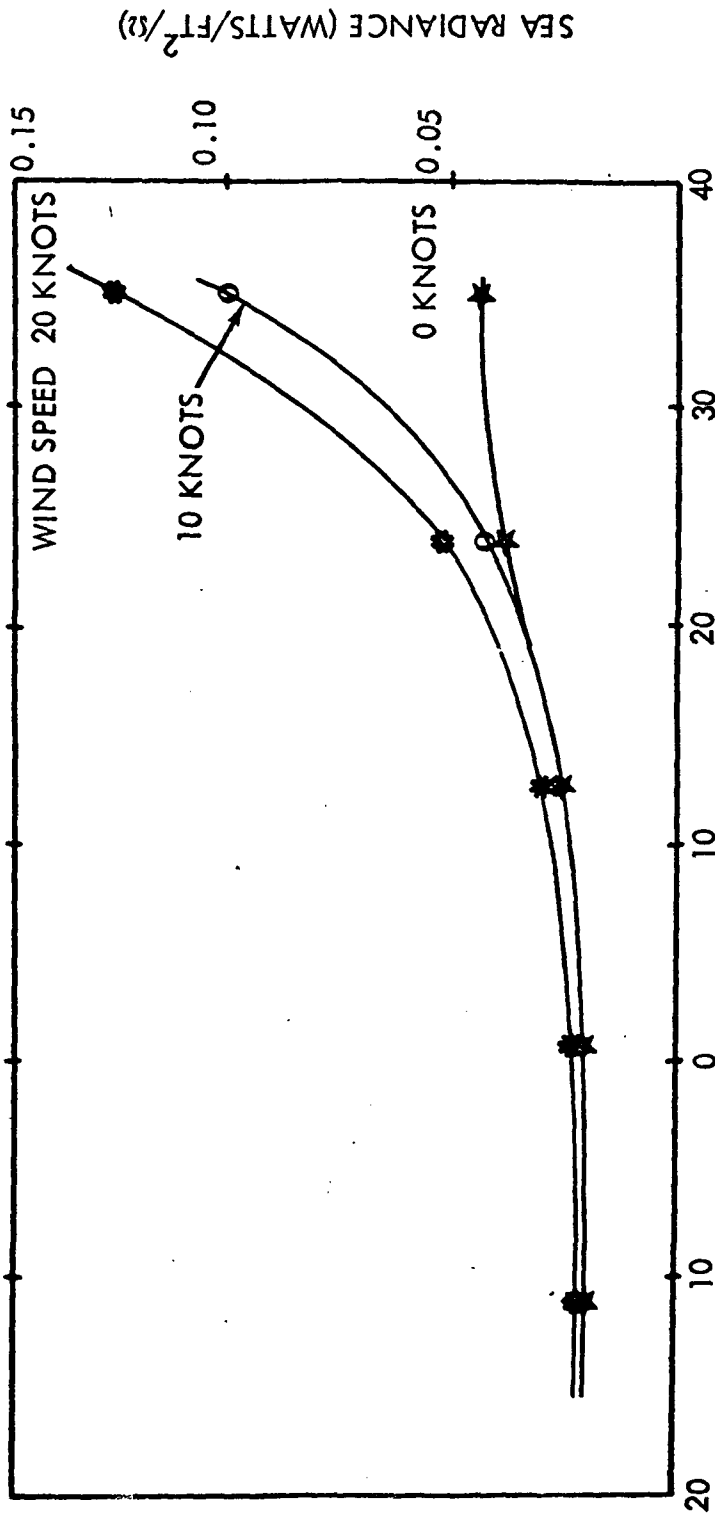


Figure 8-8. Downward Pointing Sensor, Solar Illumination Angle of 45 Degrees

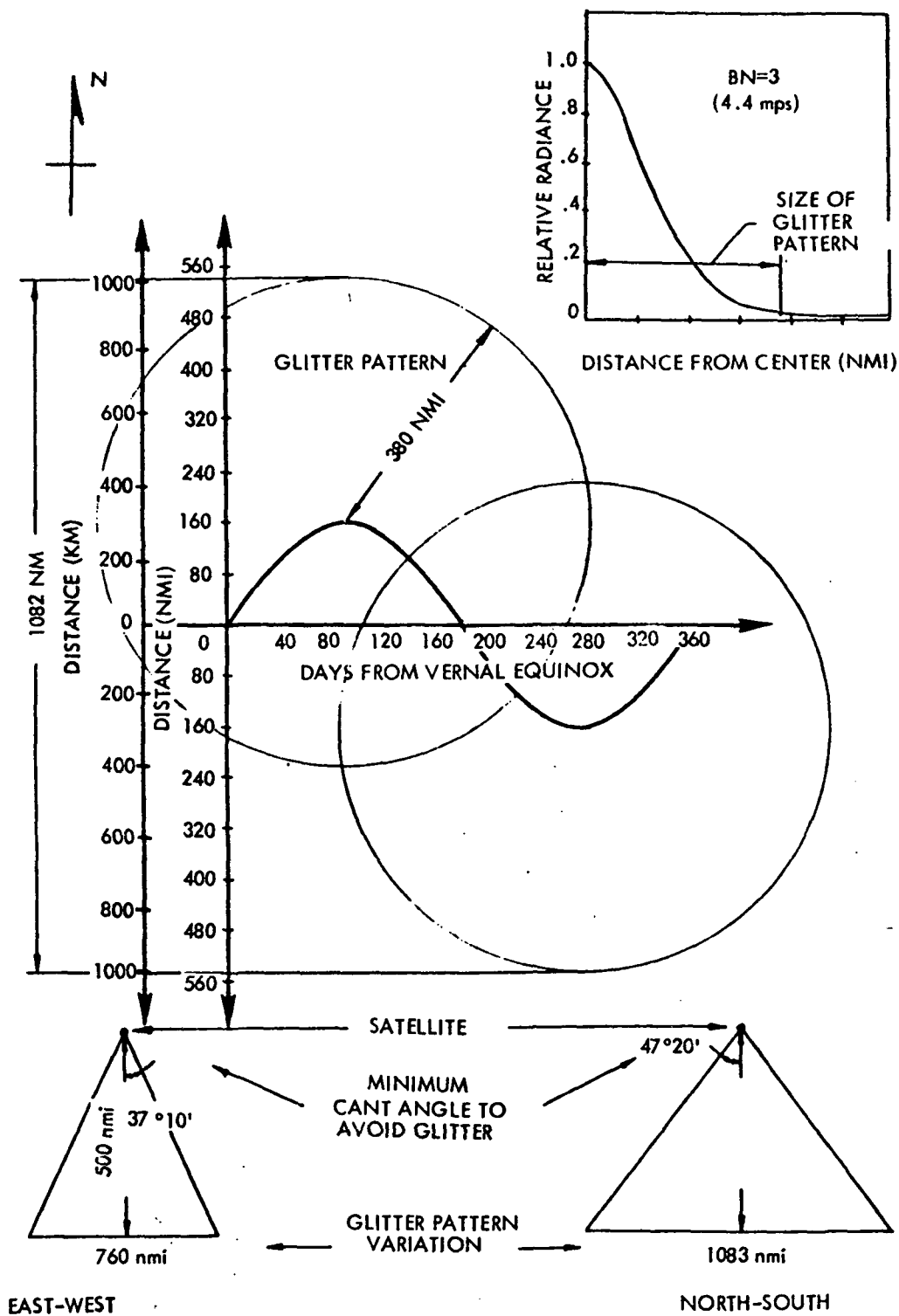


Figure 8-9. Minimum Cant Angle to Avoid the Glitter Pattern for a 926 km (500 n mi) Orbit (At the Equator for a Noon Sun)

Figure 8-9 shows the minimum cant angle the non-glitter sensors would have to use to avoid the specular reflectance associated with the glitter pattern for a 500 n mi orbit with a local noon sun at the equator. A sea state with a beaufort number (BN) of three (wind speed 4.4 mps) was used to determine the cant angle because this is the lowest sea state at which white caps occur. At this level even if the non-glitter sensors are canted away from the glitter pattern some data will be destroyed because of the specular reflectance of the white caps. To avoid the BN3 glitter pattern, the non-glitter sensors would have to cant cross-track approximately 37 degrees off the local vertical or fore and aft 47 degrees. To avoid the glitter pattern throughout the year, the sensor would have to use two-axis gimbaling because of the variation in pattern size and position.

Scene Contrast/Instrument Sensitivity. In order to satisfy the scene contrast and instrument sensitivity requirements associated with visible spectroscopy the ten o'clock geometry with the sensor canted off the local vertical, away from the sun, should be chosen. This arrangement gives the best coverage with the requirements mentioned above, especially at the equator. (See Appendix G.) The final decision is made by comparing orbits with similar geometries; the ascending and descending orbits for both the 10:00 AM and 2:00 PM geometries.

Assuming the sensor will be pointed 20 degrees off nadir away from the sun, the final selection resulted in a 2:00 PM orbit which gave the best hazy day coverage, since the 2:00 PM orbit was an afternoon orbit in which most coastal morning fog would have cleared away.

8.3.1.2 Image Distortion

Another constraint at the lower altitudes (an upper constraint on Q) is image distortion at the fringe of the swath width due to viewing obliquity. The degree of distortion is directly related to the spacecraft altitude as shown in Figure 8-10. For instance, in a global coverage scheme with a cyclic frequency of two days the obliquity angle at an altitude of 1074 km (580 n mi) is 40 degrees where as at 417 km (225 n mi)

the obliquity angle is 60 degrees. Because of these high angles, observations requiring near vertical viewing could not be achieved at lower altitudes. In a global oceanographic mission this constraint is rarely applicable.

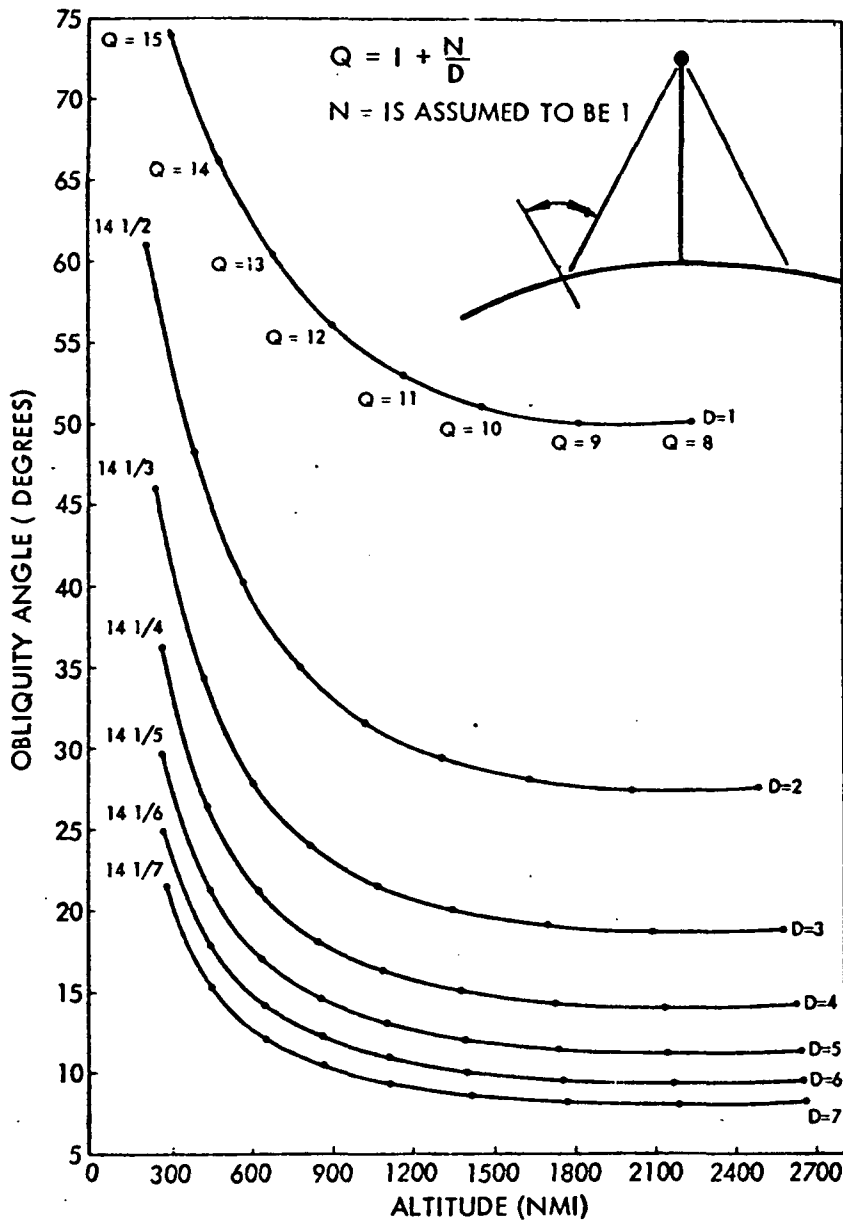


Figure 8-10. Obliquity Angle Versus Altitude for Various Cyclic Frequencies Assuming $n = 1$

8.3.1.3 Illumination Conditions

As shown in Table 8-2, the range of sensor sun angle requirements is only constrained in the visible spectrum. For sun-synchronous orbits the sun angle is dependent upon the following parameters: right ascension of the ascending node, latitude, and days from vernal equinox.

Figure 8-11 illustrates the geometry associated with solar illumination. The sun angle is the angle between the sun line and the local vertical at the subsatellite point. The time-varying inputs to the problem for sun-synchronous orbits are $\alpha - kt - \Omega_0$, the angle between the sun's hour circle and the hour circle of the ascending node, and δ , the angle representing the sun's declination. The former angle can be divided into components: Ω_0 , as stated above, represents the initial right ascension of the ascending node, and $\alpha - kt$ is the angular difference between the apparent solar time and the mean solar time. γ is the true anomaly measured from the line of apsides to the spacecraft, but in this case, since the orbit is circular the true anomaly is measured from the ascending node. ψ is the angle between the sun line and the normal to the orbit plane.

Given a specific Ω_0 and a range of latitudes, one can determine the variation of η within those latitudes. In a near polar orbit a spacecraft crosses almost every latitude twice, once ascending and once descending. Corresponding to each of these crossings is a theoretical illumination angle where $\eta > 90$ degrees is considered to be a valid subsatellite sun angle because the sun is clearly visible.

By plotting δ as a function of $\alpha - kt$ the motion of the sun during the course of a year is shown to be a figure-eight pattern with a maximum deviation off the equator of $23\ 1/2^\circ$ (see Figure 8-12). Consequently, even with sun-synchronism the solar illumination conditions vary throughout the year. By accurately choosing Ω_0 , the variation at any given latitude can be held within the operational range of the sensors.

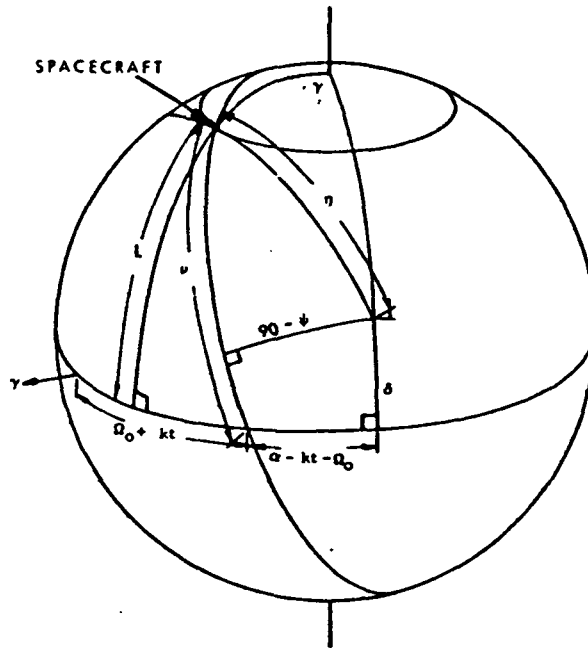


Figure 8-11. Solar Illumination Geometry

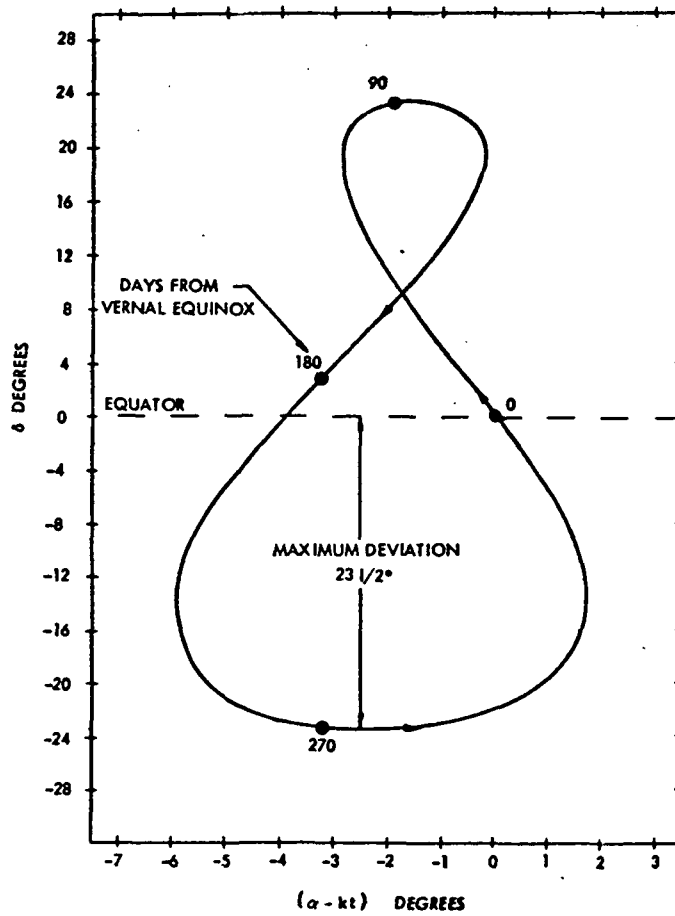


Figure 8-12. Motion of the Sun During the Course of the Year

Figures 8-13 through 8-16 express the sun angle as a function of days from vernal equinox for a latitude range of ± 70 degrees and an Ω_0 of zero degrees (twelve o'clock) and an Ω_0 of 30 degrees (two o'clock) as generated by TRW's IPCO computer program. After making a decision as to what latitudes are of prime concern, the orbit can be optimized to give these latitudes acceptable sun angles during a good portion of the year. This can be accomplished by varying Ω_0 .

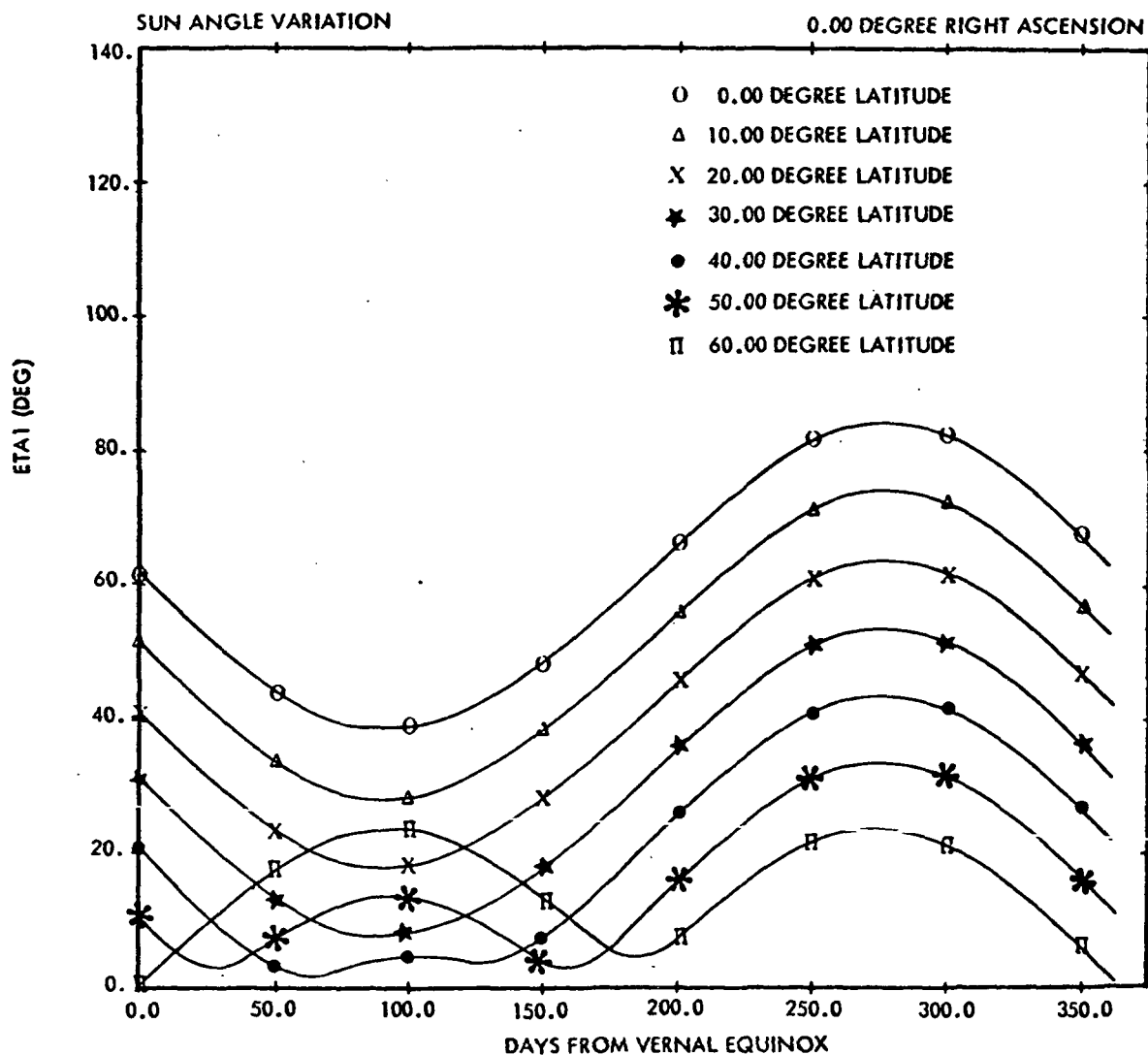


Figure 8-13. Sun Angle Variation Throughout the Year for Positive Latitudes ($\Omega_0 = 0$ degree)

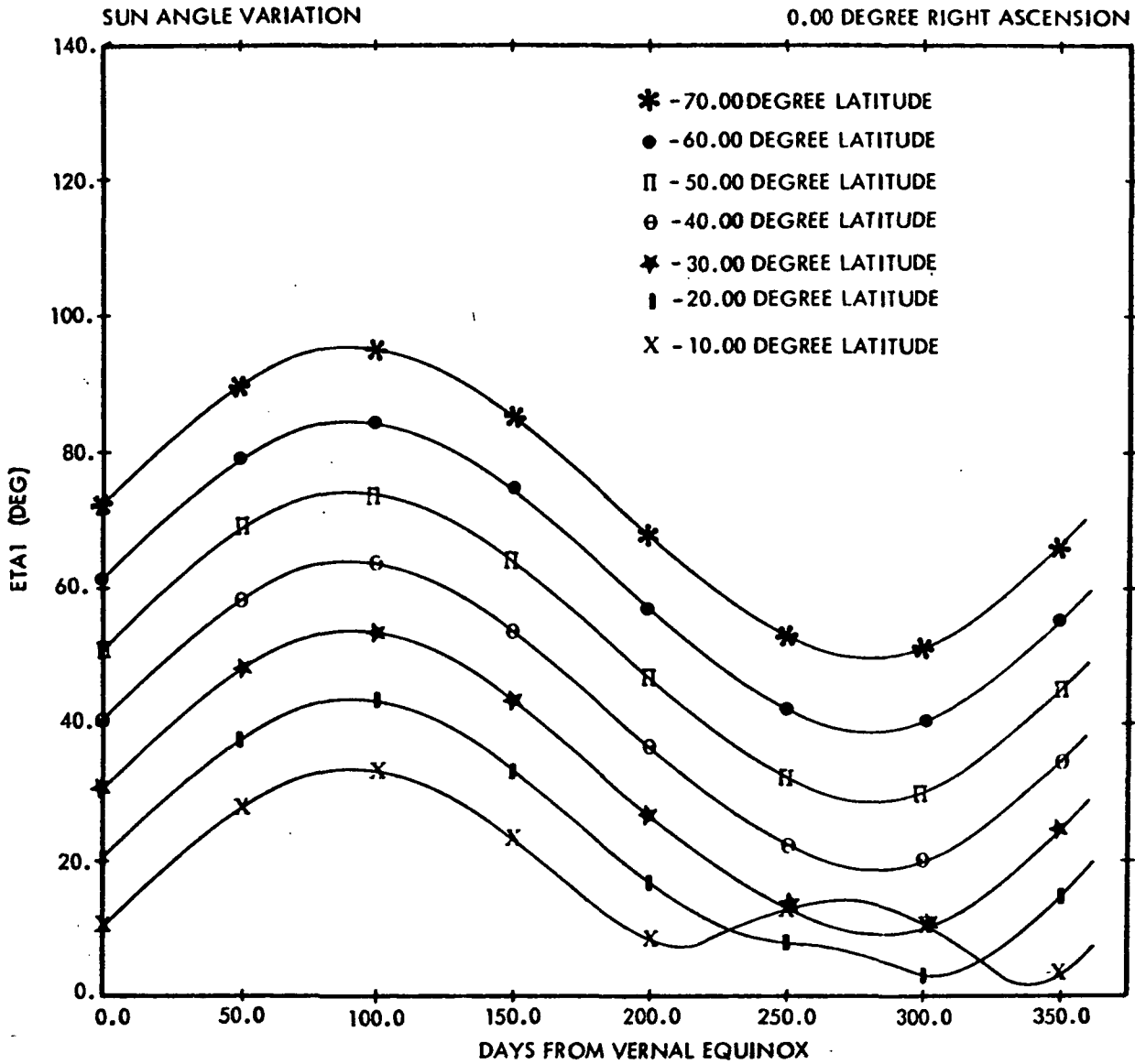


Figure 8-14. Sun Angle Variation Throughout the Year for Negative Latitudes ($\Omega_0 = 0$ degree)

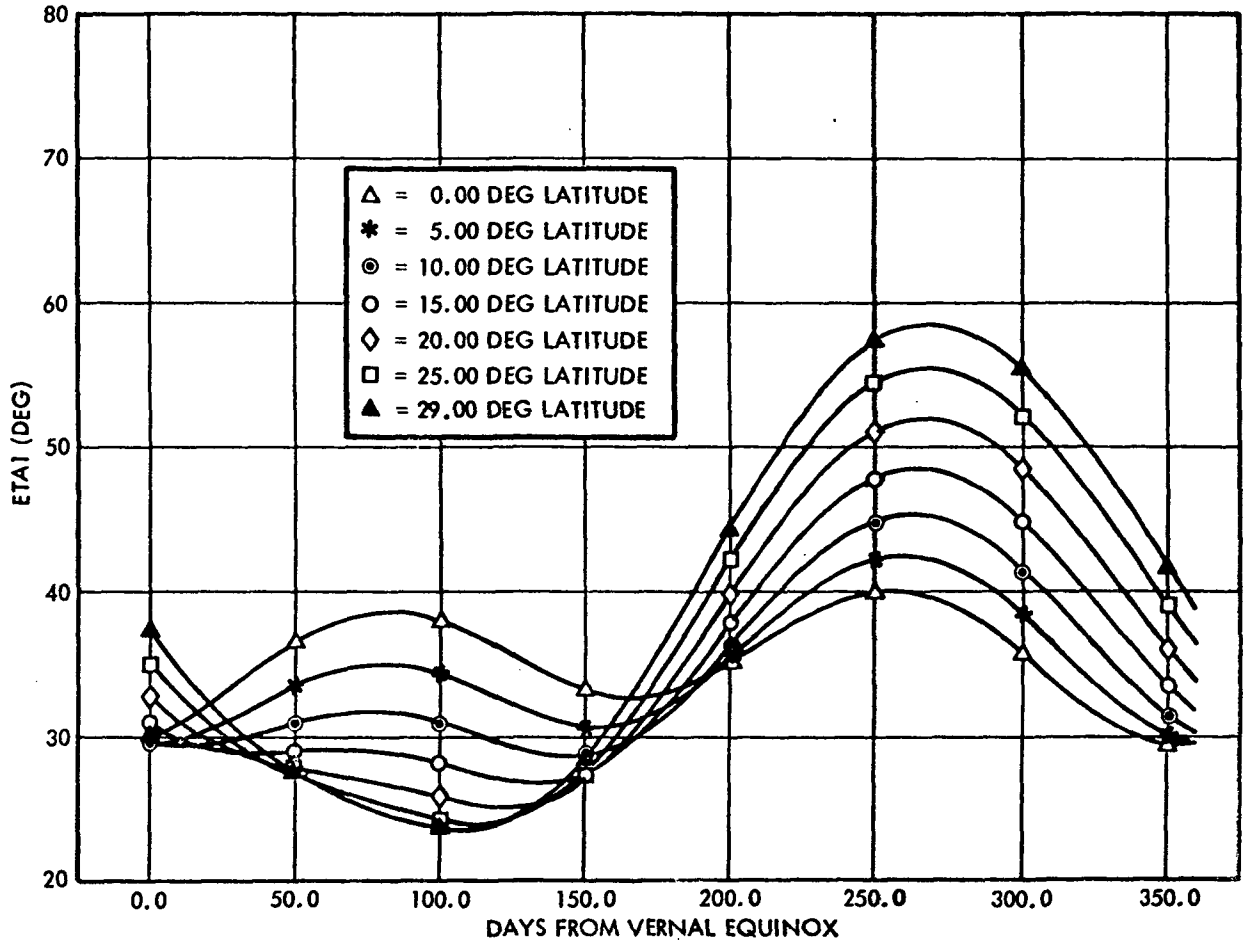


Figure 8-15. Sun Angle Variation Throughout the Year for Positive Latitudes ($\Omega_0 = 30$ degrees)

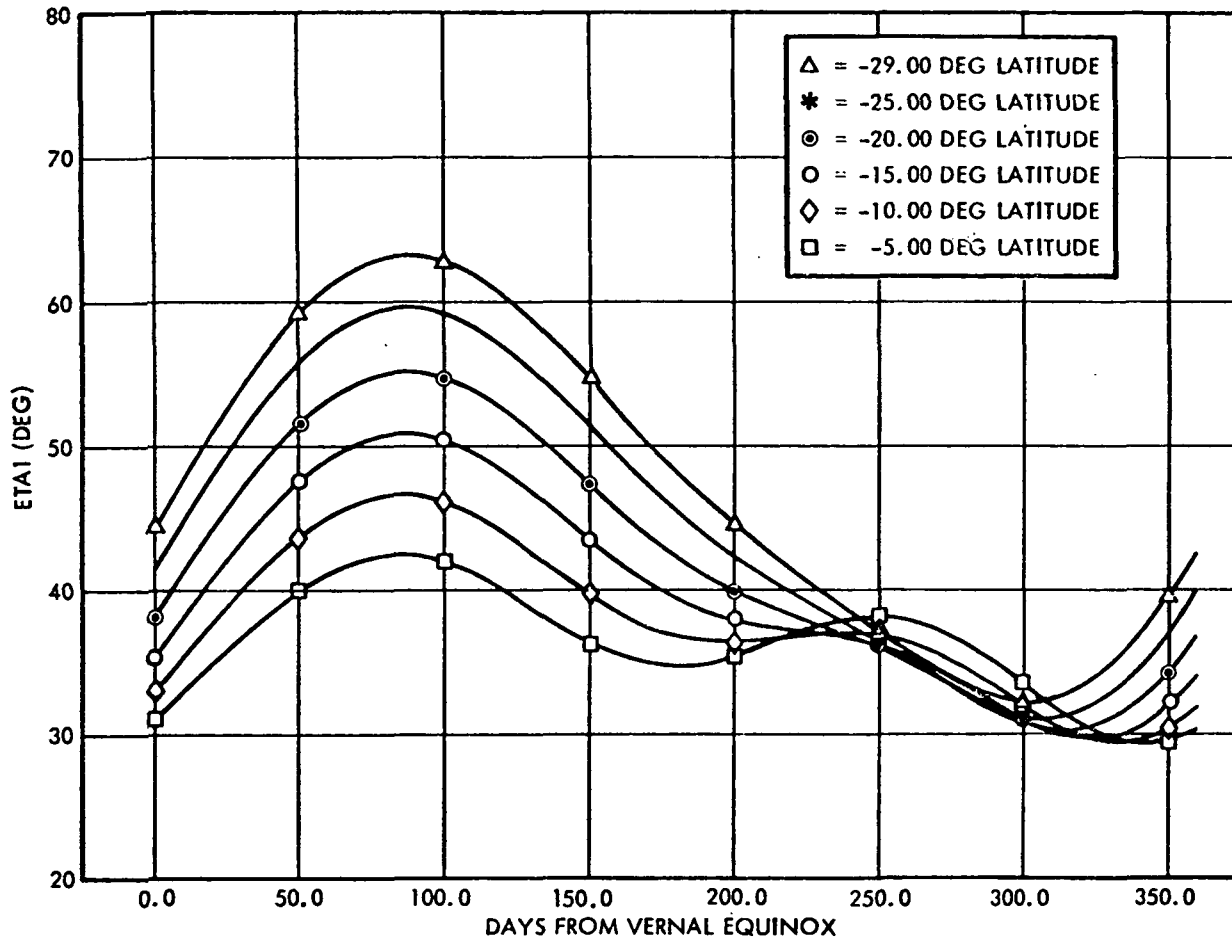


Figure 8-16. Sun Angle Variation Throughout the Year for Negative Latitudes ($\Omega_0 = 30$ degrees)

8.3.1.4 Ground Station Visibility Times

Because of the need to relay large amounts of data, strategically located ground stations maximizing the time of contact with the spacecraft are of great importance. The spacecraft altitude and antenna elevation angle establish this time for a given right ascension of the ascending node. As a result, varying the altitude has a predictable effect upon the contact time. If top priority is given to coverage of the global oceans, three possible ground station locations would be Fairbanks, Alaska; Goldstone, California; and Greenbelt, Maryland.*

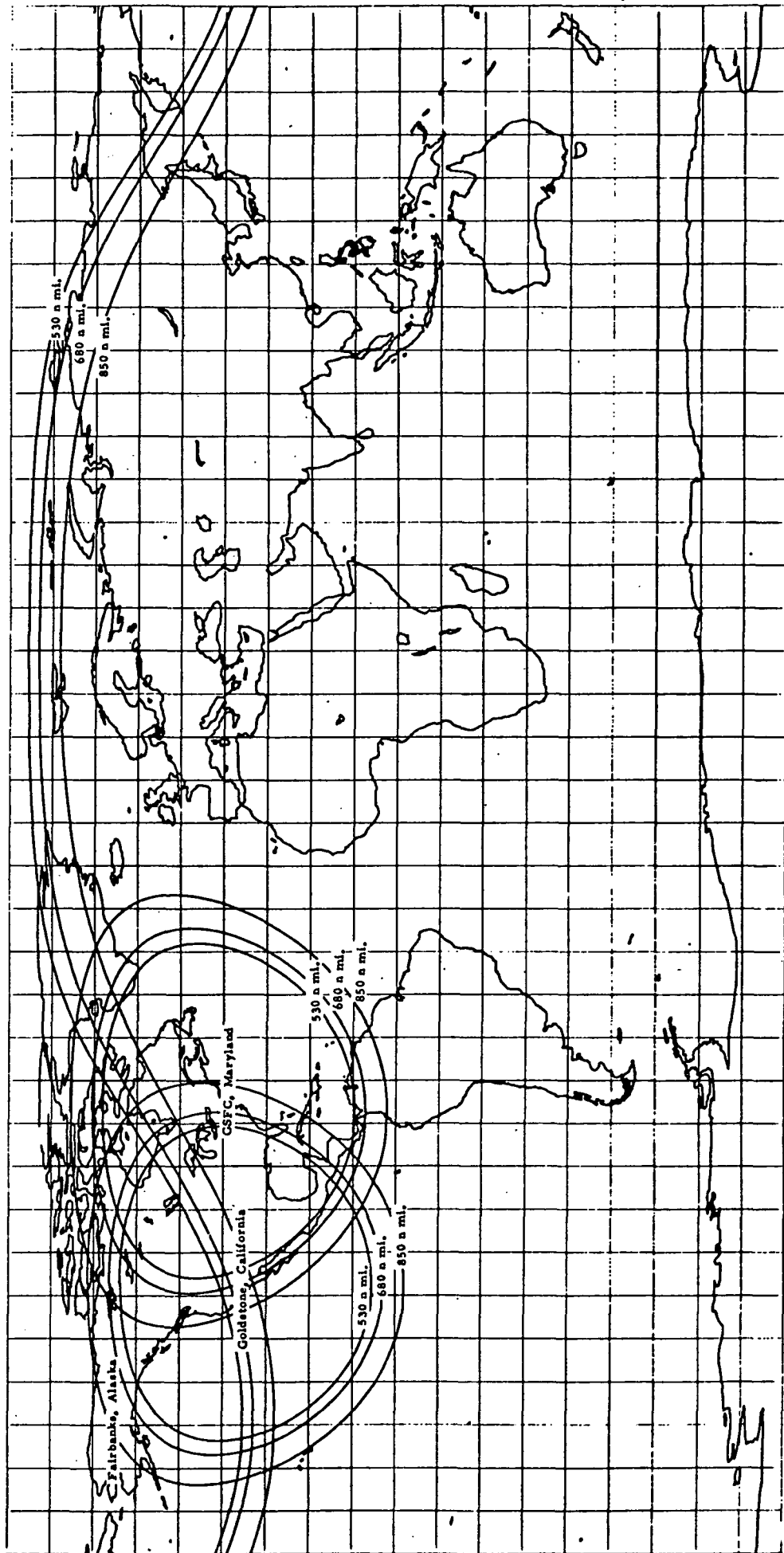
For the ERTS A/B orbit, at an altitude of 492.6 n mi, an initial right ascension of the ascending node of 142.5 degrees and a minimum elevation angle of five degrees, the maximum contact time in any orbit of the 18-day cycle is 15 minutes. Generally, any time under approximately five minutes is avoided because of the tasks which have to be done at every data dump (e.g., command uplink, and video downlink). Holding the initial time of nodal passage constant and decreasing the altitude increases the ground speed of the spacecraft and alters the subsatellite path. The result is a decrease in contact time. As a result, ground station contact time must be considered in placing a lower bound on the altitude (an upper bound on Q).

8.3.1.5 Cloud Cover

The observation frequency of coverage for the visible and near IR sensors will actually be less than the orbital frequency because of intermittent atmospheric interference. As a result, regions of interest from a phenomenological standpoint may have to be skipped or marginally covered. On the other hand, observation of the distribution and appearance of interference in the form of atmospheric moisture can be a valuable indicator of certain oceanographic phenomena such as:

*Through the use of TRW's Cartography Program, Figure 8-17 and overlays 8-1, 8-2, and 8-3 show the amount of time a spacecraft would be visible from the three ground stations per day in a typical orbit where the altitude is 1570 km (848 n mi), 1259 km (680 n mi), 1006 km (543 n mi), respectively.

Page intentionally left blank



Page intentionally left blank

- Distribution of water temperature (water maps and current boundaries, convergences, upwellings).
- Direction and magnitude of land-sea breezes, and character of the wind field over major ocean areas.
- Relative moisture content of the marine atmosphere.
- Relative sea-air temperature difference.

The effect of the intervening atmosphere is to degrade, or in many instances preclude nearly all observations that can be made from space. A statistical model of atmospheric effects on a global scale (e. g., the Arakawa-Mintz model) is a necessary first step in the development of a realistic set of procedures for planning and evaluating potential earth oriented missions.

The main form of atmospheric interference encountered in a remote mission is clouds. By defining a statistical measure of experiment success, i. e., the probability of encountering cloud cover, one can obtain an optimum orbit for the experiment. The probability of encountering cloud cover generally increases with latitude. On a yearly average, the cloudiness over the Southern Hemisphere is 10 to 15 percent greater than over the Northern Hemisphere. The ratio of ocean area to total area in the Southern Hemisphere is about 81 percent as compared to about 61 percent in the Northern Hemisphere.

Present climatological maps have been modified through information provided by existing cloud amount summaries based on both conventional and satellite data. The climatological modifications were generally limited to the area between 60°N and 60°S. Figure 8-18 shows the regions in which satellite data has been incorporated into surface statistics. The data was extremely useful in ocean regions where ship stations were scarce. Due to a large amount of ocean in tropical areas, cloud summaries based on conventional data were of limited value. Therefore, the design of the climatological regions in the tropical areas was based primarily on satellite-observed cloudiness.⁽³⁾ Few cloud data were available for the polar regions.

The mean monthly cloud amount was the principle factor in differentiating between climatological regions (see Table 8-4). The absolute cloud amount, the season of maximum cloudiness, and the magnitude of the seasonal change were all taken into account. Some consideration was also given to cloud type, with each region being designated as having predominantly convective cloudiness (tropics) or predominantly synoptic-scale cloudiness (extratropical areas). For example, areas off the West coasts of the continents where widespread stratus is common were also designated.⁽⁴⁾

Separate climatological regions have generally been designed for land and ocean areas. Certain regions contain continental land areas, islands and ocean (e. g. , 03, 04). (See Figures 8-18 and Table 8-4.) Since most of these regions are tropical, there are considerable differences in cloud regions particularly in the diurnal variations. In these regions the statistics were generally based on land stations, and therefore, properly apply to land areas.

The extremes in mean monthly cloud amount occur in the summer (June-August) and winter (December-March). A swath running along the West coast of the United States during the early summer months would have more than 70 percent mean monthly cloud amount over Southern California, 50 percent over Northern California and Oregon, and 70 percent over Washington. During the winter months the mean monthly cloud amount is less than 30 percent, 50 percent, and 70 percent, respectively. As shown above the occurrence of clouds is a significant factor in determining the phasing of the orbit.

8.3.1.6 Atmospheric Drag

The four major sources of orbital perturbation are the following:

- Atmospheric drag
- Solar perturbations
- Higher earth harmonics
- Lunar perturbations

Page intentionally left blank

Table 8-4. General Description of Climatological Regions (3)

1	2	3	4	5	6	7	8	9
REGION NUMBER	GENERAL DESCRIPTION	LOCATION	SEASONAL CHANGE IN CLOUD AMOUNT	MEAN MONTHLY CLOUD AMOUNT (JUN-AUG)(%)	MEAN MONTHLY CLOUD AMOUNT (DEC-MAR)(%)	PREDOMINANT CLOUD TYPE	DAILY VARIATION IN CLOUD AMOUNT	HOUR OF MAXIMUM CLOUD AMOUNT (LOCAL TIME)
01	ESSENTIALLY CLEAR	MAJOR DESERT AREA	SMALL	<20	<20	----	SMALL	----
02	LITTLE CLOUDINESS	SUB-DESERT AREAS	SMALL	<40	<40	----	SMALL	----
03	TROPICAL CLOUDY	NEAR EQUATOR	SMALL	>60	>60	CONVECTIVE	LARGE	1600
04	TROPICAL MODERATE CLOUDINESS	NORTH OR SOUTH OF REGION 03	SMALL	~50	~50	CONVECTIVE	LARGE	1600
05	DESERT MARINE	OVER OCEAN - OFF W. COASTS	SMALL	~50	~50	STRATIFORM	LARGE	0800
06	DESERT MARINE CLOUDY WINTER	OVER OCEAN - W. OF PERU	EXTREME	>70	<30	STRATIFORM	LARGE	0800
07	DESERT MARINE CLOUDY SUMMER	OVER OCEAN - W. OF BAJA CALIFORNIA	EXTREME	>70	<30	STRATIFORM	LARGE	0800
08	MID-LATITUDE CLEAR SUMMER	NORTH AMERICA	EXTREME	<40	~70	SYNOPTIC SCALE	SMALL	----
09	HIGH LATITUDE CLOUDY SUMMER	NORTH AMERICA ASIA	MODERATE	~70	~50	SYNOPTIC SCALE	SMALL	----
10	HIGH LATITUDE CLEAR WINTER	ASIS, NORTH AMERICA	EXTREME	~70	<30	SYNOPTIC SCALE	SMALL	----
11	MID-LATITUDE LAND	NORTHERN HEMISPHERE	MODERATE	~50	~70	SYNOPTIC SCALE	SMALL	----
12	TROPICAL CLOUDY SUMMER	NORTH OF REGION 03	MODERATE	>60	~50	CONVECTIVE	LARGE	1600
13	MID-LATITUDE OCEAN	NORTHERN HEMISPHERE	MODERATE	~60	>70	SYNOPTIC	SMALL	----
14	HIGH LATITUDE OCEAN	NORTHERN HEMISPHERE	MODERATE	>80	~70	SYNOPTIC SCALE	SMALL	----
15	POLAR	NORTHERN HEMISPHERE	SMALL	~60	~60	SYNOPTIC SCALE	SMALL	----
16	TROPICAL SEASONAL CHANGE	NORTH OF REGION 03	EXTREME	>70	<40	CONVECTIVE	LARGE	1600
17	TROPICAL CLEAR WINTER	NORTHERN HEMISPHERE NR REGION 16	MODERATE	~50	<30	CONVECTIVE	LARGE	1600
18	MEDITERRANEAN	NORTHERN HEMISPHERE EUROPE, WESTERN NORTH AMERICA	EXTREME	~30	--	CONVECTIVE	SMALL	----
19	SUBTROPICAL	NORTHERN HEMISPHERE 30° N	MODERATE	<50	--	CONVECTIVE	LARGE	1600
20	SUBTROPICAL OCEAN	NORTHERN HEMISPHERE 30° N	MODERATE	~50	--	CONVECTIVE	SMALL	----
21	TROPICAL CLOUDY SUMMER	SOUTH OF REGION 03	MODERATE	~50	>60	CONVECTIVE	LARGE	1600
22	MID-LATITUDE OCEAN	SOUTHERN HEMISPHERE	MODERATE	>70	~60	SYNOPTIC SCALE	SMALL	----
23	HIGH LATITUDE OCEAN	SOUTHERN HEMISPHERE	MODERATE	~70	>80	SYNOPTIC SCALE	SMALL	----
24	POLAR	SOUTHERN HEMISPHERE	SMALL	~60	~60	SYNOPTIC SCALE	SMALL	----
25	TROPICAL SEASONAL	SOUTH OF REGION 03	EXTREME	<40	>70	CONVECTIVE	LARGE	1600
26	TROPICAL CLEAR WINTER	SOUTH OF REGION 25; AFRICA, AUSTRALIA	MODERATE	<30	~50	CONVECTIVE	LARGE	1600
27	MEDITERRANEAN	SOUTHERN HEMISPHERE AUSTRALIA, CHILE	EXTREME	--	~30	CONVECTIVE	SMALL	----
28	SUBTROPICAL LAND	SOUTHERN HEMISPHERE ~30° S	MODERATE	~60	<50	CONVECTIVE	LARGE	1600
29	SUBTROPICAL OCEAN	SOUTHERN ~30° S	MODERATE	>60	~50	CONVECTIVE	SMALL	----

Page intentionally left blank

For the range of orbits considered for EOS A/B missions, the latter two are negligible. Of the three sources of solar perturbations, solar gravity gradient, solar tides, and solar radiation pressure, the former could produce longitudinal variations in the node, but these effects were considered beyond the scope of this report.

Atmospheric drag seems to exert the most significant influence on the orbit, and is therefore evaluated for the 1974-1976 launch period. An upper limit on Q can be obtained by considering the altitude decay due to drag. For the launch period considered, solar activity (which has a predictable effect on atmospheric density) will be at a minimum; at any given altitude, the decay due to drag will be low because of a reduced atmospheric density.

The effects of drag can be negated by a propulsive system in one of two ways: by continuous thrust or impulsive thrust. The thrust can be computed in terms of energy as follows:

$$\frac{dE}{dt} = \frac{\mu}{2a^2} \frac{da}{dt} \quad (9)$$

where

$$\frac{dE}{dt} = \text{change in energy per unit mass}$$

Knowing $\frac{dE}{dt}$, the continuous thrust can be computed

$$T_h = \frac{dE}{dt} \frac{P}{2\pi a} = \frac{F}{m} \quad (10)$$

where

where T_h = continuous thrust per unit mass

P = period of the orbit

The impulsive thrust is evaluated in terms of the velocity increment needed to correct the error, ΔV , and can be computed as follows:

$$\frac{\Delta E}{V} \approx \Delta V \text{ (a linear approximation)} \quad (11)$$

where

$$\Delta E = \frac{dE}{dt} t$$

t = time impulse is applied

At an altitude of 570 km (308 n mi), and an early 1975 launch, the altitude decay on a spacecraft with a frontal area of 1.86 m^2 (20 ft^2) is 662 m/yr (2173 ft/yr). This decay could be corrected with propulsive thrusting: one could use a continuous thrusting of $2.36 \times 10^{-5} \text{ kg}$ ($5.2 \times 10^{-5} \text{ lb}$) or, if the impulse were applied every year, a ΔV of .4 mps (1.3 fps). At an altitude of 370 km (200 nmi) the altitude decay would be increased by an order of magnitude and the yearly ΔV needed to correct this decay is approximately 0.36 mps (12 fps). This error could easily be corrected through propulsive thrusting (e.g., a hydrozine system). Consequently, drag considerations would not preclude use of an altitude as low as 390 km (200 n mi). (See Figure 8-19.)

8.3.2 Coverage Schemes

For a limited swath width and high repetition rates, coverage is acquired in a series of transects (making use of narrow swath widths separated by standard distances of hundreds of nautical miles). Depending upon the phasing of these transects, crucial global oceanographic phenomena could be missed.

Conceivably, global oceanography on an operational basis may require a substantial number of satellites to provide the data needed at frequent enough intervals. Conventional synoptic oceanography is based upon large gaps between successive swaths: ship tracks on major oceanographic expeditions are commonly separated by hundreds of miles. EOS A/B data, together with data from other spacecraft, aircraft, merchant, naval and scientific ships would be fed into a computer system for interpolation. In such a system, EOS A/B would couple extremely well in obtaining coverage

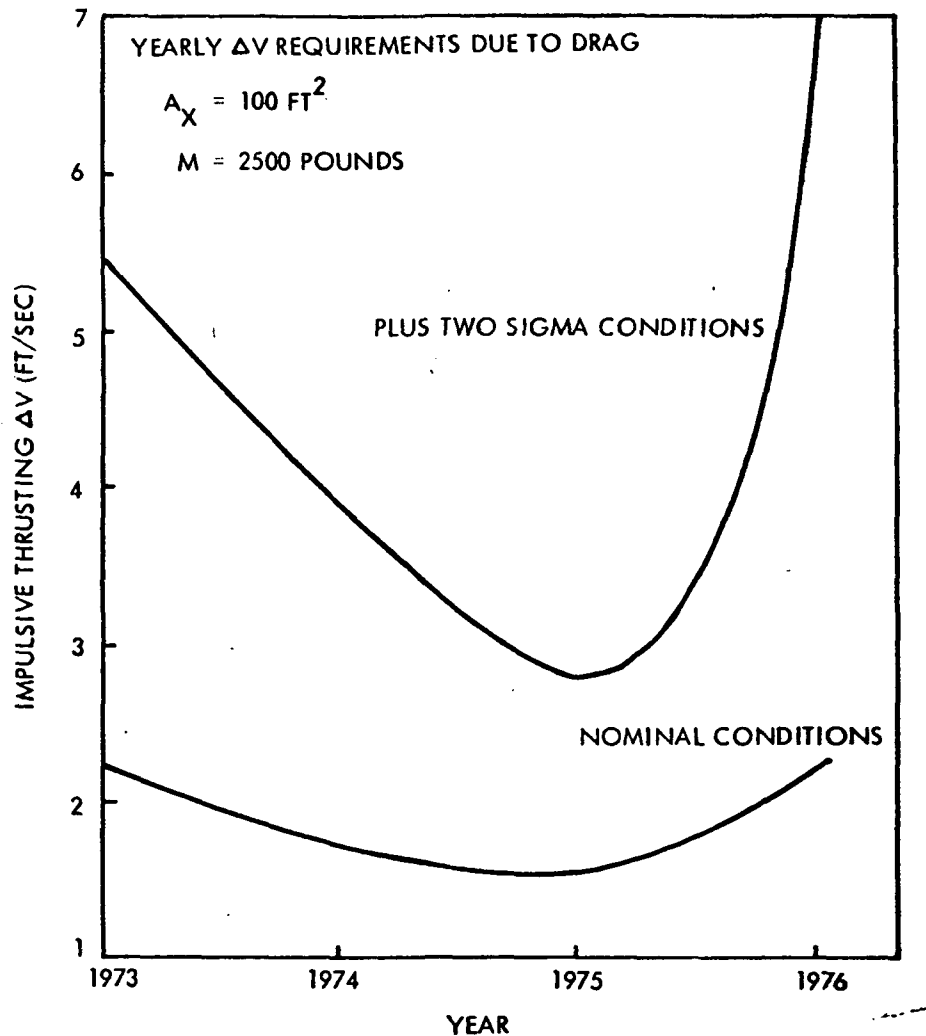


Figure 8-19. Drag Considerations

of selected regions of interest. On the other hand, using one spacecraft, coverage of oceanographic phenomena on a global basis could be obtained by lowering the resolution requirements (increasing the field of view), reducing the cyclic frequency, or resorting to some combination thereof.

8.3.2.1 Coverage Frequency

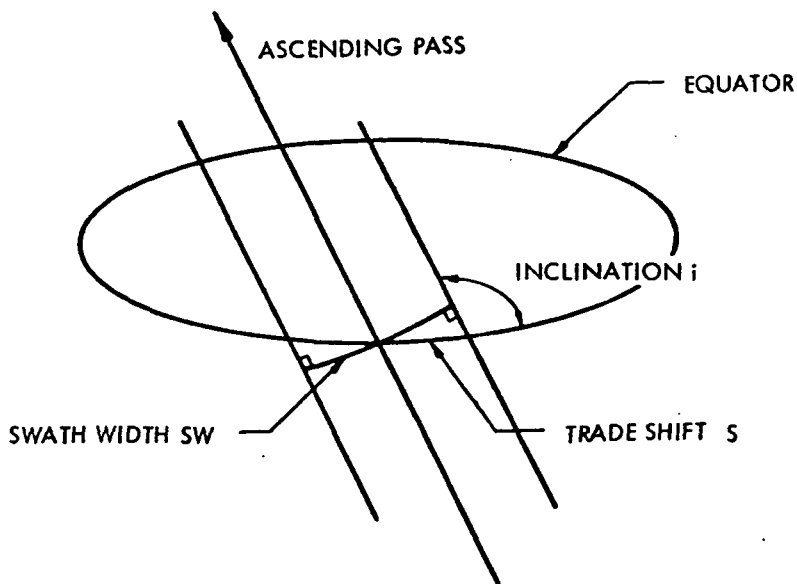
Choosing an integer for Q results in a trace pattern which repeats itself daily, and if the swath width is small (e. g., ERTS A/B has a swath width of $\sim 185 \text{ km}$ (100 n mi) complete coverage can never be obtained. Increasing the denominator, the coverage pattern repeats itself in a number of days equal to the denominator, and for complete

coverage the swath width is approximately equal to S/d (see Figure 8-20). Using the Karrenburg technique, two valid schemes are constructed for a seven-day cyclic frequency (see Figure 8-7). For $I = 14$ and $n/d = 2/7$ or $6/7$ the swath width for complete coverage (assuming an ideal perturbation free orbit in which overlap is unnecessary) is 400 km (216 n mi) and 383 km (207 nmi), respectively. If one continues to increase the swath width beyond the value corresponding to complete coverage in d days a point is reached at which the coverage frequency rises to a value higher than the cyclic frequency.

$$SW = 120 \sin^{-1} (\sin(i) \sin(S/2))$$

EXAMPLE

GIVEN $S = 25^\circ$ OR 1500 NM } $\Rightarrow SW = 2731$ KM (1476 NMI)
 EQ
 $i = 100^\circ$ } 1.6% ERROR



NOTE: AS THE SATELLITE PASSES OVER HIGHER LATITUDES THE ANGLE $i-90^\circ$ INCREASES; THEREFORE THE ERROR INCREASES. AS A FIRST ORDER APPROXIMATION THE TRADE SHIFT OR ANY FRACTION THEREIN WILL BE CONSIDERED THE SWATH WIDTH.

Figure 8-20. An Approximation to the Actual Swath Width

A further increase in the swath width results in a second point being reached at which the coverage frequency rises to an even higher value. If this process is continued until the swath width equals the trace shift, complete coverage is acquired daily. The coverage frequency, for

a given Q , is therefore a function of the swath width where the resulting dependence is a step function as displayed in the Appendix. For a cyclic frequency of seven days there are six possible rational fractions which can be grouped into three coverage patterns: $(1/7, 6/7)$ sequential coverage, $(2/7, 5/7)$ cyclic coverage, and $(3/7, 4/7)$ cyclic coverage (see Figure 8-2 and Appendix D). The first element in each group is an eastward progression across the trace shift and the second is a westward progression. In the first pattern the coverage frequency is increased at steps of one day every time one normalized unit is added to the swath width where one normalized unit equals S/d .

Depending upon the distribution of phenomena being observed this technique could be used to optimize coverage. By basing the subsatellite trace pattern upon the sensor with the narrowest swath width (e. g. , visible spectrometer) and obtaining complete global coverage, (for a visible sensor at an altitude of 370 km (200 n mi) this would be approximately 370 km (200 n mi), a sensor employing a fairly large swath width would provide global coverage at a higher frequency.

The choice of a specific rational fraction depends upon two considerations: the requirements of the sensor subsystem and the frequency of observation of global phenomena. In Figure 8-21 a rational fraction of $2/7$ or $5/7$ gives the largest increase in coverage frequency for the smallest increment in swath width where a rational fraction of $3/7$ or $4/7$ minimizes the swath width needed to achieve the largest coverage frequency under one day. In considering sensors with a field of view larger than the one used as a basis for the trace pattern the former scheme would be used to optimize resolution and the latter for optimizing the coverage frequency.

Transectional coverage of the ocean areas of interest on a global basis using narrow swath widths allows observations to be made at frequent enough intervals to satisfy the dynamic nature of some phenomena, but large voids occur in important regions leaving gaps in the data. To optimize a trace pattern employing transectional coverage, phasing must be used to insure coverage of the areas of interest. A majority of the regions lie between 80°N and 80°S as shown in Figures 8-1 and 8-2.

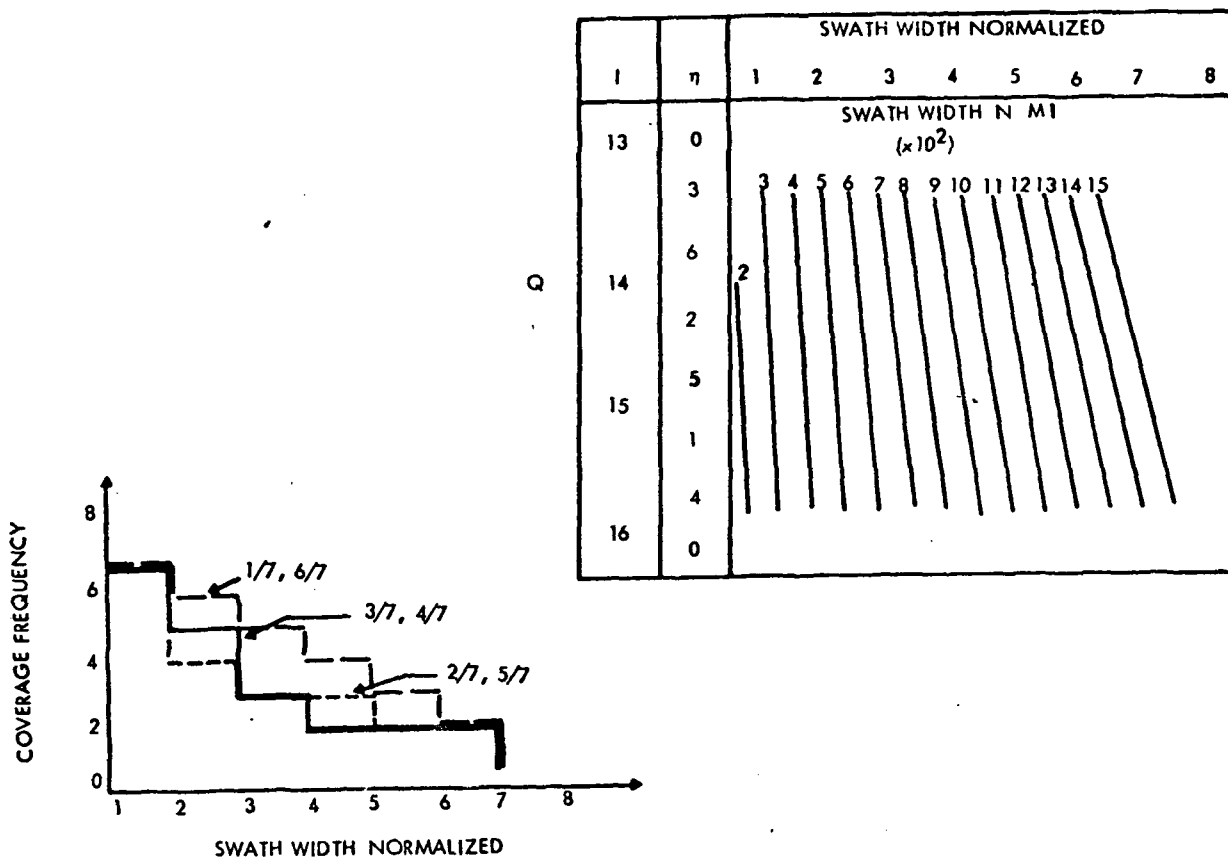


Figure 8-21. Seven-Day Cyclic Frequency

Once the trace pattern is phased to optimize coverage, the swath width can be increased to cover a larger portion of a particular region of interest by sacrificing resolution. Overlays 8-1 through 8-4 are representative trace patterns based upon the previous parametric definitions. (Table 8-6 shows the orbits considered.) Each overlay shows the first day's subsatellite trace pattern, both ascending and descending.

In order to correctly position the overlays on the base maps, Figures 8-1, 8-2 and 8-17 line up the 50°N and 50°S latitude lines on the overlays with the same latitudes on the maps. Since launch is arbitrary, one can shift or phase the overlay in a horizontal direction (west or east) to vary the areas covered and as a result there is no need to set the overlay over a specific longitude. Sliding the overlay along

Table 8-6. Representative Orbits

	Overlay				
	8.1	8.2	8.3	8.4	8.5
Q	12 1/4	13 0/1	13 1/2	13 2/3	133/4
S	29.390	27.5°	26.6°	26.3°	26.18°
i	102.3°	101.1°	99.8°	99.5°	99.4°
h	848 n mi	680 n mi	585 n mi	546 n mi	531 n mi
P	117.55 min	111 min	106.4 min	105.4 min	104.76 min

the two guide latitudes changes the phase. The grid surrounding each subsatellite pass represents a 740km (400 n mi) swath width. There is also a climatological overlay which can be placed on the base map before the subsatellite trace overlays are used (Overlay 8-6). One can then observe the seasonal cloud cover probability associated with a specific trace pattern.

8.3.2.2 Periodic Daily Coverage

Near daily coverage can be accomplished by using an extremely low cyclic frequency and a narrow swath (several hundred kilometers) assuming that regions of interest could go unobserved for long periods of time. This method would give daily coverage for periods of several days to a week and go unobserved for several months. This is accomplished by employing a consecutive progression across the trace shift which takes d days to return to the initial cyclic trace ($n = 1$ or $n = d-1$). In other words, global coverage is acquired in d days.

At high latitudes a phenomenon can be observed for longer periods of time due to an increasing overlap of consecutive swaths. As shown in Figure 8-22 a phenomenon 60 n mi in width can be seen daily for four consecutive days at 25 degrees latitude, five consecutive days at 40 degrees, and 13 days at 75 degrees by using a 370 km (200 n mi) swath width in a near polar, 902 km (487 n mi) orbit with a 36-day cyclic frequency and a sequential coverage scheme.

If in its steady progression across the trace shift, the spacecraft observed a particular phenomenon of interest, a small tangential velocity change (ΔV_t) and a small out of plane velocity change (ΔV_o) would bring it into a scheme having an integral number of orbits per day, and thus, daily observations would be made.

By using Equation 7 to calculate the normalized semi-major axis, a/a_e , substituting this into Equation 1, and taking the total derivative, an expression for a change in the nodal regression rate in terms of a change in the trace repetition parameter and inclination can be computed:

$$\frac{\Delta \dot{\Omega}}{\dot{\Omega}} = \frac{7}{3} \frac{\Delta Q}{Q} - (\tan i) \Delta i \quad (12)$$

For a sun-synchronous orbit the nodal regression rate is constant ($\Delta \dot{\Omega} = 0$) and for small velocity changes $\Delta V_o / V_t = \Delta i$. Therefore:

$$\Delta V_o = \frac{7 V_t \Delta Q}{3 Q \tan i} \quad (13)$$

By using the energy equation,

$$\frac{1}{2} \left(\dot{r}^2 + r^2 \dot{\nu}^2 \right) - \frac{\mu}{r} = \frac{-\mu}{2a} \quad (14)$$

where

- r = radial position of the spacecraft as measured from the center of the earth
- a = semi-major axis
- V = true anomaly
- $r \dot{\nu} = V_t$ (see Figure 8-3)

an expression for the tangential velocity change can be derived. For a circular orbit the radius remains fixed and equal to the semi-major axis

$$V_t^2 = \frac{\mu}{a} \quad (15)$$

taking the total derivative and substituting

$$\Delta a = - \frac{2 a^{5/2} \Delta Q}{3 K a_e^{3/2}}, \quad K = 0.059 \quad (16)$$

The resulting expression for the ΔV_t is:

$$\Delta V_t = \frac{\sqrt{\mu} a \Delta Q}{3 K a_e^{3/2}} \quad (17)$$

For the orbit considered in Figure 8-22 a ΔV_t of 4.895 m/sec (16.06 ft/sec) and a ΔV_o of 5.151 m/sec (16.9 ft/sec) is needed to bring the cyclic frequency to 1 (a daily revisit time).

This is an unlikely coverage scheme for a global oceanographic mission because of the need for global synoptic data generally every 1-5 days in the visible spectrum and one to three days for the infrared measurements of sea surface temperature.

8.3.2.3 Stereo Viewing

For narrow swath widths and trace patterns which give complete coverage at the end of each cycle, many subsatellite points are observed from only one direction or aspect angle and some points are viewed only marginally at the fringe of the swath. In many cases it is desirable to view points of interest from several directions (e. g., coastal bathymetric measurements). This can be accomplished through a careful choice of the rational fraction of Q . For example, the bathymetry observation frequency and field of view requirements vary from 1-14 days and 80-150 n mi. Assuming that Nimbus E and ERTS A/B will be operational when EOS A/B is launched, a great deal of the meteorology and terrestrial cartography, geology and hydrology could be performed by these spacecraft. As a result, a global oceanographic mission dedicated primarily to synoptic observations of the global oceans and some coastal oceanography could have a cyclic frequency of 14 days and a visible sensor swath width of 120 n mi.

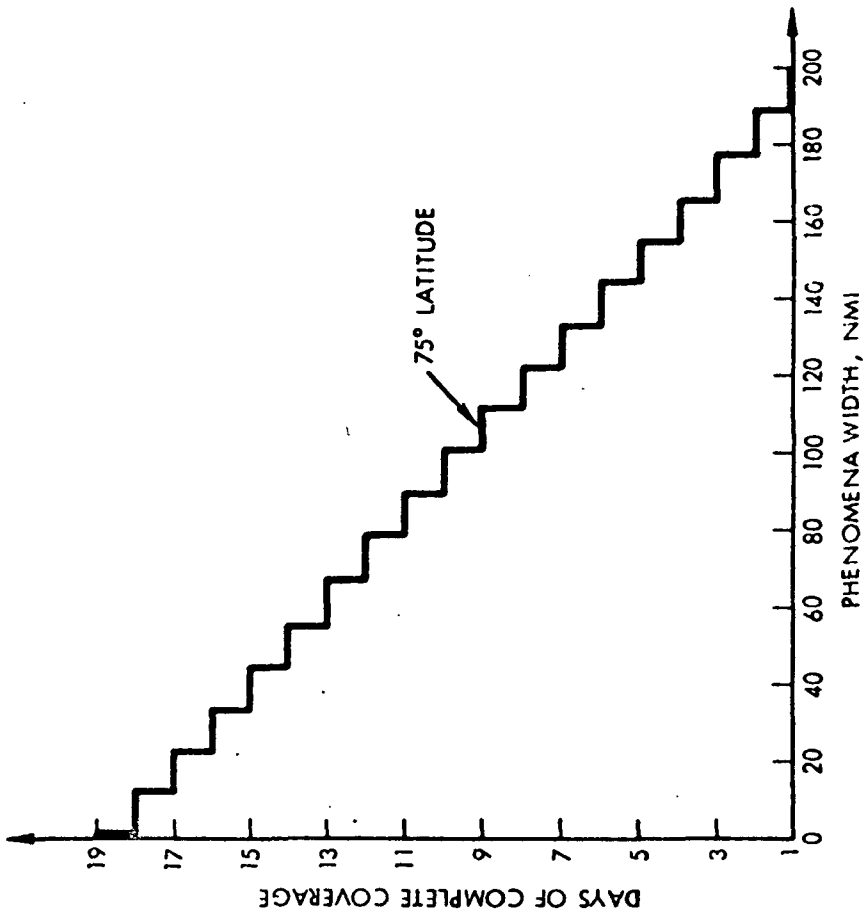
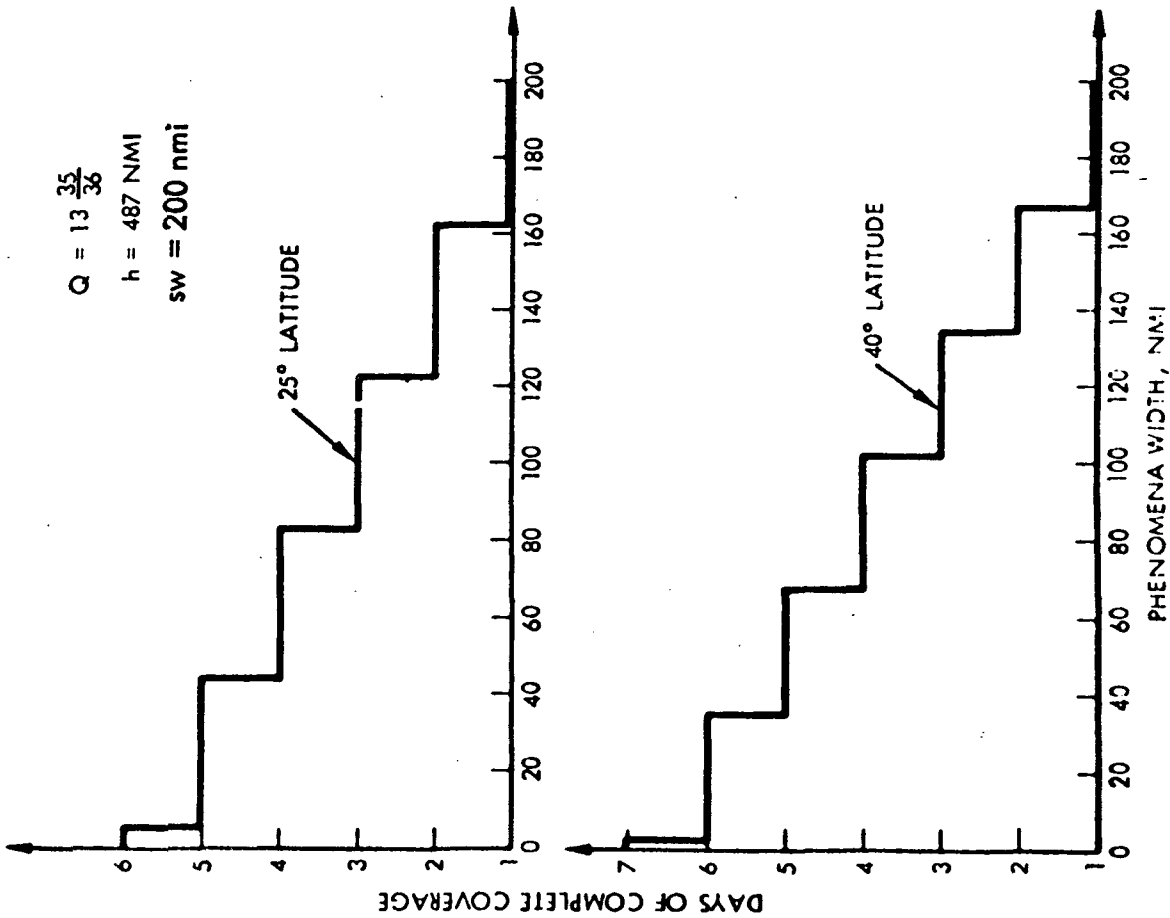


Figure 8-22. Days of Complete Daily Viewing of a Specific Phenomenon

For the orbit to lie within the mission domain, assume the integral part of Q must be 13, 14, or 15. Since a value of Q will be chosen between 13 and 15, the trace shift S will be between 24- and 27.6-degrees of longitude. Coverage of the interval S at the equator insures global coverage (except for small regions at the poles) since the longitudinal width of the swath increases steadily with latitude. To accomplish complete coverage of S the minimum number of two degrees (equatorial degrees, one degree = 60 n mi) swaths required is the smallest integer greater than S/2, which is nothing more than the cyclic frequency. If it is desirable to view points of interest from a variety of directions, an integral value of d greater than a multiple of S/2 should be considered for the coverage frequency. Table 8-7 lists several of these multiples.

Table 8-7. Values of d Corresponding to One or More Aspect Angles⁽²⁾

<u>No. of Aspect Angles</u>	<u>Value of d</u>
1	12-14
2	24-28
3	36-42
4	48-56

For a one year mission it is desirable to have a whole number of coverage cycles. This is another consideration in choosing d; Table 8-8 lists these integral multiples (assuming a year has 366 days).

Table 8-8. Frequencies Corresponding to Integral Coverage Cycles⁽²⁾

Table 8-8 Frequencies Corresponding to Integral Coverage Cycles⁽²⁾

<u>Cycles/Year</u>	<u>Cyclic Frequency</u>
1	366
2	183
3	122
4	91, 92
5	73
6	61
7	52
8	46
9	41
10	36, 37
11	33, 34
12	30, 31
13	28
14	26
15	24, 25
16	23

Solving the above two conditions simultaneously results in the following candidates for d:

24, 25, 26, 28	2 Aspect Angles
36, 37, 41	3 Aspect Angles
52	4 Aspect Angles

Assuming that 3 aspect angles are desirable there are three choices: 36, 37, and 41. A value of 36 was initially chosen for d. However, in choosing the numerator in the rational fraction, 4, 6, 8, 9, 12, 16 and 18 were avoided because the trace closes in less than 10 days; consequently for a 2° swath width voids would be left in the coverage pattern. Values such as 2, 3, 10, 14, and 15 close in less than 20 days which provides fewer than the desired three aspect angles. Furthermore, none of the remaining primes, 1, 5, 11, etc., are compatible with d (the coverage pattern is laid down in such a manner that some points are observed repeatedly, week after week, while others remain unobserved for weeks at a time).

Each of the two remaining values are good choices for d from the standpoint that they are primes of all lesser integers and the trace will not close in less than d days regardless of the choice of numerator. On the other hand these values result in a great deal of incompatibility; in fact for d = 41 there is no numerator that will result in a trace pattern which obtains complete coverage in 14 days with a 2° swath width. Similar difficulties are encountered when considering d = 37 with the exception of a numerator value of 29 (i. e., $Q = 14 \frac{29}{37}$, see Figure 8-23). Note that complete coverage is obtained every 14 days with an overlap of 0.03 degree or 3.3 km and at the end of the 37th day cycle every point is viewed from at least three-aspect angles.

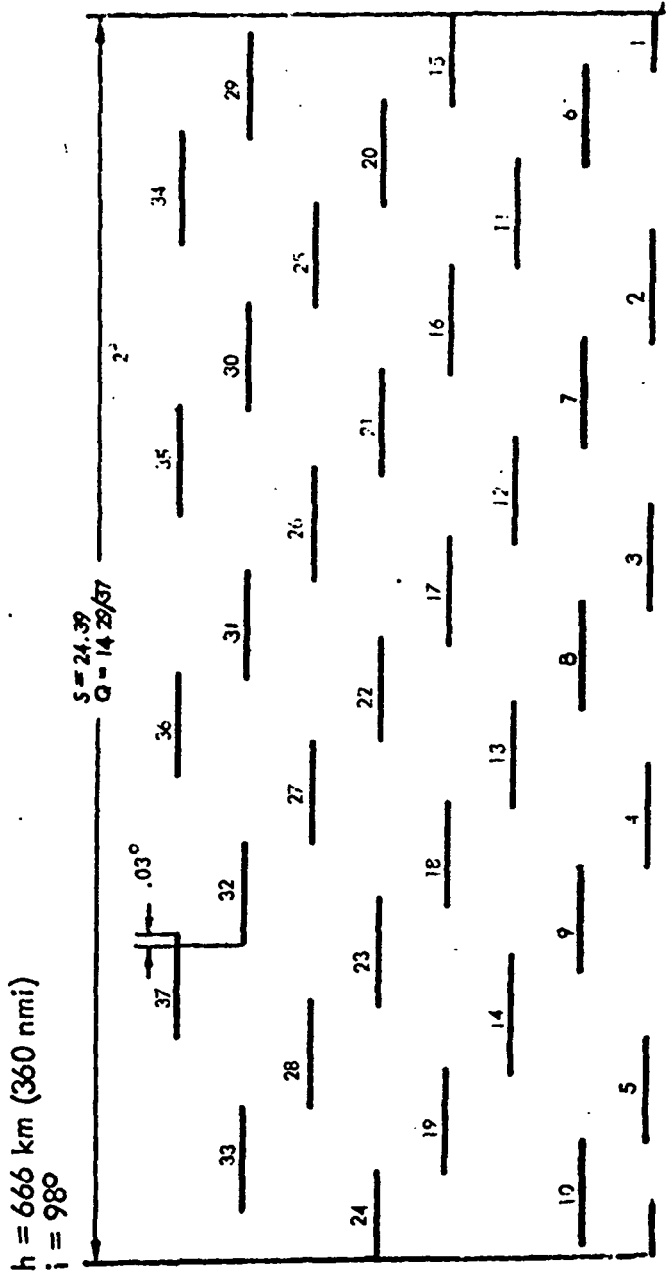


Figure 8-23. Ideal Drag Free Trace Pattern and Coverage in 14 Days with Three-Aspect Angles

8.4 FINAL ORBIT SELECTION

The final selection of an EOS Global Oceanographic Orbit depends upon the phenomenology and sensor requirements used, and the parametric coverage tradeoffs made. The logic associated with these tasks is shown in Figure 8-24. The orbital parameters are bounded and a final selection is made.

An evaluation of the ground station visibility times for the global oceanographic orbit is shown in Figures 8-25 through 8-27. Seventy percent of the visibility times are between 9 and 15 minutes and five percent are less than 5 minutes

PARAMETRIC TRADEOFF

PHENOMENOLOGY AND SENSOR REQUIREMENTS

- PHENOMENA OF INTEREST LIE BETWEEN 80° N. LAT. AND 80° S. LAT.
- OBSERVATION FREQUENCY

PRIORITY AREA	FREQUENCY RANGE
POLLUTION	3 - 30 DAYS
MARINE RESOURCES	1/2 - 14 DAYS
PHYSICAL PHENOMENA	1 - 5 DAYS



GLOBAL OCEANOGRAPHY → OBSERVATION FREQUENCY (1-5) DAYS

- FIELD OF VIEW

GLOBAL OCEANOGRAPHY → FIELD OF VIEW 100-1000 km*

* GLOBAL COVERAGE IN VISIBLE SPECTRUM REQUIRED

- SUN ANGLES

VISIBLE	
SEA STATE SENSOR	0-80°
SPECTROMETER	0-50°

PARAMETERS
 Q - ORBITS/DAY (h - ALTITUDE)
 e - ECCENTRICITY
 i - INCLINATION
 ω - ARGUMENT OF PERIGEE
 Ω_0 - INITIAL RIGHT ASCENSION OF ASCENDING NODE

- CIRCULAR ORBIT $e = 0$

- UNIFORMITY OF GROUND STATION VISIBILITY TIME
- CONSTANT SENSOR RANGE



ω IS ARBITRARY, THEREFORE IT IS SET EQUAL TO 0 $\omega = 0$

- SUN-SYNCHROMISM

- DATA CAN BE STANDARDIZED
- SUN ANGLE VARIATION IS BOUNDED
- MANY POINTS RECEIVED DAY AND NIGHT COVERAGE
- GLOBAL COVERAGE (EXCEPT AT POLES)



i and h ARE INTERDEPENDENT

- RANGE FOR Q (h)

- SENSOR REQUIREMENTS
 MICROWAVE RADIOMETER - $h \leq 850$ NMI
 VISIBLE SPECTROMETER - $h \geq 545$ NMI
 FREQ. ≥ 3 DAYS

- ATMOSPHERIC DRAG
 MINIMUM SOLAR ACTIVITY - $h \geq 150$ NMI

- OBLIQUITY - NOT A PROBLEM IN GLOBAL OCEANOGRAPHY (FOR ABOVE ALTITUDE RANGE)

- GROUND STATION VISIBILITY TIMES - NOT TOO IMPORTANT IN DETERMINING Q . (SEE COVERAGE Ω_0)



$545 \leq h \leq 850$ NMI
 $3 \geq \text{FREQ.} \geq 5$ DAYS
 $13.7 \geq Q \geq 12.2$ ORBITS/DAY

$99.5^\circ \leq i \leq 102.3^\circ$
 SUN-SYNC.

- CHOICE OF PHASING (EXCLUDING COVERAGE CONSIDERATIONS)

- CLOUD COVER IMPLIES A LOCAL EQUATORIAL CROSSING OF 9 AM - 3 PM
- FOR GLITTER MEASUREMENTS A 2 O'CLOCK SUN IS BEST
- THE SPECTROMETER CAN BE CANTED TO AVOID THE GLITTER PATTERN (HIGH NOON SUN GIVES MAX PENETRATION)



$\Omega_0 = 0^\circ$ OR 180°

COVERAGE

PARAMETERS:
 S = TRACE SHIFT
 d = CYCLIC FREQUENCY
 SW = SWATH WIDTH

- GLOBAL COVERAGE IS REQUIRED ON AN OPERATIONAL BASIS



POSSIBILITY OF MORE THAN ONE SATELLITE

- HIGH FREQUENCY COVERAGE

- d = OBSERVATION FREQUENCY
- $SW = S/d$, $S = \frac{360^\circ}{Q}$ (VISIBLE SPECTROMETER)



$3 \leq d \leq 5$ DAYS
 $1581 \leq S \leq 1763$ NMI
 $320 \leq SW \leq 600$ NMI

- PERIODIC DAILY COVERAGE
 RULED OUT BECAUSE OF THE NEED FOR GLOBAL SYNOPTIC DATA

- STEREO VIEWING
 RULED OUT BECAUSE OF THE NEED FOR GLOBAL SYNOPTIC DATA AND THERE IS NO STRONG REQUIREMENT FOR MULTI-ANGLE VIEWING

- SHIFTING Ω_0 CAN SET PHASING TO COVER IMPORTANT PHENOMENA.

GLOBAL OCEANOGRAPHIC ORBIT

- $e = 0$
- $\omega = 0$
- $h = 531$ NMI.
- $i = 99.4^\circ$
- $\Omega_0 = 30^\circ$ (2 O'CLOCK)
- $Q = 13 \frac{3}{4}$ ORBITS/DAY
- $d = 4$ DAYS
- $sw = 400$ NMI. (VISIBLE SPECT.)

Figure 8-24. Summary of the Orbital Trade-offs and the Orbit Selected

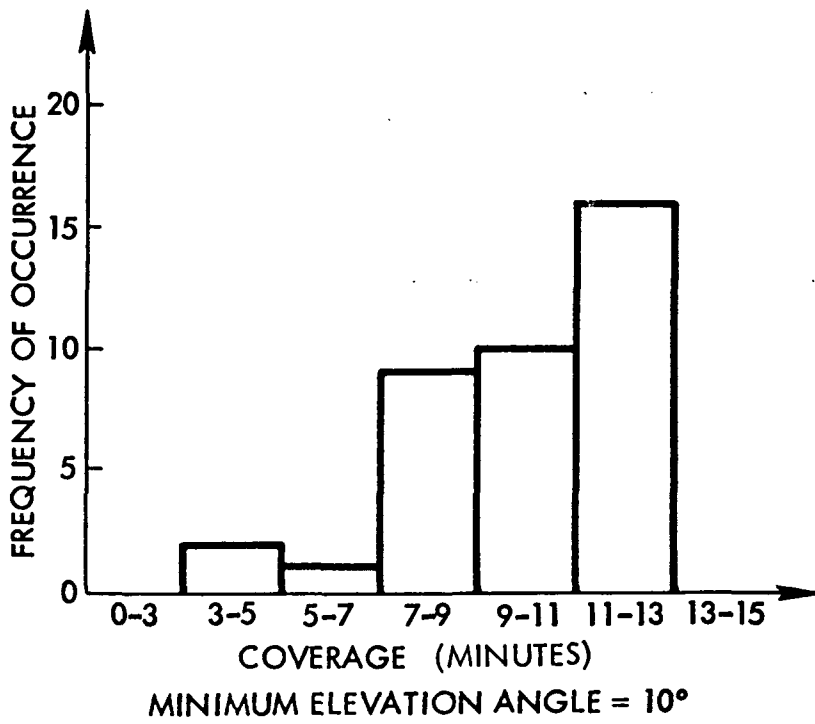
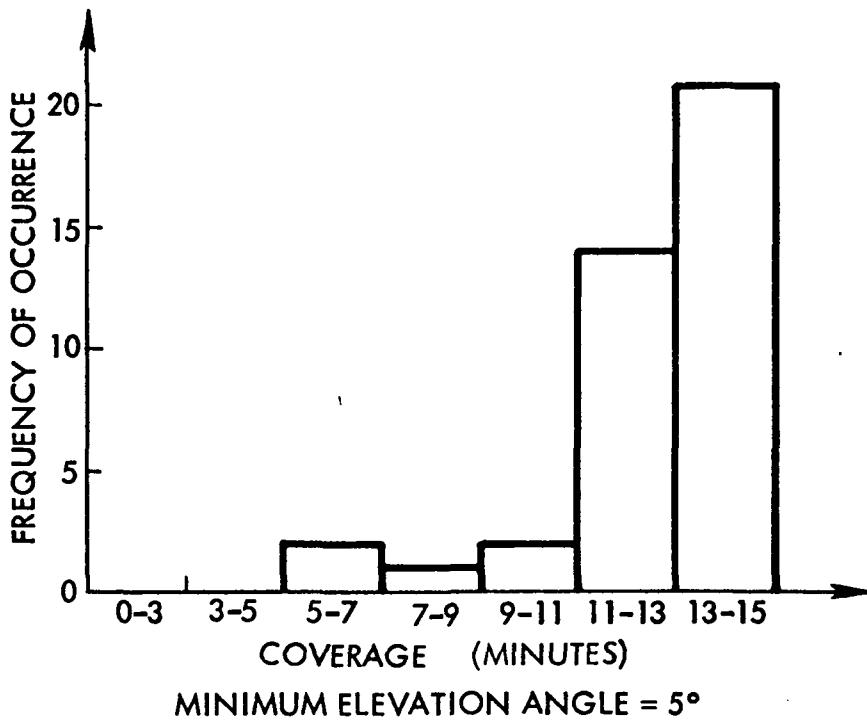


Figure 8-25 Ground Station Coverage Histogram for Fairbanks, Alaska using the EOS Global Oceanographic Orbit

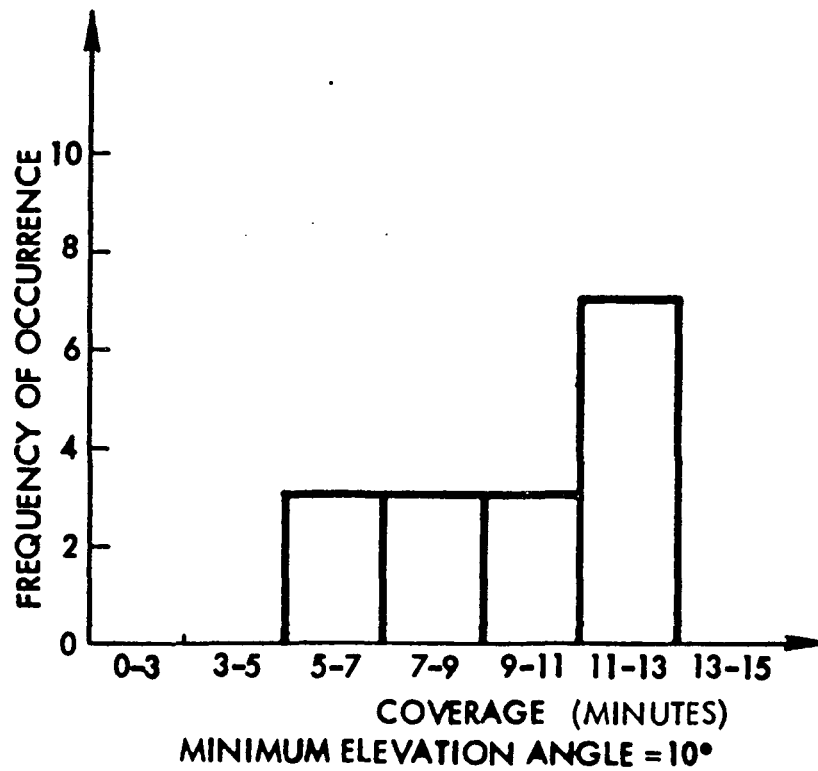
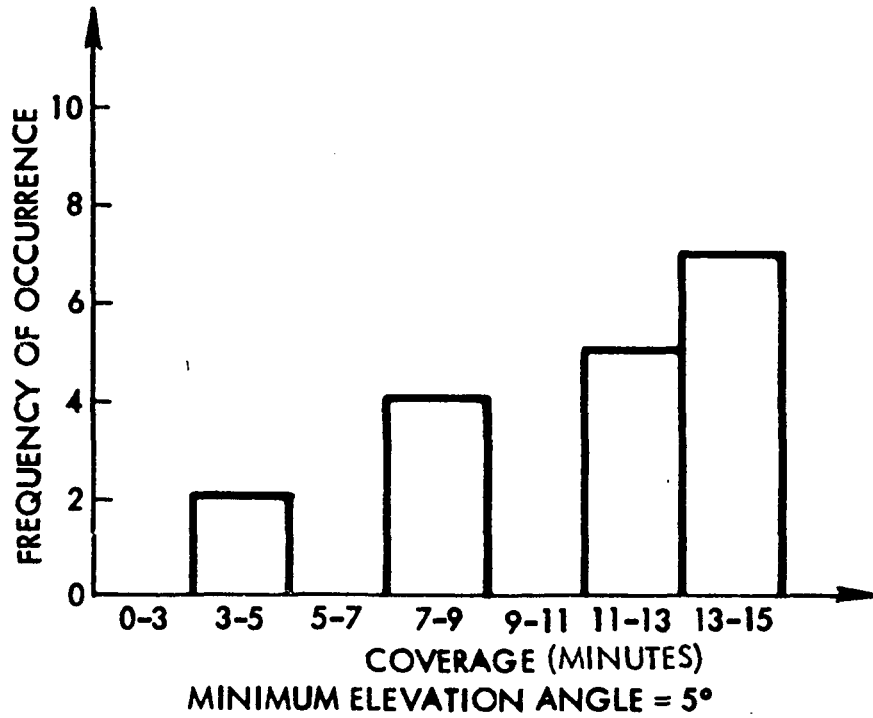


Figure 8-26. Ground Station Coverage Histogram for Goldstone, California Using the EOS Global Oceanographic Orbit

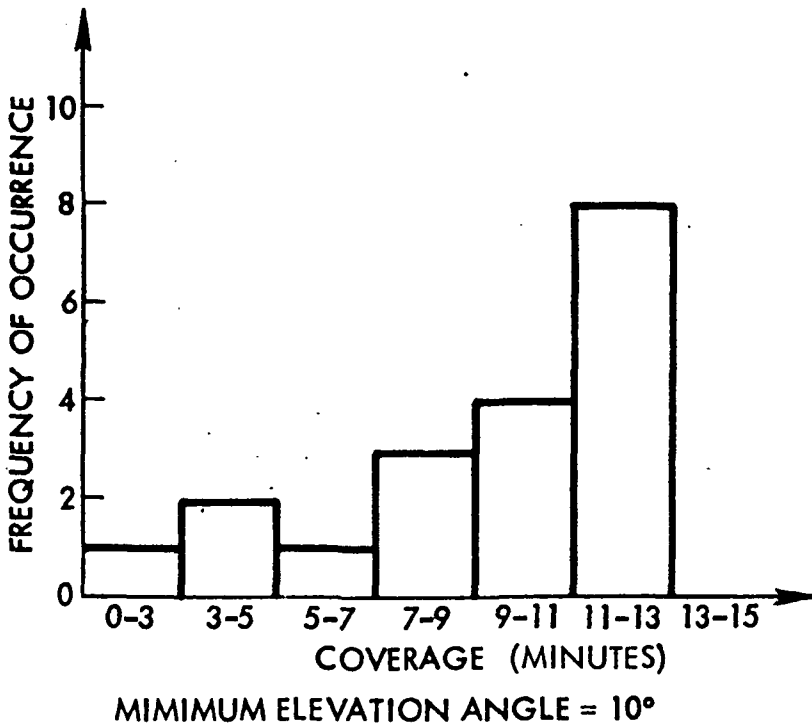
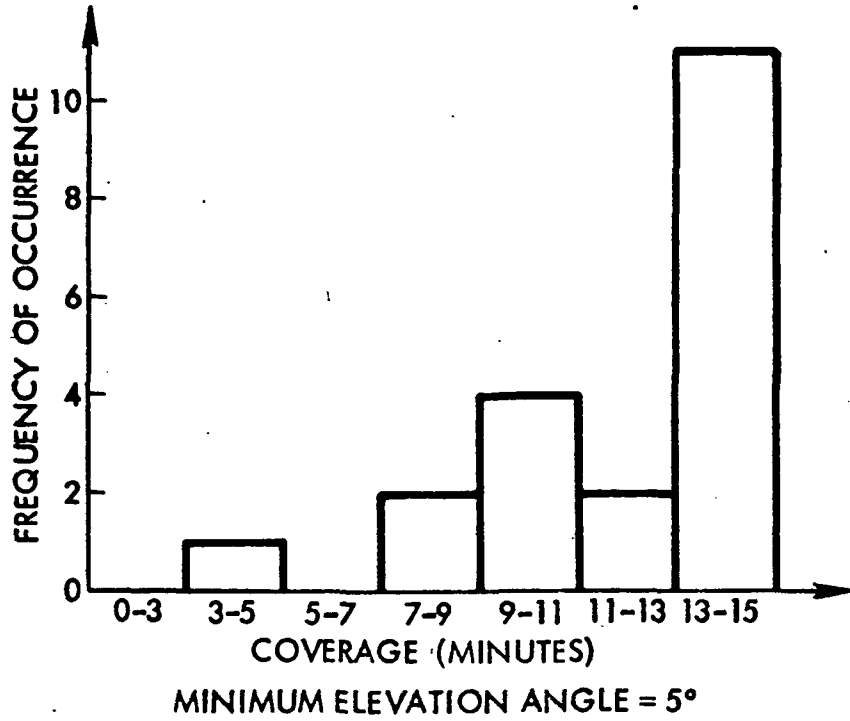


Figure 8-27. Ground Station Coverage Histogram for the Goddard Space Flight Center using the EOS Global Oceanographic Orbit

BIBLIOGRAPHY FOR SECTION 8

1. Hela, I., and T. Laevastu, "Fisheries Hydrography," Fishing News (books) Ltd., 1961.
2. Karrenberg, H. K., E. Levin, and R. D. Luders, "Orbit Synthesis," AAA/AIAA Astrodynamics Specialist Conference, Jackson, Wyoming, September 3-5, 1968
3. World Wide Cloud Cover Distributions for Use In Computer Simulations - Final Report, Allied Research Associates, Inc. for NASA/Marshall Space Flight Center, Contract No. CR-61345.
4. Development of a Global Cloud Model for Simulating Earth Viewing Space Missions - Final Report, Allied Research Associates, Inc. for NASA/Marshall Space Flight Center, Contract No. CR-61345.

Reference was made to the following report throughout the study:

Coastal Zone Requirements for EOS A/B - Final Report, Part I, TRW Systems Group for NASA/Langley Research Center, Contract No. NAS1-10280, February 4, 1971.

9. SUPPORTING MEASUREMENTS AND EXISTING DATA PROGRAMS

9.1 BACKGROUND

In the broadest sense, any environmental measurements from platforms other than EOS (which exceed EOS data in precision and accuracy, or address phenomena or aspects of phenomena which cannot be directly measured by EOS sensors) would be of potential utility as supporting measurements for EOS A/B. General categories of in situ measurements that would constitute valuable supporting information for ocean-oriented remote measurement programs are listed in Table 9-1.

Existing data sources should be relied upon wherever practical in order to reduce the need and associated high costs of new measurement capability. Future measurement programs planned by global ocean users should also be considered for possible supporting measurement contributions. Where there are identifiable measurement gaps, new programs should be instituted to ensure needed coverage.

Although it is the specific experiment which dictates the required ground truth measurement, it is the purpose of this section to examine all relevant existing and planned data sources and programs which could possibly contribute to such measurements. Measurement accuracy, frequency and time of day are important in determining whether to take advantage of data from other programs; when inadequate or not compatible, additional measurements must be made.

It is appropriate to consider measurement programs in terms of two primary categories: national programs and international programs. All relevant national measurement programs are accounted for in the Department of Commerce's (NOAA) Marine Environmental Prediction (MAREP) program. MAREP's charter is to integrate all federal marine environmental monitoring systems, to assess and improve

Table 9-1. Supporting Environmental Measurements

PHYSICAL OCEANOGRAPHY

CURRENT SPEED AND DIRECTION
 MASS TRANSPORT
 WATER MASS STABILITY
 WIND-DRIVEN AND THERMOHALINE CIRCULATION
 WATER TEMPERATURE
 WATER DENSITY
 PROPERTIES OF SEA ICE
 OPTICAL PROPERTIES OF WATER
 SEA AND SWELL DIRECTION, HEIGHT, PERIOD
 SOLAR RADIATION INTENSITY
 TIDAL AMPLITUDE AND FREQUENCY

CHEMICAL OCEANOGRAPHY

SALINITY
 DISSOLVED OXYGEN
 CO₂, CARBONATE, BICARBONATE CONTENT
 NUTRIENTS (NITRATES, PHOSPHATES, SILICATES)
 H₂S CONTENT
 TRACE ELEMENT CONTENT (INORGANIC MICRONUTRIENTS)
 pH
 OXIDATION-REDUCTION POTENTIAL
 CONDUCTIVITY
 CONCENTRATION OF SELECTED POLLUTANTS (DISSOLVED AND
 IN MARINE ORGANISMS)
 SOLUBLE ORGANIC MATTER CONTENT
 ORGANIC AND INORGANIC PARTICULATE CONTENT

BIOLOGICAL OCEANOGRAPHY

PRIMARY PRODUCTIVITY
 PHYTOPLANKTON STANDING CROP
 ZOOPLANKTON STANDING STOCK
 NEKTON STANDING STOCK
 TAXONOMIC DIVERSITY
 TROPHO-DYNAMIC INFORMATION
 LIFE HISTORY DATA ON IMPORTANT SPECIES
 SPECIES-SPECIFIC TOLERANCE LIMITS FOR
 ENVIRONMENTAL EXTREMES

MARINE GEOLOGY

SEDIMENTARY DEPOSITION AND EROSION RATES
 BOTTOM COMPOSITION
 BOTTOM TOPOGRAPHY
 TURBIDITY

METEOROLOGY

AIR TEMPERATURE
 SEA SURFACE TEMPERATURES
 ATMOSPHERIC MOISTURE CONTENT
 CLOUD COVER
 CLOUD CHARACTER
 PRECIPITATION (SNOW, RAIN, ICE)
 FOG AND SMOG DISTRIBUTION
 SURFACE AND HIGH-ALTITUDE WIND VECTOR
 ATMOSPHERIC VISIBILITY
 ATMOSPHERIC CONTENT OF SEA SPRAY AND SALT NUCLEI
 ATMOSPHERIC PRESSURE

these systems, and to provide better marine prediction and warning services. This includes analyzing and forecasting the physical, chemical, biological, and hydrodynamic conditions of the oceans, coastal zone waters, and Great Lakes plus the overlying atmosphere and their interaction. When fully implemented, the program will provide a basic service of data analyses and forecasts for use by government agencies and the general public. The basic service will utilize existing and future observational or monitoring networks, analysis and forecast centers, telecommunications services, and other federal facilities. In addition to the basic service provided, specialized users will benefit from specialized services for maritime navigation, for water pollution control, for fisheries interests, for mineral exploration, and for specialized military application.

Four interlocking systems -- data acquisition, data collection and relay, data processing and product formulation, and product and services dissemination -- comprise the MAREP system. Ultimately, the data

acquisition system will require an integrated mix of sensor platforms including satellites, aircraft, balloons, oceanographic ships, ocean station vessels, ships of opportunity, unmanned buoys, manned buoys, fixed ocean platforms, submersibles, and island and coastal stations. The MAREP systems concept is depicted in Figure 9-1.

According to the MAREP charter, all routine federal special and aperiodic marine environmental monitoring will be accounted for -- this includes broad ocean surveys as well as one-time federal research cruises. Since the majority of university research cruises are federally sponsored, for purposes of this discussion these can also be considered as components of MAREP.

MAREP programs which involve the acquisition and near-real-time dissemination of environmental data include, for example,

- The National Weather Service (NWS)
- The Fleet Numerical Weather Central (FNWC) Marine Analysis and Prediction Service
- The Marine Resources Monitoring, Assessment, and Prediction (MARMAP) program
- The National Data Buoy System (NDBS)
- The National Marine Fisheries Service (NMFS) Fish Advisory Programs
- The U. S. Coast Guard - Infrared Radiation Thermometer (USCG - IRT) Aircraft Surveys
- The Geochemical Ocean Sections Study (GEOSECS)^(*)

An important adjunct to the MAREP program is the Interagency Coordinating group (ICMAREP) composed of officials from each of the principal marine-related agencies who provide planning and guidance for the MAREP staff.

The meteorological counterpart to MAREP is the Federal Plan for Meteorological Services and Supporting Research (FPMSSR). The coordinating staff for FPMSSR, which is in the Office of the Federal Coordinator for

*The GEOSECS program, one of the International Decade of Ocean Exploration (IDOE) programs, is funded by NSF. Although IDOE is international in scope, the national role is reflected in the MAREP programs plans.

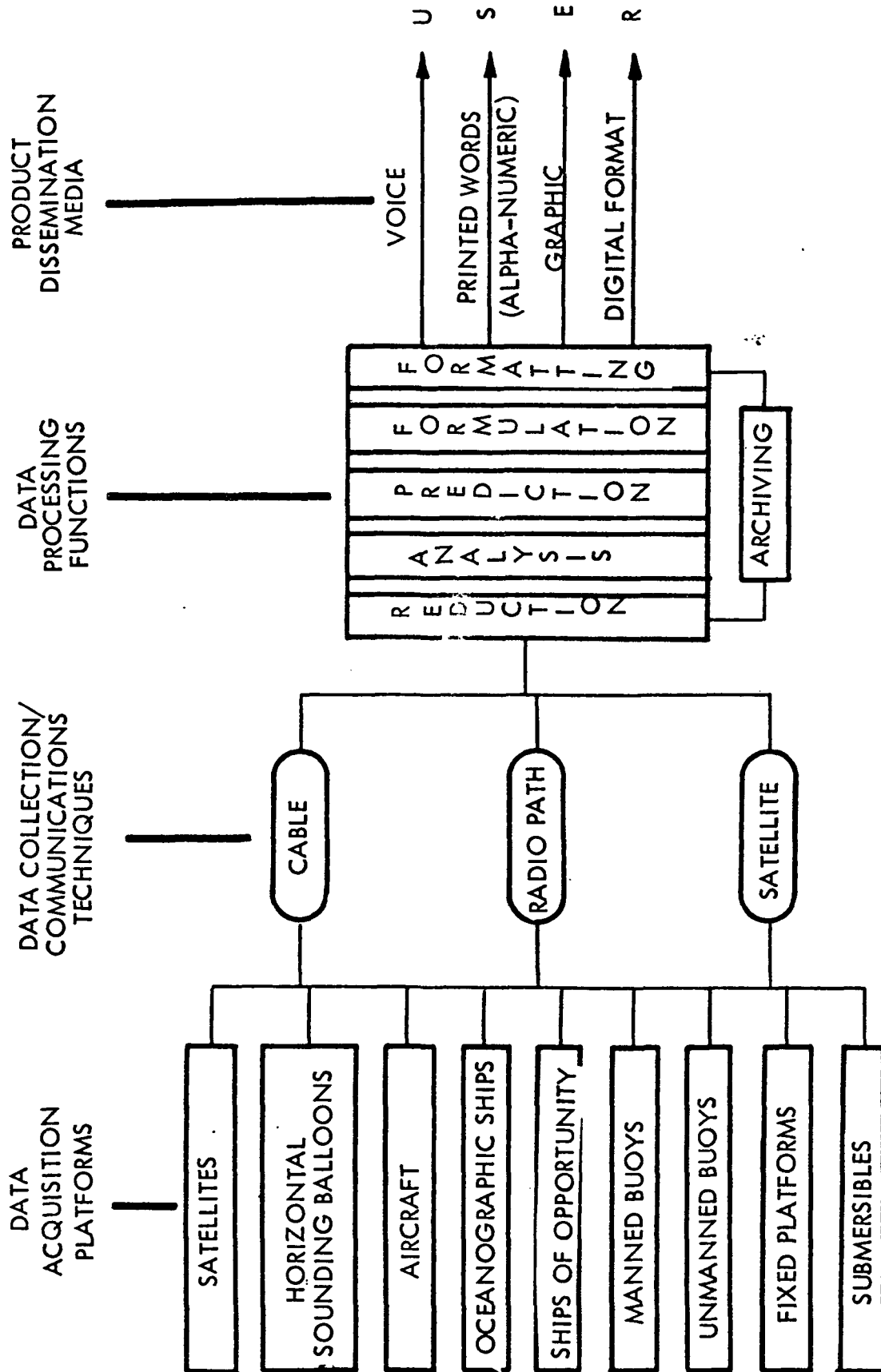


Figure 9-1. MAREP Systems Concept

Meteorology (OFCM), has cognizance over such meteorologically-oriented programs as Barbados Oceanographic and Meteorological Experiment (BOMEX). For obvious reasons, there is continuous interaction between the MAREP and OFCM staffs.

International programs are coordinated either through the World Meteorological Organization's (WMO), World Weather Watch (WWW), or the Intergovernmental Oceanographic Commission (IOC). Several projects are of interest for possible ground truth measurements:

- The Global Atmospheric Research Program (GARP)
- The Integrated Global Ocean Station System (IGOSS)

GARP is an outgrowth of a United Nations resolution that recommended the improvement of weather forecasting capability.⁽¹⁾ It was established as an international cooperative research effort aimed at increasing understanding of the general circulation of the atmosphere and laying the mathematical and physical basis for methods of long-range prediction. The ultimate goal is to predict accurately the atmospheric circulations on a global scale. It is hoped that this will lead to better prediction and eventual control of the weather through:

- Economically useful, long-range weather prediction
- Identification of consequences of inadvertent modifications of weather
- Identification of consequences of purposeful modifications of weather

In addition to traditional methods of gathering data, ocean drift platforms (approximately 700) and atmospheric balloon platforms (approximately 1000) will be employed to transmit randomly timed data signals which also provide information from which platform positions could be computed. Constant level "mother balloons" have been proposed to carry about 100 dropsondes to be released upon command and OMEGA will track the sondes for wind information. Polar orbiting spacecraft (other than or in addition to EOS) will also be used as well as aircraft, ships of opportunity and any other available data gathering programs. GARP initial data set accuracy is as follows:

- Component wind velocities $\pm 3 \text{ m/sec}^{-1}$
- Air temperature $\pm 1^\circ \text{ C}$
- Air pressure $\pm 0.5 \text{ mb}$
- Sea surface temperature $\pm 0.2^\circ \text{ C}$

The participants in the program include universities, industry and governmental agencies working mainly under associated national programs. In the long-term, the technology developed under GARP will be incorporated into the routine operation of the World Weather Watch (WWW) which is sponsored by the World Meteorological Organization (WMO).

GARP can provide EOS with ground truth from its many data gathering operations and experiments. The meteorological experiments such as BOMEX, TROPEX and FGGE (First GARP Global Experiment) should be particularly helpful. In addition to this type of experiments, there are planned GARP sub-programs which will furnish EOS with ground truth:

- Vertical atmospheric profiles with sounding rockets for atmospheric circulation studies
- Inflow and outflow of energy in polar regions
- Monsoon area studies
- Air mass transformations over the seas adjacent to continents.

EOS contributions to GARP would be to provide additional synoptic data for their experiment correlation. A primary objective of the GARP free drifting, floating data platforms is to provide a better knowledge of surface currents of the ocean and of momentum exchange between the sea and atmosphere. EOS can contribute to this surface current experiment.

IGOSS is contemplated as a worldwide system for observing the marine environment, communicating and processing the data, and disseminating the products in real-time for use by marine interests. IGOSS is an outgrowth of a joint WMO-IOC task group and will be closely related to and coordinated with the WWW program.

Data from international program measurements is disseminated through the world data centers which are closely tied to NOAA's Environmental Data Service (EDS). Thus, data will be readily available through the MAREP program.

9.2 RELEVANT DATA PROGRAMS

For supporting measurements planning purposes, it is essential to consider environmental data programs that will be in existence during the 1974-75 time frame. The programs meriting closest consideration may be grouped into four basic categories:

- routine data programs
- special operational data programs
- special experimental data programs
- aircraft support programs

In the sub-sections that follow, the programs falling under each of these categories will be examined in some detail. A listing of these programs and their estimated implementation schedules is given in Table 9-2.

9.2.1 Routine Data Programs

The charter of certain large environmental data programs is to acquire, process, and disseminate data products to a great variety of general users on a routine basis. Programs of this nature likely to significantly interact with EOS A/B include the National Weather Service, the Fleet Numerical Weather Central, and the National Data Buoy System.

9.2.1.1 National Weather Service (NWS)

NOAA is concerned with describing man's physical environment and predicting its physical state. Where this mission of NOAA relates to the atmosphere, it is the task of NWS, NOAA's weather bureau, to provide the nation's basic and specialized weather services and issue timely warning of impending atmospheric and hydrologic hazards.

As part of the World Weather Watch (WWW) being planned by the World Meteorological Organization (WMO), three World Meteorological Centers (WMC) have been established. They are in Moscow, Melbourne, and Washington, D. C. The WMC in Washington includes NOAA's National Environmental Satellite Center (collocated with NWS),

Table 9-2. Environmental Data Programs (71-76)

PROGRAM/ACTIVITY	CALENDAR YEAR					
	71	72	73	74	75	76
GARP			▲ TROPEX			
IGOSS						
NWS						
FNWC						
NDBS						
MARMAP						
NMFS FISHERY-ADVISORY PROGRAM						
GEOSECS						
AUTEC						
MTF (MISSISSIPPI TEST FACILITY)						
U.S. COAST GUARD A/C IRT PROGRAM						
NASA A/C REMOTE SENSING PROGRAM						

(OPERATIONAL)

(OPERATIONAL)

▲ EEP BUOYS ▲ LOW-CAPABILITY BUOYS ▲ PROTOTYPE NET

(OPERATIONAL)

▲ ATLANTIC PACIFIC

(OPERATIONAL)

▲ APPROX.

(OPERATIONAL)

(DEVELOPMENTAL)

▲ START INTERIM/DEVELOPMENT MODE
 ▲ START/END OPERATIONAL MODE

Environmental Data Service, and NWS. The National Environmental Satellite Center is linked directly with the Goddard Space Flight Center in Greenbelt, Maryland, and is thereby able to perform remote command and control functions with orbiting environmental satellites.

Every day, the NWS receives:

- 12,000 synoptic reports from surface stations
- 25,000 hourly synoptic aircraft reports
- 1,500 synoptic reports from ships at sea
- 1,500 upper-air reports
- 400 weather reconnaissance reports
- 2,500 detailed aircraft reports
- 500 radar reports
- 200 satellite photographs

These data are computer processed and analyzed each day on observations taken over the Northern Hemisphere at 0000 hours and 1200 hours GMT. Each computer cycle begins with a preliminary analysis, made after an hour and a half of collection over North America from the surface to 18,000 feet. The operational analysis is made after three and a half hours of collection, when 70 percent of all data has come in. This analysis describes ten levels of the atmosphere over the Northern Hemisphere from the surface to 53,000 feet. It is completed before the measurements are four hours old, and takes the computer half an hour.

Computer products are reproduced on curve followers, photographic systems, and a facsimile converter. Manual analyses are made for the surface, 18,000 feet, and 30,000 feet, as a check on the computer. These are also used to prepare data cards for ocean areas, where measurements are insufficient for accurate machine analysis. A final machine analysis is made once a day after ten hours of collection, when most information is in, and covers the Northern Hemisphere from the surface to 53,000 feet.

NWS's meteorologists are now preparing daily forecasts extending 72 hours into the future; forecasts out to a week ahead three times per week; and out to a month ahead twice per month. Long-range forecasts, based on numerical prediction techniques and broad-scale, simultaneous

observations, are prepared routinely for three-and five-day periods. Thirty-day forecasts are also prepared based on numerical and statistical techniques.

General area meteorological warnings and forecasts of wind, weather, visibility, and sea conditions when wave heights in excess of 8 feet are expected, are provided all maritime activities by Weather Service Offices on the Atlantic and Pacific Coasts. Forecasts and warnings are provided to commercial shipping, government and nongovernment research and survey vessels, recreational boating, commercial fishing vessels, sports fishermen and mineral exploration/production platforms. These forecasts cover a 24-hour period and are updated every six hours. Figure 9-2 shows areas of NWS shipping forecast and warning responsibilities.

Computer-produced ocean wave forecasts are now being transmitted from the Weather Bureau's National Meteorological Center for use in high seas weather broadcasts and to alert coastal forecasters to the possibility of dangerous breakers and surf. The new ocean wave forecasting program began 1 October 1968. The forecasts are based on surface wind predictions supplied by NWS's Six-Layer Primitive Equation Model. North Atlantic and North Pacific forecasts for 24 and 48 hours include significant height of wind waves (waves generated by the action of local winds on the water), swell (previously-generated wind waves which have propagated out of their generating area), and combined, or overall, wave height conditions.

In addition to providing these weather services, plans are to provide predictions of surface and subsurface temperatures, depth of the mixed layer, and currents for commercial fishing interests.

Each day, NWS transmits 450 facsimile charts and 200 teletypewriter messages, and distributes locally more than 2,500 copies of weather maps. Products flow out of NWS on the 40 teletypewriter circuits which bring the data in, and on a dozen facsimile circuits - circuits which transmit weather maps and computer-prepared photomosaics. In the United States alone, there are more than 1,000 facsimile receivers. Weather information goes to other nations and to ships at sea over international cable and radio links from coastal relay points. Radiofacsimile weather maps are transmitted daily by the NWS to mariners on the high seas in the North Atlantic. The maps cover almost the entire North Atlantic and include all major shipping lanes between the United States and Europe.

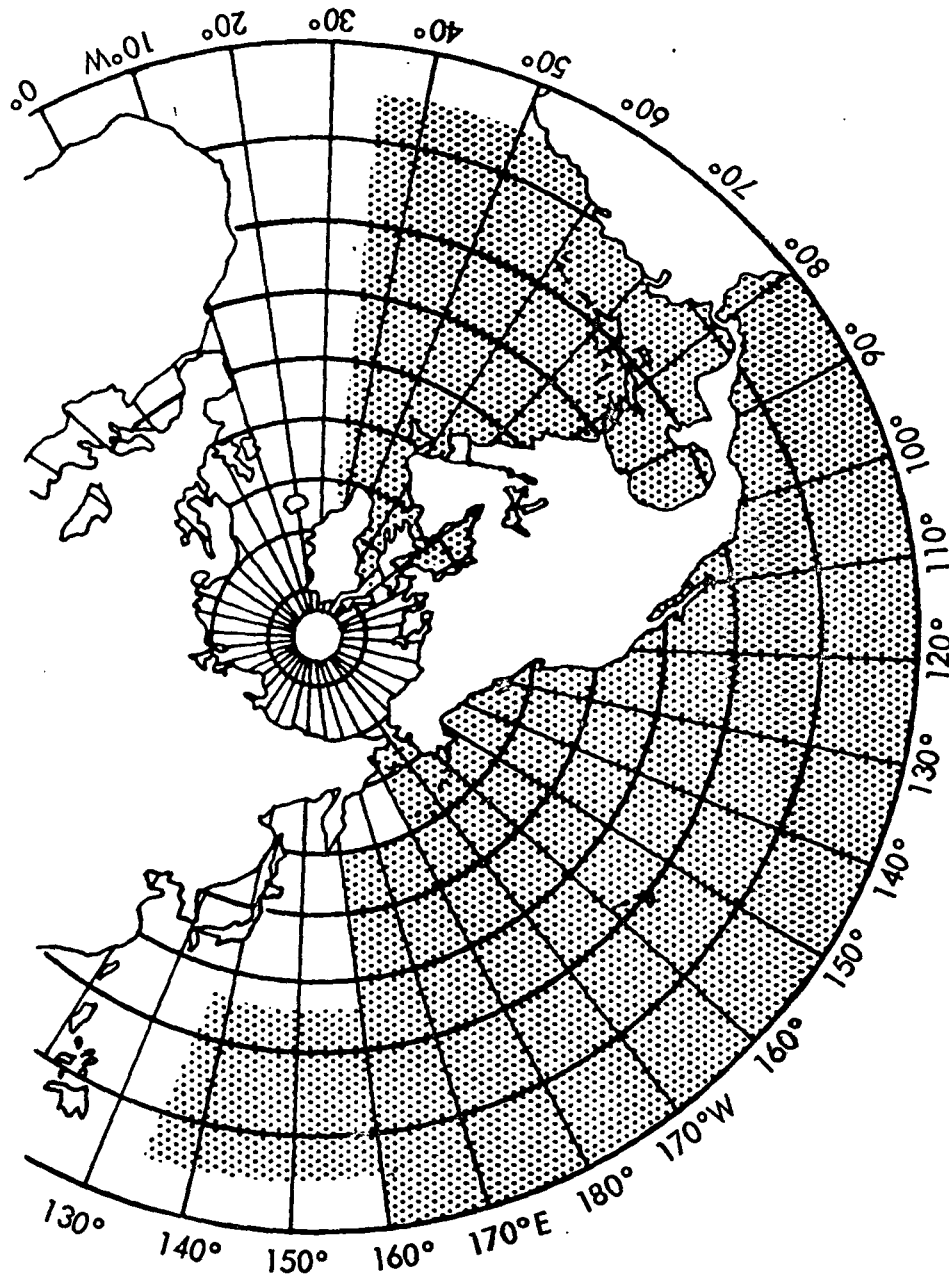


Figure 9-2. Areas of United States Responsibilities for Shipping Forecasts and Warnings Under International Agreements

Ocean and atmospheric processes are closely interrelated and hard to treat as separate systems. NWS information on weather conditions over ocean areas will add greatly to EOS environmental ground truth. The upper air and atmospheric observations are especially important for heat exchange processes. At present, there are insufficient ocean area measurements available to NWS for computer analysis.

EOS contributions to NWS on ocean area measurements in the form of surface wind speed and direction, sea state, surface temperature, and cloud patterns would help to narrow the gap of missing information.

9.2.1.2 Fleet Numerical Weather Central

The Fleet Numerical Weather Central, which operates under the auspices of the U. S. Naval Oceanographic Office (NAVOCEANO), is the largest of marine information systems. NAVOCEANO is responsible for developing oceanographic analysis and prediction techniques and applying them to naval operations on an experimental basis. As programs of proven utility are developed, they are transferred to the Naval Weather Service Command for application in operational forecasts. The Fleet Numerical Weather Central, located in Monterey, California, is the hub of a vital computer network established to process data for product formulation. Since 1962, activities of FNWC have centered around application of the techniques of synoptic meteorological analysis and numerical weather prediction to the analysis and forecasting of meteorological-oceanographic phenomena over the ocean areas of the Northern Hemisphere.

The facility uses an iterative engineering approach in refining data products to meet user requirements. Computer solutions of combined theoretical and empirical equations are continually applied to real-time data on new oceanographic variables. Then, steps are taken to improve the data base for these variables. Finally, the original empirical approximations and constants are replaced by more exact relations determined from data.

While a major function of FNWC is to upgrade environmental monitoring and predictive capability for military applications, important non-military environmental data programs benefit greatly from services provided by this facility. Basic categories of users of the kind of synoptic ocean analyses/predictions provided by FNWC are listed in Table 9-3.

Table 9-3 User Categories for FNWC Analyses/Forecasts

Users by Activity	Areas and Depths of Concern	Principal Use
Weather forecasting	Near coasts and open ocean Surface to bottom of thermocline	Weather forecasting over continents not possible without consideration of oceans
National security	Near coast and open ocean Surface to bottom	Naval operations and planning; surveillance, ASW (sound propagation)
Navigation	Open ocean and near coast Surface	Safety of navigation; ship routing
Fisheries	Near coast and open ocean Surface to 500m	Fish location; fishing operations and planning
Coast and beach users	Shallow water, coasts	Storm surge and pollution forecasts
Coastal engineering	Shallow water, coasts	Effect of ocean on structures
Oil drilling	Shallow water near coast	Safety of operation; pollution

Forecasts on the following synoptic parameters are developed routinely (every 12 hours) and disseminated among users:

- sea surface temperature
- wind waves (direction, period, height)
- combined sea (direction, period, height)
- ocean currents (stream function and transport)
- ocean-atmosphere heat exchange (total, latent and sensible)
- potential mixed layer depth (including transients)
- subsurface thermal structure (temperatures at any level)
- temperature versus depth profiles (for any ocean point)
- sound velocity versus depth profiles (for any ocean point)
- oceanic fronts
- underwater sound fields (ray trace plots and sound loss plots)

Previously the analyses and forecasts were restricted to the Northern Hemisphere. Recently, however, the coverage on some of these has been extended to 20°S. The accuracy of the forecasts is a function of the accuracies of the input meteorological forecasts. As general limits of the forecasting accuracy, the following values have been given: ⁽²⁾

- | | |
|-------------------------------------|------------------|
| ● sea surface temperature | 0.3 to 1.8°C |
| ● temperature below the thermocline | 0.3 to 1.3°C |
| ● mixed layer depth | 20 to 50 feet |
| ● wave height | 1.5 to 4 feet |
| ● current speed | 0.1 to 0.4 knots |
| ● current direction | 10 to 50° |

A variety of media are utilized to distribute the above products to the users. These include: fleet broadcast teletype, facsimile (FAX), digital data link, U. S. mail, and local hand delivery.

Major data sources which provide input to FNWC include merchant, military, and scientific ships, U. S. Coast Guard aircraft, buoys, and permanent ocean stations.

Permanent ocean stations provide some of the most comprehensive data inputted to FNWC. Observations are made and reported at 3 hour intervals on:

- dry bulb air temperature
- dew point temperature
- sea surface temperature
- air/sea temperature difference
- pressure at sea level
- surface wind direction and speed
- percent frequency of cloud types
- low cloud percent frequency
- height of lowest clouds
- precipitation amount
- visibility
- sea height, direction, period
- swell height, direction, period

Twice a day, rawinsondes are released to measure wind velocities aloft.

Permanent ocean stations are now located as follows:

November	30°N	140°W	} Pacific Ocean
Papa	50°N	145°W	
Victor	34°N	154°E	
Tango (during typhoon season)	29°N	135°E	
Delta	44°N	41°W	
Charlie	52°45'N	35°30'W	
Bravo	56.5°N	51°W	
—	39°N	74°W	
Alpha	62°N	33°W	
Echo	35°N	48°W	
India	59°N	19°W	
Juliet	52°30'N	20°W	
Kilo	45°N	16°W	
Mike	66°N	02°E	
—	39°N	74°W	

FNWC Data Base

The major impediment to improved forecasting capability is lack of sufficient data on two critical parameters: subsurface soundings (temperature versus depth), and upper atmosphere conditions. Specifically, subsurface soundings should be expanded to one sounding per water mass every two days to provide minimum data for air-ocean heat exchange analyses and predictions. The lack of synoptic subsurface observations precludes direct structural analysis and accordingly requires computation of oceanographic conditions from a knowledge of atmospheric conditions and boundary layer processes and the nature of their coupling to the ocean. Thus, a good portion of synoptic oceanographic analysis derives from concurrent atmospheric analysis. ⁽³⁾ This points up a critical immediate data need -- expanded data on the atmosphere, in particular the upper atmosphere. Principal investigators at FNWC strongly recommend that priorities for expenditures among environmental data programs be reordered to encourage new developments which will provide expanded data in conventional radiosonde format - the present coverage simply is not adequate. Figure 9-3 illustrates the discrepancy between the existing and recommended upper atmosphere network for Northern Hemisphere winter.

The primary FNWC data source is represented by reporting vessels at sea. There are some 5,000 of these in the Northern Hemisphere. The system suffers because vessel observations are not distributed evenly in time and space over all ocean areas. The most accurate and comprehensive data is provided by scientific ships, a representative distribution of which is depicted in Figure 9-4. The scarcity of ship activities in the Southern Hemisphere is particularly noteworthy. Figures 9-5 and 9-6 show a typical distribution of vessel reports for two synoptic hours. Another problem is that of communications. Reception of radioed reports from certain isolated areas is often quite poor. This problem may eventually be remedied by data relay satellites. Navigational satellites may also be of great value eventually. FNWC now uses a data resolution of 25 km for small-scale analyses, and this may be adequate to meet most user needs. However, an ideal goal would be about 5 km resolution. It is at about this resolution that navigational uncertainties enter the picture.

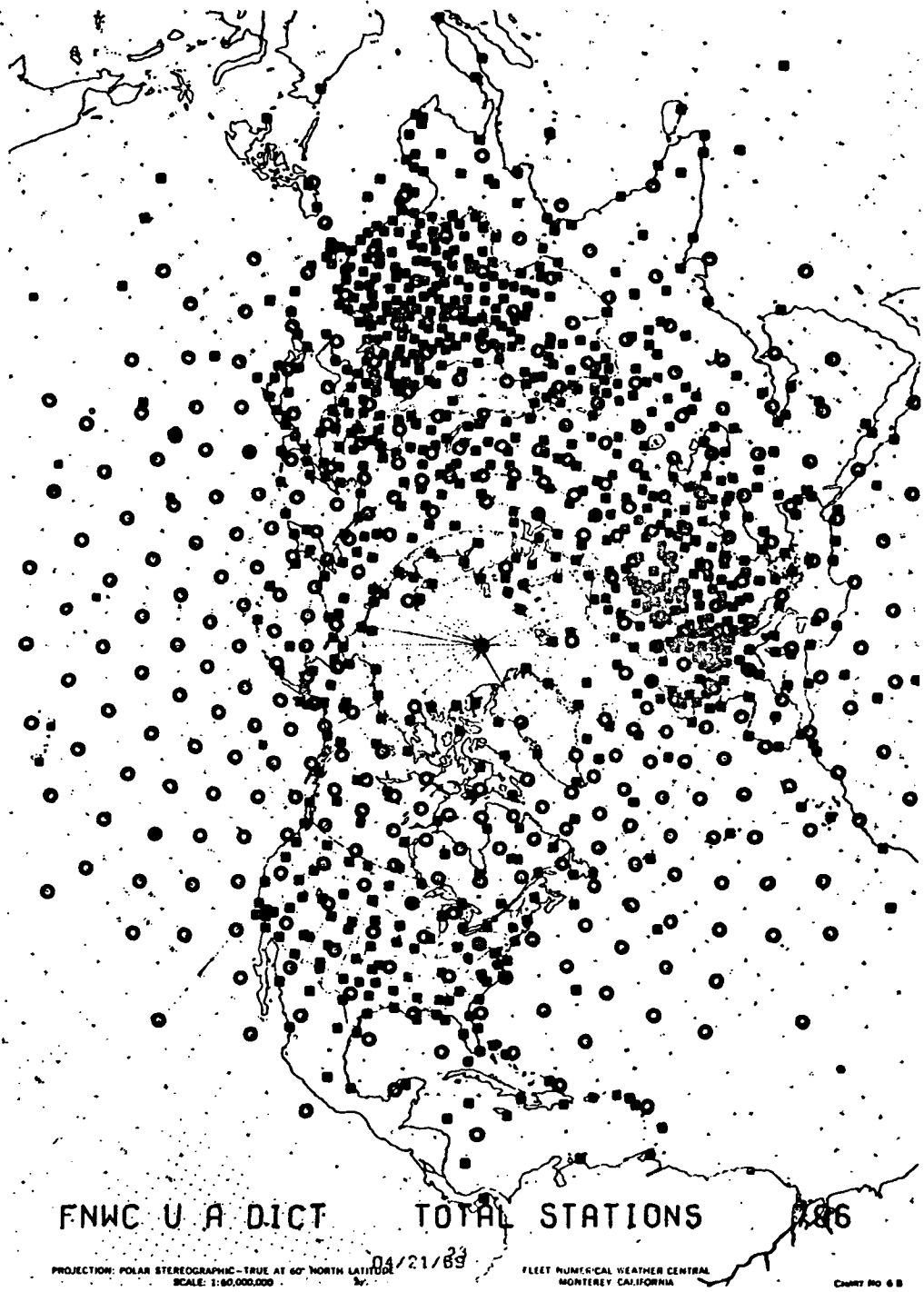
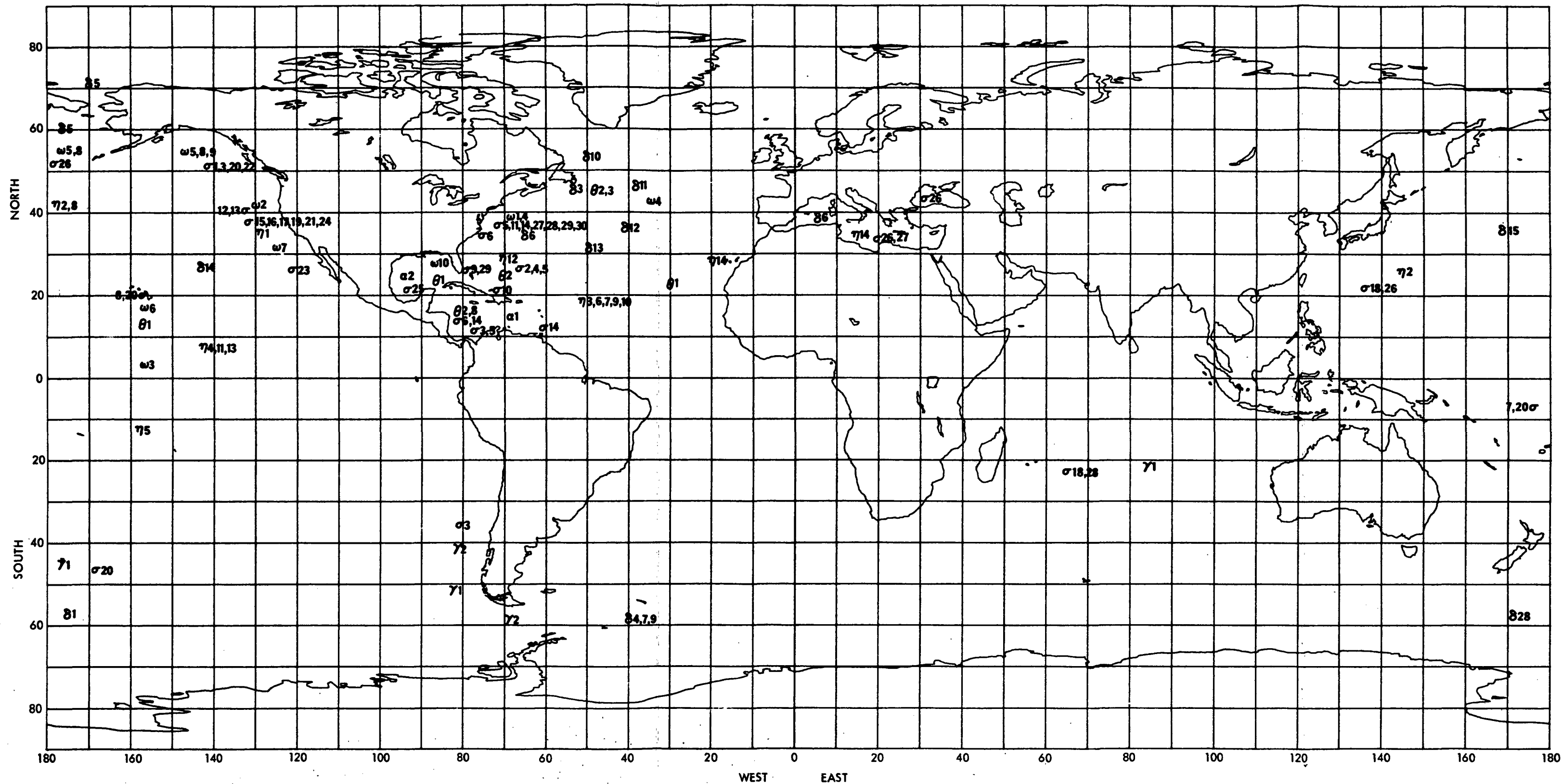


Figure 9-3 Existing Upper-Air Network (Squares) Compared With Recommended Coverage for Winter (Circles), (from Wolff⁴)

Page intentionally left blank



- α DEPARTMENT OF COMMERCE, ESSA**
- 1. DISCOVERER
- 2. PEIRCE
- ω DEPARTMENT OF THE INTERIOR, NMFS**
- 1. ALBATROSS IV
- 2. JOHN N. COBB
- 3. TOWNSEND CROMWELL
- 4. DELAWARE II
- 5. MILLER FREEMAN
- 6. CHARLES H. GILBERT
- 7. DAVID STARR JORDAN
- 8. GEORGE B. KELEZ
- 9. R/V OREGON
- 10. R/V OREGON II
- γ NATIONAL SCIENCE FOUNDATION**
- 1. ELTANIN
- 2. HERO
- 8 U. S. COAST GUARD**
- 1. USCGC BURTON ISLAND
- 2. USCGC EDISTO
- 3. USCGC EVERGREEN
- 4. USCGC GLACIER
- 5. USCGC NORTHWIND
- 6. USCGC ROCKAWAY
- 7. USCGC SOUTHWIND
- 8. USCGC STATEN ISLAND
- 9. USCGC WESTWIND
- 10. OCEAN STATION BRAVO
- 11. OCEAN STATION CHARLIE
- 12. OCEAN STATION DELTA
- 13. OCEAN STATION ECHO
- 14. OCEAN STATION NOVEMBER
- 15. OCEAN STATION VICTOR
- η U. S. NAVAL OCEANOGRAPHIC OFFICE**
- 1. USNS BARTLETT
- 2. USNS SILAS BENT
- 3. USNS BOWDITCH
- 4. USNS CHAUVENET
- 5. USNS DE STEIGUER
- 6. USNS DUTTON
- 7. USNS HARKNESS
- 8. R/V F. V. HUNT
- 9. USNS ELISHA KANE
- 10. USNS SGT G. D. KEATHLEY
- 11. USNS KELLAR
- 12. USNS LYNCH
- 13. USNS MICHELSON
- 14. USNS SANDS
- θ U. S. NAVAL RESEARCH LABORATORY**
- 1. USNS GIBBS
- 2. USNS MISSION CAPISTRANO
- 3. USNS MIZAR
- σ UNIVERSITIES AND OTHERS**
- 1. ACONA
- 2. PANULIRUS II
- 3. ROBERT D. CONRAD
- 4. SIR HORACE LAMB
- 5. VEMA
- 6. R/V EASTWARD
- 7. M/V MAHI
- 8. R/V TERITU
- 9. GERDA
- 10. JOHN E. PILLSBURY
- 11. R. V. KYMA
- 12. R/V CAYUSE
- 13. R/V YAQUINA
- 14. TRIDENT
- 15. ALEXANDER AGASSIZ
- 16. ALPHA HELIX
- 17. ELLEN B. SCRIPPS
- 18. MELVILLE
- 19. OCONOSTOTA
- 20. WASHINGTON
- 21. VALERO IV
- 22. PROTEUS
- 23. ALASKA
- 24. N. B. SCOLFIELD
- 25. ALAMINOS
- 26. THOMAS G. THOMPSON
- 27. ATLANTIS II
- 28. R/V CHAIN
- 29. R/V GOSNOLD
- 30. R/V KNORR
- U. OF ALASKA
- BERMUDA BIOLOGICAL STATION
- COLUMBIA UNIVERSITY
- COLUMBIA UNIVERSITY
- COLUMBIA UNIVERSITY
- DUKE UNIVERSITY
- U. OF HAWAII
- U. OF HAWAII
- U. OF MIAMI
- U. OF MIAMI
- NEW YORK UNIVERSITY
- OREGON STATE UNIVERSITY
- OREGON STATE UNIVERSITY
- U. OF RHODE ISLAND
- SCRIPPS
- U. OF SOUTHERN CALIFORNIA
- STANFORD UNIVERSITY
- STATE OF CALIFORNIA
- STATE OF CALIFORNIA
- TEXAS A&M UNIVERSITY
- U. OF WASHINGTON
- WOODS HOLE
- WOODS HOLE
- WOODS HOLE
- WOODS HOLE

Figure 9-4 Oceanographic Ship Operations, March 1970 - September 1970

Page intentionally left blank



Figure 9-5 Synoptic Ship Coverage Received at FNWC for 00 GMT.
29 December 1969 (from Wolff⁴)

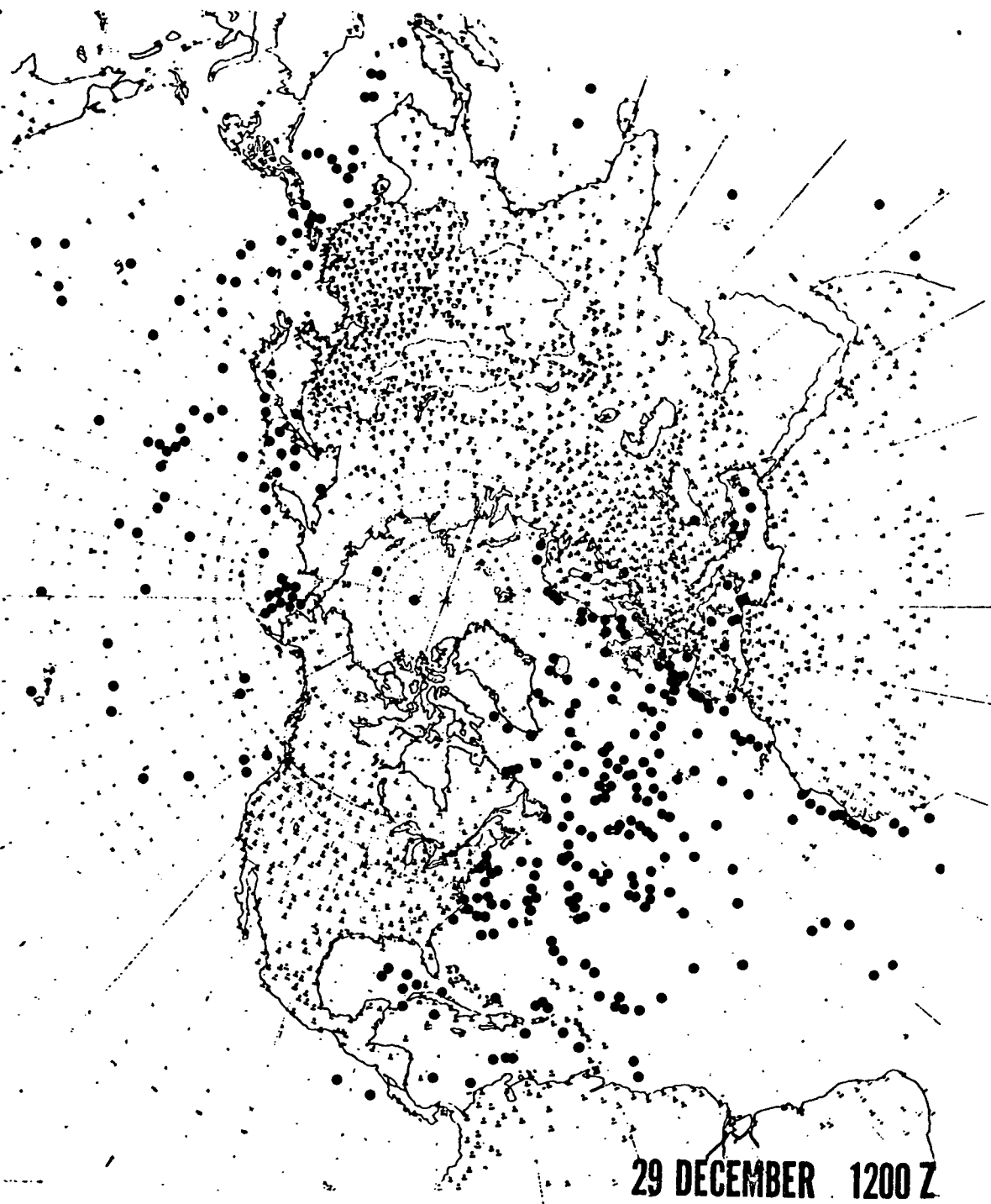


Figure 9-6 Synoptic Ship Coverage Received at FNWC for 12 GMT, 29 December 1969 (from Wolff⁴)

The quantity of sea surface temperature (SST) data that enters the FNWC system, while adequate for many applications, could stand improvement -- especially for the Southern Hemisphere. Although about 1200 SST reports are available every 12 hours from the Northern Hemisphere, this quantity is insufficient for effective synoptic analysis, requiring that data for each 12-hour analysis be accumulated over a 3 1/2-day period. Since SST changes are not exceptionally abrupt in most locations, being on the order of 0.3°C or less in 12 hours over major parts of the oceans (near sharp current boundaries, however, changes may be as great as 4°C in 12 hours)⁽²⁾, it is feasible to retain 3 1/2 days' data in the analysis.⁽⁴⁾ Quality of the SST data input to FNWC, most of which is represented by ship engine room injection temperatures, is relatively poor, being accurate to approximately ±1°C.⁽²⁾ In general, accuracies approaching ±0.1°C would be desirable for most applications -- ambient thermal noise in the sea surface is approximately of the order of ±0.1°C.⁽⁴⁾ For the scientist investigating first principles, desired accuracy would be as great as ±0.05°C.

Data on cloud patterns is of limited value to FNWC at the present time. For predictive purposes, clouds are analyzed at three layers mainly for computation of insolation. However, cloud cover is computed rather than ascertained from imagery. The accuracy of sea and swell observations is notoriously poor, primarily owing to a lack of objective measurement technique. Single observations, the most reliable of which originate from weather ships, are used for verification. Unfortunately, verification errors may be as high as observation errors (standard errors of 0.3 m and 6.0 m for wave heights of 1.5 m and 6.0 m, respectively; standard error in wave direction of 10° to 13°; standard error in wave period of 1.8 seconds). According to Wolff⁽⁴⁾ this implies that "further improvement of models requires either a drastic improvement of the accuracy of wave observations, or an improvement of the computation and forecasting of surface wind over the sea, or both."

The EOS program and the FNWC program would be likely to interact in a number of beneficial ways. Many of the elements contributing to the FNWC data grid which acquire high quality data would represent EOS calibration sources and would provide valuable ground truth data to aid in

interpretation of EOS sensor output. Furthermore, the FNWC program would provide information useful in delineating critical areas requiring greater temporal or spatial data density. On the other hand, the synoptic contribution of surface observations from EOS -- especially temperature and sea state -- would be expected to reduce much of the uncertainty involved in interpolating isopleths between widely-separated observations.

FNWC Future Plans and Developments

Included among FNWC's anticipated future developments is expanded use of expendible oceanographic instrumentation - particularly the XBT. Further plans, as excerpted from the Federal Planning Guide for MAREP, ⁽⁵⁾ are as follows:

Oceanographic sensors are being developed that use miniaturized modular design with digital and/or analog output to facilitate data handling with EDP methods. Insofar as is practicable, the concept is to provide a flow of information-- from oceanographic observation to computer to forecast product (with transformation to tactical indices) to user-- that is untouched by hand, but originating from a system with a "manual override" capability. Additionally, the Navy is striving to develop new programs to provide completely computerized products that are tailored to the needs of Operating Forces.

A comprehensive ocean-air-space synoptic environmental measuring system is envisioned for the time frame 1972-1977. This system will include improved satellite readout interpretation, more instrumented aircraft to provide better control in data collection and to improve density of observations, and an ocean buoy system.

The total system requirements envision: manned and unmanned platforms with accompanying local and remote sensors; facilities to collect, process, disseminate, and display ocean/air data; and a means to provide conversion factors to integrate ocean/air data into command and control systems. The state-of-the-art of ocean/air data gathering will be thoroughly examined to ensure that the development of hardware and techniques meet future requirements, and to ensure an orderly progression from exploratory development to operational use.

The key to better forecasting of oceanic conditions may well depend, as meteorological forecasting has, upon a better understanding of the circulation. Heat budget information, now largely unavailable, will be of considerable value in predicting large-scale patterns for an entire hemisphere.

9.2.1.3 National Data Buoy System

The National Data Buoy System (NDBS) is currently under development by NOAA. The mission of NDBS is to gather and report environmental information from global ocean regions on a real-time, scheduled basis using unmanned instrumented buoys. The data will be transmitted via radio communications links to shore stations for dissemination to users in near real-time.

The NDBS long range development plan ⁽⁶⁾ calls for the eventual deployment of an operational network of 150 high-capability buoys and an unspecified number of both drifting and moored low capability buoys in the 1980-81 time frame. The intermediate stages leading to the operational buoy system include the deployment of ten engineering experimental phase (EEP) buoys by late 1971, about 30 preprototype low-capability buoys by mid-1972, and a prototype net of about 35 buoys by mid-1977. The EEP buoys, which will be updated with new components and equipment as they become available, will be located in the Gulf of Mexico. Low capability buoys will be located between 20 and 60 degrees north latitude, being moored up to 400 nautical miles off shore from the North American coastline, with drifting buoys in the Western Atlantic and Eastern Pacific Oceans and in the Gulf of Mexico. The eventual high-capability operational buoys system will cover the Western Atlantic and Eastern Pacific ocean regions between the equator and 60 degrees north latitude, with the possibility of future expanded deployment as the program proceeds. Typical buoy spacing ranges from 100 nautical miles in the coastal North American waters (400 miles off shore) to 500 nautical miles in the deep ocean.

The high capability buoys, including the developmental models, are to make extensive meteorological and oceanographic measurements as shown in Table 9-4. Synoptic observations are to be made every three hours by the coastal buoys and every six hours by the deep ocean buoys. Provisions will also be made to permit shorter observation intervals down to one hour, being initiated either by command from shore or under prespecified environmental conditions. All measured data shall be screened for accuracy, formatted, and made ready for transmission to the users within one hour of the synoptic measurement time.

Table 9-4 Measurement Requirements - High-Capability Buoy System

PARAMETER	UNITS	RANGE	ALLOWABLE ERRORS (rms)		SAMPLING DURATION (MINUTES)	LEVELS
			DESIGN GOAL	INITIALLY ACCEPTABLE		
AIR-SEA INTERFACE TO 15 METERS ALTITUDE:						
INSOLATION	ly/min	0 TO 2	0.02	0.05	10	1 LEVEL, NOT SPECIFIED
PRECIPITATION RATE	cm/hr	0 TO 20	0.025 OR 1%**	***	60	1 LEVEL, NOT SPECIFIED
AIR TEMPERATURE	°C	-10 TO 40	0.1	0.5	10	5, 10, 15 METERS
AIR PRESSURE	mb	900 TO 1100	0.1	1.0	10	10 METERS
DEW POINT	°C	-10 TO 40	0.2	0.5	10	10 METERS
WIND SPEED	m/sec	0 TO 80	0.25 OR 3%**	0.5 OR 5%**	15	5, 10, 15 METERS
WIND DIRECTION	degrees	0 TO 360	2.0	5.0	15	5, 10, 15 METERS
VISIBILITY*	km	0 TO 20	0.5 OR 10%**	1.0 OR 15%**	10	1 LEVEL, NOT SPECIFIED
AIR-SEA INTERFACE TO 10 METERS DEPTH:						
WATER TEMPERATURE	°C	-2 TO 40	0.1	0.5	30	1 METER
WAVE DIRECTION	degrees	0 TO 360	5.0	-	10	1 LEVEL, NOT SPECIFIED
WAVE HEIGHT	meters	0 TO 30	0.5	-	10	1 LEVEL, NOT SPECIFIED
WAVE PERIOD	sec	2 TO 40	0.1	0.5	10	1 LEVEL, NOT SPECIFIED
SALINITY	0/00	20 TO 40	0.01	0.05	10	1 METER
CURRENT SPEED	m/sec	0.1 TO 3.0	0.1	-	10	2 METERS
CURRENT DIRECTION	degrees	0 TO 360	5.0	10.0	10	2 METERS
*SECONDARY PARAMETER						
**WHICHEVER IS LARGER						
***YES OR NO INDICATION ACCEPTABLE						
PARAMETER	UNITS	RANGE	ALLOWABLE ERRORS (rms)		SAMPLING DURATION (MINUTES)	LEVELS
			DESIGN GOAL	INITIALLY ACCEPTABLE		
10 TO 500 METERS DEPTH:						
WATER TEMPERATURE	°C	-2 TO 35	0.01	0.1	30	12 (LAPSO)***
SALINITY	0/00	20 TO 40	0.01	0.3	10	12 (LAPSO)***
CURRENT SPEED	m/sec	0.1 TO 3	0.05	0.1	10	12 (LAPSO)***
CURRENT DIRECTION	degrees	0 TO 360	5.0	10.0	10	12 (LAPSO)***
WATER PRESSURE	kg/cm ²	0.5 TO 55	0.5	-	10	12 (LAPSO)***
SOUND SPEED	m/sec	1410 TO 1580	0.3	-	10	12 (LAPSO)***
AMBIENT LIGHT*	ly/min	0 TO 0.3	0.01 OR 5%**	-	10	10, 100 METERS
AMBIENT NOISE*	db	-80 TO -20	3.0	-	10	10, 100 METERS
TRANSPARENCY*	%/m	0 TO 70	2.0	-	10	10, 100 METERS

*SECONDARY PARAMETERS

**WHICHEVER IS LARGER

***INTERNATIONAL ASSOCIATION OF PHYSICAL SCIENTISTS IN OCEANOGRAPHY (LAPSO) LEVELS:
10, 20, 30, 50, 75, 100, 150, 200, 250, 300, 400, AND 500 METERS

The low capability buoys are to make the synoptic measurements shown in Table 9-5 four times a day with no provision for additional observations. Data shall be ready for transmission to users as soon after the observation as possible.

Although only limited buoy deployment is planned during the EOS A/B time frame, those coastal regions in which the buoy prototypes will be operating should be excellent ground truth sites. In particular, both high and low capability buoy prototypes will be operating in the Gulf of Mexico for several years prior to, as well as during, the EOS A/B time frame. The prior detailed observations of environmental phenomena in this area, as well as the buoy measurements taken concurrently with EOS A/B operation will provide extensive ground truth data for the interpretation and identification of satellite-observed phenomena.

Table 9-5. Measurement Requirements - Low-Capability Buoy System

MOORED BUOY	DRIFTING BUOY	PARAMETER	UNITS	RANGE	ALLOWABLE ERRORS (rms)	LEVELS
X	X	AIR TEMPERATURE	°C	-10 TO 40	0.5	AIR-SEA INTERFACE
X	X	AIR PRESSURE	mb	900 TO 1100	1.0	—
X	X	WATER TEMPERATURE	°C	-2 TO 40	0.2	—
X	X	WIND SPEED*	m/sec	0 TO 80	1.0 OR 5%**	—
X	X	WIND DIRECTION*	DEGREES	0 TO 360	5.0	—
X	—	WATER TEMPERATURE	°C	-2 TO 35	0.1	10, 20, 50, 100, 200 METERS
X	—	WATER PRESSURE	kg/cm ²	15 TO 23	0.5	200 METERS

*SECONDARY PARAMETERS
**WHICHEVER IS LARGER

9.2.2 Special Operational Data Programs

A number of large environmental data programs serve a specialized user community. Examples of such programs with which EOS A/B might interact in especially beneficial ways include the MARMAP program of National Marine Fisheries Service and the Geochemical Ocean Sections Study.

9. 2. 2. 1 Marine Resources Monitoring Assessment and Prediction (MARMAP) Program

The MARMAP Program is currently in the planning and development stage. The overall objectives of the program⁽⁷⁾ are to:

- Develop techniques for obtaining accurate measures of the abundance and geographic distribution of living marine resources available to the United States.
- Monitor seasonal and annual fluctuations in the distribution and abundance of the various life stages of pelagic and demersal fishery resources and relate them to environmental factors and exploitation by man.
- Assess the productive capacity of these resources on a sustained yield basis and develop models for predicting future yields.
- Establish a comprehensive description of the marine ecosystem in terms of the distribution, composition, and interrelationship of biological communities.

Achievement of these objectives is to be accomplished under the MARMAP Program by development of an integrated national system for acquisition, compilation, analysis, and dissemination of information on the resource populations and their environment.

The basic data acquisition function will consist of large-scale quantitative ocean surveys for monitoring the abundance, composition, and distribution of the principal biological communities, as well as concurrent monitoring of the physical environment. NMFS vessels will be utilized as the primary survey platform for obtaining the biological information, although ships of opportunity will also be employed. Other types of platforms such as buoys, aircraft, and land and island stations will be incorporated as part of the MARMAP data acquisition capability in ocean regions where detailed supplementary environmental data is required.

Biological processes will be studied in detail by small scale, high intensity "zoom" surveys or experiments. This type survey effort would be concentrated in specific ocean regions and would only be performed for a limited time period as opposed to the broad scale, continuous surveys. These surveys will be defined as the need arises and are not detailed in the current MARMAP planning document.

The continuous ocean surveys of MARMAP involve the sampling of three kinds of biological communities: Survey 1 - ichthyoplankton (i. e., fish eggs and larvae), Survey 2 - demersal fish and benthic invertebrate communities, and Survey 3 - harvestable pelagic fishes. These surveys will initially be concentrated in those areas where a limited base of biological and environmental knowledge is available and eventually will be expanded into areas for which little or no information is available. As shown in Figure 9-7, the most intensive sampling (up to six surveys per year) of all three types of communities would be conducted in the waters over the continental shelves and slopes adjacent to the United States. Less intensive surveys (up to four surveys per year) would be done on plankton and pelagic communities and environmental factors adjacent to these intensive sampling areas. Interim operational surveys are to begin in mid-1972 with full scale operational surveys scheduled by mid-1975.

The preliminary requirements for taking concurrent environmental measurements at survey stations are shown in Table 9-6, while continuous measurements to be taken along the vessel cruise track are shown in Table 9-7. The preliminary Survey One plan calls for cruise tracks orientated perpendicular to the coastline at intervals of approximately 100 to 200 miles. The data stations are to be spaced at approximately 30-mile intervals along the cruise tracks. The preliminary Survey Two plan has not yet been established although a more closely spaced sampling grid will be necessary. Survey Three requires a continuous sampling technique (such as sonar) which will probably be incorporated with Survey One.

In addition to the survey vessel measurements, the other data platforms mentioned previously will be incorporated as part of the MARMAP Program to obtain data of higher temporal or spatial frequency in certain ocean regions. The following data is of primary interest:

- current speed and direction
- runoff information
- rainfall
- wind speed and direction
- sea level
- chlorophyll
- sea surface temperature

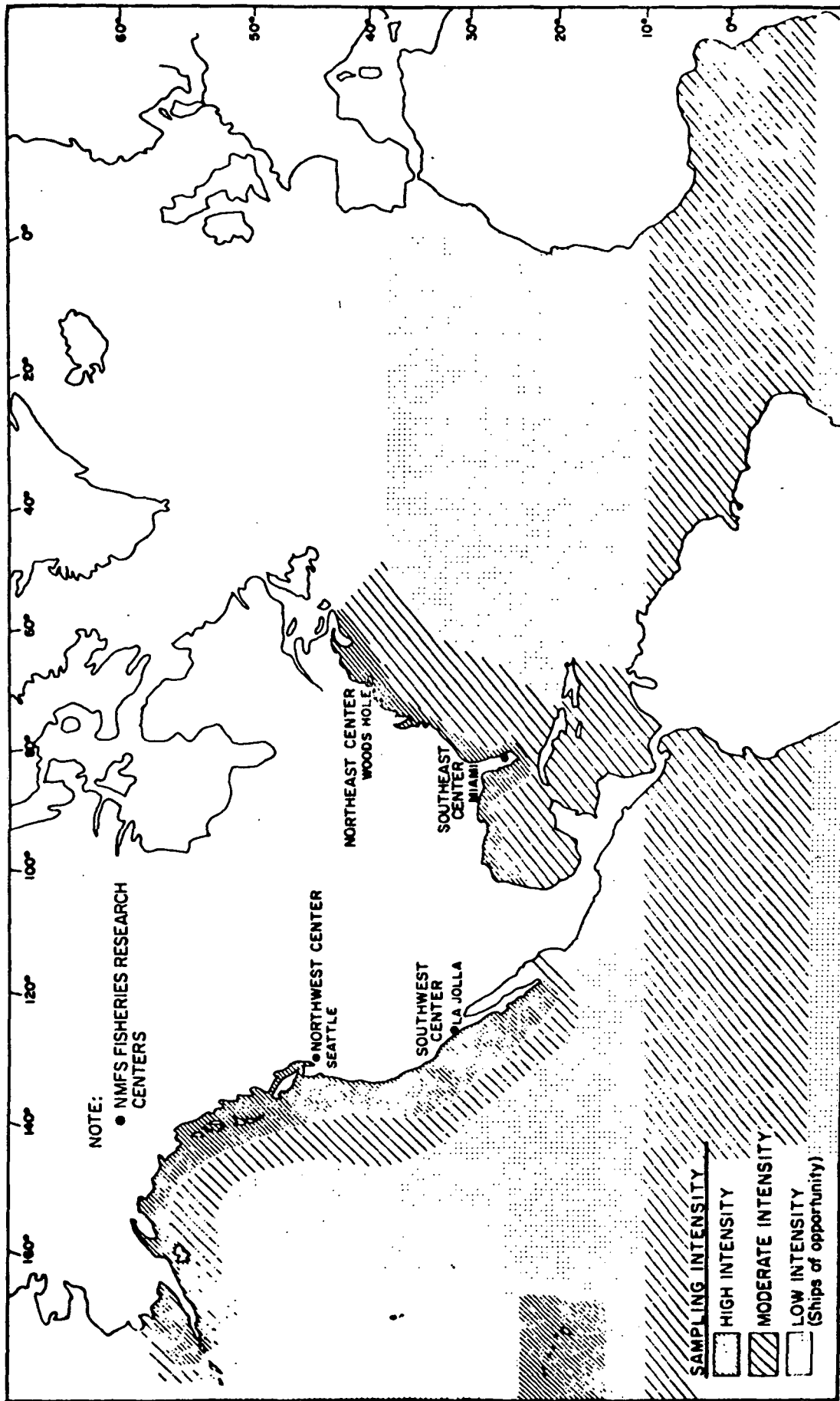


Figure 9-7. MARMAP Survey Area

Table 9-6. Environmental Measurements at MARMAP Survey Stations

VARIABLE MEASURED	SAMPLING TECHNIQUE	MAXIMUM DEPTH (METERS)
TEMPERATURE SALINITY	STD CAST STD CAST AND ROSETTE WATER SAMPLER (1)	1500 1500
OXYGEN	SAMPLER AND (IF AVAILABLE) A CONTINUOUS TRACE OXYGEN SENSOR ON THE STD UNIT.	1500
NUTRIENTS (1) NITRATES (2) PHOSPHATES (3) SILICATES (4) AMMONIA	ROSETTE WATER SAMPLER (2)	300
OPTICAL PROPERTIES (1) BEAM ATTENUATION (2) DIFFUSE ATTENUATION	COMBINED CAST WITH TRANSMISSOMETER IRRADIANCE METER	250
CURRENT SPEED AND DIRECTION	IMPRACTICAL ON SURVEY OPERATIONS (EXCEPT AS DETERMINED FROM SHIP- DRAFT WITH PROPER NAVIGATION)	-
BOTTOM DEPTH	ECHOSOUNDER	?

1. THE ROSETTE SAMPLER ATTACHED ON LINE WITH THE STD UNIT SHOULD BE A STANDARD EQUIPMENT TO ALLOW THE COMBINATION OF: (1) THE DETAIL FROM CONTINUOUS VERTICAL PROFILES BY THE STD, (2) THE ACCURACY OF NANSEN CAST DETERMINATIONS AND, (3) THE POSSIBILITY OF CALIBRATING A STD AT EVERY STATION.
2. WATER SAMPLES CAN BE DRAWN FOR DISSOLVED OXYGEN AND NUTRIENT DETERMINATIONS FROM THE NISKIN BOTTLES OF THE ROSETTE SAMPLER. NANSEN CASTS ARE THE ALTERNATIVE SAMPLING METHOD, WHICH WOULD REQUIRE AN ADDITIONAL 45 MINUTES PER STATION.

The two Environmental Data Centers (Pacific and Atlantic) to be established under the MARMAP Program will serve as the coordinator for the collection, analysis, and dissemination of all biological and environmental data from MARMAP-dedicated platforms as well as that obtained from external data resources. These centers should serve as the focal point for an EOS A/B - MARMAP interface, providing valuable

Table 9-7. Environmental Measurements Made Underway and Continuously Along MARMAP Survey Cruise Tracks

VARIABLE MEASURED	MEASUREMENT/FREQUENCY	STANDARD SAMPLING TECHNIQUE
SURFACE TEMPERATURE SALINITY	CONTINUOUS	THERMO OR FREQUENT SAMPLING (1)
INSOLATION	CONTINUOUS	PYRAHELIOMETER
SURFACE CHLOROPHYLL	CONTINUOUS	FLUOROMETER
SURFACE NUTRIENTS	CONTINUOUS	AUTOANALYZER (2)
BATHYTHERMOGRAPH	UNDERWAY AT ABOUT A 30 NAUTICAL MILE SPACING BETWEEN, BUT NOT AT STANDARD STATIONS	MECHANICAL OR EXPENDABLE BT
WEATHER AND SEA STATE	AT BATHYTHERMOGRAPH AND STANDARD STATIONS	STANDARD EQUIPMENT (3)
OCCURRENCE OF FISH SCHOOLS, BIRD FLOCKS, AND MAMMALS	CONTINUOUS	SHIP'S WATCH
BOTTOM DEPTH	CONTINUOUS	ECHOSOUNDER

1. THE RECORDING THERMOSALINOGRAPH SHOULD BE EQUIPPED WITH AN ANALOG OUTPUT, OR AN ALARM SYSTEM FOR MAJOR CHANGES (FRONTS, ANOMALIES, ETC.).
2. DESIRABLE TO HAVE CERTAIN VESSELS SO EQUIPPED.
3. ANEMOMETER AND WET BULB/DRY BULB SENSOR HEIGHT SHOULD BE INCLUDED IN REPORT.

ground truth information and a historical data base for EOS A/B and high spatial and temporal frequency environmental data coverage for MARMAP. The MARMAP Program is compatible with EOS A/B in terms of regions of coverage. Further, the EOS A/B data obtained on a frequent basis will complement the detailed low frequency measurements to be made by the MARMAP Program.

9.2.2.2 Fishery Advisory Services

A small number of advisory services have been set up on an experimental or pilot basis for certain United States fisheries. Their function is to prepare forecasts of fishing conditions for the benefit of the individual fisherman. Domestic forecasting services, which are largely empirical in nature, contrast with the advanced and vital forecasting programs supported by more aggressive fishing nations, notably Japan. Japan is vitally dependent upon the sea for food, and her high seas fishing industry is government-operated. All elements cooperate in reporting environmental and fishing information in real time to the forecasting agency. The United States fishing industry, on the other hand, is comprised of a competitive system of "rugged individuals". A vessel captain will guard very closely any strategies he may develop or any information he may have acquired on optimal fishing areas rather than share such information with fellow fishermen. Under these circumstances, it appears that the most direct way in which the U. S. government can aid the domestic fisherman is by promoting services that will supply him with environmental and stock location and abundance information -- information that provides a basis for his individual tactical fishing decisions. Under the MAREP program, responsibility for providing this kind of service to fisheries interests rests with the National Marine Fisheries Service (NMFS) of NOAA.

The largest and most sophisticated of the advisory or forecasting programs that have been implemented to date is the fishery-advisory service for Eastern Pacific tuna fisheries of the NMFS Fishery-Oceanography Center (FOC) in La Jolla, California. The nature of this program and its potential interaction with the EOS A/B mission will be examined in some detail here.

The FOC program generates fishery forecasts of two kinds -- tactical and strategic. The tactical forecasts, radioed daily to the fleet, deal with short-term changes in locations of fish concentrations and/or with short-term changes in environmental conditions that influence fish distribution or affect navigation and fishing operations. The tactical forecasts directly aid the fleet in its harvesting activities. Strategic forecasts, on the other hand, are long-range environmental and abundance forecasts of fundamental importance for management and conservation of the fishery resources.

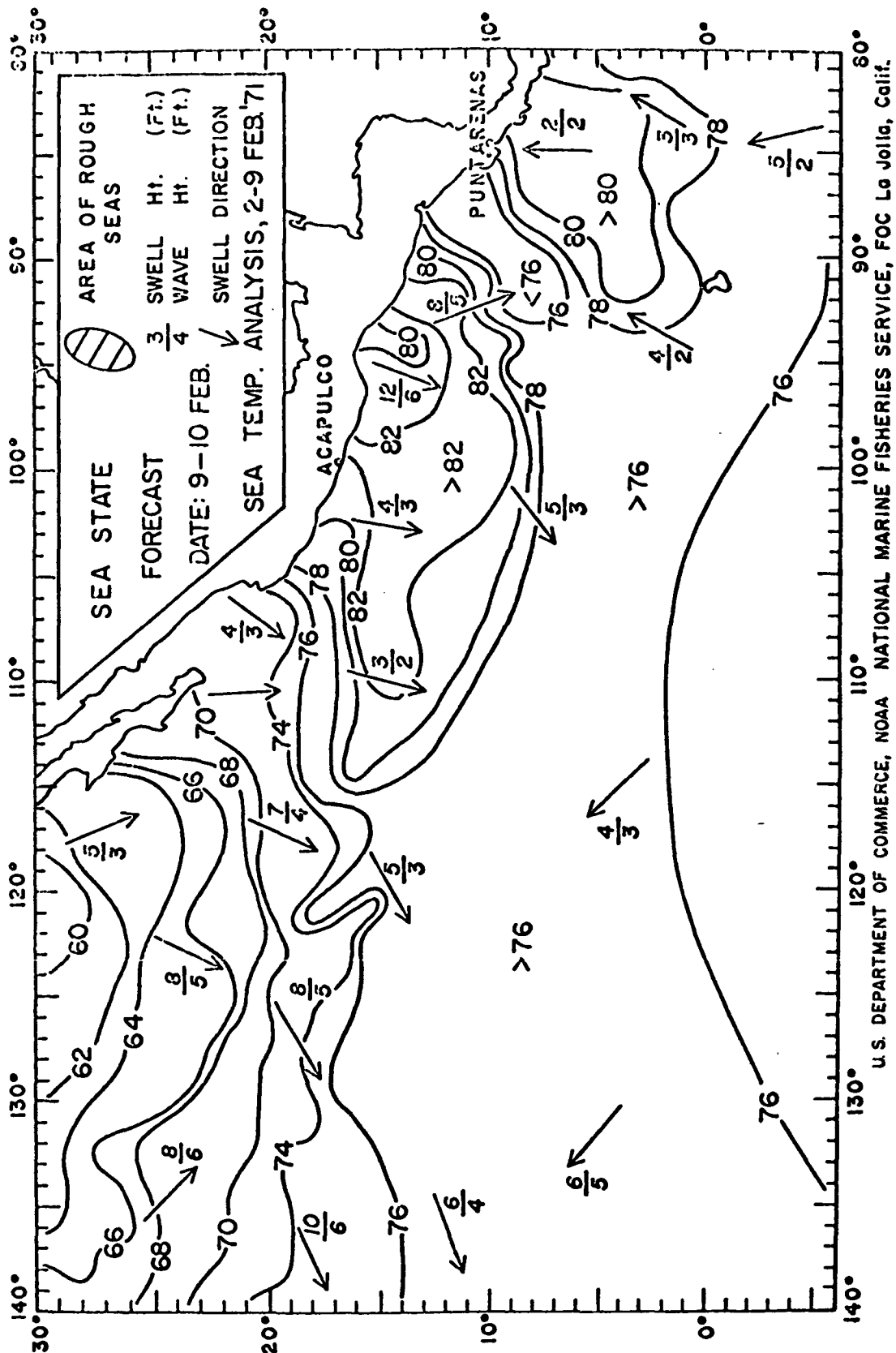
It is an experimental program designed to encourage the flow of valuable environmental data from fishing vessels in exchange for information which may assist vessel operators in making tactical fishing decisions. Environmental data which serves as a basis for the advisory service, derives from a variety of sources, including: merchant fleet weather and sea surface temperature observations; the Automatic Picture Transmission (APT) installation at the Fishery-Oceanography Center; the Fleet Numerical Weather Central at Monterey; the National Weather Service and cooperating fishing vessels.

Output to the fleet includes:

- Daily radioed weather advisories
- 15-day sea surface temperature charts of the eastern Pacific Ocean between latitudes 30°N and 30°S .
- Monthly mean sea surface temperature and temperature anomaly charts for the entire North Pacific
- Daily radio facsimile (FAX) broadcasts to the tropical Pacific tuna fleet containing oceanographic and weather information specifically tailored to fishermen's needs. Examples of these charts appear as Figures 9-8 and 9-9. (Weekly analyses of thermocline depth will be included on the charts in the near future).

Eventually, the location of surface thermal fronts and perhaps the distribution of chlorophyll as indicated by satellite measurements may be included in the charts.

During the 1971 tuna fishing season, NMFS provided 13 cooperating tuna vessels operating in the Eastern Tropical Pacific with FAX equipment with the agreement that they would transmit at least on XBT or bathythermograph report, or one synoptic marine weather observation per day while on the fishing grounds. This is an attempt to foster expanded cooperation from the fleet in providing environmental data to the system. Since fishermen ply sea routes seldom traversed by merchant and military vessels, a valuable source of environmental data will exist to the extent that fishermen can be encouraged to report weather and ocean conditions. Currently only about 15 percent of the tuna fleet operating in the Eastern Tropical Pacific, which is comprised of about 120 vessels, radios data from the fishing grounds. In January of this year, however, a special encoding system was



U.S. DEPARTMENT OF COMMERCE, NOAA NATIONAL MARINE FISHERIES SERVICE, FOC La Jolla, Calif.

Figure 9-8. Fishery information chart, showing swell direction and height, wind wave height, and seven-day sea surface temperature analysis.

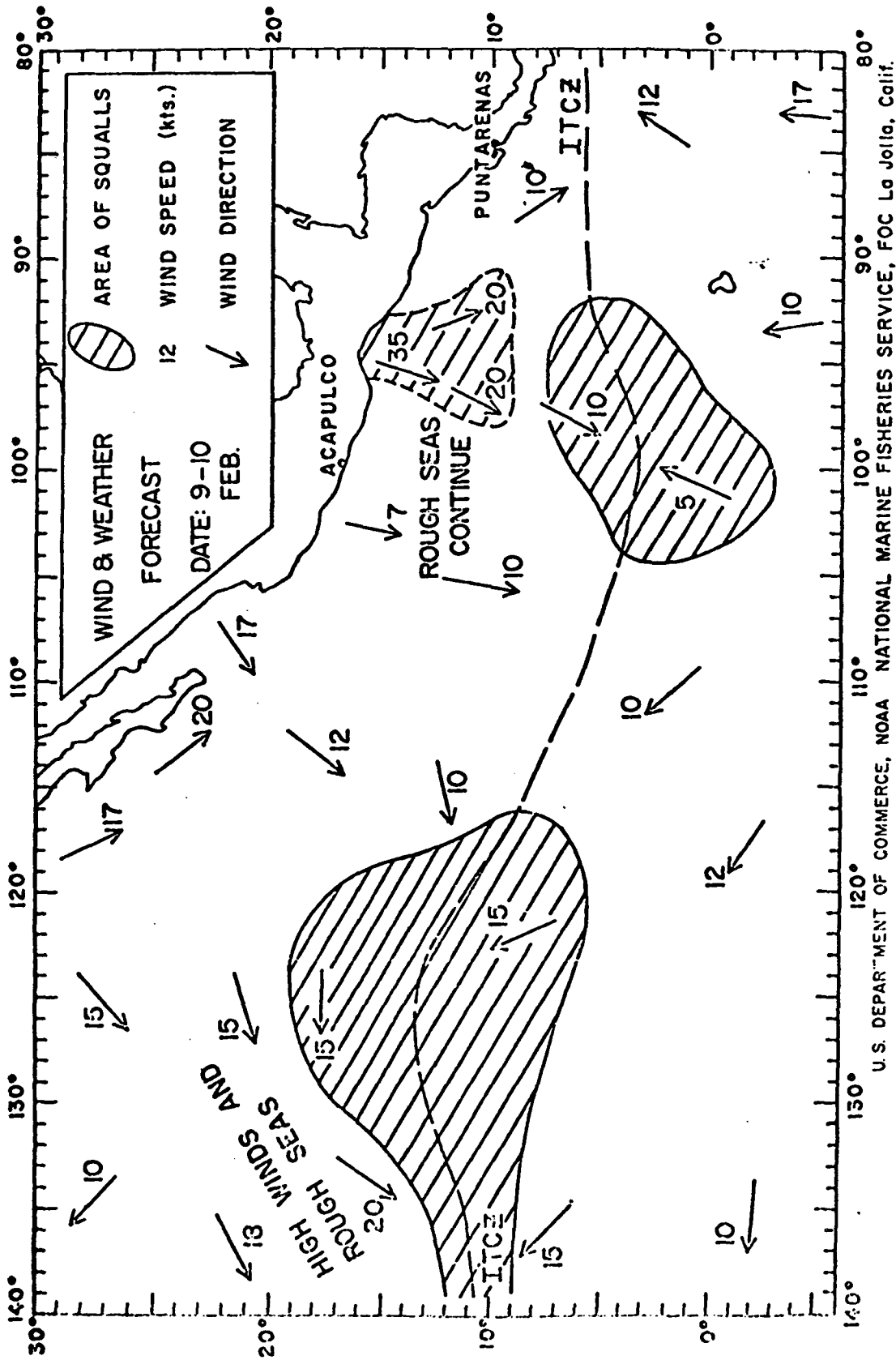


Figure 9-9. Fishery information chart, containing information on speed and direction of surface winds, location and direction of movement of tropical storms, location of areas of swells and other inclement weather conditions, and location of the Intertropical Convergence Zone.

adopted which makes it unnecessary for reporting vessels to identify themselves, thereby giving away their location to the rest of the fleet. This factor, plus continuing distribution of FAX receivers among the fleet, should lead to improved cooperation from the fishermen.

The existing system of communications with the fleet is not without its shortcomings. Many of these, however, might be alleviated eventually by means of data relay equipment aboard satellites. The major existing problems will only be mentioned here, as the problem of two-way communication with the fleet could easily form the subject of a separate study.

Vessels in the Eastern Tropical Pacific receive FAX transmissions from FOC of very good quality, however, a more rapid means is needed for getting vessel reports into the U. S. synoptic weather data schedule. Although a data collection facility has been set up in the Canal Zone, it is apparently somewhat of a bottleneck. In addition, fishermen apparently have great difficulty in reaching radio stations from the tropical Pacific when in need of weather information. Furthermore, there is virtually no communication in near-real time with the entire tuna fleet operating off the West Coast of Africa.

The principal potential EOS A/B contribution toward fishery-advisory services will be in its synoptic coverage of surface phenomena. Comprehensive areal coverage of certain ocean sectors where ship observations are reasonably dense should provide valuable supplementary data. In remote areas, where shipboard observations are scarce or lacking, the EOS satellite may represent a major data source for information on sea state, ocean color, sea surface temperature and the location of thermal fronts and regions of upwelling. Data acquired by the fishing vessels, on the other hand, represents a valuable source of ground truth data for the EOS A/B program.

9.2.2.3 Geochemical Ocean Sections Study (GEOSECS)

GEOSECS is the first major research effort of the IDOE. The lead agency for the United States' involvement is the National Science Foundation. The project involves dividing the world's oceans along north-south lines and measuring the vertical distribution of key chemicals and chemical

processes at fixed points, with emphasis on development of baseline data for comparison with future measurements of the environment and measurement of changes to enable prediction of impact of pollution conditions.

Specific program objectives are as follows:

- Identification of major suspected and unsuspected pollutants and their sources
- Identification of ocean processes affecting the dispersal, sedimentation, and fate of pollutants
- Identification or prediction of the impact of pollutants on the biosphere as well as their effect on aesthetic and commercial uses of the oceans
- Identification of ocean areas where high concentrations of pollutants may be expected to be found.

A pilot project is currently in progress in the Pacific Ocean (28°N , 121°W). The profiling program is expected to be implemented in the Atlantic in 1972 and in the Pacific in 1973.

Measurements provided by the GEOSECS program are expected to be of great importance to understanding the advection-diffusion field of the general circulation of the global ocean. It is primarily in this area that the GEOSECS and EOS A/B programs are likely to be most synergistic.

9.2.3 Special Experimental Data Programs

Certain programs are planned or are in existence which are largely problem-oriented rather than chartered for routine applications.

Three which appear to be of particular significance to EOS A/B are project "Little Window", the Atlantic Undersea Test and Evaluation Center, and the Mississippi Test Facility.

9.2.3.1 Project "Little Window II"

Project "Little Window II" ⁽⁸⁾ is a combined satellite/aircraft/ship survey of the sea surface temperature over a 100 nmi square area of the Gulf of California. The field phase of the project took place during the first week of May, 1971. The specific purpose of the project is to ascertain the limitations for measuring sea surface temperature of the infrared sensors aboard the Nimbus IV, ITOS I, and NOAA I satellites in terms of

spatial resolution and accuracy (the sensors aboard these satellites were designed to furnish meteorological information utilizing a temperature range several times larger than is necessary for oceanographic purposes). Measurements from surface vessels are used to calibrate aircraft infra-red radiometer data, which is then compared to simultaneously-recorded satellite radiation data.

A pilot project, called "Little Window I" was conducted over a smaller area (60 x 30 nmi) in the same location during March of 1970. Due to the fact that correlative satellite data has only recently been made available, the field data accumulated during project "Little Window I" is being retained for analysis concurrently with "Little Window II" data. At the time of this writing, the raw data had been compiled and a comprehensive data catalogue⁽⁹⁾ had been prepared which summarizes information on what data was acquired, and where, when, and how the data was taken. The catalogue has been distributed to project participants who are processing the data according to their individual requirements. Plans now call for a meeting in February, 1972, at which all participants in the project will present results of their individual analyses and compare their findings with those of other investigators. Subsequently, the official results of the "Little Window II" experiment will be published by the Naval Oceanographic Office.

Pending final evaluation of the results of these two special projects, there is good reason to expect that similar projects will be undertaken in future years. Because of the potential value to advances in spacecraft oceanography represented by projects of this nature, the scope of the field measurement phase of project "Little Window II" will be examined in some detail here.

The following characteristics of the Gulf of California figured into its selection as the study area:

- an extremely dry atmosphere with a minimum of clouds
- land masses distinctive enough to position the spacecraft results within the desired oceanographic tolerances
- fairly uniform sea surface temperature with surface wind speeds of less than 10 knots
- proximity to U. S. -based aircraft and ships.

The instrument platforms involved in the data collection included conventionally-equipped research vessels, infrared radiometer-equipped aircraft and satellites, and a shore satellite receiver station. Surface temperature data from ITOS I and NOAA I were collected by receivers on shore and aboard one of the research vessels, making use of the satellites' APT and DRIR (Automatic Picture Transmission and Direct Readout Infrared) capabilities. These data, together with stored Nimbus IV data collected at the NASA Goddard Space Flight Center, and stored data collected from the satellites at the National Environmental Satellite Service, constitutes the body of satellite data that will be utilized for comparison with aircraft and vessel data.

The study area and the basic aircraft tracks, ship cruise tracks, and coastal vessel anchor stations appear in Figures 9-10 & 9-11. Three research aircraft participated in daily surveys of the area, collecting day and night low-altitude (<500 feet) infrared radiometric measurements of sea surface temperature. In addition, one of the research aircraft conducted a series of experiments over one of the oceanographic vessels to determine the effect of atmospheric interference with altitude. Atmospheric temperature and moisture content were measured at various altitudes ranging from 300 feet, and radiometric readings were obtained for comparison with the ship's infrared radiometer. The oceanographic vessels acquired standard oceanographic data to establish the stability of the area and to aid in its assessment for future satellite thermal sensor studies. One of the oceanographic vessels was equipped with a bow-mounted infrared radiometer for measuring sea surface temperature, and a laser to provide backscattering profiles of cloud and haze layers in the direction of the satellite and to enable day and night measurements of cloud height and geometrical thickness. In addition, radiosondes were released from this vessel and from Mexican weather stations at Mazatlan and Empalme during the actual times of satellite overflights. Regularly scheduled weather reports were made six times daily by all stations.

9.2.3.2 Atlantic Undersea Test and Evaluation Center (AUTEK)

The primary mission of AUTEK is test evaluation of naval weapons, both in-air and in-water. Range instrumentation consisting of radars and theodolites satisfy in-air tracking requirements while a large number of hydrophones installed on the floor of the Tongue of the Ocean (TOTO)

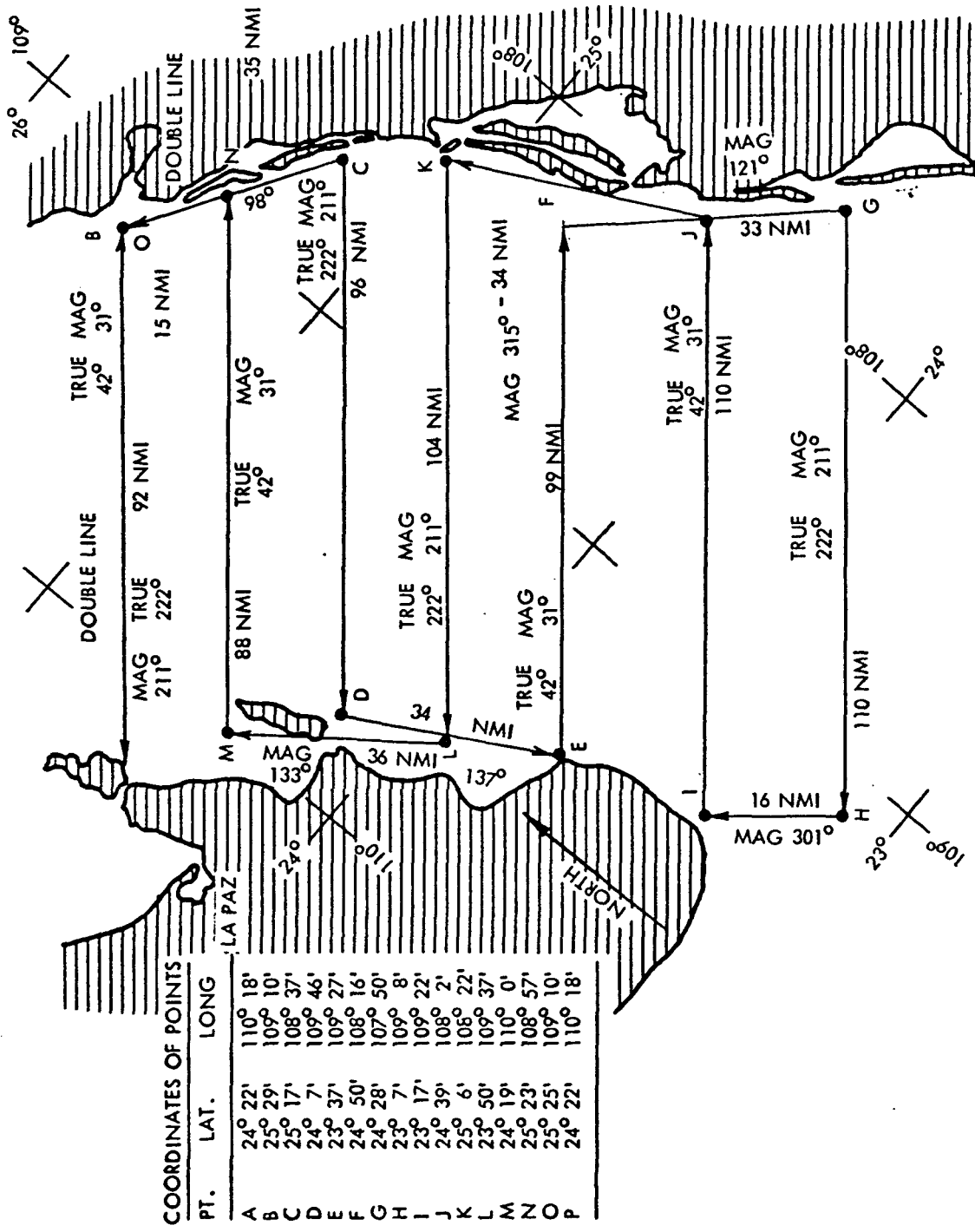


Figure 9-11. Basic Aircraft Tracks

adjacent to Andros Island, British West Indies, are the basis for in-water tracking. In addition to this Weapons Test Range there are an Acoustic Range for measurement of in-water sound levels generated by both surface and submersible vessels and a Fleet Operational Readiness Accuracy Check Site (FORACS) which measures ship/fire control /weapon alignment by means of in-water acoustic transponders and shore-mounted theodolite transits. Environmental support services are provided by oceanographic and meteorological instrumentation including remote weather stations located around the periphery of the TOTO which can be interrogated by radio command to furnish information for mesoscale climatology plots. Other test programs not involving weapons are also supported by AUTEK. These programs have included hydrographic surveys, ecological baselines, bottom contouring by isodensity plots of reflected light and IR airborne temperature sensing. AUTEK has been selected for a permanent ground truth site for water color remote sensing with the first test program in the fall of 1970 and yearly repetitions of this test are scheduled.

AUTEK can provide accurate ground truth calibrations for EOS from water temperature measurements, wind speed and velocity, wave staff readings and meso-climatological information. Additional calibration/correlation information can be provided EOS by the various environmental test programs which are supported by AUTEK during the year.

EOS contributions to AUTEK would be additional water color data for correlation with the permanent ground truth site/aircraft remote sensing program, surface temperature isotherms for possible detection of saline lenses which form over the shallow bank areas of the TOTO and generate anomalies in sound propagation, synoptic sea-state determination for test operations information and large scale weather information.

9.2.3.3 Mississippi Test Facility (MTF)

The Mississippi Test Facility is involved in research in the application of remote sensing techniques, making use of data generated by NASA Earth Resources projects such as Earth Resources Aircraft, Earth Resources Technology Satellites and the manned orbiting Skylab Earth Resources Experiment package. The applications studies and associated research effort will be directed toward the economics, needs and/or the environment

of the region encompassing of the states of Louisiana and Mississippi and a significant distance into the Gulf of Mexico. The effort shall capitalize on the collocation at MTF of other government agencies such as the Coast Guard Buoy project, Federal Water Quality Administration (FWQA), National Marine Fisheries Service (NMFS) and the National Oceanic and Atmospheric Agency (NOAA). Mutual interest projects include ground truth for remote sensing provided by in-situ buoy measurements, monitoring of water pollution, marine resources assessment and harvesting, and the TROPEX atmospheric/oceanic research program.

MTF can provide EOS with ground truth for the Gulf of Mexico which should be extensive and accurate. The scope of activity at the MTF and the existence of the collocated agencies (Coast Guard, FWQA, and NOAA) provides an advantage of mutual interests and data accessibility seldom encountered.

EOS contributions to MTF would be to provide additional data for their applications studies and associated research efforts. All of the EOS data could be utilized by MTF.

9.2.4 Aircraft Programs

Various government agencies such as NASA, the U. S. Navy, the U. S. Coast Guard and the University of Michigan have aircraft remote sensing programs currently in operation or being planned for the near future. These programs utilize sensors that are similar to those being considered for the EOS A/B satellite and require similar ground truth information. This ground truth information obtained in support of the aircraft programs is directly applicable to EOS A/B and correlation is also possible between data from the satellite and aircraft sensors.

NASA's aircraft remote sensing program is primarily a proof-of-technology vehicle concerned with determining feasibility of monitoring the earth's resources by remote sensing and is not geared for operational application. Three aircraft are based at the Manned Spacecraft Center (Ellington AFB), consisting of an RB-57, a C-130 and a P3A. The flight schedules for these and other aircraft participating in the MSC program during the first quarter of FY 1972 are shown in Figure 9-12. Table 9-8

Table 9-8. Types of sensors and support systems currently used onboard aircraft in MSC's Earth Observations Program.

EARTH OBSERVATIONS AIRCRAFT SENSORS				
TYPE OF SENSOR	NP-3A	NC-130B	RB-57F	U. OF MICH. C-47*
Photographic:	9-Inch Format RC-8 Metric Cameras (2) KA62 Multifband Camera Cluster (4) Boresight Cameras (SLAR, IR Spectrometer, Microwave Radiometer) (3)	9-Inch Format RC-8 Metric Cameras (2) Hasselblad Multifband Camera Cluster (6) Boresight Cameras (13.3 Scatterometer, 2 Spares)	9-Inch Format RC-8 Metric Cameras (2) Hasselblad Multifband Camera Cluster (6) 9-Inch Format Zeiss Metric Camera (12-inch F.L. or 6-inch F.L.) Boresight Camera (IR Spectrometer/Radiometer) (1)	K-17 Camera (1) KB-8 Cameras (2) P-2 Cameras (2)
Radar:	16.5 GHz Side Looking Airborne Radar (SLAR) 400 MHz Dual-Polarization Scatterometer 13.3 GHz Single Polarization Scatterometer	13.3 GHz Single Polarization Scatterometer		
Microwave (Passive):	Multifrequency Microwave Radiometer (MFMR) (4-Frequency)			
IR Scanner:	RS-14 Dual-Channel Imager	Reconofax IV Single Channel Imager	RS-7 Single-Channel Imager	Double-Ended Multi-spectral Imagers (2)
IR Pallet:	IR Spectrometer IR Radiometer		IR Spectrometer IR Radiometer	
Laser:	Profiler			
Support Systems:	Precision Radiation Thermometer (PRT-5) Total Air Temperature Probe (TAT) Liquid Water Content Indicator Auxiliary Data Annotation System (ADAS) 14 Channel Analog Magnetic Tape Recorder APN-153 Doppler Radar LTN-51 Inertial Navigation System APN-159 Radar Altimeter Dew Point Hygrometer	Precision Radiation Thermometer (PRT-5) Total Air Temperature Probe (TAT) Liquid Water Content Indicator Auxiliary Data Annotation System (ADAS) 14 Channel Analog Magnetic Tape Recorder Closed Circuit Television LN-120 Inertial Navigation System APN-159 Radar Altimeter	Radar Altimeter Air Mass Computer ARN-21C Tacan Navigation System Auxiliary Data Annotation System (ADAS) 14 Channel Analog Magnetic Tape Recorders (2) Closed Circuit Television APN-159 Radar Altimeter	Precision Radiation Thermometer (PRT-5)
*Contract Aircraft				

----- AIRCRAFT PROJECTED MISSION
 _____ AIRCRAFT ACTUAL MISSION

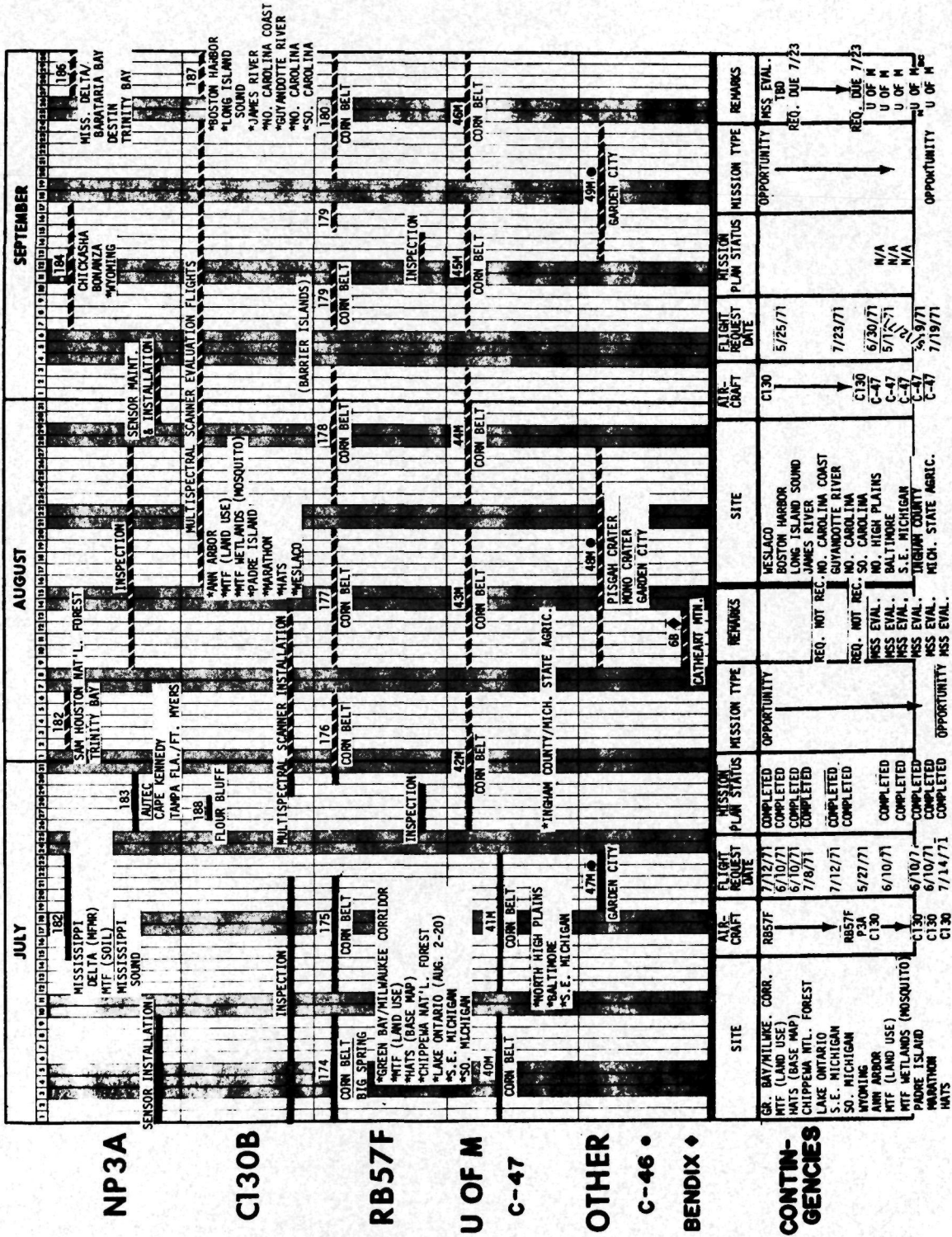


Figure 9-12. Aircraft Schedule First Quarter FY 72

DATE JULY 30, 1971

▲ AIRCRAFT PROJECTED MISSION
 ■ AIRCRAFT ACTUAL MISSION

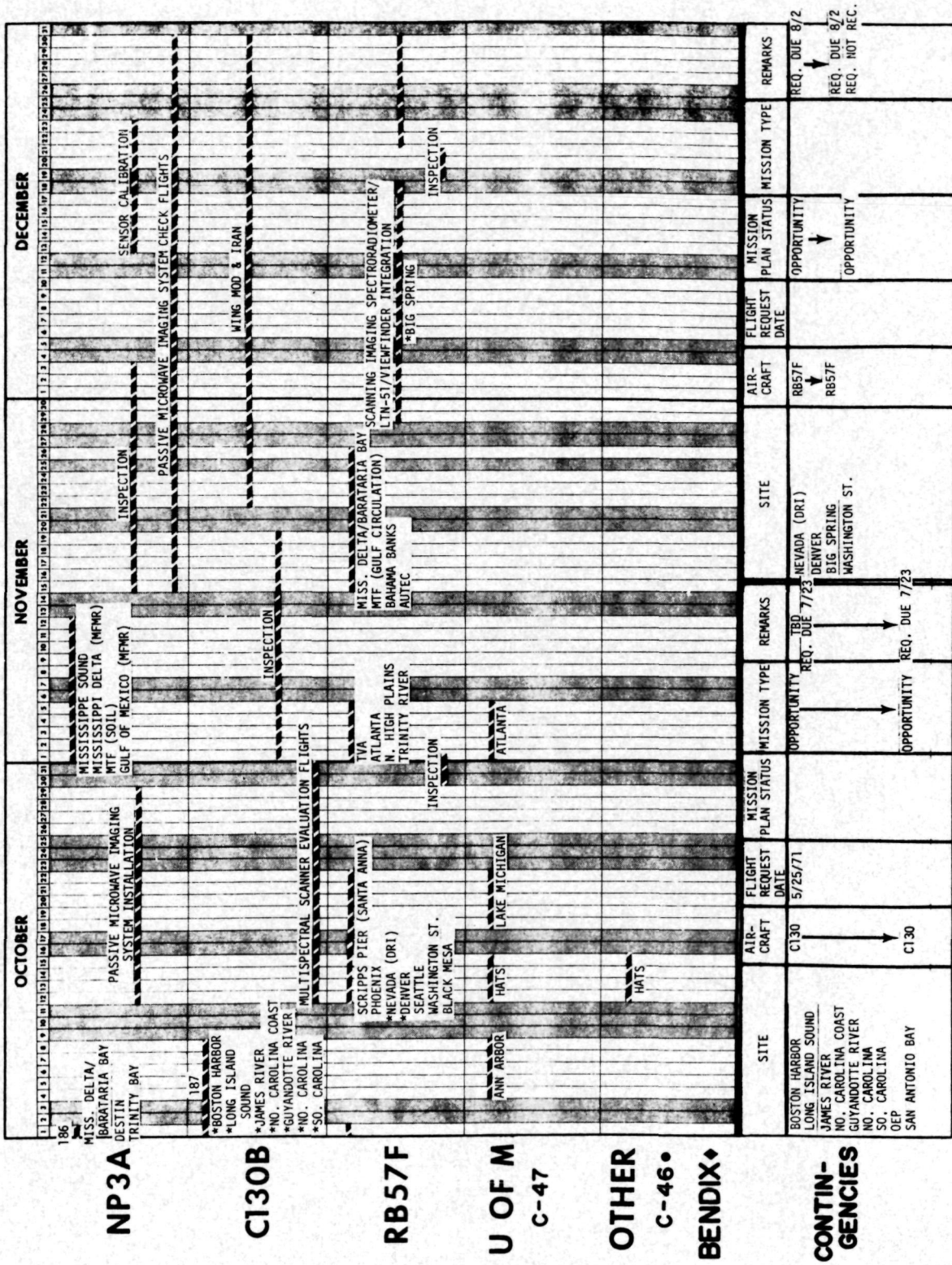


Figure 9-12. Aircraft Schedule Second Quarter FY 72 (Continued)

lists the sensors currently in use aboard aircraft participating in MSC's Earth Observations Program. Table 9-9 lists proposed sensors for these aircraft. Two U-2 aircraft outfitted with sensors similar to those to be flown in ERTS A/B are based at Ames Research Center, Moffett Field Colitorium. Four sites have been selected for U-2 remote sensing of earth resources data:

- Los Angeles - San Francisco area
- California Feather River area
- Arizona - including Phoenix and Tucson
- Maryland - Chesapeake Bay

In California the remote sensing studies will be made of agriculture and hydrology; in Arizona, arid lands will be studied; and in Maryland's Chesapeake Bay, the emphasis will be on oceanography. The aircraft are to make repetitive flights over the test sites, photographing each area every 18 days at the same local time to simulate the coverage that will be provided by the satellite. Another Ames Research Center Project is the air sampling program which is a joint venture of NASA and the U. C. Riverside Statewide Air Pollution Research Center. Twelve times annually for three years a twin engine Cessna will overfly the Los Angeles basin at altitudes ranging to 17,000 feet. This program will be duplicated for the San Francisco area. Air collecting instruments will gather particulates, ozone, carbon monoxide, hydrocarbons, oxides of nitrogen, and acetylene. Cameras and other instruments will obtain information in the visible spectrum. Satellites will be the principal benefactor of the air pollution measurement flights.

The Navy conducts extensive oceanographic reconnaissance flights with specially equipped aircraft for data collection and research project support. These efforts vary from employing fleet patrol aircraft in an ice reconnaissance role to specially equipped aircraft for data collection and research project support. Instruments flown include IR, laser, microwave and radar in addition to visible sensors.

The Coast Guard conducts regular monthly surface temperature overflights off the east and west coasts of the U. S. and in the Gulf of Mexico. These flights cover the coastal regions in a zig-zag type pattern out to

Table 9-9. Proposed sensors for MSC's Earth Observations Aircraft

TYPE OF SENSOR	NP-3A	NC-130B	RB-57F	U. OF MICH. C-47*
Microwave	10.69 GHz Passive Microwave Imaging System (PMIS)			
Photographic			70-mm Panoramic Cameras (3" Focal Length)(2)	
Imaging Scanners		24-Channel Multi-spectral Scanner	Scanning Imaging Spectroradiometer (SIS)	
Support Systems	Environmental Sensor Station	Panametrics Hygrometer System LTN-51 Navigational System	Optical Viewing System LTN-51 Navigational System	

*Contract Aircraft

approximately 100 miles offshore. Sightings of marine bird flocks and surface-swimming animals are also recorded. Resulting charts are mailed monthly to users.

Aircraft program data is particularly valuable to EOS A/B for determination of atmospheric effects on data. Aircraft flying below cloud layers can eliminate cloud attenuation effects and obtain valuable data for comparison purposes.

EOS A/B can benefit the aircraft programs by furnishing synoptic data over large areas which in some cases can explain aircraft sensor data anomalies.

9.3 DEDICATED GROUND TRUTH PROGRAM FOR THE EOS A/B MISSION

Despite the range of possibilities for beneficial interaction with the relevant data programs examined in the preceding section, ground truth requirements are only partially satisfied -- especially for concise evaluation of sensor performance. Ad hoc programs in the style of project "Little Window" would appear to be in order to best meet this objective. The Gulf of Mexico represents a very good area for sensor evaluation in terms of the three major applications identified in this study: ocean pollution, management of living resources, and monitoring/prediction of physical processes/phenomena. For the management of living resources application, an alternative area -- off the West Coast of Baja California -- was considered. In addition, the components and possible scope of a ground truth program were considered for this area.

9.3.1 Gulf of Mexico Sensor Evaluation Area

The Gulf of Mexico is well suited as a sensor evaluation area by virtue of the anticipated concentration of surface data platforms -- especially those of the National Data Buoy System, the accessibility of the region to vessels from marine labs and to aircraft, and the relatively small percent of cloud cover (roughly 20 percent on a yearly average). The region is oceanographically complex, permitting observations to be made on all aspects of phenomena of interest. The circulation is dominated by inflow through the Yucatan Channel, and outflow through the Straits of Florida, between Cuba and Florida. The surface current entering the Channel loops

through the eastern Gulf, entraining waters in the central and western regions in the circulation, thereby setting the rest of the Gulf in motion. Two major clockwise gyres exist, one in the northeast Gulf and the other off the western tip of Cuba. A highly variable deep water exchange also occurs at the Yucatan Channel. The deep underflow seems to loop in a counterclockwise direction throughout the entire Gulf and may actually be the primary driving force in the Western Gulf. Additionally, the influx of Mississippi River water has a significant influence in the northern Gulf region, many miles from its mouth.

9.3.2 Baja California Sensor Evaluation Area

Several factors make the area off Baja California, shown in Fig.9-13, ideal for measurements related to management of living marine resources.

- Since 1951 data on physical, chemical and biological properties of the water column have been collected through the California Cooperative Oceanic Fisheries Investigations (Cal COFI). In addition, numerous vessels from Scripps Institution of Oceanography and other research institutions have collected data in this area on other than Cal COFI Stations.
- Considerable research on the distribution of chlorophyll, and its relationship to the standing crop of tuna food, such as red crab, has been carried out by the Scripps Tuna Oceanography Research (STOR) group, and others, in the area shown.
- Information on project "Little Window" which took place off the eastern coast of the Baja Peninsula will be available prior to the EOS A/B mission. The data and results of this experiment will provide excellent planning information since project "Little Window" was in effect carried out to calibrate the IR sensors aboard Nimbus and NOAA satellites.
- There apparently will be a continuing number of ground truth platforms available in this area through the EOS A/B time period.
- The continental shelf is very narrow and precipitation in the area is minimal; consequently, the terrestrial influence on ocean color is nearly insignificant relative to the effect of biological factors.

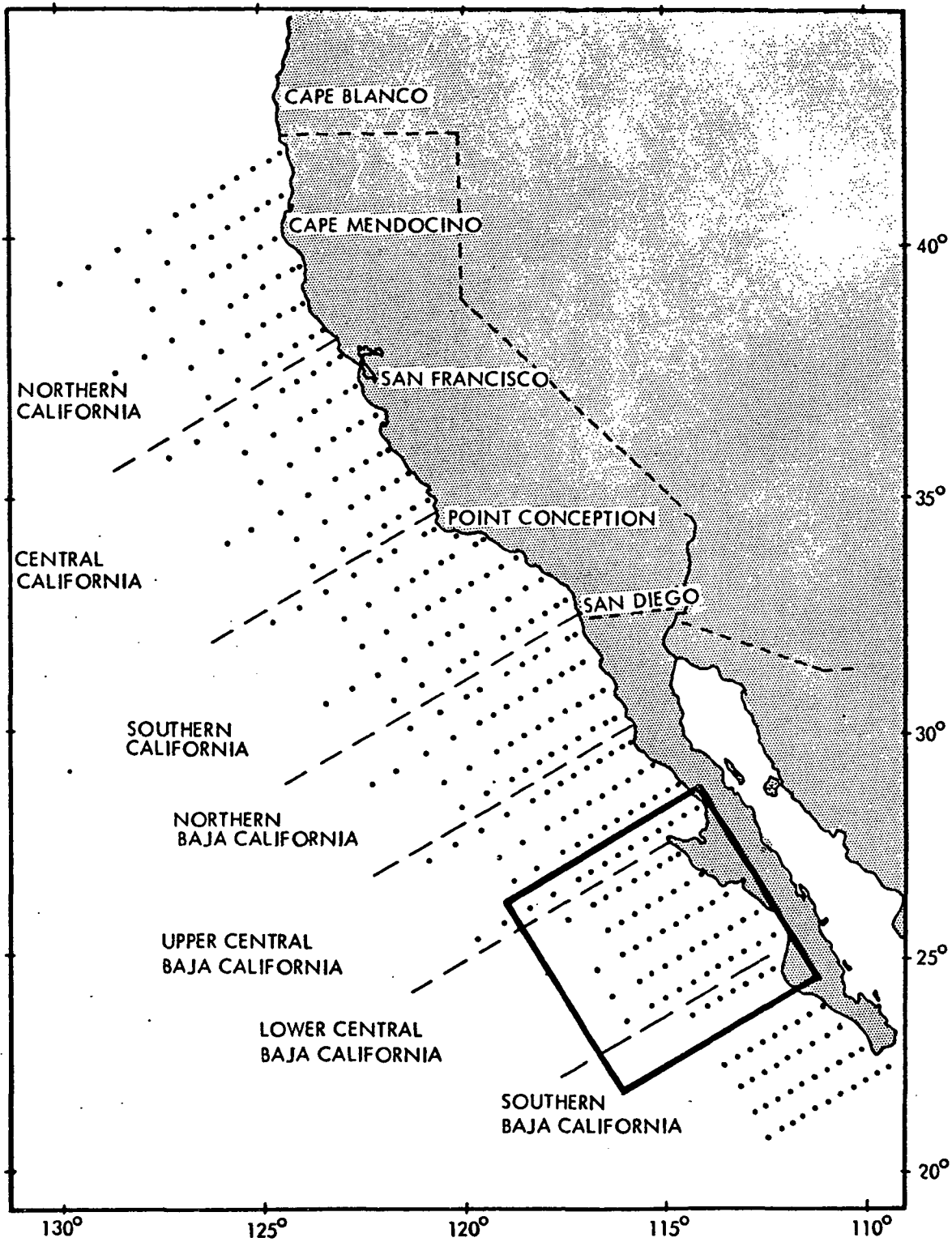


Figure 9-13 Station Pattern of the California Cooperative Oceanic Fisheries Investigation (CalCOFI), and Suggested Experiment Area

The recommended ground truth exercise would be a high-intensity, short duration effort specifically directed toward documentation of atmospheric and oceanic properties simultaneously with overflight of the EOS A/B satellite. The basic experiment, which would be of two or three days' duration, might be performed more than once - before and after the upwelling season, for example. This would permit analysis of sensor performance under a variety of environmental conditions.

Assuming that an area approximately 300 miles square is selected as the study area, reasonably good oceanographic sampling density could be achieved in one day with three or four oceanographic vessels (or in two days with half as many vessels) occupying stations every 6 hours along parallel cruise tracks. Grid spacing would be approximately 60 nmi. Complete aerial coverage could be provided daily by two instrumented aircraft, assuming transects separated by about 60 nmi, and a 5 hour period of optimal sun angle conditions for visible observations. Ideally, the following kinds of measurements would be included in a comprehensive ground truth program:

- Atmospheric constituents
 - infrared-active molecules (H_2O , CO_2 , O_3 , N_2O , CH_4)
 - atmospheric haze
 - water clouds
- Ocean surface temperature (by aircraft and surface vessels, continuously along tracks) and surface salinity (by vessels, continuously along tracks)
- Ocean temperature and salinity profiles (expendable bathy-thermograph every 10 nmi, salinity-temperature-depth recorder every 30 nmi)
- Biological data
 - standard oceanographic sections for nutrients and dissolved oxygen every 60 nmi.
 - primary productivity measurements (one or two per vessel per day)
 - phytoplankton standing crop (chlorophyll a) - (continuous surface measurements along vessel cruise tracks, vertical profiles every 30 nmi)
 - catch and effort data from fishing vessels in the area.
 - aircraft observations of fish schools, and ocean color data from multispectral sensors
 - zooplankton and midwater trawl tows (every 60 nmi.)
- Standard weather observations - every 6 hours.

9.4 SUMMARY

The preceding review of existing and anticipated EOS A/B-compatible data programs indicates that a multi-faceted and comprehensive simultaneous ocean surface data coverage will be available from which ground truth information in support of EOS A/B may be drawn. Ground truth support of the following nature will enhance the utility of the EOS mission:

- Data of value for direct point-to-point calibration - particularly for atmospheric effects - of EOS sensors
- Detailed documentation of phenomena (horizontal and vertical spatial patterns and intensity) to facilitate interpretation of what was seen by the satellite's sensors
- Information on related phenomena and driving forces to permit analysis of satellite measurements in the broad context of cause and effect.

Where gaps exist in the surface truth coverage, special aircraft or surface vessel experiments in the style of project "Little Window" are appropriate.

The EOS A/B mission configured in this study, while relying upon existing data programs for surface truth data, will in return afford an important and unique contribution to the data resources of many of the data programs examined. In particular, the synopticity and frequency aspects of the satellite data will be valuable.

REFERENCES FOR SECTION 9

1. U. S. Committee for the Global Atmospheric Research Program, Plan for U. S. Participation in the Global Atmospheric Research Program, National Academy of Sciences, Washington D. C. , 1969.
2. Wolff, P. M. , T. Laevastu, and P. Patro, 1969, "Synoptic Analyses and Prediction of Conditions and Processes in the Surface Layers of the Sea," Oceans from Space, Gulf Publ. Co. , Houston, 234 pp.
3. Wolff, P. M. , 1970, "Environmental Forecasting - Largest of Marine Information Systems," MTS Journal 4 (6) : p. 7-18 .
4. Wolff, P. M. , 1970, "Problems in the Operational Prediction of the Environment," FNWC Tech. Note 56, 76 pp.
5. Federal Planning Guide for MAREP, Executive Summary, 1969, U. S. National Council on Marine Resources and Engineering Development, prepared for the Interagency Committee on Ocean Exploration and Environmental Services.
6. Sperry Rand Corporation Pub. No. GB-2520-1032, National Data Buoy Development Plan, January 1970.
7. Program Development Plan for Marine Resources Monitoring, Assessment, and Prediction (MARMAP) Program, 1971, prepared by TRW Systems Group for the National Marine Fisheries Service (NOAA).
8. U. S. Naval Oceanographic Office, 1971. Little Window II - A Satellite/Ocean Station Sea Surface Temperature Experiment in the Gulf of California, Operational Plan, February, 1971, 25 pp.
9. U. S. Naval Oceanographic Office, 1971, "Little Window II" - Data Catalogue, July 1971, 79 pp.

10. DATA MANAGEMENT

The general problems of data acquisition and management have been discussed in Section 8 of the Final Report on Coastal Zone Requirements for EOS A/B (NASA document CR-111816, dated 4 February 1971, prepared by TRW Systems under NASA Contract NAS 1-10280). The present discussion is concerned with the specific problems associated with the suggested global oceanographic satellite payloads. Moreover, the subject is treated primarily within the context of taking the currently planned ERTS A/B data handling capabilities as a baseline. The emphasis is thus on a comparison of global oceanographic satellite data acquisition, transmission and processing requirements with those of ERTS A/B and the impact that these requirements would have on the data handling system to be established for ERTS A/B. Most of the estimates of ERTS A/B ground station capabilities, data link capacities and, in particular, NASA Data Processing Facility (NDPF) characteristics are based on the ERTS A/B Study performed by TRW Systems under Contract NAS 5-11260 (especially Volume 14, "Ground Data Handling System Design," of the final report).

The ground data handling capabilities estimated for ERTS A/B are assumed to be available for receiving and preprocessing the data from the sensors considered in the present study. (The terms "processing" and "preprocessing" are used throughout almost interchangeably; the introduction of the latter term is intended to emphasize the fact that processing of the data involving analysis or interpretation is generally performed by the users and not by the NDPF.) The discussion of data management to follow will indicate that the space-to-ground data link capabilities intended for ERTS A/B will be adequate for the proposed global oceanographic payload configuration and usage, but that some additional communications capabilities between the ground stations and the NDPF would be desirable. The NDPF has adequate capabilities for handling the global oceanographic data preprocessing requirements in general except for the SAR data, which will require modest hardware additions. Of course, specialized software must be provided for treating the oceanographic data.

10.1 DATA ACQUISITION

For the purpose of estimating the amount of data which will be acquired, the total payload is taken to consist of six sensor assemblies. In the order of the volume of data to be handled they are:

- Side Looking Radar
- Multispectral Mechanical Scanner
- Visible Imaging Spectrometer
- Glitter Pattern Sensor
- Microwave Radiometer
- Radar Altimeter

10.1.1 Synthetic Aperture Radar

The synthetic aperture radar (SAR), configured to give a 600 km swath width and 1 Km crosstrack resolution, has a bandwidth of 0.5 MHz. This provides a potential of about 6-meter resolution along track; the normal processing to give image-type data for square (1 Km x 1 Km) resolution elements will reduce the data rate by more than two orders of magnitude, but this cannot be accomplished in the vehicle, so the raw data will have to be transmitted to the ground. On-board digitization of the data is not absolutely necessary, but it will probably be useful, and for comparison with other payload outputs it is assumed here that sampling twice per cycle and digitizing to an 8-bit level will be done. Thus the data rate is 8 M bits/sec, much larger than that of any other sensor.

The most important use for the SAR information is for the mapping of ice in the polar regions, and daily coverage is desirable. Since the sensor looks only to one side of the spacecraft, an orientation designed to obtain measurements up to one pole will miss the other by a substantial distance. A reasonable compromise is to have the SAR swath begin at 20° from the spacecraft nadir (about 3° in earth central angle) and pointed so that the region near the north pole is covered. Measurements can then be obtained to within 63 Km of the north pole, or to about latitude 89.5° N, and to within about 1340 Km of the south pole, or to about latitude 78° S. Typical swaths showing these coverage characteristics are shown in Figure 10-1. The region never seen near the south pole is entirely over

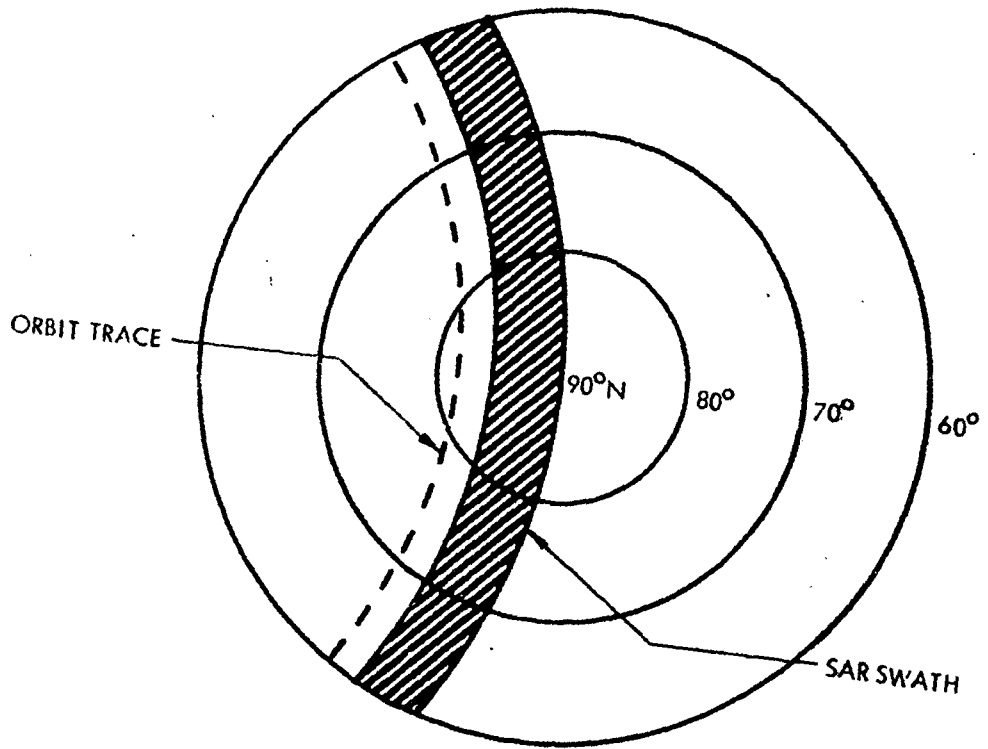


Figure 10-1a. Typical SAR Swath Near North Pole

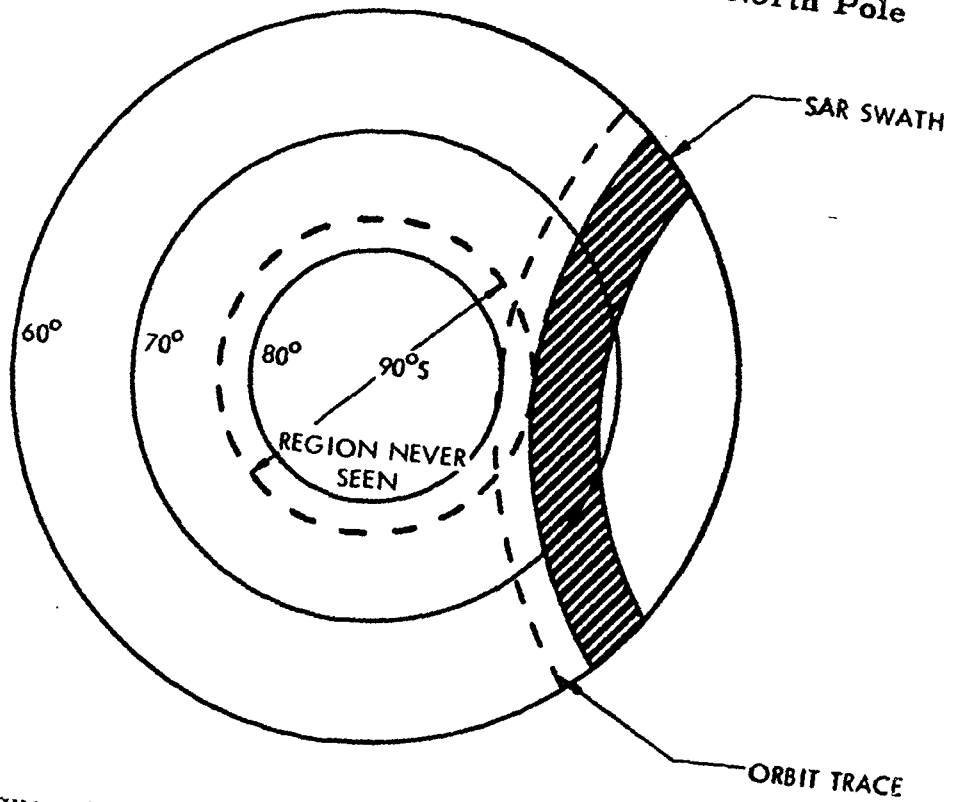


Figure 10-1b. Typical SAR Swath Near South Pole

land except for a small portion of the Weddell Sea, so the loss of coverage of this area is not as significant as would be that of the corresponding region near the north pole.

The fraction of the orbit above latitude 60° is about 0.14 near either pole so coverage of these regions requires operation about 0.28 of total orbit time. Considering, on the one hand, that the coverage becomes quite redundant in the high latitudes and, on the other, that selective coverage may be desired at latitudes less than 60° , especially in the northern hemisphere, the average fractional time of operation of the SAR is estimated at 0.25, which gives a total of 1.24×10^4 M bits of SAR data collected per orbit.

10.1.2 Multispectral Mechanical Scanner

The multispectral mechanical scanner has three channels in the thermal infrared region plus three or four more in the near UV, visible, and near infrared. With all channels operating, this gives a data rate of about 1.5 M bits/sec with a two-thirds duty cycle, for an average rate of 1 M bit/sec. It is intended for use over the ocean; the areas of interest cover about 0.6 of the area overflown, on the average. All the wavelengths used are affected by cloud cover but, for sizing the data load, only the maximum case (no cloud cover) is considered. The thermal IR channels are equally useful night and day, but the UV, visible and near IR channels are measuring only reflected sunlight and thus are effective only when the sun is appreciably above the horizon. The thermal IR channels therefore require half the data rate for 0.6 of the time; the others require half the data rate for 0.3 of the time (half of the over ocean time), for a total effective fractional time of use of 0.45, or about 2800 seconds per orbit average. Thus 2.8×10^3 M bits of multispectral scanner data will be acquired per orbit.

10.1.3 Visible Imaging Spectrometer

The visible imaging spectrometer has a data rate during operation of 0.3 M bits/sec. It is to be used over ocean areas at times when the sun angle is $\leq 60^{\circ}$. The ocean areas comprise about 0.6 of the total area overflown and the fraction of the orbit with acceptable sun angles is 0.33, so the fractional time is 0.2, assuming no cloud cover.

This gives about 1,240 seconds of coverage per orbit or 3.7×10^2 M bits of visible spectrometer data acquired per orbit, on the average.

10.1.4 Glitter Pattern Sensor

The glitter pattern sensor is the only major payload component that operates in a framing mode. Its instantaneous data rate thus depends on the time used to slow-scan the vidicon after each exposure; for a choice of a 5-second scan time, the data rate is 0.2 M bits/sec. With about 25 seconds between frames, the average is then 0.04 M bits/sec (note that this average is essentially independent of the scan rate, since faster scans with higher instantaneous rates have a correspondingly shorter duty cycle). The coverage capabilities are essentially the same as for the visible spectrometer, i. e., about 0.2 of the time, 1,240 seconds per orbit. The average glitter pattern data acquisition is thus about 50 M bits/orbit.

10.1.5 Microwave Radiometer

The microwave radiometer acquires data at about 200 bits/sec, much less than any of the previously considered sensors. It will operate at all times while over ocean areas, thus about 0.6 of the time, for 3,700 seconds, or about 0.74 M bits total per orbit.

10.1.6 Radar Altimeter

The altimeter, like the microwave radiometer, operates whenever the spacecraft is over ocean areas. It has a data rate less than 100 bits/sec, for a total of 0.37 M bits acquired per orbit.

10.1.7 Summary

The data acquisition volumes discussed in the foregoing are summarized in Table 10-1. It can be seen that in terms of data which must be sent to the ground, the SAR acquires about four times the volume of data of all the other together. Taken as a whole, however, the data load imposed on spacecraft and ground capabilities by the EOS sensors is considerably less than the data load for ERTS A/B.

Table 11-1. Data Acquisition

Sensor	Operating Data Rate (MB/S)		Average Coverage Factor		Average Total Data Per Orbit (MB)
	Instantaneous	Average	Fraction of orbit	Operating time/orbit(sec)	
SLR	8 MB/S	8 MB/S	0.25	1550	1.24×10^4 MB
Multispectral Scanner	1.5	1.0	0.3	1850	} 2.8×10^3
	0.75	0.5	0.3	1850	
Visible Spectrometer	0.3	0.3	0.2	1240	3.7×10^2
Glitter Sensor	0.2	0.04	0.2	1240	50
Microwave Radiometer	0.0002	0.0002	0.6	3700	0.74
Radar Altimeter	0.0001	0.0001	0.6	3700	0.37
					Total 1.56×10^4 MB

10.2 DATA STORAGE AND TRANSMISSION

10.2.1 Space-to-Ground Considerations

The ground stations proposed to receive the global oceanographic data are the NTTF, Goldstone, Calif., and Fairbanks, Alaska. The read-out times available from these stations should not differ materially, on the average, from those available from stations considered for ERTS A/B, i. e., NTTF, Corpus Christi, and Fairbanks. A typical daily schedule (ref. Volume 14, ERTS A/B Studies Final Report) showed a total of 223.3 minutes of readout time, or an average of 16 minutes per orbit, for these three stations, based on the ERTS A/B orbit (altitude 492.6 nmi and inclination 99°) and pass duration defined as the time the spacecraft is 5° above the horizon at the station. The times for an individual orbit varied from zero to 36.8 minutes. Thus it is evident that on-board storage must be provided to accumulate at least up to two orbits worth of data, and that the data must be transmitted at a higher than real-time rate.

The SAR presents by far the greatest problem and must be considered separately. The video tape recorder being developed for ERTS A/B MSS data provides both data rate and data capacity characteristics suitable for handling the SAR output, and thus it can be taken to represent realizable state-of-the-art recording and give an estimate of size, weight, and power requirements. Pertinent estimated characteristics are:

1. 24 data tracks which record or read out 16.4 MB/S total
2. Total capacity 30 minutes of recording or 2.95×10^4 MB
3. Weight 45 pounds
4. Transport package size 12" x 20" x 4.5"
5. Electronic package size 20" x 8" x 6"
6. Power consumption 83 watts (record), 75 watts (playback)

This VTR could thus store about 2.4 orbits worth of SAR data, if efficiently packed. Although it is a single speed device, it would be possible to read in on 12 tracks half the time, and on the other 12 tracks half the time, while reading out all 24 tracks at once, thus effectively doubling the read-out data rate. This mode of operation would permit reading out all the SAR data in an average time of 13 minutes per orbit, which is below, although not comfortably below, the available 16 minutes per orbit. The current state-of-the-art in VTR's permits a specially developed design which could use 30 MB/S capacity of the ground station receivers, and reduce the average readout time to 7 minutes/orbit. However, the foregoing shows the basic feasibility of storing and transmitting the suggested volume of SAR data.

All the rest of the sensors could be recorded on a similar VTR, but of perhaps a third to a half the total capacity. The data from each sensor could be recorded on several tracks each a fraction of the time, with all tracks read out at once, in a mode similar to that for the SAR, to achieve an effective increase in data rates, and hence acceptable readout times. The extremely low data rates and correspondingly small data volumes of the microwave radiometer and the radar altimeter suggest perhaps the use of small buffers, which would intermittently read out at a much higher rate and be interleaved with the data from another sensor on a single track. Even more strongly than with the SAR data, however, it appears that a recorder design tailored specifically to the problem is both desirable and readily attainable.

In summary, the global ocean payload data can be transmitted to the ground stations using established technology in the spacecraft and the two 30 MB/S data link capabilities of the ground stations.

10.2.2 Ground Data Links

The ERTS A/B data handling system is predicated on recording the wideband video data at ground stations other than the NTTF, with physical transportation of the data tapes to the NDPF at Goddard. With a data processing cycle of several days, and with data for which there is no requirement for immediate dissemination, this is an economical and satisfactory solution to the problem of getting the data from the ground stations to the data processing center. It is evident from the preceding section that the capabilities intended for ERTS are fully adequate, with respect to both data volume and format, for the global ocean data. Also, in so far as the primary mission for the global oceanographic data being considered is experimental in nature, the delays incurred by the ERTS method are probably tolerable. However, from the synoptic oceanographer's point of view, most of the data are highly perishable, becoming of marginal value typically after about one day. It is desirable that as much operational utility as possible should be derived from the data, notwithstanding its primarily experimental nature. Moreover, it is appropriate to include investigation and trial of potentially expeditious and effective methods of dissemination as part of the total experimental program. For these reasons it is appropriate to consider augmentations of the ground data link system which would be useful for oceanographic data distribution. Of course, the routine recording of all the payload data received, as a precaution against the loss of the data in any subsequent transmission or processing, is desirable regardless of what the subsequent operations may be.

As before, the SAR data present the greatest problem, both because of the amount of raw data and because of the need for rapid dissemination. Synoptic oceanographers would like high latitude ice mapping data at least within a day, and this is clearly incompatible with physical shipping of data tapes. Conventional processing of raw SAR data to produce image-type data results in an enormous reduction in the data volume. Specifically, the 1.24×10^4 M bits of data acquired per orbit, expressed in terms of picture elements of 1 km x 1 km size, and digitized to eight bits per element, become only about 27 M bits of picture data. In the present state-of-the-art, the processing can be done by primarily optical means (the current most common method) or by special purpose electronic data processing equipment

of modest size, which can be readily fitted, for example, into an aircraft but not into a spacecraft of the EOS class. This suggests that very modest additions to the equipment at Goldstone and Fairbanks for the purpose of doing the standard initial processing of the SAR data would greatly facilitate its subsequent distribution for further processing and ultimate dissemination to the users. In fact, if this initial processing is done, the SAR data volume becomes less than that of most of the sensors.

If we look at the total data acquired per orbit with the SAR output partially processed, as indicated, the average amount becomes 3.25×10^3 M bits. This total is of course shared by the receiving stations, but not in equal amounts. As would be expected, the total readout time available at Fairbanks is much larger than at the other stations; in fact, for the typical day quoted earlier it amounted to 119.9 minutes, or slightly over half the total of 223.3 minutes. Thus we may take Fairbanks as the worst case, with 1.67×10^3 M bits acquired per orbit. A data link dedicated to transmitting the payload information to the NDPF would have to transmit this amount in about 6000 seconds, at a data rate of 280 K bits/sec. It can thus be roughly estimated that communication links capable of transmitting at least 300 K bits/sec from Fairbanks to Goddard, and about 150 K bits/sec from Goldstone to Goddard, will eventually be needed to transmit global oceanographic data from an EOS satellite if these data are to be useful to synoptic oceanographers and meteorologists. The earlier these links are achieved, the greater the operational benefit that will be derived, in addition to the experimental value of information obtained from satellite oceanographic data.

10.3 DATA HANDLING AT NDPF

The data acquired by the global oceanographic EOS satellite will all come to the NDPF for appropriate processing, storage, and distribution. Because of the experimental nature of the data obtained, the NDPF may have a larger role than with later, more operationally oriented satellites. The basic philosophy, however, should be applicable to the handling of data from any satellite. Thus the processing done will be that associated with spacecraft and instrumentation effects, rather than analysis or interpretation requiring expertise within the disciplines of the ultimate users. This includes adjustment of data values for calibration, correction of spacecraft

or sensor induced distortions in image data, and correlation of payload data with time and spacecraft position and attitude to provide position or other pertinent annotation.

In addition, the information must be put into a format or formats which are convenient for the users. This includes for imagery the size of the pictures, whether negative or positive or false-color, roll film or individual frames, additions of sensitometric control data, choice of projection, annotation, and many other factors. Numeric data can be in the form of magnetic tape, electron beam recorder or laser beam recorder film, computer printouts, etc., and may be organized in a variety of ways. However, there are options of a more fundamental nature as well as the above important but rather straight forward considerations. Each kind of information suggests a natural method for its presentation; for example, visible imagery is basically analog in nature and continuous in spatial coordinates, while altimeter data seems most appropriately given in numeric form for discrete locations. The natural presentation is generally to be preferred, but frequently it is not compatible with the merging of the data with that from other sources, or with some important uses of the data. A good illustration is given by satellite cloud data, which are very convenient for synoptic meteorologists to use in the mosaics or other pictorial formats employed, but they are very difficult for climatologists to merge with data based on point observations; indeed, up to the present climatologists have generally felt that the effort required to put these data into the forms they need is not justified by the results to be achieved. The transformation of image-type data to numeric values on a standard grid is usually most efficiently and economically done during preprocessing. Similarly, basically point-type data is usually obtained for locations dictated by spacecraft and sensor operating conditions, and may need to be transformed to a standard grid. Thus all the oceanographic data need to be studied to determine the most useful output formats, and the accomplishment of the required transformations will usually be a function of the NDPF.

10.3.1 Processing

The output of the oceanographic satellite sensors represents a data volume about one order of magnitude less than that of ERTS A/B, but the types of data are more diversified, and in addition, the desired throughput

time is much shorter (less than a day versus six days for ERTS A/B). The data management philosophy therefore is shifted from batch methods for efficient use of main frame computer time and reproduction facilities in order to handle large volumes of data to methods providing much faster reaction to smaller amounts of data. This will probably result in somewhat lower efficiency, for example, incomplete utilization of computational capabilities because of a relatively greater amount of set-up time and use of peripheral equipment. There still remains, however, a large excess of basic capability. Some modest additions of special purpose equipment will be needed, and, of course, software specific to the individual sensor data processing requirements must be provided.

10.3.1.1 SAR

It has already been shown that special processing equipment is needed for the initial processing of SAR data at Goldstone and Fairbanks. The same requirement applies to the NTTF/NDPF, where it is assumed that because of the existing wideband link between these two neighboring facilities, the SAR processing equipment would be located at the NDPF. The required processing will utilize the equipment no more than 3 to 4 hours a day, so that if it were decided to send all the raw SAR data to the NDPF one set of equipment would still be adequate for that mode of operation. The equipment can be either essentially optical or wholly electronic. The optical equipment would occupy on the order of 150 square feet of space in the controlled photographic area; the electronic version, a few racks of equipment. If electronic processing is selected, it could no doubt be accomplished by the central computer facility, but this would almost certainly be much less efficient than to provide special purpose equipment.

The output of the initial processing of SAR data is in the form of imagery of the swaths covered, uncorrected for geometric factors and spacecraft body rates. This imagery, whether generated at the NDPF or received from the other ground stations, should therefore be given further preprocessing before it is transmitted to the users. The techniques developed for producing mosaics of satellite cloud pictures on specified projections are probably easily adaptable to SAR imagery, and the polar stereographic projection seems the obvious one to select. In view of the experience of the Weather Service in this area, it might be advisable to provide

them only the swath imagery corrected for satellite motions along with ephemeris data, and have them make the desired mosaics. It would be quite feasible, however, to carry the processing through to the production of mosaics at the NDPF.

10.3.1.2 Multispectral Mechanical Scanner

The data from the multispectral mechanical scanner are very similar in nature to ERTS A/B MSS imagery. Although the area covered is much greater, each pixel covers about 200 times as much area, so the pixel volume is about an order of magnitude less. There are other significant differences also. The larger resolution elements and the conical scan pattern make corrections for geometric errors very much simpler, while on the other hand, the conical scan makes the picture reconstruction algorithms quite different and probably more complicated than for MSS. The output formats will also be different. False color composites of several channels do not have any particular utility, so the image output should consist only of separate pictures for each of the channels, and possibly only of the UV, visible, and near IR channels. The selection of the three thermal IR channels at 4.9, 9.1, and 11.0 μ provides a method to remove atmospheric effects from the determination of sea surface temperatures by using measurements from all three channels for each location. Therefore, the output from these channels should be a single thematic map of sea surface temperatures, a tabulation of temperatures at selected grid points, or most likely, both. The NDPF computing capability, with the addition of specific software, and the photographic production capability, with little or no modification, should be adequate. The analog or hybrid equipment designed specifically for geometric correction of ERTS A/B imagery may not, however, be adaptable to multispectral mechanical scanner data.

10.3.1.3 Visible Spectrometer

Pictorial representation of the data from the twenty spectral channels of the visible spectrometer in a single or a small number of false color composites is impossible without seriously compromising the original information. A few selected channels may be used to produce false color composites for screening purposes, but serious ocean color analyses must use the basic spectral data in some explicit form. This will probably take the form of digital data tapes in which the information is organized by

spectral data per location, after suitable preprocessing to introduce calibration adjustments and correct geometric errors. Such an organization is easy to obtain from the sensor data output format. The number of data points, while over two orders of magnitude less than that anticipated for the ERTS MSS, is still formidable, and each point represents 20 channels as compared with 4 or 5 for the MSS. Thus the screening function, performed by the user on false color composites, or from indications from other information sources, is mandatory. For a small number of locations of interest, the spectral data can be examined in detail, either from a table of reflectance values per channel, or a graphically presented spectrum for each point. From the point of view of the NDPF, however, the problems of analysis and interpretation affect the required preprocessing only in so far as they dictate output formats. The likely output products suggested above are well within NDPF hardware capabilities, and development of the required software does not present a major problem.

10.3.1.4 Glitter Pattern Sensor

The glitter pattern sensor generates a modest amount of raw data, and the output requirements are correspondingly small. The wind velocity information consists of discrete values for no more than 70 locations per orbit, easily amenable to distribution as data tapes or even computer print-outs. The data reduction is expected to be entirely automatic, requiring very little computer time and a modest software development effort. It may turn out that operator screening for cloud cover, with subsequent direction of the data reduction, is desirable; this could require up to 30 minutes operator time per orbit, at a console communicating with the computer. The second objective of the sun glitter information, the location of areas of reduced sea state, definitely requires operator examination of glitter pattern imagery. Thus the two functions, assuming that operator guidance is used in the data reduction, could be efficiently combined. The operator would probably examine CRT presentations of the glitter imagery, and select only those frames of interest for rectification and hard copy output, but even routine production of images of all glitter pattern sensor frames received would not entail a serious photographic production problem.

10.3.1.5 Microwave Radiometer

The theory of the dual channel, dual angle microwave radiometer requires very straight forward computer processing, and the volume is so small that the computer utilization is almost negligible. The output could be either in the form of thematic maps or as data tapes giving sea surface temperature and roughness at each location. It should be noted that the same physical parameters are measured by several sensors; both the IR scanner and the microwave radiometer give surface temperatures, and both the glitter pattern sensor and the microwave radiometer give indications of sea state. Simply following the natural order of the data will in general not give the data for the same geographic locations, so consideration should be given to transforming the data for the above three sensors to a standard grid network common to them all. This procedure would, at least in theory, slightly degrade the accuracy of the original information, but in these cases, the effect will be very small, and represents nothing essentially different from what the user would have to do to correlate the data himself. It would represent no great problem, either in data processing or in the volume of output products, to present both the glitter sensor and microwave radiometer outputs in both the original and standard grid formats, and the IR data, being of much higher resolution, will probably provide data close enough to the standard locations without further manipulation. However, the calculation of interpolated IR data at points on a standard grid of density consistent with the glitter sensor and microwave radiometer coverage, would also represent a very small effort.

10.3.1.6 Radar Altimeter

The radar altimeter information needs very little processing, other than correlation with spacecraft data to get accurate locations, and the total volume is small. Transformation to a standard grid would also be advisable and easily accomplished.

10.3.2 Data Storage

Many of the questions associated with data storage design philosophy are fully answered, or the options greatly restricted, when the output data formats have been established, since they define the data some or all of

which must be stored, and go a long way toward indicating the organization of the files. The questions remain, however, of how much of the data should be stored, how long it should be kept, and whether or not multiple copies of some data should be kept on hand.

In an experimental program, it is advisable that all the raw, or nearly raw, data be kept throughout the length of the program, or at least as long as physical limitations permit, since originally unanticipated uses may be identified, or improved methods of data reduction may be developed, which require reprocessing of the original data. Most of the fully preprocessed outputs should probably also be kept, since users will not always identify their complete requirements at the beginning of the program, and it is very convenient to have a central repository for the program-generated data. These guidelines must be tempered by practical considerations, but it is not anticipated that the volume of experimental global oceanographic data generated will grow to unmanageable proportions.

The nature of expected user requests has considerable bearing on exactly what is stored and in what quantities. In an area in which very few requests are anticipated after the initial distribution, it is most efficient to keep only the bare minimum of processed data necessary to generate outputs on special requests. Thus for computer-generated thematic maps which are not likely to be called for again, only the digital data, and no hard copies need be kept. Certainly where imagery has been distributed as negative and positive transparencies, and as paper prints, there is no need to keep all these forms. Even when requests are expected, the philosophy of regenerating specific output formats from more basic data on request results in a workable system, and is almost mandatory when the volume of data which must be stored is very large. On the other hand, in areas where frequent user requests occur, the regeneration of output formats may disrupt the orderly operation of the facility and the delays attendant on getting data out of the system can be annoying, at least, to the users. Thus, where it is possible, it is advisable to have copies of much used material physically on hand. In the absence of specific knowledge of program details and user participation, answers to most of the foregoing questions must be deferred.

10.3.3 Distribution From NDPF

The details of the initial distribution of the global oceanographic data and of the handling of later requests are difficult to anticipate at this time. Two general observations can be made, however. First, the rapid decrease in the value of the data for many users, along with the low volume and the digital or alphanumeric form in which it can be cast, make routine distribution over electronic data links a significant characteristic of the program. This will be true, in particular, of the data supplied to synoptic meteorologists and oceanographers, to users within the fisheries, and to agencies concerned with hazards. In this respect, the requirements placed on the NDPF, both with regard to methods of operation and availability of communication channels, are markedly different from those of ERTS A/B. Planning for distribution of ERTS A/B products involved exclusively the physical shipment of either hardcopy imagery or data tapes. On the other hand, later requests, i. e., those for previous data, will come largely from a different set of users, and, obviously, will be far less time-constrained. Thus the data distribution will follow two distinct patterns, one well defined and predictable, using mostly communications links, and the other more sporadic and nearly always involving physical products, much as the non-routine requests for ERTS A/B are expected to be.